

**ROLE OF A C-TERMINAL AMPHIPATHIC HELIX IN THE F  
PLASMID SEGREGATING PROTEIN SopA IN MEMBRANE  
BINDING, POLYMERISATION, DNA BINDING AND PLASMID  
MAINTENANCE**

*By*

**DIPIKA MISHRA**

**LIFE11201504005**

**National Institute of Science Education and Research**

*A thesis submitted to the*

*Board of Studies in Life Sciences*

*In partial fulfillment of requirements for the*

*Degree of*

**DOCTOR OF PHILOSOPHY**

*of*

**HOMI BHABHA NATIONAL INSTITUTE**



**January, 2022**

## Recommendations of the Viva Voce Committee

As members of the Viva Voce Committee, we certify that we have read the dissertation prepared by Dipika Mishra entitled "ROLE OF A C-TERMINAL AMPHIPATHIC HELIX IN THE PLASMID SEGREGATING PROTEIN SopA IN MEMBRANE BINDING, POLYMERISATION, DNA BINDING AND PLASMID MAINTENANCE" and recommend that it may be accepted as fulfilling the thesis requirement for the award of Degree of Doctor of Philosophy.

Chairman - Name & Signature with date

-Prof. Moley Sarkar

*Moley Sarkar*

07/02/2022

Guide / Convener - Name & Signature with date

-Dr. Ramanujam Srinivasan

*R. Srinivasan*

04/02/2022

Co-guide - Name & Signature with date (if any)

Examiner - Name & Signature with date

-Dr. Sunish Radhakrishnan

*Sunish*

06/02/2022

Member 1- Name & Signature with date

-Dr. Debasish Chaudhuri

*Debasish Chaudhuri*

06/02/2022

Member 2- Name & Signature with date

-Dr. Renjith Mathew

*Renjith Mathew*

08/02/2022

Member 3- Name & Signature with date

-Dr. Rudresh Acharya

*Rudresh*

07/02/2022

Final approval and acceptance of this thesis is contingent upon the candidate's submission of the final copies of the thesis to HBNI.

I/We hereby certify that I/we have read this thesis prepared under my/our direction and recommend that it may be accepted as fulfilling the thesis requirement.

*D. Srinivasan*  
21/02/22

## **STATEMENT BY AUTHOR**

This dissertation has been submitted in partial fulfillment of requirements for an advanced degree at Homi Bhabha National Institute (HBNI) and is deposited in the Library to be made available to borrowers under rules of the HBNI.

Brief quotations from this dissertation are allowable without special permission, provided that accurate acknowledgement of source is made. Requests for permission for extended quotation from or reproduction of this manuscript in whole or in part may be granted by the Competent Authority of HBNI when in his or her judgment the proposed use of the material is in the interests of scholarship. In all other instances, however, permission must be obtained from the author.

*Dipika Mishra*  
Dipika Mishra

## **DECLARATION**

I, hereby declare that the investigation presented in the thesis has been carried out by me. The work is original and has not been submitted earlier as a whole or in part for a degree / diploma at this or any other Institution / University.

*Dipika Mishra*

**Dipika Mishra**

## List of Publications arising from the thesis

### Journal

1. **Mishra, D., Pahujani, S.,** Mitra, N., Srivastava, A. & Srinivasan, R. Identification of a Potential Membrane-Targeting Sequence in the C-Terminus of the F Plasmid Segregation Protein SopA. *The Journal of Membrane Biology* 1–15 (2021) doi:10.1007/s00232-020-00157-8.
2. **Mishra, D.,** Jakhmola, A., Srinivasan, R. A role for the C-terminal helix of the F plasmid segregating protein SopA in plasmid maintenance. *Plasmid* (2022) doi: 10.1016/j.plasmid.2022.102617.
3. **Mishra, D.,** Mitra, N., Sakshi, P., Gayathri, P., Anand, S. and Srinivasan, R. The C-terminal helix in F plasmid segregating protein SopA regulates polymerization, DNA binding and interaction with SopBC complex. (Manuscript under preparation).

### Other Publications:

1. **Mishra, D &** Srinivasan, R. Catching A Walker in the Act – DNA Partitioning by ParA family of Proteins. *Frontiers in Microbiology* (Communicated)
2. **Mishra, D.,** Mitra, N. & Srinivasan, R. World War II, Sex and Antibiotics. (Communicated).

### Conferences

#### International

#### Talks:

1. C-terminus of SopA- A key player in mediating segregation. *Boston Bacterial Meet (BBM) 2020*, 16<sup>th</sup> July-17<sup>th</sup> July 2020. (Virtual)
2. SopA C-terminus plays a crucial role in nucleoid binding and mediating F plasmid segregation. **Mishra D,** Srinivasan R. *Caulocon 2.0*, 6<sup>th</sup> November 2020. (Virtual)
3. SopA mediated plasmid segregation- A tale through the C-terminus. **Mishra D,** Srinivasan R. *ISPB series on Plasmids around the globe*, 8<sup>th</sup> June 2021. (Virtual)

#### Posters:

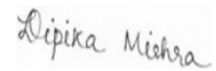
1. Chromosomal segregation in bacteria: role of actin like proteins and Walker A ATPases. **Mishra D,** Prugnaller S, Funaya C, Mishra M, Antony C, Balasubramanian MK, & Srinivasan R. *International Conference of Cell Biology 2018-The Dynamic Cell: Molecules and networks to form and function*. 27<sup>th</sup> Jan-31<sup>st</sup> Jan 2018, Leonia Holistic Destination, Hyderabad.

2. The role of SopA C-terminus in F plasmid Segregation. **Mishra D**, Srinivasan R. *Young Microbiologists Symposium on Microbe Signalling, Organisation and Pathogenesis 2020*. 26<sup>th</sup> Aug-27<sup>th</sup> Aug 2020. (Virtual e-poster)

**National:**

**Talks:**

Dissecting the role of SopA C-terminus in F plasmid maintenance. **Mishra D**, Srinivasan R. *National seminar on “Advances and challenges in Biological sciences” [ACBS-2020]*, 12<sup>th</sup>Feb-13<sup>th</sup> Feb 2020. **Awarded Best Oral Presentation.**



Dipika Mishra

**Dedicated to my dearest Baba**

## ACKNOWLEDGEMENTS

This work would not have been complete without the guidance, support and encouragement of my mentor, Dr. Ramanujam Srinivasan. I express my sincere gratitude to him for the time he invested in guiding me through this project. He was always available for discussions on the project and allowed me to work independently in my project.

I am grateful to all members of my Doctoral Committee (Prof. Moloy Sarkar, Dr. Debasish Chaudhuri, Dr. Rudresh Acharya, Dr. Renjith Mathew) for their useful suggestions on the project. Special thanks to Dr. Sanjita Banerjee for her help and advice. I would also thank Dr. Anand Srivastava and for his collaboration in the membrane binding aspect of SopA. I extend my gratitude to Dr. Dileep Vasudevan Lab, Dr. Gayathri Pananghat Lab, Dr. Abdur Rahman lab and Dr. Tirumala Kumar Chowdary lab for allowing me to use their lab facilities and discussions. Special thanks is extended to Dr. Srikhant Harne for help with initial cloning and purification protocols of SopA, to IISER Pune facilities and hospitality. I am thankful to DAE for providing me with the fellowship for carrying out my research. I am also indebted to SBS, NISER and the common instrumentation facility.

This work would not have been complete without the strains and plasmids received from various labs across the globe. Thanks to Dr. David Lane, Dr. Jean Yves Bouet, Dr. Ajitkumar Parthasarathi, Dr. Anjana Badrinarayanan, Dr. Gayathri Pananghat, Dr. Chandra Mohan Joshi, Dr. Tushar K Beuria and all other people who provided us with the strains as well as plasmids.

To all the past and present members of the lab (Ajay, Nivedita, Sakshi, Sakshi Pahujani, Dr. Vimal Kishore, Dr. Supriya Pandit, Bhagyashri, Rudra), thanks for always being there for me and creating a friendly environment and a healthy workspace in the lab. It was fun working with you guys.

PhD is a difficult journey especially when you do not have friends to fall back upon. Thanks to Saumya and Rojalin for sharing our bit of difficult journeys together. Thanks to Rojalin for our discussions on a wide range of topics ranging from science and meandering through the lanes of Literature.



My family has been my biggest strength. To my Mother, without your backing, I could have never made it here. Thanks a lot for always being beside me when I needed you the most. To my elder brother Debasish, thank you for your advice, inspirations in life and your trust in me. To my younger brother Deepak, thank you for patiently listening to my struggles and keeping faith in me dear. This journey would not have been complete without the most important person in my life, my dearest Baba. I wish you were with me Baba today as I finish this journey.

A big thank you to all the COVID warriors, without whom, even thinking about completion of this Thesis would have been a distant dream.

For those whose names I have not mentioned, you know who you are and your contributions in my journey, thanks to all.

# CONTENTS

<b>SUMMARY</b>	<b>i</b>
<b>LIST OF FIGURES</b>	<b>iii</b>
<b>LIST OF TABLES</b>	<b>vi</b>
<b>LIST OF ABBREVIATIONS</b>	<b>vii</b>
<b>1. CHAPTER 1: INTRODUCTION</b>	<b>1 - 44</b>
<b>1.1 INTRODUCTION</b>	<b>1</b>
<b>1.2 PLASMID MAINTENANCE AND PARTITIONING MACHINERY</b>	<b>5</b>
1.2.1 MULTIMER RESOLUTION SYSTEMS	7
1.2.2 POST SEGREGATIONAL KILLING	7
1.2.3 ACTIVE PARTITIONING OR ‘MITOTIC’ SYSTEMS	8
<b>1.3 EVENTS PRIOR TO PARTITIONING</b>	<b>12</b>
A) <i>DIF</i> , <i>XERC</i> AND <i>XERD</i>	12
B) TOPOISOMERASE IV	13
<b>1.4 BASIC ARCHITECTURE OF THE BACTERIAL MITOTIC SEGREGATION MACHINERY</b>	<b>13</b>
<b>1.5 THE TYPES OF PLASMID SEGREGATION MACHINERY</b>	<b>15</b>
1.5.1 <i>TYPE-I/ WALKER A-TYPE ATPASES</i>	15
1.5.2 <i>TYPE-II/ ACTIN-LIKE PROTEINS IN SEGREGATION</i>	18
1.5.3 <i>TYPE-III/ TUBULIN/ FTSZ-LIKE GTPASE FAMILY OF PARTITIONING PROTEINS</i>	20
<b>1.6 PARA/ SOPA – A <u>W</u>ALKER <u>A</u> TYPE <u>C</u>YTOSKELETAL <u>A</u>TPASE (WACA)</b>	<b>22</b>
<b>1.7 CENTROMERE BINDING PROTEIN (CBP) OR THE ADAPTOR PROTEIN – PARB</b>	<b>26</b>

<b>1.8 BACTERIAL NUCLEOID AS A HOST FACTOR</b>	27
<b>1.9 PARA HOMOLOGS INVOLVED IN PARTITIONING BACTERIAL GENOMES</b>	29
<b>1.10 WACA PROTEINS IN ARCHAEAL DNA PARTITIONING</b>	29
<b>1.11 THE MECHANISM AND MODELS OF DNA PARTITIONING BY PARA</b>	30
<b>1.12 DIVERSE BIOLOGICAL FUNCTIONS OF WACA / PARA SUPERFAMILY OF PROTEINS</b>	39
1.12.1 ROLE OF MIND IN CHROMOSOME SEGREGATION	40
1.12.2 PARA LIKE PROTEINS IN CARBOXYSOME MAINTENANCE IN CYANOBACTERIA	41
1.12.3 ORPHAN PARA PROMOTING CHEMORECEPTOR CLUSTER FORMATION	42
1.12.4 GENOMIC ISLAND MEDIATED INCOMPATIBILITY	42
1.12.5 ORPHAN PARA INVOLVED IN CELLULOSE BIOSYNTHESIS	42
<b>1.13 SUMMARY</b>	44
<b><u>2. CHAPTER 2: MATERIALS AND METHODS</u></b>	<b>45 - 81</b>
<b>2.1 BACTERIAL STRAINS AND GROWTH CONDITIONS</b>	45
<b>2.2 REAGENTS</b>	45
<b>2.3 ANTIBIOTICS</b>	55
<b>2.4 PLASMID DNA EXTRACTION</b>	55
<b>2.5 CLONING</b>	56
<b>2.6 GENERATION OF C-TERMINAL DELETION MUTANTS</b>	58
<b>2.7 GENERATION OF SITE-DIRECTED MUTANTS</b>	59
<b>2.8 TRANSFORMATION OF <i>S. POMBE</i> (FISSION YEAST) - LITHIUM ACETATE METHOD</b>	70
<b>2.9 POLYMERASE CHAIN REACTION (PCR)</b>	71
<b>2.10 PROTEIN PURIFICATION</b>	73

<b>2.11 ELECTROPHORETIC MOBILITY SHIFT ASSAY (EMSA)</b>	75
<b>2.12 MEMBRANE FRACTIONATION</b>	75
<b>2.13 LIVE CELL IMAGING</b>	76
2.13.1 CHLORAMPHENICOL AND CEPHALEXIN TREATMENT CELLS FOR NUCLEOID CONDENSATION AND CELL DIVISION INHIBITION, RESPECTIVELY	77
2.13.2 LOCALISATION OF THE MUTANTS IN $\Delta$ MINB STRAIN	77
<b>2.14 PLASMID STABILITY ASSAY</b>	77
<b>2.15 BACTERIAL TWO-HYBRID ASSAYS (BACTH)</b>	79
<b>2.16 PROMOTER REPRESSION ASSAY</b>	80
2.16.1 LACZ ACTIVITY INDICATOR PLATE ASSAY (QUALITATIVE)	80
2.16.2 B-GALACTOSIDASE ASSAY/ ONPG ASSAY (QUANTITATIVE)	80
<b><u>3. CHAPTER 3: IDENTIFICATION OF AN AMPHIPATHIC HELIX WITHIN THE C-TERMINAL 360 – 388 RESIDUES OF SOPA</u></b>	<b>82 - 107</b>
<hr/>	
<b>3.1 INTRODUCTION</b>	82
<b>3.2 RESULTS</b>	84
3.2.1 THE C-TERMINUS OF SOPA IS PREDICTED TO FORM AN AMPHIPATHIC HELIX	84
3.2.2 ASSOCIATION OF SOPA WITH THE MEMBRANE IN A $D\Psi$ -SENSITIVE MANNER	90
3.3.3 ROLE OF HOST FACTORS IN SOPA LOCALISATION	93
3.3.4 MEMBRANE ASSOCIATION OF SOPA PROTEIN	94
3.3.5 SOPA ASSOCIATION TO THE MEMBRANE IS DIMERISATION INDEPENDENT	99
3.3.6 C-TERMINAL MUTANTS ARE DEFECTIVE IN MAINTAINING PLASMIDS	102
<b>3.3 DISCUSSION</b>	104

<b><u>4. CHAPTER 4: ROLE OF THE C-TERMINAL HELIX OF SOPA IN</u></b>	
<b><u>NUCLEOID BINDING AND PLASMID STABILITY</u></b>	<b><u>108 - 132</u></b>
<b>4.1 INTRODUCTION</b>	108
<b>4.2 RESULTS</b>	110
4.2.1 SOPA $\Delta$ CT29 AND SOPA W369E MUTANTS ARE DEFECTIVE IN NSDNA BINDING	110
4.2.2 PERTURBED NUCLEOID BINDING OF SOPA C-TERMINAL DELETION MUTANTS	113
4.2.3 INFLUENCE OF THE SOPBC PARTITIONING COMPLEX ON THE NUCLEOID LOCALISATION OF C-TERMINAL DELETION MUTANTS OF SOPA	117
4.2.4 SOPA $\Delta$ CT5 IS DEFECTIVE FOR PLASMID MAINTENANCE	119
4.2.5 RESIDUES IMPORTANT FOR DNA BINDING WITHIN THE C-TERMINAL HELIX OF SOPA	121
4.2.6 INFLUENCE OF THE SOPBC PARTITIONING COMPLEX ON THE NUCLEOID LOCALIZATION OF C-TERMINAL POINT MUTANTS OF SOPA	125
4.2.7 PLASMID MAINTENANCE IS AFFECTED IN C-TERMINAL MUTANTS	128
<b>4.3 DISCUSSION</b>	130
<b><u>5. CHAPTER 5: C-TERMINAL RESIDUES Q351 AND W362 REGULATE</u></b>	
<b><u>POLYMERISATION AND NUCLEOID BINDING OF SOPA</u></b>	<b><u>133 - 172</u></b>
<b>5.1 INTRODUCTION</b>	133
<b>5.2 RESULTS</b>	135
5.2.1 MUTATIONS IN SOPA Q351 OR W362 RESULT IN STABILISATION OF SOPA POLYMERS	135

5.2.2 INTERACTION OF SOPA Q351H AND SOPA W362E WITH WILD-TYPE SOPA AND WITH THEMSELVES	143
5.2.3 POLYMERISATION OF SOPA Q351H AND SOPA W362E IS ATP DEPENDENT	144
5.2.4 POLYMERISATION REQUIRES CONTINUOUS PROTEIN SYNTHESIS	146
5.2.5 SOPA Q351H AND SOPA W362E ARE DEFECTIVE IN PARTITIONING DNA	154
5.2.6 SOPA Q351H AND SOPA W362E FILAMENTS ARE NOT NUCLEOID-ASSOCIATED	154
5.2.7 SOPA Q351H AND SOPA W362E ACT AS SUPER-REPRESSORS OF THE <i>SOP</i> PROMOTER, P <sub>SOP</sub>	162
5.2.8 SOPA Q351H AND SOPA W362E FAIL TO INTERACT WITH SOPB	167
<b>5.3 DISCUSSION</b>	<b>169</b>
<b><u>6. CONCLUSION</u></b>	<b><u>173 - 175</u></b>
<b><u>REFERENCES</u></b>	<b><u>176 - 196</u></b>

## SUMMARY

Most bacterial genomes and plasmids carry a Walker A type Cytoskeletal ATPase belonging to the ParA superfamily of proteins to partition their genetic material during cell division cycles. ParA constitutes the ATP-dependent motor protein, and the adaptor protein ParB stimulates ParA activity and drives the dynamicity of the system. The F plasmid also carries the *parABC* locus and is known as *sopABC*. Recent studies have established that the binding of SopA to non-specific DNA is vital for its function in plasmid maintenance. A chemophoretic gradient of SopA across the bacterial chromosome (nsDNA) drives the unidirectional movement of the plasmid DNA towards the cell poles. Further, earlier studies had also shown that SopA could polymerise and bind to the plasma membrane.

However, the molecular details of SopA polymerisation, membrane-association and interaction with nsDNA remain unclear. Using a combination of *in silico*, cell biological and genetic approaches, we identify that the last 360 – 388 residues in the C-terminus of SopA contain a hitherto unidentified amphipathic helix. Helical wheel projections and hydrophobic moment calculations indicated an evident hydrophobic face characteristic of amphipathic helices, and membrane pelleting assays revealed the presence of SopA in bacterial membranes (Mishra et al., 2021). We thus identify a plausible membrane targeting sequence within the last C-terminal helix in SopA and further show that it also plays an important role in polymerization, non-specific DNA binding and interaction with SopB.

Further, using a series of C-terminal deletion mutants and several point mutants in the C-terminal helix, which affect plasmid stability and nsDNA binding activity of SopA, we elucidate the role of the C-terminal helix of SopA nucleoid binding, interaction with SopBC complex and polymerization. Deleting the last seven amino acids (Ct7) abolished nsDNA binding and interaction with the SopBC complex. Although the deletion of the last five amino acids did not affect nsDNA binding and its interaction with the SopBC complex, it led to a

complete loss of plasmids from cultures. Among the several point mutants generated, K385A was fully functional, R363A and F377A exhibited nucleoid localization and assembled into weak foci in the presence of SopBC, suggesting interaction with the SopBC complex, but failed to maintain plasmids stably. E375A was unable to maintain plasmids in cultures stably and was unable to localize to the nucleoids, suggesting a critical role for this residue in nsDNA binding. Surprisingly, mutation of the aromatic residue W362 to glutamic acid (E) resulted in stabilization of the SopA polymers and led to the formation of cytoplasmic filaments by SopA. Such cytoplasmic filaments were also reported for another mutant of SopA, i.e., SopA1 (M315I Q351H). We show that Q351H mutation is sufficient for stabilizing SopA polymers. Time-lapse imaging revealed that polymers were dynamic and prone to depolymerisation upon depletion of ATP or inhibition of new protein synthesis. Most importantly, these mutations disrupted the non-specific DNA binding activity of SopA, as has been shown *in vivo* by localization of the filaments in the inter nucleoid space and in minicells in a *AminB* strain. Interestingly, the mutants were capable of sequence-specific DNA binding at the P<sub>sop</sub> promoter region and repress gene expression in the absence of SopBC. Consistently, we failed to detect the interaction of SopB with these mutants by Bacterial-two hybrid assays. In summary, these studies reveal a fundamental role for the C-terminal amphipathic helix in polymerisation, DNA binding and plasmid partitioning functions of SopA and have implications for the transfer and spread of multi-drug resistance in bacteria.



## LIST OF FIGURES

**Figure 1-1.** Schematic representation of the eukaryotic segregation machinery

**Figure 1-2.** The different types of plasmid maintenance mechanisms

**Figure 1-3.** The different types of NTPase based DNA partitioning systems in bacteria

**Figure 1-4.** Schematic representation of the basic components of the bacterial segregation machinery

**Figure 1-5.** Genetic organisation of Type-Ia, Type-Ib, Type-II and Type- III partition loci

**Figure 1-6.** The conserved domains of F plasmid partitioning protein SopA

**Figure 1-7.** Sequence alignment of P1 ParA and SopA proteins and their secondary structure.

**Figure 1-8.** Timeline: Important milestones in our understanding of the models proposed for the mechanism of DNA segregation.

**Figure 1-9.** Model depicting the mechanisms of ParA proteins in DNA partitioning.

**Figure 1-10.** A molecular model depicting the mechanism of DNA partitioning by ParA / SopA

**Figure 1-11.** The deviant Walker A motif in different members of P loop ATPase

**Figure 2-1.** Schematic diagram representing the protocol used for estimating plasmid loss rates in bacteria

**Figure 2-2.** Depiction of vector maps of (A) pUT18C-SopA, (B) pKT25-SopB

**Figure 3-1.** Prediction of a C-terminal amphipathic helix in SopA

**Figure 3-2.** SopA localisation to nucleoids is sensitive to the membrane potential  $\Delta\Psi$

**Figure 3-3.** SopA relocalisation to membrane periphery is independent of *ugpA*

**Figure 3-4.** SopA in bacterial membrane fractions

**Figure 3-5.** SopA relocalisation to the membrane periphery is independent of its ATP binding

**Figure 3-6.** Deletion of the predicted C-terminal amphipathic helix of SopA lead to plasmid loss

**Figure 3-7.** The C-terminus of SopB might be a potential membrane targeting sequence

**Figure 4-1.** SopA  $\Delta$ Ct29 and W369E mutants are impaired in non-specific DNA binding

**Figure 4-2.** The C-terminal deletion mutants exhibit abrogated nsDNA binding

**Figure 4-3.** Influence of the partitioning complex on the localisation of SopA C-terminal deletion mutants

**Figure 4-4.** The last five amino acids in the C-terminal helix are essential for plasmid maintenance

**Figure 4-5.** C-terminal helix residues in SopA critical for nsDNA

**Figure 4-6.** Influence of the partitioning complex on the localisation of C-terminal point mutants

**Figure 4-7.** Plasmid Stability Assay using C- terminal point mutants depicts plasmid loss in the case of most C-terminal mutants

**Figure 5-1.** Assembly of SopA, SopA1, Q351H and W362A/E into polymers

**Figure 5-2.** SopA Q351H and SopA W362E retain the ability to interact with the wild-type SopA

**Figure 5-3.** The polymerisation of SopA Q351H and SopA W362E is dependent upon ATP binding

**Figure 5-4.** Polymers are dynamic and exhibit the property of growth as well as shrinkage

**Figure 5-5.** SopA Q351H and SopA W362E are defective in plasmid partitioning

**Figure 5-6.** SopA Q351H and W362E are not nucleoid bound and show ns DNA binding defects

**Figure 5-7.** SopA Q351H and SopA W362E can bind the SopA promoter to repress transcription

**Figure 5-8.** SopA Q351H and W362E mutants are impaired in interaction with SopB

## **LIST OF TABLES**

**Table 1-1.** A few examples of active DNA partitioning systems in bacteria

**Table 2-1.** Bacterial and Yeast strains used in this study

**Table 2-2.** Antibiotics used in this study and their specific concentrations used

**Table 2-3.** Plasmids used in this study

**Table 2-4.** Oligonucleotides used in this study

**Table 2-5.** The PCR reaction conditions in the thermocycler

**Table 2-6.** The components of the PCR reaction

**Table 2-7.** The composition of the buffers used for protein purification.

**Table 4-1.** Residues mutated in the C-terminal stretch of SopA

**Table 4-2.** Table summarising the effects of deletion mutants and the site-directed mutants on SopA activity

## LIST OF ABBREVIATIONS

ATP	Adenosine -5`-triphosphate
ADP	Adenosine 5'-diphosphate
$\beta$ -Gal	beta-Galactosidase
bp	base pair(s)
BACTH	Bacterial Two Hybrid Assay
BSA	Bovine Serum Albumin
CaCl <sub>2</sub>	Calcium Chloride
Car	Carbenicillin
Cam	Chloramphenicol
DTT	Dithiothreitol
DNA	Deoxyribonucleic acid
EDTA	Ethylenediaminetetraacetic acid
EM	Electron Microscopy
EMM	Edinburg Minimal Medium
EMSA	Electrophoretic Mobility Shift Assay
GFP	Green fluorescent protein
His	histidine
IPTG	isopropyl- $\beta$ -D-thiogalactopyranoside
kb	kilobase
kDa	kilodaltons
KCl	Potassium Chloride
LB	Luria Bertani

MgCl <sub>2</sub>	Magnesium Chloride
μg	microgram (10 <sup>-6</sup> g)
mg	milligram (10 <sup>-3</sup> g)
μl	microliter (10 <sup>-6</sup> L)
ml	millilitre (10 <sup>-3</sup> L)
μM	micromolar(10 <sup>-6</sup> Mo)
mM	millimolar (10 <sup>-3</sup> Mo)
NaCl	Sodium Chloride
nsDNA	non-specific DNA
PAGE	Polyacrylamide gel electrophoresis
PMSF	phenylmethylsulfonyl fluoride
SDS	sodium dodecyl sulfate
X-Gal	5-bromo-4-chloro-3-indolyl-β-galactopyranoside

# **CHAPTER 1**

## **INTRODUCTION**

## 1.1 INTRODUCTION

The genetic material in all organisms needs to be equi-partitioned during each round of cell division. This mechanism has been very well studied in eukaryotes. The initial study on eukaryotic chromosome segregation dates back to the later part of the nineteenth century with the discovery of thread-like structures within the nucleus of the stained newt cells. These thread-like structures, observed with a light microscope, were named chromatin (Flemming, 1882). Subsequently, the entire mechanism of eukaryotic chromosome segregation was characterised further and is now known to be carried out by the microtubules. These microtubules or the so-called 'spindle fibers' pull the chromosomes apart and assist in segregating the replicated genetic material during cell division cycles (Scholey et al., 2003; Kline-Smith and Walczak, 2004) (**Fig. 1-1**). This entire mechanism is very well coordinated and takes place during the mitotic (M) phase in the programmed cell cycle and is organised into four different phases- S, G1, M and G2 (Cooper, 2000; Walczak et al., 2010).

The prokaryotes, on the other hand, were long believed to lack such sophistication for DNA segregation. The need for machinery to drive such cellular processes was deemed unnecessary, and the mechanisms by which bacteria partitioned their DNA remained poorly understood. Similarly, cell division and septum closure in bacteria were thought to be processes that did not involve any cytoskeleton function (Koch, 1985; Nanninga, 1998). However, the discovery of the bacterial cell division protein FtsZ and shape maintenance protein MreB sharing sequence and structural similarities with the eukaryotic tubulin and actin, respectively (Bork et al., 1992; Lowe and Amos, 1998; Van den Ent et al., 2001; Van den Ent et al., 2014) led to the acceptance of the presence of cytoskeleton in bacteria (Shih and Rothfield, 2006;



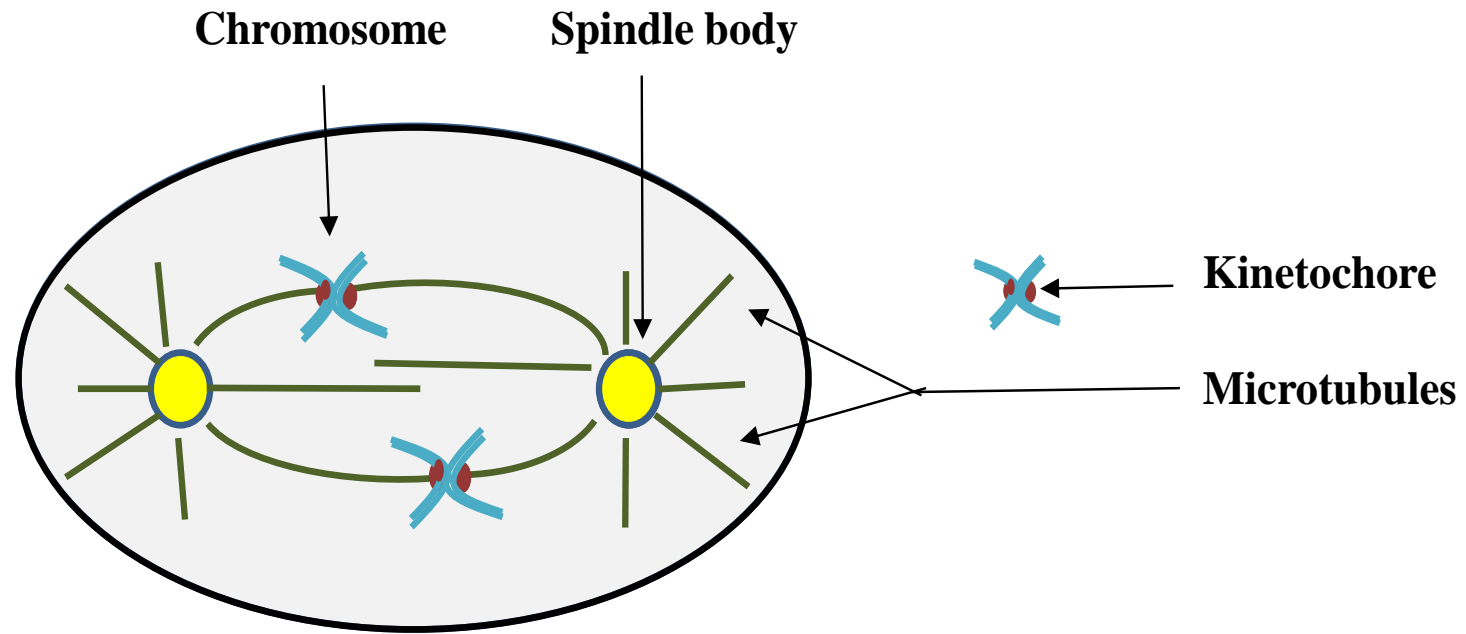


**Figure 1-1. Schematic representation of the eukaryotic segregation machinery.**

Representation of a section through an animal cell wherein the mitotic spindle is attached to the kinetochores of chromosomes, and depolymerising microtubules pull the chromosomes apart. The spindle pole body is represented as a small yellow circle.

Green lines represent the spindle, while blue represents the chromosomes and red their kinetochores.

Michie and Lowe, 2006). Thus, two families of cytoskeletal proteins, namely the Tubulin/ FtsZ family and the Actin/MreB family, became widely recognised. The recognition of bacterial origins of the eukaryotic cytoskeleton (Erickson, 2007; Nogales, 2010; Wickstead and Gull, 2011; Wagstaff and Lowe, 2018; Akil et al., 2019; W Stairs and J.G Ettema, 2020) and discovery of several cytoskeletal proteins across both Bacterial and Archaeal domains of life (Cabeen and Jacobs-Wagner, 2010; J.G Ettema et al., 2011) has dramatically changed our view of the cellular processes in prokaryotes. Today, we understand that different bacteria employ a variety of mechanisms to segregate their DNA into daughter cells. While almost all eukaryotes utilise tubulin to partition DNA, the process is carried out by diverse cytoskeletal proteins in different bacteria. These include the actin homologs (Actin-like proteins / Alps), tubulin/ FtsZ family of proteins and a unique but more widespread family of Walker A Cytoskeletal ATPases or simply known as WACA family of proteins (Shih and Rothfield, 2006; Derman et al., 2009; Salje et al., 2010; Gerdes et al., 2010; Ingerson-Mahar and Gitai, 2012; Gayathri et al., 2012; Lutkenhaus, 2012). Moreover, most bacterial and archaeal chromosomes and single / low-copy number plasmids carried by them utilise the WACA family of proteins for equi-partitioning during cell division (Motallebi-Veshareh et al., 1990; Koonin, 1993; Lutkenhaus, 2012). Thus, both the chromosomes as well as low copy number plasmids have served as excellent models to study the mechanisms by which the WACA of proteins mediate bacterial DNA segregation. The minimalistic machinery associated with the low copy number plasmids has allowed a detailed mechanistic study of the mechanism possible and has served as a paradigm for plasmid as well as bacterial chromosome segregation.

The DNA segregation systems in bacteria have been conveniently classified into four broad groups/ families - Type-I, Type-II, Type-III, and Type-IV (reviewed in Gerdes et al., 2000; Hayes and Barillà, 2006; Lutkenhaus, 2012). Type-I systems utilise, ParA family of proteins, a P-loop ATPase with a deviant Walker A motif for DNA partitioning. They are often found in chromosomal loci and single-copy plasmids such as the F plasmid (Fertility Plasmid that encode the Fertility factor or the F factor). The Type-II system carries the actin-like family of proteins and is found in R plasmids. They involve a polymerising actin-like protein ParM that undergoes insertional polymerisation to push apart the plasmids to the two opposite ends of the cell (Gerdes et al., 2000; Van den Ent et al., 2002; Moller-Jensen et al., 2003; Campbell and Mullins, 2007; Salje et al., 2009; Gayathri et al., 2012; Gayathri et al., 2013). The type-III mechanism is employed by pBTaxis plasmid wherein TubZ treadmills and pulls apart the two plasmids to the poles (Larsen et al., 2007). The Type-IV mechanism exemplified by the pSK1 plasmid of *Staphylococcus aureus* is the least studied one, involves only a single protein (Firth et al., 2000) and how this functions in DNA segregation is unclear. However, almost all bacterial chromosomes and single or very low copy number plasmids utilise the Type-I mechanism of DNA segregation mediated by the ParA superfamily of proteins (Abeles et al., 1985; Davis et al., 1992; Koonin, 1993; Davis et al., 1996; Lutkenhaus, 2012).

This chapter will provide a brief overview of the different types of plasmid maintenance and partitioning systems with an emphasis on plasmid segregation mediated by the Type-I systems. This will be followed by a detailed description of the current models and mechanisms by which the ParA family of proteins (in Type-I class

to which F plasmid and all chromosomal *par* systems are categorised) function in equi-partitioning of the replicated DNA into the newly born daughter cells.

## **1.2 Plasmid Maintenance and Partitioning Machinery**

Plasmids are extrachromosomal self-replicating pieces of DNA that encode genes for antibiotic resistance and pathogenicity (Sherratt, 1974; Giraldo et al., 1998; Birge, 2006; M Pinto et al., 2012). Plasmids generally vary in size from a few kilobases to hundreds of kilobases, and their geometry is commonly circular or sometimes linear. Plasmids often encode useful traits, including resistance to antibiotics, production of bacteriocins and resistance to heavy metals, ultraviolet light as well as many other metabolic functions (Sherratt, 1974; Birge, 2006). Plasmids have been traditionally classified into different types based on their replication and copy numbers (Million-Weaver and Camps, 2014). High copy number plasmids are generally small and replicate randomly during the cell cycle (**Fig. 1-2A**). These plasmids are maintained in copies  $>15$  per cell, and thus random assortment and segregation during cytokinesis ensure sufficient distribution of these plasmids into two daughter cells (Birge, 2006; Million-Weaver and Camps, 2014). In contrast, low copy number plasmids are maintained in copies of  $< 15$  per cell and thus cannot solely rely on random distribution but instead ensure their accurate distribution by possessing partitioning loci (**Fig. 1-2B**). Further, this is true for single-copy number plasmids, including bacterial genomes. Therefore, multiple mechanisms have evolved that ensure the faithful maintenance of such single-copy plasmids and prevent their loss from a host bacterial cell. These include-

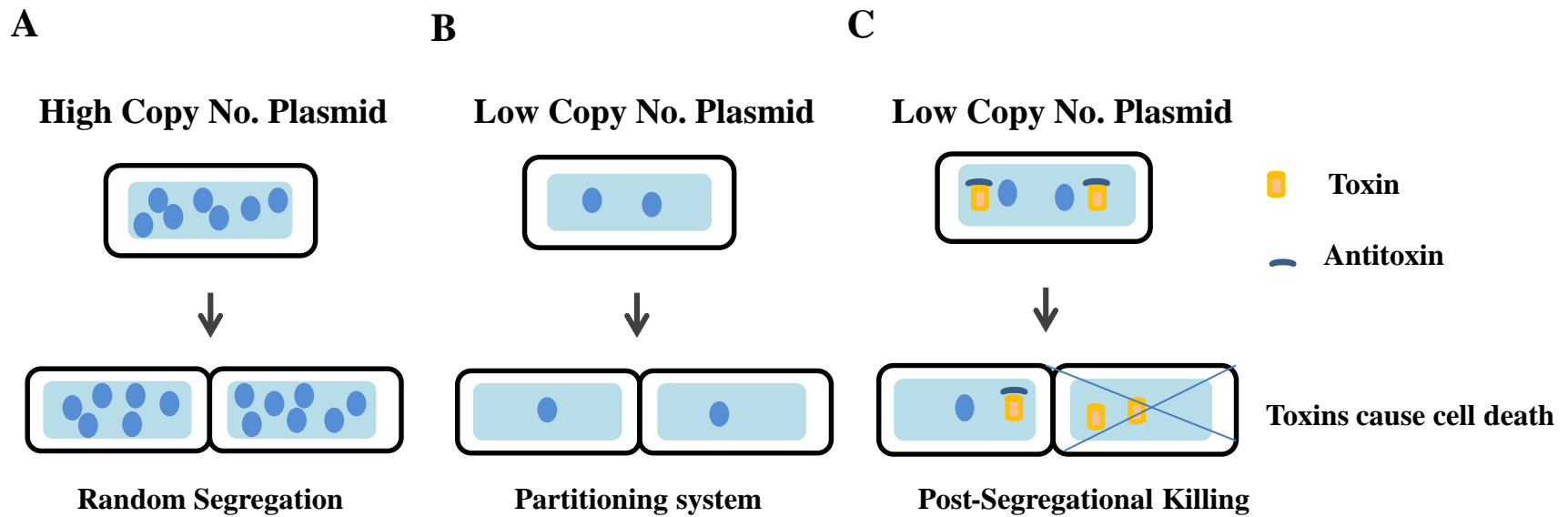


**Figure 1-2. The different types of plasmid maintenance mechanisms**

(A) High copy number plasmids employ random segregation mechanisms. (B) Low copy number plasmids depend upon a stringent segregation mechanism. (C) The detailed mechanism of Post Segregational Killing mediated by toxin and anti-toxins wherein the toxin are stable components, and the presence of anti-toxin negates their lethal effect. In the absence of anti-toxins, the cell dies. The plasmids are represented as blue spheres, toxin as a yellow rectangle, anti-toxin as a blue curve.

**1.2.1 Multimer Resolution Systems** - Due to replication and homologous recombination between sister plasmids, the formation of plasmid dimers and multimers will prevent their accurate segregation onto daughter cells. However, site-specific recombinase cleaves these multimers onto monomers and favour their segregation. This mechanism is found in the case of the P1 plasmid (Austin et al., 1981).

**1.2.2 Post Segregational Killing** – This mechanism works by ensuring that only the population that carries the plasmids survive and propagate (Jaffe et al., 1985). The maintenance of the plasmid is determined by the presence of toxin-antitoxin systems or commonly known as TA systems (Gerdes and Molin., 1986) (**Fig. 1-2C**). The plasmid encodes both these components, and while the toxins of all bacterial TA systems are proteins, the antitoxins are either proteins or small RNAs (Gerdes et al., 1990). Moreover, the toxin is a stable component and thus, once produced, stays in the cell for a longer period. On the contrary, antitoxins are unstable and thus need to be produced continuously to negate the effect of the toxin. In the event of plasmid loss, antitoxins are rapidly lost due to their instability and are no more available to negate the effects of the toxin, which is stable, stays on in the cell, leading to the death of the cell (Yarmolinsky, 1995; Hayes, 2003; Bukowski et al., 2011; Hayes and Van Melderen, 2011). Thus, the survival of the bacterial cell depends upon the continuous production of the antitoxin, which requires the plasmid to be maintained. One such example of a TA system is *hok/sok* present in the R1 plasmid (Gerdes et al., 1990; Thisted and Gerdes, 1992) and the now famous *ccdA/ccdB* (used in Gateway™ cloning) in F plasmid (Hiraga et al., 1986; Bernard et al., 1993).

**1.2.3 Active Partitioning or ‘Mitotic’ Systems** - These systems use force-generating mechanisms to partition DNA and are often found in low copy number plasmids and chromosomes that are segregated equally during each round of cell division (Thomas, 2000). The partitioning systems are primarily tripartite and are constituted by a *cis*-acting centromeric sequence present on the plasmid/ DNA and two *trans*-acting proteins – the force-generating NTPase and an adaptor protein that links the NTPase to the plasmid/ DNA to be partitioned (Ogura and Hiraga, 1983; Dam and Gerdes., 1994; Abeles et al., 1985; Mori et al., 1989; Gerdes and Molin, 1986; Friedman and Austin, 1988). The centromeric sequence is a palindromic tandem-repeat and is bound by the adaptor protein. The NTPase protein provides the force for directional movement of the DNA. Partitioning systems in bacteria have been majorly classified into three classes based on the type of NTPase present (**Fig. 1-3 and Table 1-1**) as enlisted below here :

**a) Type-I / Walker A-type ATPase** - These utilise a Walker A-type ATPase for force generation, and examples include –*parABC* or the *sopABC* system (F plasmid), *parABS* (P1 and pCXC100 plasmids),  $\delta\omega$  (pSM19035 plasmid).

**b) Type-II / Actin-like proteins** - These systems carry an actin homolog that pushes the DNA, and examples include the *parMRC* system in the R1 and pSK41plasmids.

**c) Type-III / Tubulin/ FtsZ/ TubZ Family** - These systems are marked by the presence of a tubulin/ FtsZ/ TubZ family of protein, and examples include the *tubZRC* systems found in pBTaxis and pXO1plasmids.

**d) Type-IV** - These are poorly understood systems, which share no known homologs and examples include the *par* found in pSK1 and R388 plasmid.

While the Type-II family has been extensively studied, the mechanisms by which Type-I partitioning systems function is relatively less well understood. Thus, here are various mechanisms employed by bacterial cells to ensure that the plasmids are maintained and segregated equally into the daughter cells following cell division.

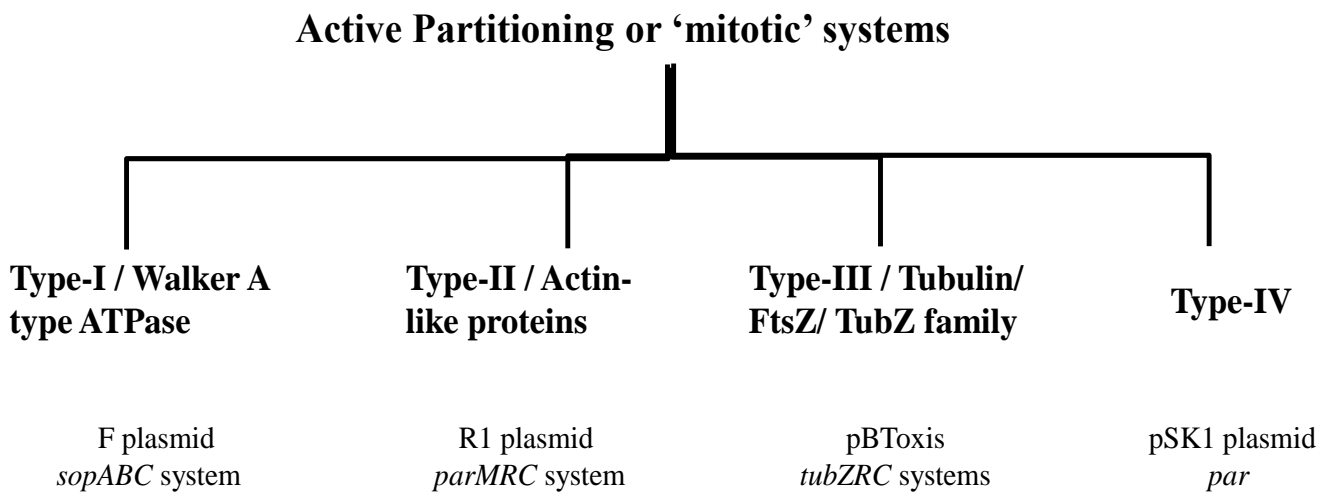


**Figure 1-3. The different types of NTPase based DNA partitioning systems in bacteria.**



**Table 1-1. A few examples of active DNA partitioning systems in bacteria**

PLASMID	ORGANISM	FUNCTION	GENES	SEGREGATION SYSTEM	REFERENCE
<b>F</b>	<i>Escherichia coli</i>	DNA transfer between bacteria by conjugation	<i>ccdA, ccdB, repE, sopA, sopB, sopC, traD, traM</i>	Type-I	Dmowski and Jagura-Burdzy, 2013
<b>TP228</b>	<i>Salmonella newport</i>	Multi drug resistance, resistance to mercuric ions	<i>parF, parG, parH</i>	Type-I	Dmowski and Jagura-Burdzy, 2013
<b>Ti</b>	<i>Agrobacterium tumefaciens</i>	Virulence, opine synthesis	<i>repA, repB, repC</i>	Type-I	Christie, 2004; Gordon and Christie, 2014
<b>R1</b>	<i>Salmonella paratyphi</i>	Multidrug resistance	<i>repA, traN, copA, hok, sok, parM, parR, parC</i>	Type-II	Jensen and Gerdes, 1997
<b>pSK41</b>	<i>Staphylococcus aureus</i>	Multidrug resistance, mobilisation of other co-resident plasmids	<i>aacA-aphD, smr, mupA, ble, aadD</i>	Type-II	Schumacher, 2008
<b>pLS20</b>	<i>Bacillus subtilis subsp. natto</i>	Interspecies plasmid transfer	<i>alp7R, alp7C, alp7A</i>	Type-II	Koehler and Thorne, 1987

<b>pB171</b>	<i>Escherichia coli</i>	Diarrhoea in children	<i>bpfA, bpfT</i>	Type-I and Type-II	Ebersbach and Gerdes, 2001
<b>pBToxis</b>	<i>Bacillus thuringiensis</i>	Virulence, insect toxin	<i>cry4Aa, cry4Ba, cry10Aa, cyt1Aa, cyt2Ba</i>	Type-III	Schumacher, 2008
<b>pXO1</b>	<i>Bacillus anthracis</i>	Anthrax toxin, edema factor, lethal factor	<i>cya, lef, pagA, atxA, pagR</i>	Type-III	Dmowski and Jagura-Burdzy, 2013
<b>pSK1</b>	<i>Staphylococcus aureus</i>	Resistance to antiseptics and disinfectants	<i>rep, orf245</i>	Type-IV	Schumacher, 2008

### 1.3 Events Prior to Partitioning

Complete DNA replication and resolution must precede the segregation process. Site-specific DNA recombinases act to resolve plasmid multimers or the linked sister chromosomes. This mechanism is taken care of by XerCD or *dif*. In the absence of *dif* or other recombination factors, around 10 % of the cells have a defect in chromosome segregation. The absence of any of these factors causes chromosome segregation defects by disentanglement of sister chromosomes, and thus, these are critical for segregation. Key players in the process include-

#### *a) dif, XerC and XerD*

Daughter chromosomes produce a circular dimer upon recombination. For segregation to proceed, these dimers must be resolved to monomers. In *Escherichia coli*, these dimers are resolved by a *dif* (deletion induced filamentation) locus, a 28 bp sequence located at the centre of the replication terminus (Blakely et al., 1991, Blakely et al., 1993; Colloms et al., 1990; Kuempel et al., 1996). FtsK positions *dif* close to the division septum (Capiaux et al., 2002). Strains with a deleted *dif* locus mainly produce a Dif phenotype that involves induction of SOS response, aberrant nucleoid morphology, filamentous cells, and reduced viability (Kuempel et al., 1996). Recombination at *dif* requires XerC and XerD resolvases that bind to 11 bp within the *dif* region. Mutation in either one of the *xer* genes leads to Dif phenotype. Thus, Xer proteins act as Type-I topoisomerases that help to relax supercoils by nicking one strand of the *dif* locus (Cornet et al., 1996).

### ***b) Topoisomerase IV***

Soon after the replication of chromosomes, intertwined structures of sister chromosomes are produced. The resolution of these structures is mediated by DNA gyrase (Reece and Maxwell, 1991). DNA gyrase also serves the function of relieving the torsional stress generated because of replication. In *Bacillus subtilis* cells, DNA gyrase has been shown to accumulate at the replication fork (Tadesse and Graumann, 2006), which might aid in resolving the linked sister chromatids soon after replication to enable proper segregation. This, in *E. coli*, is performed by Topoisomerase IV.

### **1.4 Basic Architecture of the Bacterial Mitotic Segregation Machinery**

Although the active partitioning systems have been classified based on the different types of NTPases associated with the segrosome, the basic architecture of the segregation machinery itself is somewhat similar in all the cases. The segregation machinery of bacterial chromosomes, as well as plasmids, involves a tripartite complex of a centromeric sequence, an adaptor protein, and a motor protein, that can either be an ATPase or a GTPase (Ogura and Hiraga, 1983; Mori et al., 1986; Abeles et al., 1985; Gerdes and Molin, 1986; Friedman and Austin, 1988; Dam and Gerdes, 1994; Schumacher, 2008; Lutkenhaus, 2012) (**Fig. 1-4**). The plasmids are tethered to the adaptor protein by the centromeric sequence, which is then recruited to the motor protein. The motor protein provides the energy driven by ATP/GTP hydrolysis that in turn helps in the movement of the plasmids to the two opposite ends of the cell.

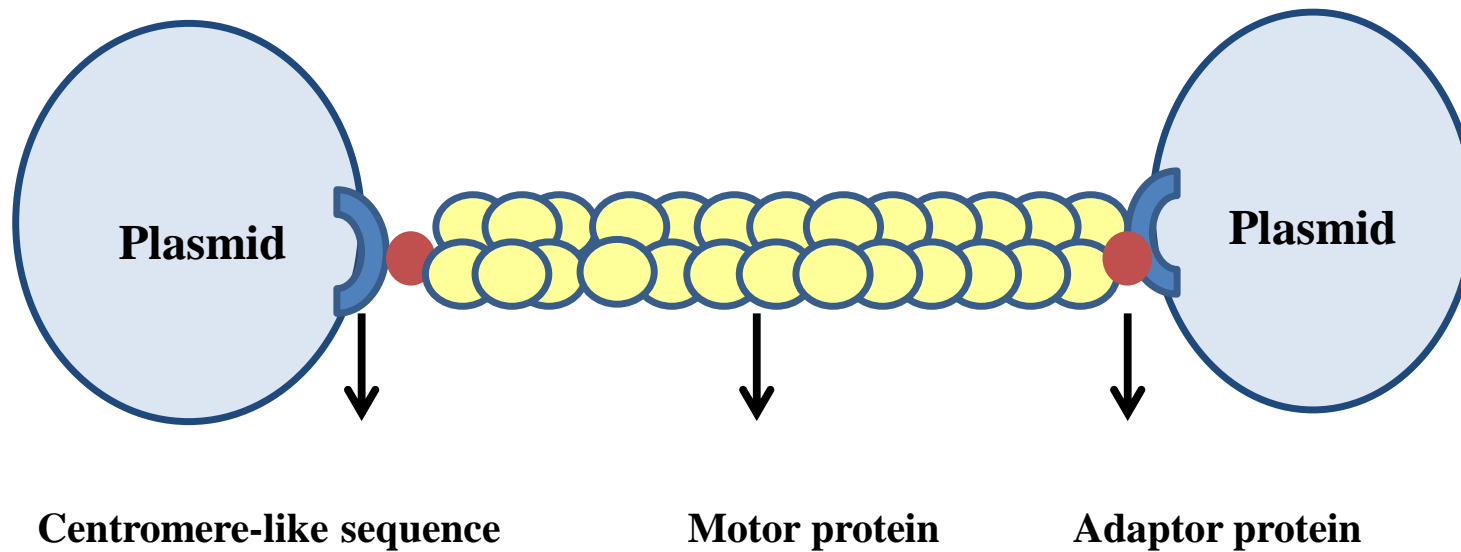


**Figure 1-4. Schematic representation of the basic components of the bacterial segregation machinery.**

The machinery involves an adaptor protein, a motor protein and a repetitive DNA sequence or centromere. The plasmids have been represented as spheres (blue), and the motor protein is represented in yellow colour.

## 1.5 The Types of Plasmid Segregation Machinery

As described briefly above, based on the genetic organisation of the modules and the evolutionary relationship with other proteins, active plasmid partitioning systems are broadly classified into the following types:

### 1.5.1 *Type-I / Walker A-type ATPases*

Most bacterial chromosomes and low copy number plasmids use the Type-I mechanism of plasmid segregation. The NTPase or the motor protein in the Type-I systems belongs to a superfamily of P loop ATPases, known as the ParA/MinD family of ATPases, that have a deviant Walker A box motif  $\text{G}\underline{\text{K}}\text{GGHGK}(\text{S/T})$  or P loop (Koonin, 1983). The Walker A motif is located at the N-terminus of an  $\alpha$ -helix in ParA proteins and is directly involved in interactions with the bound ATP molecule. This motif also has a second lysine residue near the N-terminal end (Hayes, 2000; Lutkenhaus and Sundaramoorthy, 2003; Motallebi-Veshareh et al., 1990; Wendler et al., 2012). Walker A motifs in Type-I ParA family differ from Classical Walker A motifs in having the additional signature lysine residue, and thus the term deviant Walker A motif follows. Moreover, this family of ATPases also contain a second motif, the B box, characterised by negatively charged residues (D/E) that play an important role in magnesium ion-coordination and ATP hydrolysis (Schumacher et al., 2012). The other important players in the process are the centromeric repeat sequence *parC* and a centromere binding protein (CBP) or adaptor protein ParB. Mutations in the conserved Walker A box lead to a significant loss in plasmid stability and point to a key role for ATP hydrolysis in mediating segregation (Barillà et al., 2005; Ebersbach and Gerdes,

2001; Fung et al., 2001; Pratto et al., 2008). The plasmid, via *parC* and the bound adaptor protein, interacts with the motor protein ParA, which is the ATPase that generates the required forces to move the plasmids to the opposite ends of the cell.

The type-I mechanism is further sub-divided into Type-Ia and Type-Ib based on the structure of ParA (Hayes 2000; Schumacher, 2008). Type-Ia / large ParA includes *parABS* from P1 plasmid and *sopABC* from F plasmid that have an extended N-terminal helix-turn-helix (HTH) motif (**Fig. 1-5A**). These large ParA proteins (~ 300-450 amino acids) also act as repressors of their own gene expression (Abeles et al., 1985). The HTH domains help in this sequence-specific DNA binding to operator regions near their promoters (Mori et al., 1989; Davis et al., 1992; Hayes et al., 1994; Ravin et al., 2003). The ParA proteins also bind DNA in a sequence non-specific manner and are thus localised on the bacterial nucleoid (Leonard et al., 2005; Hester and Lutkenhaus, 2007; Castaing et al., 2008; Vecchiarelli et al., 2010; Roberts et al., 2012; Le Gall et al., 2016). The larger ParAs are mainly found in the case of plasmids. However, members of the Type-Ib subfamily, like *Salmonella newport* TP228 ParA and *Helicobacter pylori* Soj (*HpSoj*), are smaller (~ 200-250 amino acids) and lack the N-terminal HTH domain and are thus also referred to as smaller ParAs (**Fig. 1-5B**). The smaller ParAs, however, have a non-specific DNA binding activity and are found in most chromosomes and a few plasmids. Specific examples of Type-Ia includes the P1 bacteriophage *parABC* system and the *sopABC* system of F plasmid.

Overall, the Type-Ia is one of the first identified plasmid maintenance systems (Ogura and Hiraga, 1983). In the case of F plasmid (the one encoding for Fertility factor), *sopABC* serves as the partitioning system wherein *sopC* serves as the centromeric sequence, SopB acts as the adaptor protein or the centromeric binding

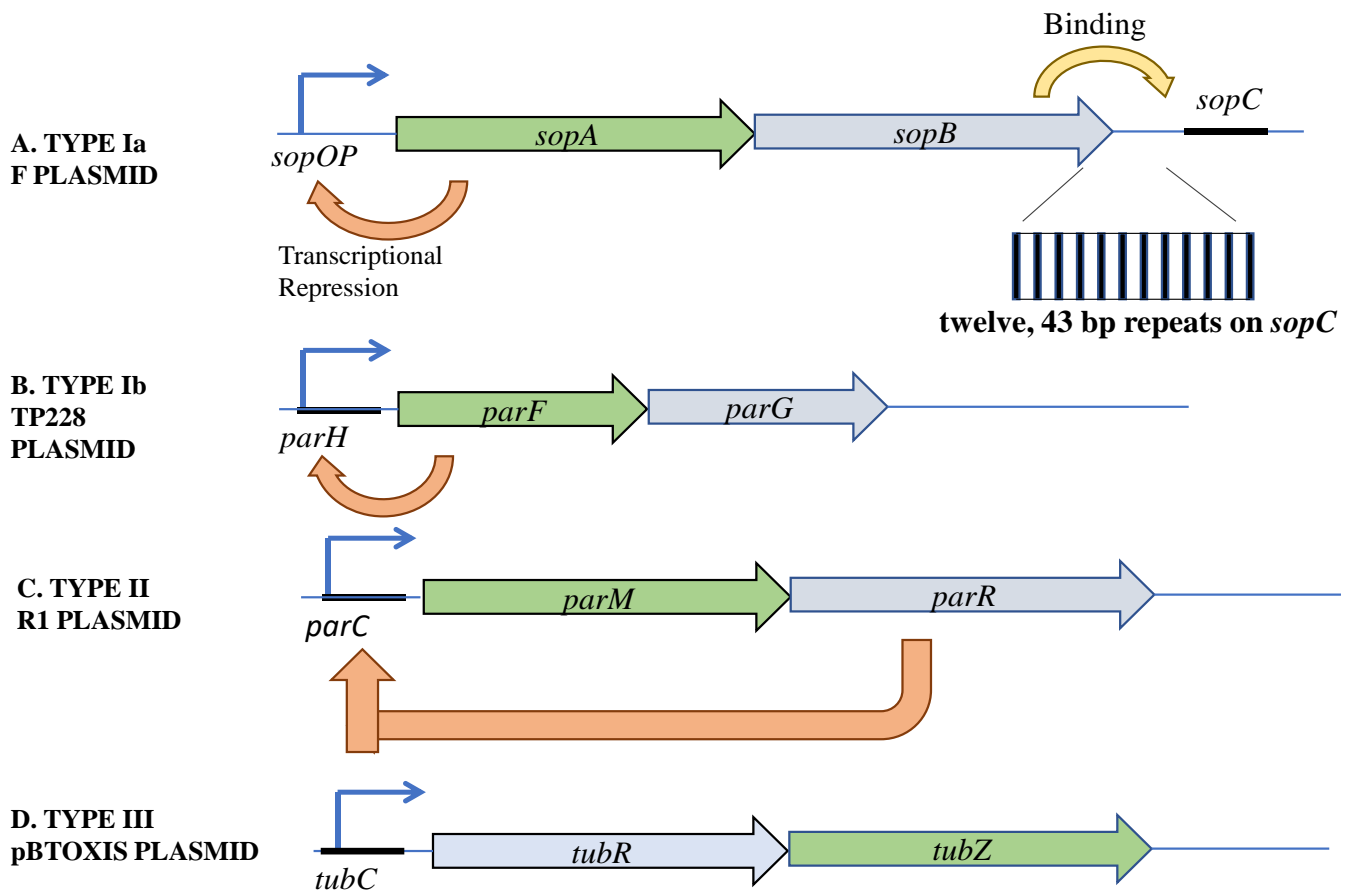


**Figure 1-5. Genetic organisation of Type-Ia, Type-Ib, Type-II and Type- III partition loci.**

Genes encoding the ATPase (green) and adaptor protein (blue) are indicated. The auto-repression activity is represented by an orange arrow. F plasmid, TP228 plasmid, R plasmid and pBToxis plasmid are used as representatives of (A) Type-Ia, (B) Type-Ib, (C) Type-II and (D) Type-III segregation mechanisms, respectively. The *sopA* (green box) and *sopB* (blue box) are expressed from the *Psop* promoter. The partition site *sopC* is located downstream of the *sopAB* genes. The *sopC* gene sequence is represented by a black line. The inset shows the repetitive stretch of twelve 43 bp repeats. The orange arrows represent transcriptional repression, whereas the yellow arrow points at *sopC* binding.



protein (CBP), which binds to *sopC* sequence and SopA functions are the motor protein, which is the NTPase (Ogura and Hiraga, 1983). At the genetic loci, the genes appear in the order of *sopA*, *sopB* and *sopC*, wherein SopA and SopB are driven by a single promoter located upstream of *sopA* (Mori et al., 1986; Hirano et al., 1998; Mori et al., 1989). The centromeric sequence *sopC* is composed of twelve forty-three base pair repeats (Hayakawa et al., 1985; Lane et al., 1987; Mori et al., 1989) (**Fig. 1-5A**). Each 43-bp sequence contains a short 16-bp inverted repeat to which SopB binds as a dimer (Hanai et al., 1986; Lane et al., 1987; Mori et al., 1989), and this complex is then recruited towards SopA. Examples of the Type-Ib system includes the *S. newport* TP228 plasmid containing the *parFGH* loci (Fothergill et al., 2005), *Streptococcus pyogenes* pSM19035 plasmid containing the *parABS* ( $\delta$ /*parA*,  $\omega$ /*parB* and *parS*) (de la Hoz et al., 2004; Pratto et al., 2008) and *H. pylori* *Soj* (*HpSoj*) (Chu et al., 2019). The ParA ATPases in the Type-Ib systems lack the N-terminal HTH domain required for site-specific DNA binding at their promoter regions and are approximately 190-310 amino acids (**Fig. 1.5B**). Moreover, since the N-terminal domain is also responsible for auto-repressor function, these small ParA ATPases do not have any repressor functions (Ebersbach et al., 2005). ParB members of the Type-Ib family are also small, i.e., ~ 45-130 residues with an N-terminal protein-protein interaction domain, central HTH domain and a self-dimerisation domain at the C-terminus. Further, residues near the N-terminus of ParB specify their interactions with the cognate ParA.

### **1.5.2 Type-II/ Actin-like Proteins in Segregation**

Type-II partitioning system was first discovered *E. coli* resistance plasmid R1 (Jenson and Gerdes, 1997). The partitioning system in this group contains an actin-like ATPase called ParM, an adaptor protein ParR and centromere site *parC* (**Fig. 1-5C**).

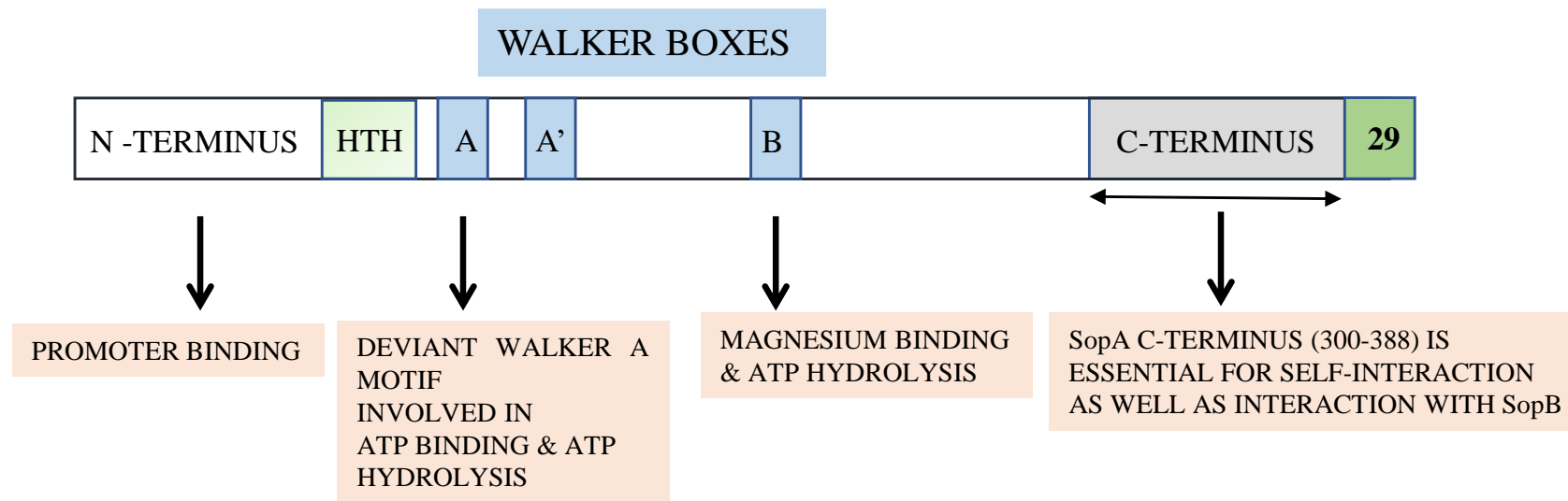
ParM monomers have an actin-like fold, and its crystal structure also bears a close resemblance to actin (van den Ent et al., 2002). Just like actin, ParM also assembles into a two-stranded helix. Despite all these similarities, there are also differences between actin and ParM, mainly with respect to the orientation of the filament, i.e., actin forms a right-handed filament, but ParM helices are mainly left-handed (Orlova et al., 2007; Popp et al., 2008). ParM grows bidirectionally with similar rates of monomer addition at both ends and exhibits dynamic instability, a feature of microtubules (Moller-Jensen et al., 2002; Garner et al., 2004). Although ParM can bind both ATP as well as GTP, the most preferred substrate is ATP, for which ParM has a 10-fold higher affinity than GTP (Galkin et al., 2009). Cryoelectron microscopy of cells overexpressing ParM showed that the protein assembles into closely packed filament bundles with an average number of 3-5 ParM filament per bundle (Salje et al., 2009). Also, ParM filaments exhibit bidirectional growth and *in vivo* data also hints at the dynamic instability of the ParM filaments (Moller-Jensen et al., 2002; Garner et al., 2004; Galkin et al., 2009; Gayathri et al., 2012; Gayathri et al., 2013). More recent studies suggest that the filaments grow by insertional polymerisation wherein new ParM subunits are inserted at the filaments ParR-*parC* interface (Moller-Jensen et al., 2003; Garner et al., 2004; Garner et al., 2007).

Reconstitution of the components of the ParMRC segregation machinery *in vitro* using polystyrene beads for immobilising *parC* and addition of ParR, ParM, and ATP resulted in the assembly of dynamic filaments of ParM (Garner et al., 2007). The addition of ATP caused the formation of short filaments that exhibited growth and then shrinkage. However, in the presence of another bead in proximity, the filaments appeared to bundle and push the beads away further. This *in vitro* reconstitution

experiment made it clear that ParMRC is an autonomous system and does not rely on other host-mediated factors for segregation. Moreover, in the presence of a non-hydrolysable analogue of ATP, these *in vitro* filaments were longer, suggesting that the growth and retraction of filaments in the presence of ATP were driven by hydrolysis (Garner et al., 2007). Based on cryoelectron microscopy, *in vitro* reconstitution experiments, and sophisticated imaging, a “search, capture and push” model for plasmid segregation by ParM and other actin-like proteins has been proposed (Garner et al., 2007; Campbell et al., 2007; Salje et al., 2009).

### **1.5.3 Type-III/ Tubulin/ FtsZ-like GTPase Family of Partitioning Proteins**

This type of partitioning machinery has been described in pBTaxis plasmid (Larsen et al., 2007) of *B. thuringiensis*, pXO1 plasmid of *B. anthracis* (Tinsley and Khan, 2006) and more recently in the form of PhuZ (Phage Tubulin/ FtsZ) in *Pseudomonas chlororaphis* phage 201 $\phi$ 2-1 (Kraemer et al., 2012; Erb et al., 2014). The segregation machinery contains the same three components (*tubZRC*) as are found in Type-I and Type-II systems, except that motor NTPase (TubZ) belongs to the tubulin/FtsZ superfamily of cytoskeletal proteins (Larsen et al., 2007) (**Fig. 1-5D**). The tubulin-fold of TubZ exhibits striking similarity with bacterial cell division protein FtsZ, although the sequence similarity of TubZ or bacterial FtsZs with eukaryotic tubulin amounts to even less than 14 % (Nogales et al., 1998; Lowe and Amos, 1998; Larsen et al., 2007; Ni et al., 2010; Aylett et al., 2010 ). This is thus an example of the involvement of tubulin-like proteins in the DNA segregation in bacteria. The CBP in this family is the TubR that binds to the *tubC* centromeric sequence. TubZ contains a tubulin-like fold and a flexible C-terminal domain.



115 - (KGGHGK(S/T)) - 121

**Figure 1-6. The conserved domains of F plasmid partitioning protein SopA.**

The N-terminal, C-terminal and the Walker A motifs have been represented. The Walker motifs in SopA have been highlighted in blue, and the function of each domain has been represented in orange boxes below. The C-terminal 29 amino acid residues, which have been studied in this thesis, has been highlighted in green colour.

TubZ polymerises to form two or four-stranded filaments upon binding to GTP (Montabana and Agard, 2014). The filaments undergo treadmilling, which assists in DNA partitioning (Larsen et al., 2007; Tang et al., 2007). The bacteriophage tubulin protein PhuZ, on the other hand, resembles the eukaryotic microtubule in some aspects. It was the first prokaryotic tubulin to be discovered that exhibited dynamic instability (Erb et al., 2014). It polymerises into a triple-stranded filament that is anchored at one end to the cell poles (Zehr et al., 2014). Also, like eukaryotic microtubules, the PhuZ filaments assemble into a bipolar spindle that helps to regulate viral reproduction by placing the viral nuclei at mid-cell (Kraemer et al., 2012; Erb et al., 2014).

### **1.6 ParA/ SopA – A Walker A type Cytoskeletal ATPase**

ParA is a protein that functions in DNA segregation of both the plasmids as well as the bacterial chromosome and constitutes the motor protein in Type-I partitioning systems. ParA belongs to the Walker A type Cytoskeletal ATPases (WACA) family of proteins. They contain a Walker A motif, a Walker A' motif, Walker B motif and a ParA specific sequence (Motallebi-Veshareh et al., 1990; Koonin, 1993) (**Fig. 1-6**). Structural analysis of ParA reveals the presence of an N-terminal  $\alpha$ -helix (H1) for dimerisation, a winged-helix turn helix motif (comprising  $\alpha 2$  and  $\alpha 3$ ) for binding specific DNA and the conserved Walker motifs for binding to nucleotides followed by ParA specific C-terminal sequence. The Walker A motif and  $\alpha 15B$  helix bind to ADP, and the  $\alpha 15B$  helix,  $\alpha 16$  helix, and the loop near these C-terminal helices make contact with non-specific DNA (Dunham et al., 2009) (**Fig. 1-7**). Moreover, in similar lines to other members of the WACA superfamily, ParA

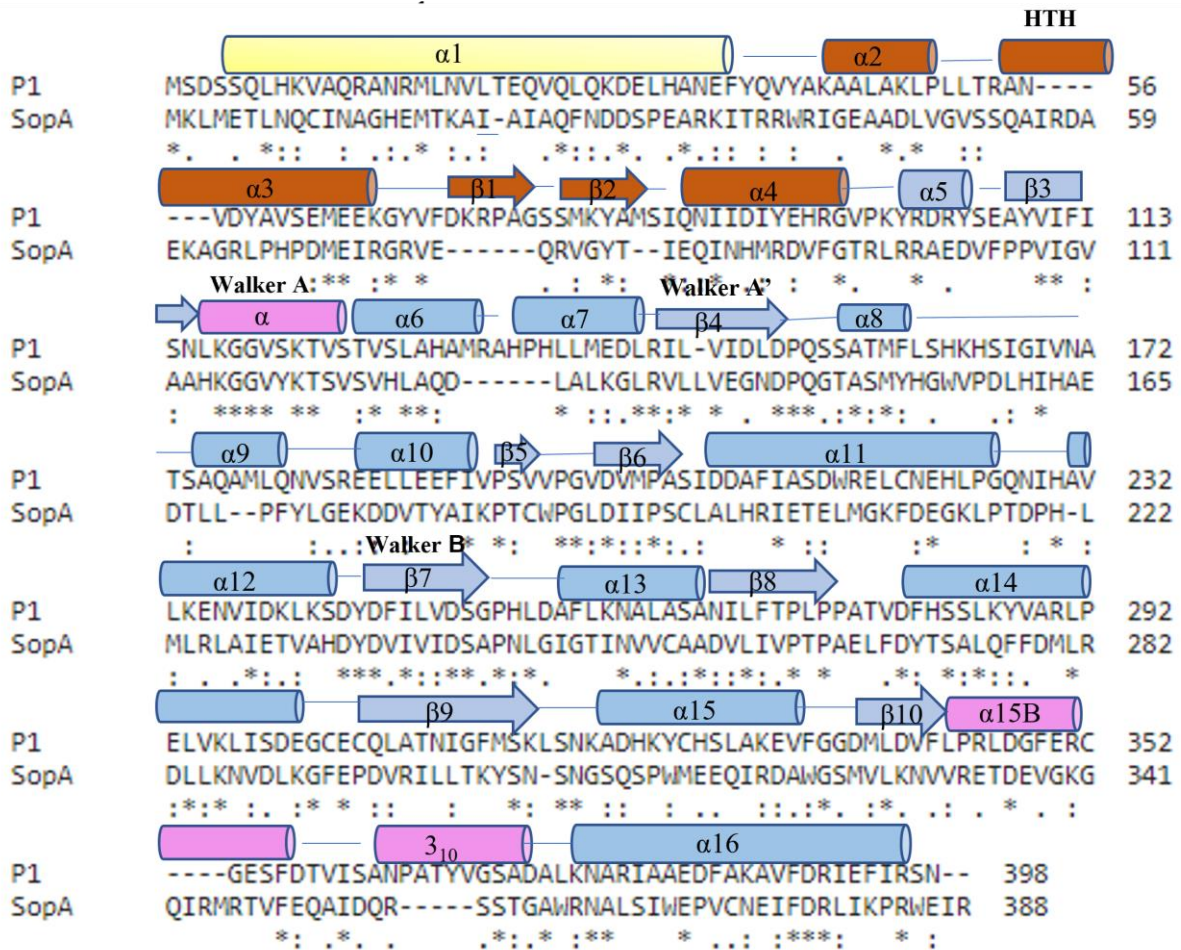


**Figure 1-7. Sequence alignment of P1 ParA and SopA proteins and their secondary structure.**

Sequence alignment of the P1 and SopA proteins. Secondary structural elements are drawn over the sequences, and the three structural regions are coloured. The HTH, Walker A, Walker A', Walker B and SopA-specific regions are labelled. (Adapted from Dunham et al., 2009)

exhibits weak ATPase activity (Watanabe et al., 1992; Davis et al., 1992; Leonard et al., 2005; Barillà et al., 2007; Havey et al., 2012), wherein the ATP hydrolysis activity is stimulated 3-fold by ParB alone and 1.5 fold by DNA. However, the presence of both ParB and DNA stimulates the ATPase activity by 10-15 fold (Davis et al., 1992; Watanabe et al., 1992; Libante et al., 2001; Bouet et al., 2007; Ah-Seng et al., 2009). Also, the larger ParA found in the Type-Ia system has an auto-regulatory function. They bind their promoter sites (**Fig. 1-5A**) and thus directly regulate the expression levels of both ParA and ParB proteins (Mori et al., 1989; Davis et al., 1992; Davey and Funnell, 1997; Hirano et al., 1998; Komai et al., 2011).

ParA exists in a monomer-dimer equilibrium in the cell wherein the monomer form is free and the dimeric form associates with the nucleoid (Vecchiarelli et al., 2010). Further, ParA exists in at least two ATP-bound states, an active state that binds to the nucleoid and an inactive conformation that is not capable of binding non-specific DNA. While both active and inactive states are an ATP dependent dimer, the active state is represented as ParA-ATP\* or, more specifically as (ParA-ATP\*)<sub>2</sub> (Vecchiarelli et al., 2010). The change involves a conformational change and a slow transition of the ATP bound inactive dimeric form into an active ATP bound dimer (ParA-ATP\*)<sub>2</sub>. Circular Dichroism experiments indicated that the ParA undergoes structural changes and exhibits greater helicity upon binding to ATP (Davey and Funnell, 1997). In the case of P1, the (ParA-ATP\*)<sub>2</sub> conformation was detected by a decrease in tryptophan fluorescence, observed in the presence of Mg<sup>+2</sup> and ATP, and confirmed to be the nsDNA binding active state of ParA (Vecchiarelli et al., 2010). In addition, results from SEC/MALS also revealed that (ParA-ATP\*)<sub>2</sub> bound form exists as a dimer (Vecchiarelli et al., 2010). The (ParA-ATP\*)<sub>2</sub> bound dimeric conformation associates with the

bacterial nucleoid. However, soon after ATP hydrolysis, ParA-ADP form is produced that can no longer associate with the bacterial nucleoid and acts as a transcriptional repressor of the ParA promoter (Bouet and Funnell, 1999; Libante et al., 2001; Hao et al., 2002; Baxter et al., 2020). ParA, bound to ATP, undergoes a slow conformational change to  $(\text{ParA-ATP}^*)_2$ , which is competent to bind to nsDNA. The ParB-parC complex interacts with the nucleoid bound  $(\text{ParA-ATP}^*)_2$ , stimulates the ATP hydrolysis and converts  $(\text{ParA-ATP}^*)_2$  to ParA-ADP form, which is then released from the nucleoid. The ADP is then exchanged with ATP, resulting in the formation of the ParA-ATP sandwich dimer, which then undergoes the conformational change to  $(\text{ParA-ATP}^*)_2$ , and the cycle follows (Vecchiarelli et al., 2010).

The ATP bound dimeric conformation  $(\text{ParA-ATP}^*)_2$  enables the binding of ParA molecules to the nucleoid (Vecchiarelli et al., 2010). In this conformation, ParA has an affinity for any DNA in a sequence non-specific manner. Majorly, the bacterial cell has much nsDNA in the form of the nucleoid, and thus ParA molecules are found localised to the nucleoid and facilitate the process of plasmid segregation (Castaing et al., 2008; Vecchiarelli et al., 2010; Roberts et al., 2012; Le Gall et al., 2016). This has been visualised *in vivo* by using sophisticated fluorescence microscopy techniques as well as in several *in vitro* studies. Further, SopA K340A, a nsDNA binding mutant, has been reported to have segregation defects suggestive of the critical role of ns-DNA binding in the process of plasmid maintenance (Castaing et al., 2008). In addition, fluorescence microscopy images of SopA had shown that the protein assembled into helical polymeric structures. Further, the polymers were shown to undergo oscillatory movements on the nucleoid, leading to suggestions that the polymerisation dynamics of ParA drive plasmid segregation (Lim et al., 2005; Hatano et al., 2007; Bouet et al.,



2007). Further, initial biochemical studies also suggested SopA to be localised to the bacterial membranes (Lin and Mallavia, 1998). However, work from several laboratories around the world on several ParA family proteins has currently led to a consensus view that ParA is predominantly nucleoid localised, and its nucleoid binding function is essential for plasmid maintenance (Leonard et al., 2005; Hester and Lutkenhaus, 2007; Castaing et al., 2008; Vecchiarelli et al., 2010; Roberts et al., 2012; Vecchiarelli et al., 2013; Volante et al., 2015; Le Gall et al., 2016).

ParA also has a weak auto-repression activity, and its full repressor function depends on the co-repressor ParB. Together with ParB, it strongly represses transcription of its promoter  $P_{par}$  (Friedman and Austin, 1988; Hayes et al., 1994; Libante et al., 2001). The ParB-parC complex further enhances the auto-regulatory function. It was initially thought that only ParA-ATP and ParA-ADP, but not ParA-ATP\* states, were competent in binding to the  $P_{par}$  site. However, recent studies on the non-specific DNA binding mutant ParA R351A suggests ParA-ATP\* to be as proficient in binding to  $P_{par}$ . The abrogated ns-DNA binding results in a free pool of excess ParA-ATP\*, resulting in the repression of transcription from *parOP* (Baxter et al., 2020). This auto-repression activity of ParA thus can solely be attributed to its specific DNA binding activity mediated by the HTH domain of the protein (Baxter et al., 2020).

### **1.7 Centromere Binding Protein (CBP) or the Adaptor Protein – ParB**

ParB is a DNA binding protein and an active component of the bacterial segregation machinery. The crystal structures of ParB proteins provide details about their domain organisation (Schumacher et al., 2007; Soh et al., 2019; Osorio-Valeriano et al., 2019; Jalal et al., 2020). ParB contains three different domains: an N-terminal

domain, a central DNA binding HTH motif and a C-terminal domain, all connected by flexible linkers (Funnell, 1991; Schumacher and Funnell, 2005; Funnell, 2016; Soh et al., 2019). The N-terminal stretch is necessary for protein oligomerisation and interaction with ParA and is defined by a conserved stretch of arginine residues, also referred to as the arginine patch (Yamaichi and Niki, 2000; Chen et al., 2015). This patch is essential for spreading of ParB, foci formation, and partitioning (Rodionov et al., 1999; Autret et al., 2001; Breier and Grossman, 2007; Kusiak et al., 2011; Graham et al., 2014; Funnell, 2016). The C-terminal domain plays a pivotal role in homodimerisation of ParB (Leonard et al., 2004; Khare et al., 2004). The DNA binding domain or HTH motif plays an essential role in specific DNA interaction as well as spreading. Spreading is an important feature of ParB, and it involves the formation of higher-ordered complexes. ParB is known to initiate binding to DNA at *parC* sites and spread over *parC* flanking regions, often covering a large span of the nsDNA. Recent studies on ParB have revealed that ParB is a CTPase (Soh et al., 2019; Osorio-Valeriano et al., 2019; Jalal et al., 2020) and has opened up new avenues of research and questions on the role of CTP in regulating the process of ParB spreading and DNA partitioning (Jalal et al., 2020).

### **1.8 Bacterial Nucleoid as a Host Factor**

Unlike the eukaryotic genetic material, the prokaryotic DNA is not encased within a nuclear membrane. Instead, it spreads over the entire cytosol of bacteria and is referred to as nucleoid. The term 'nucleoid' was first coined by Piekarski (Piekarski, 1937). With the progression of the cell cycle, the nucleoid changes its shape to a bilobed one and soon segregates into two daughter cells (Zimmerman, 2003; Yamaichi and Niki

2004). The genetic material contained in the eukaryotes is held together by histone and (Nasmyth and Haering, 2005; Zimmerman, 2006) cohesion proteins (Losado and Hirano, 2005; Nasmyth and Haering, 2005). However, in the case of prokaryotes, the chromosomes are held together by DNA binding proteins called Nucleoid Associated Proteins (NAP) (Kar et al., 2005) that help in chromosomal compaction and organisation of domains known as the high-density regions (HDRs). These NAPs include HU, HNF and IHF (Ali Azam et al., 1999; Johnson et al., 2004; Wang et al., 2011). The nucleoid occupies a major proportion of the bacterial cytosol and plays an integral and decisive role in positioning the cytokinetic Z-ring (Yu and Margolin, 1999; Harry et al., 1999; Sun and Margolin, 2001; Harry, 2001) as well as plasmid partitioning (Castaing et al., 2008; Le Gall et al., 2016). The bacterial nucleoid plays a central role in driving F plasmid segregation. The ParA ATPase positions itself within the HDR regions of the nucleoid to which the ParB-*parC* (or ParB-*parS*) complex binds. The binding of the ParBC/ParBS complex stimulates the ATPase activity of ParA to convert the nucleoid bound (ParA-ATP\*)<sub>2</sub> into ParA-ADP, resulting in the release of ParA from the nucleoid (Vecchiarelli et al., 2010; Havey et al., 2012; Vecchiarelli et al., 2013; Hu et al., 2015; Le Gall et al., 2016). The bacterial nucleoid thus forms a key substrate for the ParA in its function as a motor protein in plasmid partitioning. The diffusion ratchet and DNA relay mechanisms (described below) proposed for ParA further emphasise the importance of bacterial nucleoids in the process of plasmid and chromosome segregation.

### **1.9 ParA Homologs Involved in Partitioning Bacterial Genomes**

Several bacterial genomes utilise ParA homologs for partitioning their genetic material during cell division cycles. These organisms include the most well-studied model organisms such as *B. subtilis* (Leonard et al., 2005; Lee and Grossman, 2006; Hester and Lutkenhaus, 2007; Scholefield et al., 2010) and *Caulobacter crescentus*. Interestingly, in *C. crescentus*, two WACA family members, ParA and MipZ, coordinate with each other to promote segregation (Mohl et al., 1997; Lin et al., 1998; Thanbichler and Shapiro, 2006; Toro et al., 2008; Broedersz et al., 2014; Kiekebusch et al., 2012; Corralles-Guerrero et al., 2020). ParA homologs have also been implicated in genome segregation in many pathogenic species such as *Vibrio cholerae* (Heidelberg et al., 2000; Fogel and Waldor, 2005; Fogel and Waldor, 2006; Yamaichi et al., 2006; Parker et al., 2021), *H. pylori* (Lee et al., 2006; Chu et al., 2019), *Pseudomonas aeruginosa* (Bartosik et al., 2004; Lasocki et al., 2007; Jecz et al., 2015; Lagage et al., 2016), *Mycobacterium tuberculosis* (Sasseti et al., 2003; Maloney et al., 2011; Baronian et al., 2015) and others, highlighting the significance of studying ParA mediated DNA partitioning.

### **1.10 WACA Proteins in Archaeal DNA Partitioning**

Archaea, the third branch of life, have recently been amenable to genetic and cell biological studies. This group is an ancestral form of life and has been an attractive model for researchers to probe intracellular dynamics. In the thermophilic crenarchaeon *Sulfolobus solfataricus*, the SegAB complex is involved in chromosome segregation. SegA encodes a deviant Walker A motif with a weak ATPase activity (like ParA) and has the property to polymerise *in vitro* (Kalliomaa-Sanford et al., 2012; Barillà, 2016).

SegB, on the other hand, is an archaeon specific DNA binding protein that interacts with SegA in the presence of nucleotides and, in turn drives genome segregation by affecting SegA polymerisation (Kalliomaa-Sanford et al., 2012). Moreover, overexpression of *segAB* resulted in severe genome segregation defects similar to those observed with ParA proteins. pNOB8, an archaeal plasmid from *Sulfolobus* contains a unique partitioning system comprised of three proteins and a centromeric site (Schumacher et al., 2015). This system involves 3 proteins – AspA, ParA and ParB, with ParA forming the NTPase that carries the Walker A motif, AspA being the centromere binding protein, and an atypical ParB that bears structural similarity to the eukaryotic CenPA. AspA binds to the centromere sequence and creates a superhelix for ParB binding. To this ParB-AspA-centromeric complex, ParA binds and facilitates segregation of the genome. Moreover, the structure of pNOB8 ParA-AMPPNP-DNA complex has revealed the presence of a multifaceted nsDNA binding site (Zhang et al., 2017). The presence of Walker A motif in ParA and the structural resemblance of ParB to CenPA reveal a unifying theme that underlies the DNA segregation process in the three domains of life.

### **1.11 The Mechanism and Models of DNA Partitioning by ParA**

François Jacob put forth the very first model of DNA segregation and separation in bacteria, wherein the bacterial inner membrane and cell growth played a central role in pulling the chromosome apart during cell division. A brief timeline of the major milestones in our current understanding of bacterial DNA segregation is depicted in **Figure 1-8**. This ‘Jacob’ model was primarily derived from electron microscopy of

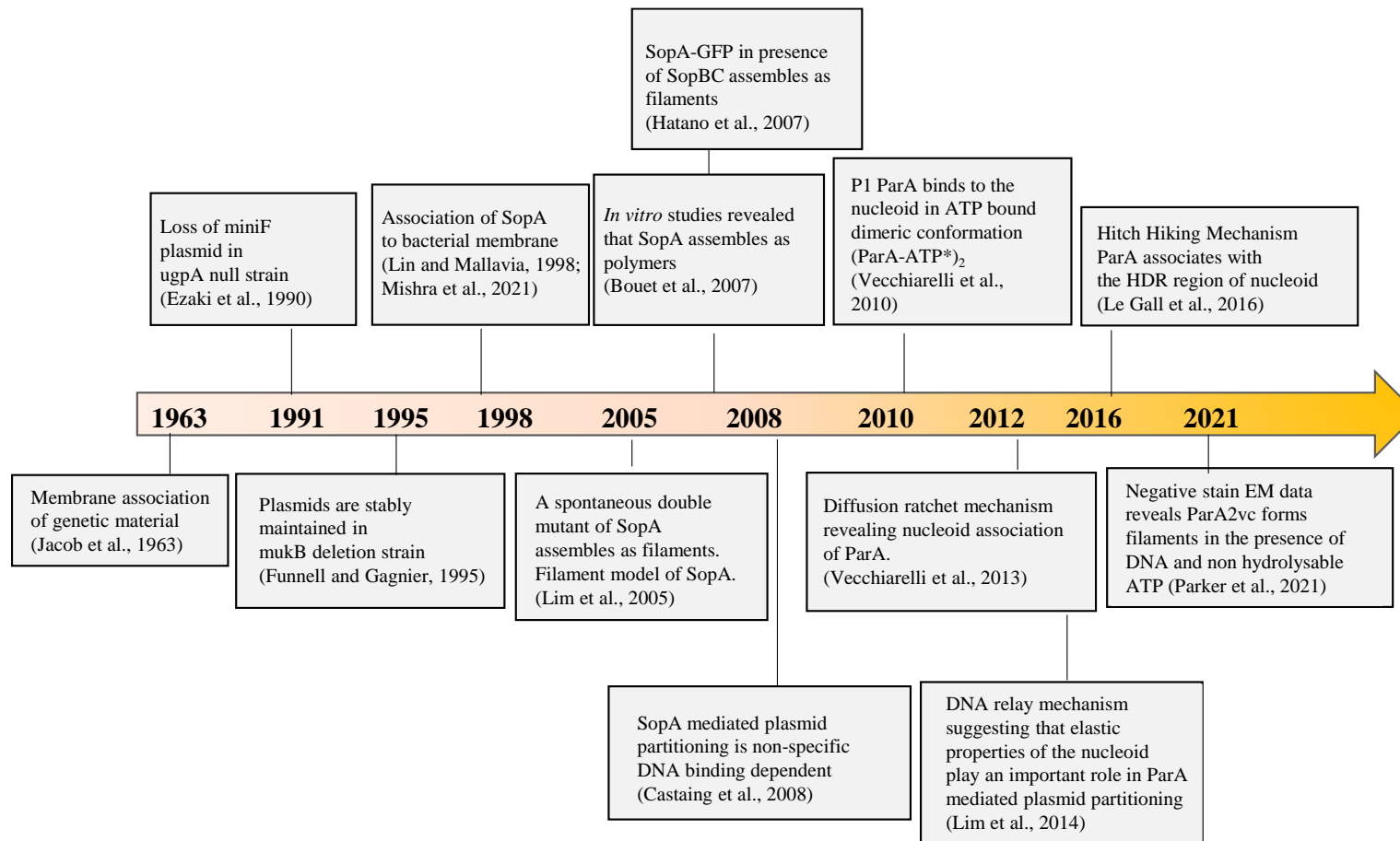


**Figure 1-8. Timeline: Important milestones in our understanding of the models proposed for the mechanism of DNA segregation.** They begin with the 1963 Jacob's membrane tethering model and goes all the way to the recently proposed DNA hitch-hiking model.

bacterial cells showing tethering of the genetic material to the bacterial inner membrane. As per this model, replicated DNA becomes tethered to the cytoplasmic membrane, and as the cell elongates, the chromosomes are pulled apart to the two opposite poles of the cells, following which cell division ensues and separates the replicated DNA (Jacob et al., 1963). This mode of DNA segregation was assumed true for F plasmids as well and further supported by the findings of Lin et. al., 1998, that plasmid partitioning protein SopA of F plasmid (FSopA) as well as that of Q plasmid (QSopA) of *Coxiella burnetii* associate with the bacterial cell membranes. The study involved biochemical membrane fractionation, floatation assays and immunoelectron microscopy, which suggested that a fraction of the respective ParA proteins were localised to the bacterial inner membranes. Further, phosphatase assays using the periplasmic PhoA protein suggested that membrane association might be specified by the N-terminal residues in FSopA and QSopA (Lin et. al., 1998). These studies resulted in a model wherein plasmid complex became associated with the membrane via ParA, and DNA partitioning was driven by cell elongation (**Fig. 1-9A**). This was further supported by beautiful genetic and plasmid localisation studies showing the abundance of F plasmids in anucleate cells (Ezaki et al., 1991), although early studies using *mukB* indicated a general role for the nucleoid as well (Niki et al., 1991)

However, further studies that directly visualised F plasmid and other partitioning proteins in bacteria using high-end imaging techniques never revealed any membrane localisation for ParA. On the contrary, ParA was predominantly found to be localised to the bacterial nucleoid. In 2005, as the concept of bacterial cytoskeleton emerged, a cytoskeletal filament model similar to the eukaryotic chromosome pulling

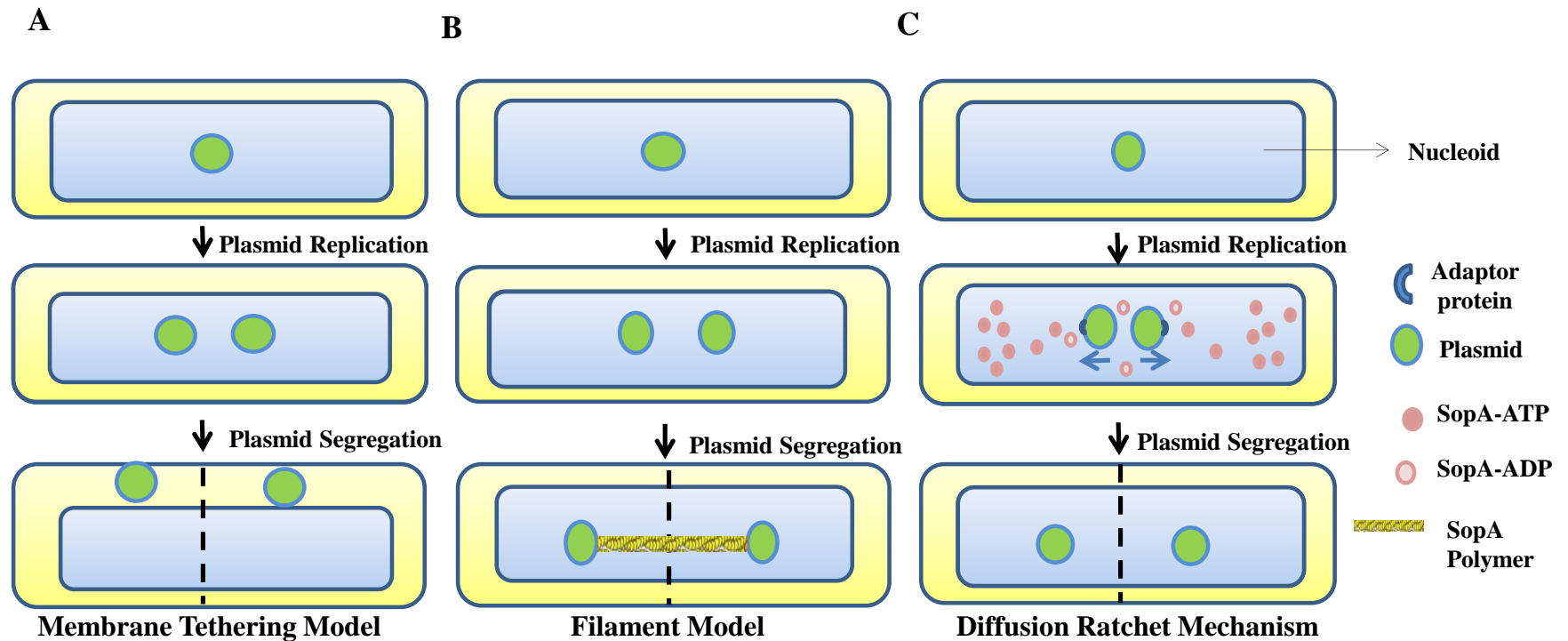


**Figure 1-9. Model depicting the mechanisms of ParA proteins in DNA partitioning.**

The initial model of (A) membrane tethering reported the association of genetic material to the chromosomes, followed by (B) filament model that involved the formation of a polymeric structure that pushes the plasmids to the poles, (C) the recent models of Diffusion ratchet mechanism wherein SopA-ATP gradient drives the localisation of the plasmid bound partitioning complex.



or burnt-bridge models were proposed (Lim et al., 2005; Ptacin et al., 2010). According to this model, ParA would require to undergo an ATP-dependent polymerisation process forming a filament that upon ATP-hydrolysis depolymerises. Dynamic polymerisation and depolymerisation cycles would eventually pull the plasmids apart via the bound ParB-*parS* complex. This was in contrast to the pushing mechanism enabled by the insertional polymerisation in the actin-like ParM protein employed by the R1 plasmid (Moller-Jensen et al., 2003; Garner et al., 2004; Garner et al., 2007; Salje et al., 2009; Gayathri et al., 2012; Gayathri et al., 2013). Pogliano and colleagues (Lim et al., 2005) found that SopA assembled into filaments *in vitro* that were visible by Nile red staining under a light microscope. The rate of filament elongation in the presence of ATP was determined as  $\sim 0.18 \pm 0.05$   $\mu\text{m}$  per minute. This polymerisation of SopA was further ascertained by *in vivo* fluorescence imaging of SopA in *E. coli* (Lim et al., 2005; Hatano et al., 2007) as well as *in vitro* by transmission electron microscopy (Bouet et al., 2007). Further, members of the smaller ParA family have also been reported to undergo polymerisation (Pratto et al., 2008; Schumacher et al., 2012). These studies led to a model of DNA segregation being mediated by a cytoskeletal polymer (**Fig. 1-9B**).

However, several research laboratories working on various ParA proteins, including those who laid the foundations for cytoskeletal polymer models, found the polymerisation and filament pulling model inconsistent with the emerging biochemical and cell biological evidence. Thus, the polymerisation mediated segregation of Type-I systems by ParA proteins was soon superseded by models favouring chemophoretic gradients and diffusion ratchet models. Interestingly, a recent work on *Vibrio cholerae* ParA2 using cryo-EM shows that ParA assembles into filaments in the presence of DNA

and non-hydrolysable ATP (Parker et al., 2021). Further, fluorometric studies on the purified ParA2 in the presence of ATP and ns-DNA, suggest that the filaments are also likely in ParA-ATP\* state (Chodha et al., 2021), a conformation that allows ns-DNA binding (Chodha et al., 2021), thus revitalising the cytoskeletal filament models, but maybe specific to these systems. However, the overwhelming amount of literature on ParA from several species and exhaustive biochemistry and super-resolution imaging argue against a polymerisation mediated partitioning and favour a diffusion ratchet mechanism (Vecchiarelli et al., 2013) or a modified version of it known as the DNA-relay mechanism, which takes into account the elastic properties of nucleoid DNA as well (Lim et al., 2014). These models were principally derived from the *in vitro* reconstitution experiments which more or less replicate the *in vivo* conditions (Vecchiarelli et al., 2013) but have been supported by recent super-resolution imaging (Le Gall et al., 2016; McLeod et al., 2017). Mizuuchi and group reconstituted the miniature version of the entire plasmid partitioning apparatus on a glass slide and were able to observe the dynamics of the partitioning machinery and the relevance of nucleoid in the process using TIRF microscopy (Hwang et al., 2013; Vecchiarelli et al., 2013; Vecchiarelli et al., 2014). Moreover, this was also supported by *in vivo* imaging data reported for other members of the ParA superfamily (Fogel and Waldor, 2005; Lim et al., 2005; Hester and Lutkenhaus, 2007; Hatano and Niki, 2010; Le Gall et al., 2016; McLeod et al., 2017). DNA-relay mechanism was first proposed to explain the movement and dynamics of *C. crescentus* ParA observed during the relocation of the replicated origin from the old pole to the new pole (Lim et al., 2014). The model also considered the elastic properties of the bacterial nucleoid that helps in segregating the plasmids (Lim et al., 2014; Hu et al., 2017). The diffusion-ratchet and DNA-relay

models assume the DNA partitioning process on the surface of the nucleoid. However, recent super-resolution imaging, using structured illumination and multi-focus microscopy, of SopA and ParF strongly suggest that the movement of plasmid (the ParB-*parC* complex) is not the surface but rather appears to be deep within the nucleoid space (Le Gall et al., 2016). These data have led to the proposition of a DNA Hitch-Hiking mechanism, a model that is entirely consistent with the diffusion ratchet and DNA-relay mechanisms (**Fig. 1-9C**).

Our current understanding of the ParA mediated DNA segregation is thus summarised as follows:

The accurate positioning and partitioning of the plasmids during each round of cell division begins with the replication of the DNA. The replicated plasmids form an inter-plasmid cluster in the presence of SopB/ParB protein. The repetitive centromeric sequence of the plasmid, *parC*, is bound by ParB, leading to clustering of ParB around *parC* sequences. This ParB bound plasmid then hovers around the cell space of the bacterium, searching for (ParA-ATP\*)<sub>2</sub> bound form of ParA. (ParA-ATP\*)<sub>2</sub> bound dimeric form remains associated within the high-density regions (HDR) within the bacterial nucleoid. The plasmid bound ParB-*parC* complex, upon encountering (ParA-ATP\*)<sub>2</sub>, stimulates the ATPase activity of ParA. This results in an altered conformation of ParA, i.e., it converts from (ParA-ATP\*)<sub>2</sub> bound state to ParA-ADP. In this conformation, ParA cannot bind to the bacterial nucleoid and is thus released into the cytosol. Such release of ParA molecule from the nucleoid creates a differential gradient of (ParA-ATP\*)<sub>2</sub> on the nucleoid, which is then chased upon by the ParB-*parS* complex, driving the directional movement of the plasmids from one end of the cell to another. Meanwhile, the ParA-ADP bound form associates with ATP attains (ParA-ATP)<sub>2</sub> that

is slowly converted to  $(\text{ParA-ATP}^*)_2$  state wherein it can reassociate with the bacterial nucleoid. Cycles of such binding and release of the ParA-ATP to the nucleoid eventually mediate displacement of the replicated plasmids away from the cell division site, ensuring equi-partitioning of the genetic material (**Fig. 1-10**). Thus, all three components act together to facilitate chromosome segregation in bacteria. The most important highlights of the currently accepted DNA Hitch-hiking model are thus listed below:

1. ParA upon binding ATP forms an ATP-sandwiched dimeric structure and further undergoes a slow conformational transition to its active dimer state -  $(\text{ParA-ATP}^*)_2$ .
2. ParA in its active ATP bound dimeric conformation  $(\text{ParA-ATP}^*)_2$  binds in patches to the high-density regions (HDR) on the nucleoid.
3. ParB-*parS* complex containing the plasmid cargo on interacting with the  $(\text{ParA-ATP}^*)_2$  -nsDNA bound form stimulates the ATPase activity of ParA and converts it into ParA-ADP, which is no longer has an affinity to nsDNA and consequently is immediately released from the HDR of nsDNA.
4. The ParA-ADP bound form is released into the cytosol, wherein it can again bind ATP to dimerise and assemble into its active state  $(\text{ParA-ATP}^*)_2$ , which is now competent to bind nsDNA in the HDR again and form new patches.
5. Meanwhile, the ParB-*parS* bound plasmid diffuses within the nucleoid, binding to another  $(\text{ParA-ATP}^*)_2$  and thus moves the cargo forward in a unidirectional manner from one part of the cell to the other.

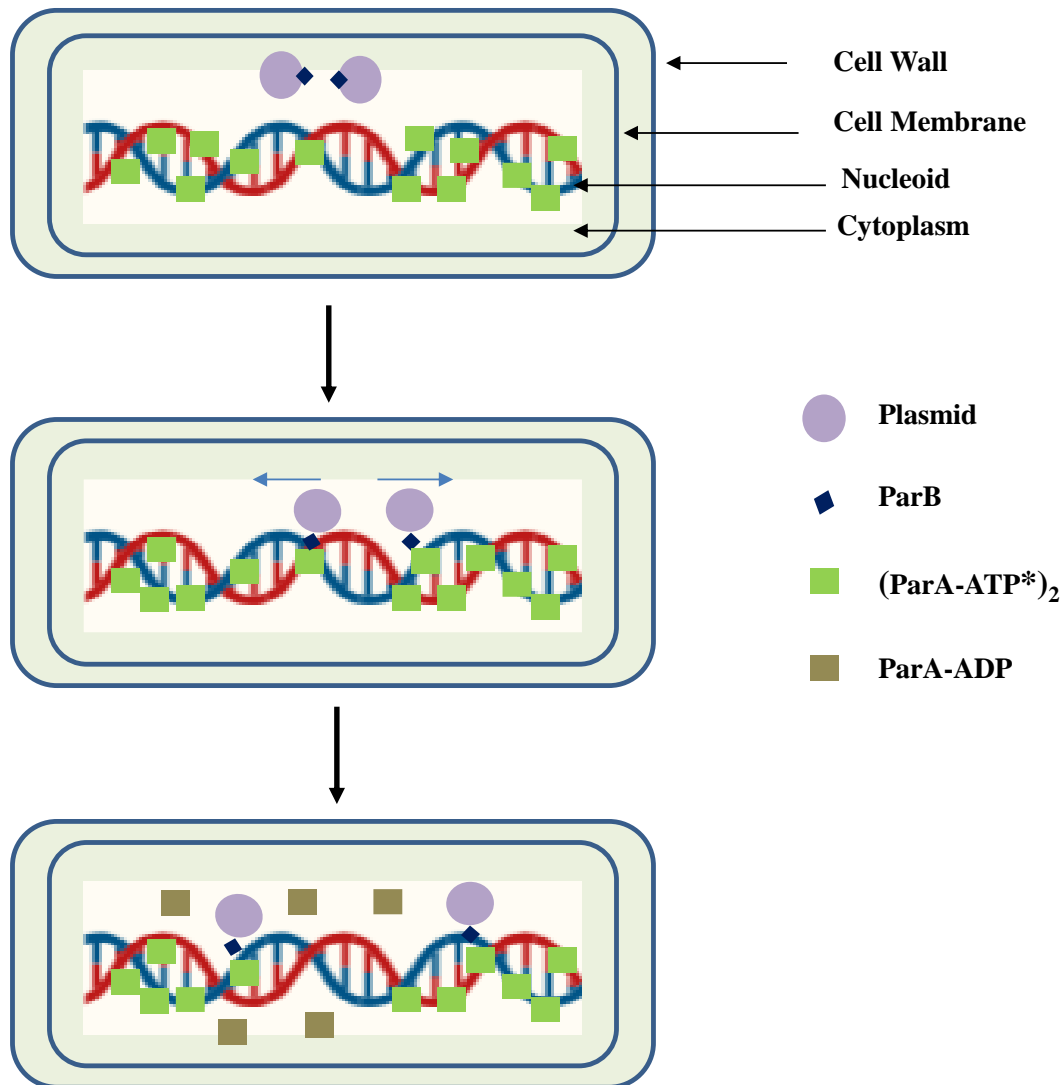


**Figure 1-10. A molecular model depicting the mechanism of DNA partitioning by ParA / SopA.**

The HDR regions of the bacterial nucleoid are associated with  $(\text{ParA-ATP}^*)_2$  molecules. Plasmid DNA, upon replication, is bound by the ParB protein. This Plasmid-ParB complex then surfs on the bacterial nucleoid. The plasmid bound ParB complex interacts with the nucleoid bound  $(\text{ParA-ATP}^*)_2$  and hydrolyses it to ParA-ADP bound form, which is no longer competent to bind to the nucleoid and thus falls off into the cytosol. The plasmid then follows the gradient and thus reaches the two extreme ends of the cell.

Thus, our current understanding of the mechanisms of ParA mediated plasmid segregation highlights the critical role of non-specific DNA as a host factor in the process, and the hitch-hiking model remains the most recent model to date (**Fig. 1-10**).

Moreover, members of the ParA superfamily are not only involved in plasmid and chromosome partitioning but are also involved in a maintenance of other cellular cargo in many bacteria. Thus, mechanisms by which the ParA family of proteins function and act will be critical in our understanding of such cellular processes. Herein, in the next section, we briefly describe and discuss various other cellular processes where ParA (WACA family) play a critical function.

### **1.12 Diverse Biological Functions of WACA / ParA Superfamily of Proteins**

Proteins with the deviant Walker A motif (Walker et al., 1982), or the P loop, serve diverse functions in different life forms. These range from DNA replication and partitioning, protein quality control, cell cycle and division and spatial organisation in cells. Examples include that above mention ParA proteins found in bacterial genomes and plasmids, which play a role in DNA segregation, a few like MinD and MipZ that are involved in cell division (reviewed in Michie and Löwe, 2006; Thanbichler and Shapiro, 2006; Du and Lutkenhaus, 2012) whereas some others play an important role in positioning large macromolecular complexes such as carboxysomes within cells (Savage et al., 2010). These motif-containing proteins are found in all life forms, ranging from archaea to bacteria and constitute a versatile system to build the spatial organisation in biological systems (**Fig. 1-11**). A few examples are briefly outlined below here.

### 1.12.1 Role of MinD in Chromosome Segregation

MinD, a component of the *min* system, is a Walker A ATPase member majorly recruited for regulating cell division in bacteria (Lutkenhaus and Sundaramoorthy, 2003; Lutkenhaus, 2012). MinD along with MinE undergoes pole to pole movement and thus produces a gradient of MinC. MinD, in its ATP binding dimeric form, binds to the membrane (Szeto et al., 2002). Following this membrane association, MinE is recruited, which stimulates the ATPase activity of MinD and thus releases it from the bacterial membrane (Hu et al., 2002). This is further followed by repeated binding and release cycles of MinD driving oscillation of MinD that act as a spatial regulator of FtsZ ring in bacteria. The oscillation of MinD drives the accurate positioning of the Z-ring, and this oscillation somewhat resembles the ParA diffusion behaviour.

As MinD is a member of the WACA superfamily of proteins and DNA binding is an attribute of other members of the family, studies have tested for the DNA binding affinity of MinD. It has been shown using numerical computer simulations that a gradient of DNA binding sites provided by the *min* system can enable the movement of the chromosome from the mid cell to the poles (Ventura et al., 2013). EMSA data also suggests that MinD, in the presence of ATP, can bind to any DNA sequence that is longer than ten bp (Ventura et al., 2013). R219 residue and the C-terminal amphipathic helix plays a critical role in the DNA binding activity of MinD. Further, sedimentation assays using labelled DNA probes and floatation assays also bear testimony to the DNA association of the protein. Also, the deletion of MinD resulted in the production of a large number of anucleate cells compared to cells lacking MinC, suggesting that MinD plays a critical role in chromosome segregation (Ventura et al., 2013).

### 1.12.2 ParA like Proteins in Carboxysome Maintenance in Cyanobacteria

Carboxysomes are membrane-bound organelles in Cyanobacteria that help in Carbon fixation. These proteinaceous microcompartments exist in low-copy numbers in the cells and thus depend on partitioning machinery to ensure their transmission during cell division (MacCready et al., 2018). By using fluorescently labelled carboxysomes, it has been shown that these organelles are arranged in a linear fashion and are equally segregated during cell division by a ParA-like Walker A ATPase partitioning machinery in *Synechococcus elongatus* (Savage et al., 2010). Recent findings (MacCready et al., 2018) suggest that a ParA homolog named McdA (for Maintenance of Carboxysome Distribution) mediates Carboxysome maintenance. McdA bears similarity to the signature Walker A motif of ParA (except for the signature ATP-binding lysine residue) and has non-specific DNA binding activity. Moreover, a small protein McdB, unrelated to ParB, also has been shown to regulate carboxysome positioning. Although McdB shows no sequence similarity to ParB, it can form higher-order oligomers like ParB (Schumacher et al., 2019). Fluorescent labelling of the nucleoid, carboxysomes and McdA inside these cells has enabled live tracking of carboxysomes. McdB (like ParB) stimulates ATPase activity of McdA driving the directed movement of carboxysome towards a higher concentration of McdA on the nucleoid by a diffusion ratchet mechanism. Thus, Carboxysomes also employ a McdAB protein complex in a manner very similar to the ParAB complex (MacCready et al., 2018).



### **1.12.3 Orphan ParA Promoting Chemoreceptor Cluster Formation**

Some ParA homologs lack both a ParB partner protein and a centromeric sequence *parC*. This ParA is located outside *the parAB* operon and is also referred to as Orphan ParA systems. These orphan ParAs are found in metabolic operons and bacterial genomes. Also, reports suggest that bacterial genomes encode multiple numbers of orphan ParAs. One such orphan ParA, "PpfA", is found to be involved in chemotactic signalling in *Rhodobacter sphaeroides* and helps segregation of protein clusters (Roberts et al., 2012). The chemotaxis protein cluster is formed by the partner proteins TlpT and CheW proteins. Mutants in the conserved Walker A motif are known to affect cluster formation.

### **1.12.4 Genomic Island Mediated Incompatibility**

ParI is an Orphan ParA member of the Walker A ATPase family present in the genomic island of *Pseudomonas putida* (Miyakoshi et al., 2012). It is a negative factor regulating the maintenance of IncP-7 plasmids as it mainly destabilises IncP-7 plasmids. Studies on ParI have revealed that mutations in the conserved Walker A motif region (mainly the ATPase domain) of ParI fail to destabilise IncP-7 plasmids. ParI tends to be an example of plasmid-mediated incompatibility residing within a genomic island.

### **1.12.5 Orphan ParA Involved in Cellulose Biosynthesis**

Cellulose is produced by bacteria as a biofilm matrix polymer to enable the cohesion of biofilms. In enterobacteria, BcsQ (bacterial cellulose synthesis) proteins help in the production of cellulose (Quéré et al., 2009). Moreover, BcsQ is a homologue of the ParA/MinD family of ATPase and is activated by binding to cyclic di-GMP. Using fluorescent-tagged BcsQ, it has been confirmed that this protein mainly localises to the cell poles in bacteria and cell-cell adhesion mainly occurs via the production of cellulose

PROTEIN	DEVIANT WALKER A MOTIF ( <u>K</u> GGHGK(S/T))
SopA	KGGVYKT
Hp Soj	KGGVGKT
McdA	SGGQGKT
MinD	KGGVGKT
PpfA	KGGVGKT
pNOB8 ParA	KGGVGKT
BcsQ	RGGVGTT
SegA	KGGVGKT
Bs Soj	KGGVGKT
MipZ	KGGAGKS

**Figure 1-11. The deviant Walker A motif in different members of P loop ATPase.**

Although both the lysines in most cases are conserved, the other residues differ.

at the cell pole. Thus, a ParA/MinD family of ATPase controls cell-cell adhesion and biofilm formation through regulating cellulose biosynthesis.

### **1.13 SUMMARY**

Segregation of chromosomes is an indispensable process in the life cycle of the bacterium, and this process needs to be stringent, consistent, and repetitive as it happens during each round of cell division. In order to accomplish this partitioning, bacteria have evolved varied mechanisms. The ParA superfamily is associated with diverse functions ranging from plasmid and chromosome segregation to carboxysome maintenance. Moreover, some other members of the ParA superfamily are also involved in chemotaxis cluster formation, Z ring positioning, cellulose biosynthesis and other functions. A clear understanding of the process of ParA mediated segregation will thus help us understand the mechanism employed by other members of this superfamily as well in more detail and will help us explore different aspects of the microbial world. Moreover, as chromosome segregation is also directly dependent on ParA, thus a clear understanding of the mechanism will help us design drugs against some of the most virulent pathogens.

## **CHAPTER 2**

### **MATERIALS AND METHODS**

## 2.1 Bacterial Strains and Growth conditions

*E. coli* strains were cultivated at 37 °C or 30 °C in LB medium (Lennox/ Miller where indicated) containing antibiotics in liquid/solid medium. MacConkey agar (Difco) plates were used for qualitative bacterial two-hybrid assays at 30 °C. These media were supplemented with appropriate antibiotics with incubation periods of 30 hours. *E. coli* DH5 $\alpha$  was used for cloning purposes. The expression of genes from the weakened Ptrc promoter of the pDSW210 vector was achieved by the addition of either 100  $\mu$ M or 400  $\mu$ M isopropyl- $\beta$ -D-thiogalactopyranoside (IPTG). Although similar results were obtained with 100  $\mu$ M or 400  $\mu$ M of IPTG, we found that the addition of 400  $\mu$ M IPTG provided more uniform expression across cells and was more reproducible and reliable. *S. pombe* cells were grown in Edinburg Minimal Medium (EMM) lacking thiamine to drive expression from nmt promoter of pREP42 plasmid. The list of bacterial and yeast strains used in this study have been listed in **Table 2-1**.

## 2.2 Reagents

Synthetic oligodeoxynucleotides were purchased from IDT or Eurofins; bovine serum albumin (BSA), IPTG and salmon sperm DNA were from Sigma-Aldrich; restriction enzymes, Q5 DNA polymerase, Taq DNA polymerase, Gibson Assembly 2x master mix were purchased from New England Biolabs and Ni-NTA agarose beads from Novagen.

**Table 2-1. Bacterial and Yeast strains used in this study.**

Strains (Lab Stock)	Name (Source)	Genotype	Source	Reference
<i>Bacterial strains:</i>				
CCD53	BW25113 <i>ΔugpA</i>	F <sup>-</sup> <i>Δ(araD-araB)567</i> <i>lacZ4787(del)::rrnB-3</i> LAM <sup>-</sup> <i>rph-1 Δ(rhaD- rhaB)568 hsdR514</i> <i>ΔugpA::kan</i>	Kind gift from Dr. Rachna Chaba (KEIO collection)	Baba et al., 2006
CCD219	DH5α	<i>fhuA2 lac(del)U169</i> <i>phoA glnV44 Φ80'</i> <i>lacZ(del)M15 gyrA96</i> <i>recA1 relA1 endA1</i> <i>thi-1 hsdR17</i>	Kind gift from Dr. Tushar K Beuria	Meselson and Yuan, 1968; Hanahan, 1985
CCD220	BL21 DE3	F <sup>-</sup> <i>ompT gal dcm lon hsd</i> <i>S<sub>B</sub>(r<sub>B</sub><sup>-</sup>m<sub>B</sub>) λ(DE3</i> <i>[lacI lacUV5-</i> <i>T7p07 ind1 sam7 nin5</i> <i>]) [malB<sup>+</sup>]<sub>K-12</sub>(λ<sup>S</sup>)</i>	Kind gift from Dr. Tirumala K Chaudhary	Studier et al., 1990
CCD252	JS964	<i>ΔlacX74 malPp::lacIq</i> <i>Δ(minCDE)::kan</i>	Kind gift from Dr. Tushar K	Pichoff et al., 1995

			Beuria	
<b>CCD253</b>	<b>MC4100</b>	<i>F</i> <sup>-</sup> <i>[araD139]<sub>B/r</sub> Δ(argF-lac)169* &amp;lambda; e14-flhD5301</i> <i>Δ(fruK-yeiR)725</i> <i>(fruA25)‡ relA1</i> <i>rpsL150(strR) rbsR22</i> <i>Δ(fimB- fimE)632(::IS1)</i> <i>deoC</i> <i>1</i>	Kind gift from Dr. Tushar K Beuria	Casadaban, 1976
<b>CCD277</b>	<b>BTH101</b>	<i>F</i> <sup>-</sup> , <i>cya-99</i> , <i>araD139</i> , <i>galE15</i> , <i>galK16</i> , <i>rpsL1</i> , <i>hsdR2</i> , <i>mcrA1</i> , <i>mcrB1</i>	Kind gift from Dr. Anjana Badrinarayanan	Karimova et al., 1998
<b>CCD322</b>	<b>Hu- pA::mCh erry</b>	MG1655 <i>hu- pA100::mcherry::kan</i>	Kind gift from Dr. Mohan Chandra Joshi	Marceau et al., 2011; Fisher et al., 2013
<b>CCD357</b>	<b>NiCo21 DE3</b>	<i>can::CBD fhuA2 [lon]</i> <i>ompT gal (λ DE3) [dcm]</i> <i>arnA::CBD</i> <i>slyD::CBD glmS6Ala</i>	New England Biolabs	Robichon et al., 2011

		<i>ΔhsdS λ DE3 = λ sBamHIo</i> <i>ΔEcoRI-B</i> <i>int::(lacI::PlacUV5::</i> <i>T7 gene1) i21 Δnin5</i>		
<b>CCD358</b>	<b>DLT1127</b>	<i>araD139, Δ(ara-</i> <i>leu)7679, ΔlacX74,</i> <i>galU, galK, rpsL, thi,</i> <i>hsdR2, mcrB, λRS88-</i> <i>Kan-PsopF::lacZ</i>	Kind gift from Dr. David Lane	Ravin and Lane, 1999
<b><i>Bacterial strains / plasmids</i></b>				
<b>CCDE257</b>		MC4100 / pCCD494		This work (Lim et al., 2005)
<b>CCDE258</b>		MC4100 / pCCD495		This work (Lim et al., 2005)
<b>CCDE312</b>		DLT1127/ pCCD479		This work
<b>CCDE313</b>		DLT1127/ pCCD810		This work
<b>CCDE314</b>		DLT1127/ pCCD825		This work
<b>CCDE315</b>		DLT1127/ pCCD809		This work



<b>CCDE316</b>		DLT1127/ pCCD494		This work
<b>CCDE317</b>		DLT1127/ pCCD479/ pCCD569		This work
<b>CCDE318</b>		DLT1127/ pCCD810/ pCCD569		This work
<b>CCDE319</b>		DLT1127/ pCCD825/ pCCD569		This work
<b>CCDE320</b>		DLT1127/ pCCD809/ pCCD569		This work
<b>CCDE321</b>		DLT1127/ pCCD494/ pCCD569		This work
<b>CCDE329</b>		BTH101/ pCCD846/ pCCD824		This work
<b>CCDE330</b>		BTH101/ pCCD847/ pCCD824		This work
<b>CCDE331</b>		BTH101/ pCCD848/ pCCD824		This work
<b>CCDE332</b>		BTH101/ pCCD850/ pCCD824		This work
<b>CCDE333</b>		BTH101/ pCCD846/ pCCD852		This work
<b>CCDE334</b>		BTH101/ pCCD847/		This work

		pCCD852		
<b>CCDE335</b>		BTH101/ pCCD848/ pCCD852		This work
<b>CCDE336</b>		BTH101/ pCCD846/ pCCD487		This work
<b>CCDE337</b>		BTH101/ pCCD847/ pCCD487		This work
<b>CCDE338</b>		BTH101/ pCCD848/ pCCD487		This work
<b>CCDE357</b>		BTH101/ pCCD490/ pCCD491		This work
<b>CCDE358</b>		BTH101/ pCCD487/ pCCD489		This work
<b>CCDE359</b>		BTH101/ pCCD851/ pCCD846		This work
<b>CCDE360</b>		BTH101/ pCCD851/ pCCD847		This work
<b>CCDE361</b>		BTH101/ pCCD851/ pCCD848		This work
<b>CCDE419</b>		MC4100/ pCCD593		This work
<b>CCDE420</b>		MC4100/ pCCD589		This work

<b>CCDE421</b>		MC4100/ pCCD590		This work
<b>CCDE422</b>		MC4100/ pCCD684		This work
<b>CCDE423</b>		MC4100/ pCCD500		This work
<b>CCDE424</b>		MC4100/ pCCD511		This work
<b>CCDE425</b>		MC4100/ pCCD687		This work
<b>CCDE426</b>		MC4100/ pCCD750		This work
<b>CCDE427</b>		MC4100/ pCCD895		This work
<b>CCDE428</b>		MC4100/ pCCD494/ pCCD569		This work
<b>CCDE429</b>		MC4100/ pCCD495/ pCCD569		This work
<b>CCDE430</b>		MC4100/ pCCD593/ pCCD569		This work
<b>CCDE431</b>		MC4100/ pCCD589/ pCCD569		This work
<b>CCDE432</b>		MC4100/ pCCD590/ pCCD569		This work
<b>CCDE433</b>		MC4100/ pCCD684/ pCCD569		This work

<b>CCDE434</b>		MC4100/ pCCD511/ pCCD569		This work
<b>CCDE435</b>		MC4100/ pCCD686/ pCCD569		This work
<b>CCDE436</b>		MC4100/ pCCD742/ pCCD569		This work
<b>CCDE437</b>		MC4100/ pCCD743/ pCCD569		This work
<b>CCDE438</b>		MC4100/ pCCD744/ pCCD569		This work
<b>CCDE439</b>		MC4100/ pCCD747/ pCCD569		This work
<b>CCDE440</b>		MC4100/ pCCD748/ pCCD569		This work
<b>CCDE441</b>		MC4100/ pCCD892/ pCCD569		This work
<b>CCDE442</b>		MC4100/ pCCD893/ pCCD569		This work
<b>CCDE443</b>		MC4100/ pCCD894/ pCCD569		This work
<b>CCDE444</b>		HupA/ pCCD494		This work
<b>CCDE445</b>		HupA/ pCCD495		This work

<b>CCDE446</b>		HupA/ pCCD511		This work
<b>CCDE447</b>		HupA / pCCD590		This work
<b>CCDE448</b>		HupA / pCCD684		This work
<b>CCDE449</b>		HupA / pCCD686		This work
<b>CCDE450</b>		HupA / pCCD742		This work
<b>CCDE451</b>		HupA / pCCD743		This work
<b>CCDE452</b>		HupA / pCCD744		This work
<b>CCDE453</b>		HupA / pCCD747		This work
<b>CCDE454</b>		HupA / pCCD748		This work
<b>CCDE455</b>		HupA / pCCD892		This work
<b>CCDE456</b>		HupA / pCCD893		This work
<b>CCDE457</b>		HupA / pCCD894		This work
<b>CCDE458</b>		NiCo21 DE3/ pCCD492		This work
<b>CCDE459</b>		NiCo21 DE3/ pCCD493		This work

<b>CCDE460</b>		NiCo21 DE3/ pCCD594		This work
<b>CCDE461</b>		NiCo21 DE3/ pCCD694		This work
<b>CCDE462</b>		NiCo21 DE3/ pCCD697		This work
<b>CCDE463</b>		NiCo21 DE3/ pCCD749		This work
<i>Yeast strains:</i>				
<b>CCDY327</b>	<b>MBY192/ KGY121</b>	<i>h2<sup>-</sup> leu1-32 ura4-D18</i>	Kind gift from Dr. Mithilesh Mishra	Rajagopalan and Balasubraman ian, 1999
<i>Yeast strains / plasmids</i>				
<b>CCDY58</b>	<b>MBY4526</b>	MBY192 / pCCD83	Kind gift from Dr. Mohan Balasubramanian	Srinivasan (un published)
<b>CCDY421</b>		MBY192 / pCCD898		This work
<b>CCDY422</b>		MBY192 / pCCD899		This work

### 2.3 Antibiotics

All antibiotics used in this work were purchased from either MP Biomedicals or Sigma-Aldrich, and the concentrations used are listed below in **Table 2-2**.

**Table 2-2. Antibiotics used in this study and their specific concentrations used**

Antibiotics	Concentration
Carbenicillin	100 µg/ml
Chloramphenicol	34 µg/ml
Kanamycin	50 µg/ml
Cephalexin	50 µg/ml

### 2.4 Plasmid DNA Extraction

Plasmid DNA was prepared from *E. coli* DH5 $\alpha$  cultures grown for approximately 16 hours in LB broth with aeration at 37 °C. Plasmid DNA was extracted using an Agilent Plasmid mini-prep Kit as follows. The stationary phase culture was harvested by centrifugation of 1.5 ml at 17350 x g for one minute. The cell pellet was re-suspended in 100 µl resuspension Buffer by thorough vortexing. 100 µl Lysis Buffer was added, and the sample was inverted four to six times carefully to lyse the cells, followed by incubation for two to three minutes at room temperature. 125 µl Neutralisation Buffer was added, the microtube was inverted gently five to six times followed by 5 minutes centrifugation at 17350 x g for precipitation of cellular debris. The supernatant was applied to a silica membrane spin column which was centrifuged at 17350 x g for one minute. The filtrate was discarded from the collection tube into which the spin column was reinserted. The membrane was washed twice by adding

750 µl from Wash Buffer. The column was centrifuged at 17350 x g. for one minute to remove any buffer. The centrifugation step was repeated once more to remove all traces of ethanol. The collection tube was discarded, and the column was placed into a sterile 1.5 ml microcentrifuge tube. 50 µl of sterile dH<sub>2</sub>O were added with incubation at room temperature for 15 minutes. Then, final centrifugation was performed for one minute at 17350 x g. to elute the DNA. The DNA concentration was measured using a Nanodrop™ and was stored at -20 °C. For low copy number plasmids, Agilent or Qiagen midiprep kit was used.

## 2.5 Cloning

The list of all the plasmid constructs used in this study are listed in **Table 2-3**. pCCD83 was constructed by Dr. Yin Yi Huang (Dr. Mohan Balasubramanian's lab) and was obtained as follows:

SopA was PCR amplified from an F<sup>+</sup> strain of *E. coli* using the oligonucleotides RSO71 and RSO79 and digested with SalI and BamHI restriction enzymes and cloned into SalI-BamHI sites of pBMB51 (Srinivasan et al., 2008) to obtain pCCD83.

pDSW210-SopA (pCCD494) construct was generated by Gibson cloning wherein the SopA fragment was initially amplified from pCCD83 construct using oligonucleotides Gbo40 and Gbo41. The vector pDSW210 was then amplified with Gibson oligonucleotides Gbo39 and Gbo42. Both the amplified fragments were checked on an agarose gel. Subsequently, the reaction mixtures were subjected to DpnI digestion overnight at 37 °C, following which ligation using Gibson assembly master mix for 1 hour at 50 °C in a thermocycler was done. The ligated product was then



transformed into DH5 $\alpha$  competent cells. The colonies thus attained were used for plasmid isolation, following which the plasmids were verified by sequencing.

pET28a<sup>+</sup>-SopA (pCCD492) construct was generated by Restriction Free cloning (van den Ent and Lowe, 2006). The SopA fragment was initially amplified from pCCD83 using RF oligonucleotides (RSO411 and RSO412) having vector-specific overhangs. The amplified PCR product was then used as a mega primer for the second PCR using pET28a<sup>+</sup> as a template such that the construct pET28a<sup>+</sup>-SopA was generated. The clone was further verified by sequencing. pET28a<sup>+</sup>-SopB (pCCD763) was also generated by Restriction Free cloning. The SopB fragment was amplified from pCCD569 (mini-F, pLtetO-1:: $\Delta$ sopA, *sopBC* +) using the RF oligonucleotides (RSO728 and RSO729), the amplified PCR product was then used as a mega primer for second PCR using pET28a<sup>+</sup> as a template, thus generating the construct pET28a<sup>+</sup>-SopB.

All the constructs used in Bacterial two-hybrid assays were generated by the Restriction Free cloning method. In case of pCCD846 (pUT18C-SopA), pCCD847 (pUT18C-SopA Q351H) and pCCD848 (pUT18C-SopA W362E) constructs, SopA or the mutants were amplified from pCCD494, pCCD593 and pCCD589 using oligonucleotides RSO804 and RSO805. This amplified product was then used as a mega primer for second PCR using pCCD489 (pUT18C) as a template. This PCR product was then DpnI digested overnight at 37 °C, following which it was transformed into DH5 $\alpha$  cells. The colonies attained were used for plasmid isolation, following which the plasmids were verified by sequencing. pCCD850 (pUT18C-SopA K340A) was generated by the QuikChange<sup>TM</sup> method using Q5 polymerase (NEB), as described in the next section.

pCCD824 (pKT25-SopB) construct was also generated similarly wherein the SopB gene was amplified from pCCD763 using oligonucleotides RSO774 and RSO775. The amplified product was used in a second PCR using pCCD486 (pKT25) as a template. For generating C-terminal T25 fusion to SopB in pKNT25 vector, oligonucleotides RSO812 and RSO813 were used in the first PCR using pCCD763 as template and pCCD487 as a template in the second PCR.

Further, for self-interaction assays, SopA and the mutants were also cloned into the pKT25 vector. In the initial step, SopA and the mutants were amplified from pCCD494 (pDSW210-SopA), pCCD593 (pDSW210-SopA Q351H) and pCCD589 (pDSW210-SopA W362E) using oligonucleotides RSO796 and RSO797. The amplified product was then used in a second PCR using pCCD486 as a template to generate pCCD851, pCCD896 and pCCD897, respectively. All these clones, thus generated, were verified by sequencing.

## **2.6 Generation of C-terminal deletion mutants**

All the deletion mutants used in this study were generated by the Restriction-free cloning method. Initially, the SopA gene from the pCCD83 construct was amplified using SopA forward primer RSGbo40 and SopA specific reverse primer (RSO682 for SopA  $\Delta$ Ct5, RSO683 for SopA  $\Delta$ Ct7, RSO684 for SopA  $\Delta$ Ct10, RSO686 for SopA  $\Delta$ Ct20 and RSO557 primer for SopA  $\Delta$ Ct29) that contains the deletion such that the deletion in SopA was incorporated. Similarly, for generating the deletions in pET28a+ SopA construct, the SopA gene was initially amplified from pCCD83 using SopA forward primer RSO411 and SopA specific reverse primer for incorporating the deletion (RSO556 for SopA  $\Delta$ Ct29). These oligonucleotides were designed to have an

overhang containing the sequence of pET28a<sup>+</sup> vector or pDSW210 vector sequence, respectively. In the next step, the first PCR product was used as a primer for the second PCR wherein pDSW210 or pET28a<sup>+</sup> vector was used as a template, thus generating the deletion. Sequential deletions in SopA include SopA  $\Delta$ Ct29 in pET28a<sup>+</sup> and SopA  $\Delta$ Ct5, SopA  $\Delta$ Ct7, SopA  $\Delta$ Ct10, SopA  $\Delta$ Ct20 and SopA  $\Delta$ Ct29 deletion in pDSW210. All the plasmids were further verified by sequencing.

## 2.7 Generation of site-directed mutants

Site-directed mutations in the C-terminus of SopA were generated using the Stratagene QuikChange<sup>TM</sup> method using Q5 polymerase (NEB). A pair of oligonucleotides containing the base changes at the desired site (**Table 2-4**) were used, and pCCD83 (pREP42-SopA-GFP) or pCCD494 (pDSW210-SopA) or pCCD492 (pET28a<sup>+</sup>-SopA) served as templates. The amplified PCR product was then run on an agarose gel to verify the band size, subjected to overnight DpnI digestion, and then transformed into DH5 $\alpha$  competent cells. The plasmids were then isolated from the colonies and sent for sequencing. The site directed mutants include SopA G116V, SopA K120E, SopA K120Q, SopAQ351H, SopA W362A, SopA R363A, SopA W369E, SopA E375A, SopAF377A, SopA R379A, SopA K382A, SopA R384A. Moreover, double mutants, SopA1 (M315I Q351H), SopA K120E W362E and SopA K120E Q351H, were also generated.

A STOP codon (TAA) was introduced between the coding sequences of SopA and GFP into the pDSW210-SopA-GFP and its variants for promoter repression as- say. Oligonucleotides RSO753 and RSO754 were used as oligonucleotides, and the plasmids carrying the respective mutations were used as template DNA. pCCD850

(pUT18C-SopA K340A) was generated using pCCD846 as template and oligonucleotides RSO816 and RSO817.

The plasmids used in this study have been listed in **Table 2-3**. The complete list of the oligonucleotides (with their sequence) used in this study has been listed in **Table 2-4**.

**Table 2-3. Plasmids used in this study.**

<b>Plasmid Stocks</b>	<b>Description</b>	<b>Vector Back-bone</b>	<b>Source</b>	<b>Reference</b>
<b>pCCD51</b>	pBMB51 (pREP42-GFP)	pREP42	Kind gift from Mohan Balasubramanian	Srinivasan et al., 2008
<b>pCCD83</b>	SopA-GFP	pREP42	Kind gift from Mohan Balasubramanian	This work
<b>pCCD479</b>	GFP under weak Ptrc promoter	pDSW210	Kind gift from TusharK Beuria	Weiss et al., 1999
<b>pCCD480</b>	A strong T7 promoter containing vector with N-terminal or C-terminal 6x His-tag	pET28a <sup>+</sup>	Kind gift from Parathasarthi Ajitkumar	Novagen

<b>pCCD486</b>	T25	pKNT25	Kind gift from Anjana Badrinarayanan	Karimova et al., 1998
<b>pCCD487</b>	T25	pKT25	Kind gift from Anjana Badrinarayanan	Karimova et al., 1998
<b>pCCD488</b>	T18	pUT18	Kind gift from Anjana Badrinarayanan	Karimova et al., 1998
<b>pCCD489</b>	T18C	pUT18	Kind gift from Anjana Badrinarayanan	Karimova et al., 1998
<b>pCCD490</b>	T25-zip	pKT25	Kind gift from Anjana Badrinarayanan	Karimova et al., 1998
<b>pCCD491</b>	T18-zip	pUT18	Kind gift from Anjana Badrinarayanan	Karimova et al., 1998

<b>pCCD492</b>	6x His-SopA	pET28a+		This work (Lim et al., 2005)
<b>pCCD493</b>	6x His-SopA1 (M315I Q351H)	pET28a+		This work
<b>pCCD494</b>	SopA-GFP	pDSW210		This work (Lim et al., 2005)
<b>pCCD495</b>	SopA1 (M315I Q351H)-GFP	pDSW210		This work (Lim et al., 2005)
<b>pCCD500</b>	SopA G116V-GFP	pDSW210		This work
<b>pCCD511</b>	SopA K120Q-GFP	pDSW210		This work
<b>pCCD564</b>	pBR322 <i>Para- BAD::SopA-6xHis</i>	pJP27	Jean-Yves Bouet	Castaing et al., 2008
<b>pCCD569</b>	mini-F, cat, pLtetO- 1:: $\Delta$ sopA, sopBC +	pDAG198	Jean-Yves Bouet	Castaing et al., 2008
<b>pCCD589</b>	SopA W362E-GFP	pDSW210		This work
<b>pCCD590</b>	SopA W369E-GFP	pDSW210		This work
<b>pCCD593</b>	SopA Q351H-GFP	pDSW210		This work
<b>pCCD594</b>	6x His-SopA Q351H	pET28a+		This work
<b>pCCD684</b>	SopA $\Delta$ Ct29-GFP	pDSW210		This work
<b>pCCD685</b>	SopA $\Delta$ Ct20-GFP	pDSW210		This work
<b>pCCD686</b>	SopA $\Delta$ Ct5-GFP	pDSW210		This work

<b>pCCD687</b>	SopA W362E K120E-GFP	pDSW210		This work
<b>pCCD694</b>	6x His-SopA $\Delta$ Ct29	pET28a+		This work
<b>pCCD697</b>	6x His-SopA W362E	pET28a+		This work
<b>pCCD742</b>	SopA F377A-GFP	pDSW210		This work
<b>pCCD743</b>	SopA K382A-GFP	pDSW210		This work
<b>pCCD744</b>	SopA R379A-GFP	pDSW210		This work
<b>pCCD747</b>	SopA $\Delta$ Ct7-GFP	pDSW210		This work
<b>pCCD748</b>	SopA $\Delta$ Ct10-GFP	pDSW210		This work
<b>pCCD749</b>	6x His-SopA K120E	pET28a+		This work
<b>pCCD750</b>	SopA K120E-GFP	pDSW210		This work
<b>pCCD763</b>	6x His-SopB	pET28a+		This work
<b>pCCD809</b>	SopA W362E (stop)	pDSW210		This work
<b>pCCD810</b>	SopA (stop)	pDSW210		This work
<b>pCCD824</b>	T25-SopB	pKT25		This work
<b>pCCD825</b>	SopA Q351H (stop)	pDSW210		This work
<b>pCCD846</b>	T18-SopA	pUT18C		This work
<b>pCCD847</b>	T18-SopA Q351H	pUT18C		This work
<b>pCCD848</b>	T18-SopA W362E	pUT18C		This work
<b>pCCD849</b>	T18-SopA R363A	pUT18C		This work
<b>pCCD850</b>	T18-SopA K340A	pUT18C		This work
<b>pCCD851</b>	T25-SopA	pKT25		This work

<b>pCCD852</b>	SopB-T25	pKNT25		This work
<b>pCCD892</b>	SopA E375A-GFP	pDSW210		This work
<b>pCCD893</b>	SopA R384A-GFP	pDSW210		This work
<b>pCCD894</b>	SopA R363A-GFP	pDSW210		This work
<b>pCCD895</b>	SopA Q351H K120E-GFP	pDSW210		This work
<b>pCCD896</b>	T25-SopA Q351H	pKT25		This work
<b>pCCD897</b>	T25-SopA W362E	pKT25		This work
<b>pCCD898</b>	SopA Q351H-GFP	pREP42		This work
<b>pCCD899</b>	SopA W362E-GFP	pREP42		This work



**Table 2-4. Oligonucleotides used in this study.**

<b>NAME</b>	<b>Sequence (5'-3')</b>	<b>Description</b>
<b>RSGbO39</b>	CTGCAGGTCGACTCTAGAG	pDSW210 amplification FP (Gibson)
<b>RSGbO40</b>	AGAGTCGACCTG- CAGATGTTTCAGAATGAAACT CATGG	SopA amplification FP (Gib- son)
<b>RSGbO41</b>	AG- TTCTTCTCCTTTACTCATCTG CAGGTTGTT- GTTTCTAATCTCCCAGCGTG G	SopA amplification RP (Gib- son)
<b>RSGbO42</b>	AACAACAACCTG- CAGATGAGTAAAGGAGAA- GAACTTTTC	pDSW210 amplification RP (Gibson)
<b>RS71</b>	GTCGTCGTCGAC- CATGTTTCAGAATGAAACTCA TG	SopA (pREP42) FP
<b>RS79</b>	GCGGCGGGATCCCGTTGTT- GTT- GTTTCTAATCTCCCAGCGTG G	SopA (pREP42) RP
<b>RS98</b>	CAGTCCCCGTGGATCGAG- GAGCAAATTCGG- GATGCCTGGGGAAGC	SopA M315I FP
<b>RS99</b>	CCGAATTT- GCTCCTCGATCCACGGG- GACTGA- GAGCCATTACTATTG	SopA M315I RP
<b>RS100</b>	CTGTTTTTGAACAC- GCCATTGATCAAC-	SopA Q351H FP

	GCTCTTCAACTGGTGCCTG- GAG	
<b>RS101</b>	CGTT- GATCAATGGCGTGTTCAAAA ACAGTTCTCATCCGGATC	SopA Q351H RP
<b>RSO411</b>	<b>GCCGCGCGG-</b> <b>CAGCCAT</b> ATGGCTAG- CATGTTCAGAATGAAACTCA TG	pET28a SopA FP
<b>RSO412</b>	CCATTTGCTGTCCACCAG- TCATGCTAGCTT <b>ATCTAATC</b> <b>TCCCAGCGTGG</b>	pET28a SopA RP
<b>RSO415</b>	GCTGCCCATAAAG <b>TT-</b> GGCGTTTACAAAACCTCAG- TTTCTGTTC	SopA G116V FP
<b>RSO416</b>	GTTTTGTAAAC- GCCA <b>ACT</b> TTTATGGGCAG- CAACCCCGATCACC	SopA G116V RP
<b>RSO417</b>	GGTGGCGTTTAC <b>CAAAC-</b> CTCAGTTTCTGTTCATCTT- GCTCAGG	SopA K120Q FP
<b>RSO418</b>	GAAACTGAGGTTT <b>GG-</b> TAAACGCCACCTTTATGGG- CAGCAAC	SopA K120Q RP
<b>RSO425</b>	CGGTTCTGGCAAA- TATTCTGAAATGAGC	pDSW210 FP
<b>RSO426</b>	GCGTTCTGATTTAATCTG- TATCAGGC	pDSW210 RP
<b>RSO460</b>	CAACTGGTGCC <b>GAGA-</b> GAAATGCTCTTTCTATTT- GGGAACC	SopA W362E FP
<b>RSO461</b>	GAGCATTCTCT <b>TCGGCAC-</b>	SopA W362E RP

	CAGTTGAAGAGCGTT- GATCAATGGCC	
<b>RSO462</b>	GCTCTTTCTATTGAGGAAC- CTGTCTG- CAATGAAATTTTCGATCGTC TG	SopA W369E FP
<b>RSO463</b>	GCAGACAGGTTCCCTCAA- TAGAAAGAG- CATTCTCCAGGCACCAG- TTGAAGAG	SopA W369E RP
<b>RSO464</b>	CTGTCTGCAATGAAATT- GCCGATCGTCTGATTAAAC- CACGCTGGGAG	SopA F377A FP
<b>RSO465</b>	GGTTTAATCAGACGATCGG- CAATTCATTGCAGA- CAGGTTCCCAAATAGAAA- GAGC	SopA F377A RP
<b>RSO556</b>	GTGGTGGTGGTGGTGGTCTCGA GGAATTCCTTAAGTTGAA- GAGCGTTGATCAA	pET28a_SopAΔCt29 RP
<b>RSO557</b>	TTACTCATCTGCAGGTT- GTTGTTGAATTCAGTTGAA- GAGCGTTGATCAATGGC	pDSW210_SopAΔCt29 RP
<b>RSO634</b>	ATG TTCAGAATGAACTCAT GGAA	SopA FP (Full length)
<b>RSO635</b>	TCTAATCTCCCAGCGTGGTT TAAT	SopA RP (Full length)
<b>RSO659</b>	CGTCTGATTAAAC- CAGCCTGGGAGATTAGA	SopA R384A FP
<b>RSO660</b>	CTCCCAGGCTGGTTTAATCA GACGATCGAAAAT	SopA R384A RP
<b>RSO661</b>	GAAATTTTCGATGCTCTGAT	SopA R379A FP

	TAAACCACGCTGG	
<b>RSO662</b>	TGGTTTAATCAGAG- CATCGAAAATTCATT- GCAGAC	SopA R379A RP
<b>RSO663</b>	GGTGCCTGGG- CAAATGCTCTTTCTATTT- GGGAA	SopA R363A FP
<b>RSO664</b>	AGAAAGAGCATTT- GCCAGGCACCAGTTGAA- GAGCG	SopA R363A RP
<b>RSO665</b>	GATCGTCTGATTGCCACCAC- GCTGGGAGATT	SopA K382A FP
<b>RSO666</b>	CCAGCGTGGTG- CAATCAGAC- GATCGAAAATTCATT	SopA K382A RP
<b>RSO667</b>	CCTGTCTG- CAATGCAATTTTCGATCGTC TGATT	SopA E375A FP
<b>RSO668</b>	ACGATCGAAAATTGCATT- GCAGACAGGTTCCCAA- TAGA	SopA E375A RP
<b>RSO682</b>	CTCATCTGCAGGTTGTT- GTT- GAATTC TGGTTTAATCAGAC GATCGAAAATTCATT	pDSW210_ ΔCT5 RP
<b>RSO683</b>	CTCATCTGCAGGTTGTT- GTTGAATTC AATCAGAC- GATCGAAAATTCATT	pDSW210_ ΔCT7 RP
<b>RSO684</b>	CTCATCTGCAGGTTGTT- GTT- GAATTC ATCGAAAATTCAT TGCAGACAGG	pDSW210_ ΔCT10 RP

<b>RSO686</b>	<b>ACTCATCTGCAGGTTGTT- GTTGAATTC</b> AATAGAAA- GAGCATTCTCCA	pDSW210_ΔCT20 RP
<b>RSO692</b>	GGTGGCGTTTAC <b>G</b> AAAC- CTCAGTTTCTGTTCATCTT- GCTCAGG	SopA_K120E FP
<b>RSO693</b>	GAAACTGAGGTTT <b>CG</b> - TAAACGCCACCTTTATGGG- CAGCAAC	SopA_K120E RP
<b>RSO728</b>	<b>CCGCGCGG- CAGCCATATGGCTAG- CAAAA</b> AATGAA- GCGTGCGCCTGTTATTCCA	pET28a_SopB FP
<b>RSO729</b>	<b>GTGGTGGTGGTGGTGGTGCT CGAG-</b> TCAGGGTGCTGGCTTTTCAA GTTC	pET28a_SopB RP
<b>RSO753</b>	AACAACAACCTGCAG <b>TAA-</b> <b>GCT</b> TAAAGGAGAA- GAACTTTTCAC	SopA-STOP FP (HindIII)
<b>RSO754</b>	TTGCTTCTCCTTTAA- <b>GCTT</b> ACTGCAGGTTGTTGTT	SopA-STOP RP (HindIII)
<b>RSO774</b>	<b>GCTG- CAGGGTCGACTCTA</b> ATGAA- GCGTGCGCCTGTTATT	pKT25_SopB FP
<b>RSO775</b>	<b>TTACTTAGGTACCCGGG- GATCCT</b> CAGGGTGCTGGCTT TTCAAGTTC	pKT25_SopB RP
<b>RSO796</b>	<b>GCTG- CAGGGTCGACTCTA</b> ATGTTC AGAATGAAACTC	pKT25_SopA FP
<b>RSO797</b>	<b>AGGTACCCGGG-</b>	pKT25_SopA RP

	GATCCTTCATCTAATCTCC CAGCGTGG	
<b>RSO804</b>	CTGCAGGTCTGACTCTAGA- GATGTTTCAGAATGAAACTCA TGG	pUT18C_SopA FP
<b>RSO805</b>	CGAGCTCGG- TACCCGTCTAATCTCCCAGC GTG	pUT18C_SopA-RP
<b>RSO812</b>	ACACAGGAAACAGC- TATGACCCATATGAA- GCGTGCGCCTGTT	pKNT25_SopB FP
<b>RSO813</b>	TAGAGTCGACCTG- CAGGCGGGTGCTGGCTTTTC AAG	pKNT25_SopB RP
<b>RSO816</b>	GATGAAGTTGGTG- CAGGTCAGATCCGGATGA- GAACTGT	SopA K340A FP
<b>RSO817</b>	CCGGATCTGACCTGCAC- CAACTTCATCCGTTTCAC- GTACAAC	SopA K340A RP
<b>Additional Bases or base changes introduced are indicated in Red</b>		

## 2.8 Lithium acetate *S. pombe* Yeast transformation

Solutions: LiAc-TE: 0.1 M lithium acetate, 10 mM Tris pH 7.5, 1 mM EDTA,  
Carrier DNA: boiled sperm DNA 10 mg/ml, LiAc-TE-PEG: LiAc-TE plus 40 %  
PEG4000.

A loopful of freshly streak *S. pombe* culture was inoculated in 3 ml of autoclaved  
YES broth and kept overnight at 30 °C. 500 ml of this primary culture was then sub-  
cultured into 50 ml autoclaved YES broth and allowed to grow at 30 °C until

OD<sub>600</sub> of 0.2-0.3. At this OD, the culture was centrifuged at 1523 x g for 8 min at room temperature. The supernatant was discarded, and the cells were washed with 50 ml sterile distilled water (D/W). This was followed by another round of centrifugation. The cells were then resuspended in 1 ml of sterile D/W and transferred into a 2 ml Eppendorf tube. 1 ml of LiAc-TE was added to the cells, centrifuged, and the supernatant was discarded. The cells were then resuspended in 1 ml of LiAc-TE, centrifuged, discarding supernatant but leaving behind 100 µl of solution. 2 ml of carrier DNA and 2-3 µg of DNA (plasmid) which needs to be transformed are added to the solution and mixed gently. This was incubated at room temperature for 10 minutes. 260 µl of 40 % PEG/LiAc-TE was added and gently mixed. It was then incubated with shaking for 60 min in a thermomixer set at 30 °C. Centrifuged again and discarded the supernatant. 43 µl pre-warmed DMSO was added and mixed gently. Heat shock at 42 °C for 5 min was given in thermomixer. The cells were then centrifuged, washed once with 1 ml sterile distilled water, resuspended in 250 µl water, and 200 µl was plated on EMM plates (without uracil) containing thiamine for pREP42 plasmid. The plates were incubated at 30 °C for 2-3 days until colonies appeared.

## **2.9 Polymerase chain reaction (PCR)**

Mutagenesis of the *sopA* gene *in vitro* (substitutions and deletions) and amplification of mutated *sopA* fragments for cloning were made by PCR. Oligonucleotides purchased from IDT/Eurofins were resuspended in dH<sub>2</sub>O to a concentration of 100 µM. PCR mixtures contained Q5 High Fidelity 2X Master mix, oligonucleotides at 500 nM and 1 – 5 ng of template DNA. After mixing all components, the reactions were subjected to thermal cycling using an Applied Biosystems Proflex™ Thermal

Cycler instrument with the instrument lid set to 105 °C. An aliquot (5 µl) of every completed reaction was checked on an agarose gel.

**Table 2-5. The PCR reaction conditions in the thermocycler.**

Step	Temperature	Time
Initial Denaturation	98 °C	30 sec
Denaturation (30x)	98 °C	30 sec
Annealing (30x)	55-72 °C	20 sec
Extension (30x)	72 °C	30 sec/kb
Final Extension	72 °C	2 min
Hold	4 °C	

**Table 2-6. The components of the PCR reaction**

Component	Volume (25 µl)
DNA template (20ng)	1 µl
Forward primer (10 µM)	1 µl
Reverse Primer (10 µM)	1 µl
Q5 Polymerase (2X)	12.5 µl
H <sub>2</sub> O	9.5 µl



## 2.10 Protein Purification

For purification of SopA, the gene was cloned into a pET28a<sup>+</sup> construct containing a strong T7 promoter upstream of the *sopA* gene and a 6x His-tag at N-terminus (pCCD492). Moreover, this construct was transformed onto NiCo21 DE3 strain of *E. coli*, which was further used for purification. The optimised condition for expression of SopA protein was standardised as - 0.5 mM IPTG; 4 hours post-induction at 30 °C. SopA protein was purified by affinity chromatography using Ni- NTA beads.

**Table 2-7. The composition of the buffers used for protein purification**

<b>LYSIS BUFFER</b>	<b>WASH BUFFER</b>	<b>ELUTION BUFFER</b>	<b>DIALYSIS BUFFER</b>	<b>ELUTION BUFFER (Di- luted)</b>
50 mM Tris- HCl [pH 8]	50 mM Tris- HCl [pH 8]	50 mM Tris- HCl [pH 8]	50 mM Tris- HCl [pH 8]	Tris-HCl [pH 8] 50 mM
400 mM KCl	400 mM KCl	400 mM KCl	400 mM KCl	400 mM KCl
--	20 mM Imidazole	500 mM Imidazole	--	150 mM Imidazole
1 mM DTT	1 mM DTT	1 mM DTT	1 mM DTT	1 mM DTT
10 % Glycerol	10 % Glycerol	10 % Glycerol	35 % Glycerol	10 % Glycerol
0.1 % CHAPS	0.1 % CHAPS	0.5 % CHAPS	0.5 % CHAPS	0.5 % CHAPS

--	--	--	1 mM EDTA	100 mM EDTA
----	----	----	-----------	-------------

### **#Purification Protocol**

NiCo21 DE3 carrying pET28a<sup>+</sup>-SopA was inoculated into 3 ml LB with added kanamycin in 50 µg/ml concentration. From the primary culture, 1/100 vol. was sub-cultured into a 200 ml culture with 50 µg/ml kanamycin. The culture was allowed to grow till OD<sub>600</sub> of 0.6. At this OD, 0.5 mM IPTG was added to the culture. The culture was allowed to grow for the next 4 hours at 30 °C, following which it was centrifuged at 13709 x g, and the pellets were resuspended in 5 ml Lysis buffer and stored at -80 °C. The following day, 10 mg/ml Lysozyme was added onto the lysate and allowed to stand for 30 minutes. The cells were then sonicated at 60 % amplitude for 30 sec. 4 such cycles were performed. The sonicated fractions were then centrifuged at 13709 x g, 20 min twice. To the supernatant attained in this step, 0.32 mg/ml of ammonium sulphate was added and allowed to mix for 30 minutes. Following this step, the fraction was centrifuged at 13709 x g for 20 min, and the pellet attained was then mixed with wash buffer and incubated for 2 hours at 4 °C. After the incubation step, the lysate was loaded onto the column and washed with 20 CV. Then, the protein was eluted with the elution buffer and collected into the diluted elution buffer. Following elution, the eluted fractions were subjected to buffer exchange through PD10 column. Protein fractions attained after a dialysis step was passed through an Amicon filter (4 ml) for concentrating the fractions. The concentrated fractions were then mixed with an equal amount of 70 % glycerol, spun at 21000 x g for 20 min. The supernatants attained after this step was run on a 10 % SDS gel to check for the protein bands. The

purified protein concentration was then measured using Bradford assay and stored at - 20 °C in aliquots. This purified protein was then thawed once and used for EMSA, as mentioned below.

### **2.11 EMSA**

Non-specific DNA binding plays an important role in F plasmid segregation. The DNA binding ability of SopA and its mutants was detected using EMSA. Reactions were performed at 25 °C in a volume of 20 µl reaction buffer (10 mM Tris (pH 8), 50 mM KCl, 5 mM CaCl<sub>2</sub>, 0.1 mg/ml BSA, 10 mM MgCl<sub>2</sub>). Each reaction included SopA (3-12 µM) and linear Hp-FtsZ DNA (100 ng) of 1,300 base pairs, with or without ATP. SopA protein was incubated with ATP for 5 min, following which the DNA was added with EMSA buffer. Incubation was done for another 10 min. Samples were analysed on 1 % agarose gel in 0.5 X TAE buffer and visualised by staining with EtBr.

### **2.12 Membrane fractionation**

After over-expression of SopA (with 0.5 mM IPTG on the similar lines as purification), the cells were centrifuged at 13709 x g, 15 minutes and the pellet was re-suspended in MBA buffer I [50 mM Tris (pH 8), 20 mM NaCl, 20 % glycerol]. In the next step, lysozyme (10 mg/ml) was added onto the resuspension and allowed to stand for 30 min, after which the samples were sonicated. Following Sonication, the sample was centrifuged at 13709 x g twice, each for 15 min. The supernatant from this step is then spun down in TLS 55 rotor at 1,00,000 x g for 1 hour at 4°C. The pellet attained in this step was split into two parts, and MBA buffer I was added to one of the pellets. To the other fraction, MBA buffer II [50 mM Tris (pH 8), 1 M NaCl, 20 % glycerol]

was added and allowed to stand for 15 min after which, it was again centrifuged in TLS 55 rotor at 1,00,000 x g for 2 hours. The pellet and supernatant attained in this step were subjected to an SDS-PAGE and stained with Coomassie Blue.

### **2.13 Live Cell Imaging-**

Plasmids were transformed into MC4100 strain for imaging purposes. Exponentially growing cells at OD<sub>600</sub> of 0.2 were induced with either 100 or 400 µM IPTG as indicated. Following 2 hours of induction, the cells were spotted on pads made up of 1.5 % agarose in LB. Nucleoids were visualised by incubating cells with 0.5 µg/ml 4',6-diamidino-2-phenylindole (DAPI) for 15–20 min prior to analysis. Alternatively, HupA-mCherry strain was used to visualise the nucleoid. For membrane staining, 0.5 µg/ml FM-4-64 was used. Images were acquired using an epifluorescence microscope (DeltaVision Elite™) equipped with a CCD camera (CoolSNAP HQ2). A 100 X oil immersion objective lens (UPLSAPO100XO) of NA 1.4 or a phase objective (PLN100XOPH) of NA 1.25 were used for imaging. Excitation filter and emission filters of 475/28 nm and 525/48 230 nm respectively were used for imaging GFP, excitation and emission filters of 575/25 nm and 625/45 nm, respectively were used for mCherry and excitation and emission filters of 390/18 and 435/48 respectively were used for DAPI. For FM4-64, the excitation and emission filters of 542/27 and 597/45, respectively, were used. Image acquisition was done using the SoftWorx™ software, and deconvolution of images was performed using SoftWorx™ software's in-built algorithm - DECON3D: 3D iterative constrained deconvolution with a maximum of 10 iterations. All images were processed with ImageJ or Fiji (Version: ImageJ 2.1.0/ 1.53c; Java 1.8.0\_172) (Schindelin et al., 2012).

### **2.13.1 Chloramphenicol and Cephalixin treatment to condense nucleoids and inhibit cell division respectively.**

MC4100 strain carrying the mutant plasmids was grown till OD<sub>600</sub> of 0.2 and then induced with 400  $\mu$ M IPTG. Chloramphenicol (100  $\mu$ g/ml) was added to the cultures for 20 minutes to 1 hour before imaging. Chloramphenicol has been used to inhibit protein synthesis and hence cause nucleoid condensation in bacterial cells. Nucleoid occupies most of the space in an *E. coli* cell, making it often difficult to distinguish the nucleoid and cytoplasmic localisation of proteins. Thus, to further confirm the cytoplasmic localisation of the SopA mutants, we resorted to nucleoid condensation using chloramphenicol (Zusman et al., 1973; Sun and Margolin, 2004). For experiments involving the characterisation of mutants' defective in nsDNA binding, cephalixin and chloramphenicol were added together. 50  $\mu$ g/ml Cephalixin was added, earlier during induction, to the cells and incubated for either 30 min or 2 hours as indicated.

### **2.13.2. Localisation of the mutants in $\Delta$ *minB* strain**

The SopA variant plasmids were transformed into the  $\Delta$ *minB* (mini-cell forming) strain of *E. coli* (CCD252). Exponentially growing cells at OD<sub>600</sub> of 0.2 were induced with 400  $\mu$ M IPTG. After 2hr of induction, the cells were spotted on pads made up of 1.5 % agarose in LB and imaged.

## **2.14 Plasmid Stability Assay**

A two-plasmid system was used to measure plasmid stability assay (Ah-Seng et al., 2013). Expression of SopA or its variants was achieved by utilising the leaky transcription from the weakened P<sub>trc</sub> promoter of pDSW210 (ampicillin-resistant; Amp<sup>R</sup>). The other plasmid (pDAG198; a kind gift from Jean-Yves Bouet, Castaing et

al., 2008) was chloramphenicol-resistant (CamR) and carried the SopBC locus ( $\Delta$ sopA, sopBC+). SopB was expressed from the constitutively active promoter pLtetO. Both the plasmids were co-transformed into MC4100 strain of *E. coli* and allowed to grow for 10 hours at 37 °C with both antibiotics. The overnight culture was sub-cultured 1:1000 and maintained in exponential phase by sub-culturing (1:100) twice into a fresh LB tube with only carbenicillin and without chloramphenicol (selecting for pDSW210 but not for mini-F plasmid) and allowed to grow for 40 generations. Various dilutions of the culture were plated on carbenicillin plates and incubated at 37°C. Colonies were then patched on plates containing either carbenicillin or chloramphenicol to estimate the retention of mini-F plasmid that carried  $\Delta$ sopA, sopBC+(pCCD569). The plasmid loss rate was calculated following the equation “ $L = 100 \times [1 - (F_f/F_i)^{\{1/n\}}]$ ” (Ravin and Lane, 1999).  $F_i$  is the fraction of cells containing plasmid initially, and  $F_f$  is the number of cells carrying the plasmid after 40 generations (n) of growth.  $F_i$  was always close to 1, considering that most cells that grew in liquid culture in the presence of both the antibiotics contained both the plasmids. Therefore, the number of colonies initially at zero generations on plates with or without chloramphenicol was more or less the same always and thus  $F_i$  was always taken to be 1 for calculating plasmid loss.

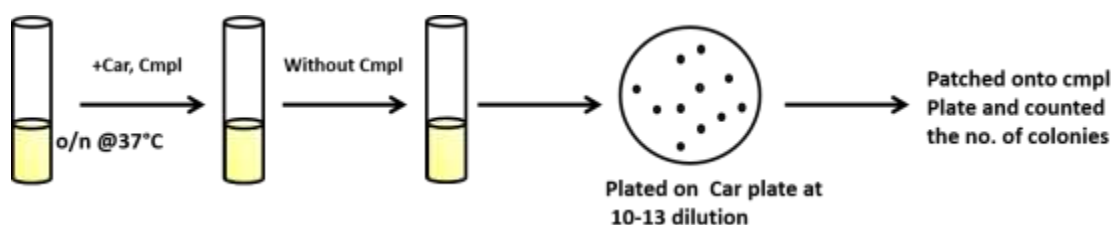


**Figure 2- 1.** Schematic diagram representing the protocol used for estimating plasmid loss rates in bacteria. Overnight cultures were grown with both antibiotics (carbenicillin, chloramphenicol) at 37 °C, following which it was sub-cultured onto fresh LB broth

with only carbenicillin and then allowed to grow for almost 40 generations. Various dilutions of the cultures were then plated on carbenicillin plates at various dilutions. The colonies that grew on the carbenicillin plate were subsequently patched on chloramphenicol plates to test for the presence of mini-F plasmids.

## 2.15 Bacterial two-hybrid analysis

A bacterial two-hybrid assay was used to detect protein-protein interactions using plasmids pUT18C and pKT25 (Karimova et al., 1998). T18 and T25 N and C-terminal fusions of SopA and SopB were constructed using plasmid pUT18C, pKT25/ pKNT25. The clones were verified by sequencing and co-transformed in- to *E.coli* BTH101 in all pairwise combinations. Colonies of pUT18C/pKT25 (or pKNT25) co-transformants were grown in LB medium with 100 µg/ml ampicillin, 50 µg/ml kanamycin and 0.5 mM IPTG overnight at 30 °C. Overnight cultures were spot-ting on indicator MacConkey plates supplemented with 100 µg/ml ampicillin, 50 µg/ml kanamycin and 0.5 mM IPTG and incubated at 30 °C for up to 48 hours before imaging the plates. SopB was cloned both as N-terminal fusion (in pKT25 vector) as well as C-terminal fusion (in pKNT25 vector). However, since interaction was also observed in the case of N-terminal fusion of SopB (in pKT25) and N-terminal fusion of SopA (in pUT18C), all results presented in this thesis are with these sets of vectors.

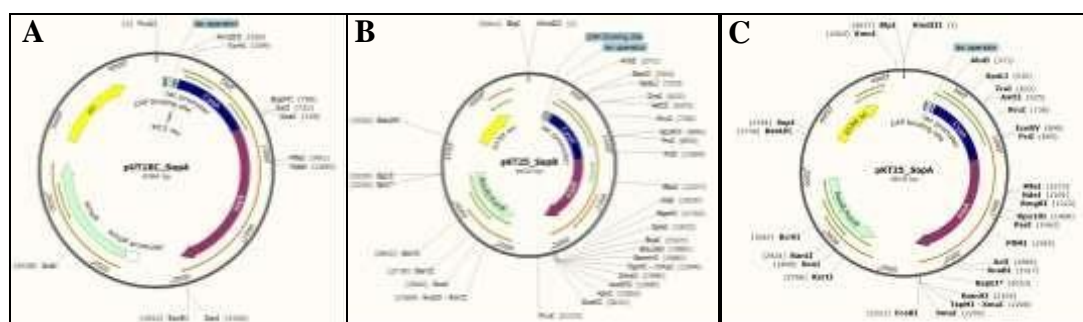


**Figure 2-2.** Depiction of vector maps of (A) pUT18C-SopA, (B) pKT25-SopB

and (C) pKT25-SopA sequences created using Snapgene<sup>TM</sup>. The SopA and SopB genes were cloned as N-terminal fusion in all the cases. The *cyoA* gene has been highlighted in blue colour.

## **2.16 Promoter repression assay**

### **2.16.1. LacZ activity indicator plate assay (Qualitative)**

A qualitative assay using X-gal+IPTG or MacConkey agar plates was used to detect the LacZ activity. We initially transformed the wild-type SopA clone as well as SopA(stop) mutants with or without mini-F plasmids ( $\Delta$ sopAsopBC+; pCCD569) into DLT1127 strain (CCD358; *Psop::lacZ*). The colonies thus attained were inoculated into 3 ml LB media with all the three antibiotics carbenicillin, chloramphenicol and kanamycin (in case of strains carrying mini-F plasmid) or carbenicillin and kanamycin (in case of strains without the SopBC plasmid). The overnight culture was then sub-cultured 1/100<sup>th</sup> volume into fresh LB with the antibiotics. Growth was continued until the cultures reached an OD<sub>600</sub> of 0.2, following which the cultures were induced with 400  $\mu$ M IPTG for 2 hours. Subsequently, the OD<sub>600</sub> of all the cultures were determined and normalised. In the next step, serial dilutions of the cultures were made in a 96 well plate and then spotted on indicator plates- X-gal (40  $\mu$ g/ml) + IPTG (0.5 mM) or X-gal + Glucose (2 %) or MacConkey agar plates. These plates were then incubated at 37 °C for overnight, following which they were imaged.

### **2.16.2. Beta-Galactosidase assay (Quantitative)**

Beta Galactosidase assays were performed as described (Griffith and Wolf Jr, 2002). Briefly, 2 ml culture at OD<sub>600</sub> of 0.6 was used for all assays. OD<sub>600</sub> values of all the samples were normalised. All samples were centrifuged at 1523 x g, 10 min, 4 °C.



The pellet was mixed with Z-buffer (0.06 M Na<sub>2</sub>HPO<sub>4</sub>, 0.04 M NaH<sub>2</sub>PO<sub>4</sub>, 0.01 M KCl, 0.001 M MgSO<sub>4</sub>, pH 7.0). Immediately before use, 50 µM β-mercaptoethanol was added to Z-buffer. The OD<sub>600</sub> values were further measured to confirm that all the samples have the same cell density. CHCl<sub>3</sub> (20 µl) and SDS (20 µl of 0.1 % solution) were added to the cultures to permeabilise the cells. Samples were then vortexed for one minute and incubated at 28 °C for 10 minutes. Then 4 mg/ml nitrophenyl-β-D-galactopyranoside (ONPG) (0.13 mM final concentration) was added as a substrate for the reaction. This was recorded as time zero for the assay. When ONPG is hydrolysed by β-galactosidase into galactose and o-nitrophenol, the solution colour turns yellow. The reaction was stopped by adding 100 µl of 1 M Na<sub>2</sub>CO<sub>3</sub> after a sufficient yellow colour had developed and the time of colour development was recorded (in minutes). OD<sub>420</sub> and OD<sub>550</sub> were measured for each sample. Values of the β-galactosidase activity were determined in Miller units using the formula:

$$\text{Miller Units (MU)} = 1000 \times [\text{OD}_{420} - (1.75 \times \text{OD}_{550})] / (\text{T} \times \text{V} \times \text{OD}_{600}).$$

T is reaction time (minutes), V is the volume of culture used (ml).

## **CHAPTER 3**

# **IDENTIFICATION OF AN AMPHIPATHIC HELIX WITHIN THE C-TERMINAL 360 – 388 RESIDUES OF SOPA**

### 3.1 INTRODUCTION

SopA is one of the members of the ParA superfamily of proteins that enables segregation of low copy number F plasmid. The Sop system includes a centromeric sequence *sopC*, an adaptor protein SopB and an ATPase SopA (Ogura and Hiraga, 1983). SopB binds to the centromeric sequence on the plasmid *sopC* forming fluorescent foci. Localisation pattern of SopA protein plays a major role in giving directionality to SopB-*sopC* complex (or simply called as SopBC complex), which is essentially the F plasmid, and thus driving the segregation process. SopBC complex chases the gradient of SopA-ATP on the nucleoid. Visualisation of ParA using immunofluorescence microscopy reveals that these proteins are associated with the nucleoid (Hirano et al., 1998; Marston et al., 1999; Ebersbach and Gerdes, 2001), and migration of ParA is restricted to the nucleoid region of the cell (Marston and Errington, 1999; Quisel et al., 1999; Ebersbach and Gerdes, 2001; Hatano et al., 2007). Moreover, more recently, the *in vitro* reconstitution of Sop system using DNA carpeted flow cell and whole-chromosome labelling using multicolour super-resolution microscopy also hints at the role of the nucleoid in segregation (Vecchiarelli et al., 2013; Le Gall et al., 2016). However, on binding to nucleoid-associated SopA-ATP\*, SopB stimulates the ATP hydrolysis of SopA and thus removes the SopA-ATP bound form from the nucleoid creating a gradient of SopA-ATP\* on the nucleoid. Generation of this gradient of SopA-ATP\* is mainly associated with the formation of SopA-ATP/ ADP and its release from the nucleoid. Moreover, the SopA-ATP form needs to undergo a conformational change to bind to the nucleoid again. Thus, the time lag of conversion of SopA-ADP to SopA-ATP or, more specifically the SopA-ATP\* state plays a vital

role in maintaining the gradient. Earlier work has revealed that both F plasmid, as well as P1 plasmid, are stably maintained in a *mukB* deletion strain (Funnell and Gagnier, 1995). Further, Hiraga and group (Ezaki et al., 1991) have also provided evidence of F plasmid segregating efficiently onto anucleate cells highlighting that some additional host factors along with nucleoid binding play a key role in the process of segregation. Moreover, a mini-F plasmid is unstable in a *ugpA* null strain, further suggesting that UgpA might be a relevant host factor involved in the process (Ezaki et al., 1990). Earlier studies on SopA (Lin and Mallavia, 1998) have revealed 63% of SopA protein in the membrane fractions as against the 32.7% in the cytosolic fraction, further proving that SopA might be a membrane associating protein (Lin and Mallavia, 1998). Consistent with all these studies, it has also been reported that changes in membrane composition and imbalance in phospholipid, as well as lipid II biosynthesis, lead to plasmid loss (Inagawa et al., 2001), indicative of a greater role of membrane in plasmid segregation.

Interestingly, a spontaneous double mutant of SopA, SopA1 (M315I Q351H), produces filament phenotype in contrast to the nucleoid localisation pattern of SopA (Lim et al., 2005). On careful analysis of the sequence, it was observed that the mutation in SopA1 mapped to the C-terminal stretch of the protein. Similar filament phenotype has been observed in case of membrane binding protein FtsA upon deletion of MTS (membrane targeting sequence). Moreover, many membrane-binding proteins found in bacteria have either a C-terminal (e.g., FtsA, MinD) or an N-terminal (e.g., Noc) stretch of an amphipathic helix, acting as MTS (Pichoff and Lutkenhaus, 2005; Szeto et al., 2002; Strahl and Hamoen, 2010). All these data led us to postulate that SopA, like other membrane-binding proteins, might have an MTS at the C-terminal stretch, perturbation of which leads to filament phenotype.

In this chapter, we describe our findings on the role of the C-terminal helix in F plasmid segregation. We find the SopA contains a potential amphipathic helix within the C-terminal helix and is required for stable maintenance of plasmids. Further, using membrane fraction assays, we confirm that a proportion of SopA is indeed associated with bacterial membranes. In an independent study, we have carried out *in silico* molecular dynamics simulation analysis (Pahujani, 2020), which reveals that the predicted amphipathic helix has a weak affinity to membranes. Taken together, we identify a potential amphipathic helix in the C-terminus of SopA and show that the last C-terminal helix of SopA has a role in plasmid maintenance (Mishra et al., 2021).

## **3.2 RESULTS**

### **3.2.1 The C-terminus of SopA is predicted to form an amphipathic helix**

SopA is a member of the Type-Ia family of P loop ATPase wherein other major members of this family are recruited for either plasmid or chromosome segregation. These proteins exhibit non-specific DNA binding activity and are thus always found localised to the nucleoid (Castaing et al., 2008; Vecchiarelli et al., 2010; Roberts et al., 2012; Le Gall et al., 2016). Nonetheless, earlier work on F plasmid has revealed its presence in anucleate cells independently of the bacterial chromosome (Ezaki et al., 1991). Biochemical assays have established that a significant proportion of the SopA protein exists in membrane fractions, and this accounts up to 63% (Lin and Mallavia, 1998). Interestingly, unlike the nucleoid binding activity of wild-type SopA, one of SopA mutants, SopA1 (M314I Q351H), exhibits polymerisation and assembles into filaments in *E. coli* (Lim et al., 2005 and **Fig. 3-1A**). This spontaneous double mutant maps close to the last C-terminal helix of the protein (**Fig. 3-1B**). Membrane binding

protein FtsA also exhibits a similar filament phenotype (like SopA1) upon deletion of its C-terminal MTS (Pichoff and Lutkenhaus, 2005). A Multiple Sequence Alignment (MSA) using Clustal Omega of different members of ParA family-like MinD, QSopA, ParA, SopA and ParF proteins (Madeira et al., 2019) revealed subtle differences in the C-terminal stretch among members of ParA superfamily (**Fig. 3-1C**). The last C-terminal helix of SopA might thus behave differently from other well studied members of this family.

Since many known membrane-binding proteins have either a C-terminal or an N-terminal amphipathic helix functioning as an MTS, we set out to identify whether SopA C-terminal residues carry the potential to form an amphipathic helix. To do so, we used AMPHIPASEEK, a software designed to identify amphipathic residues (Sapay et al., 2006). AMPHIPASEEK data revealed that the C-terminus of SopA has a membrane targeting amphipathic residues that span from A361 to V373 amino acids (**Fig. 3-1D i**). However, no such amphipathic helix was detected in the case of a related ParA superfamily member P1 ParA (**Fig. 3-1D ii**). Further, helical wheel projections using Softwares HeliQuest (Gautier et al., 2008) as well as Netwheels (Mól et al., 2018) revealed the presence of a hydrophobic face in the C-terminal helix (**Fig. 3-1E**). Such hydrophobic patch was also predicted for other membrane-binding proteins like FtsA and MinD (**Fig. 3-1E**). Taken together, these data suggest that C-terminus of SopA is divergent from other members of ParA family and has amphipathic residues that might contribute to membrane binding. Moreover, molecular dynamics simulation of the C-terminal amphipathic helix of SopA revealed weak membrane affinity of the SopA protein (Pahujani, 2020; Master thesis work by undergraduate student Sakshi Pahujani, in collaboration with Dr. Anand Srivastava lab, IISc).

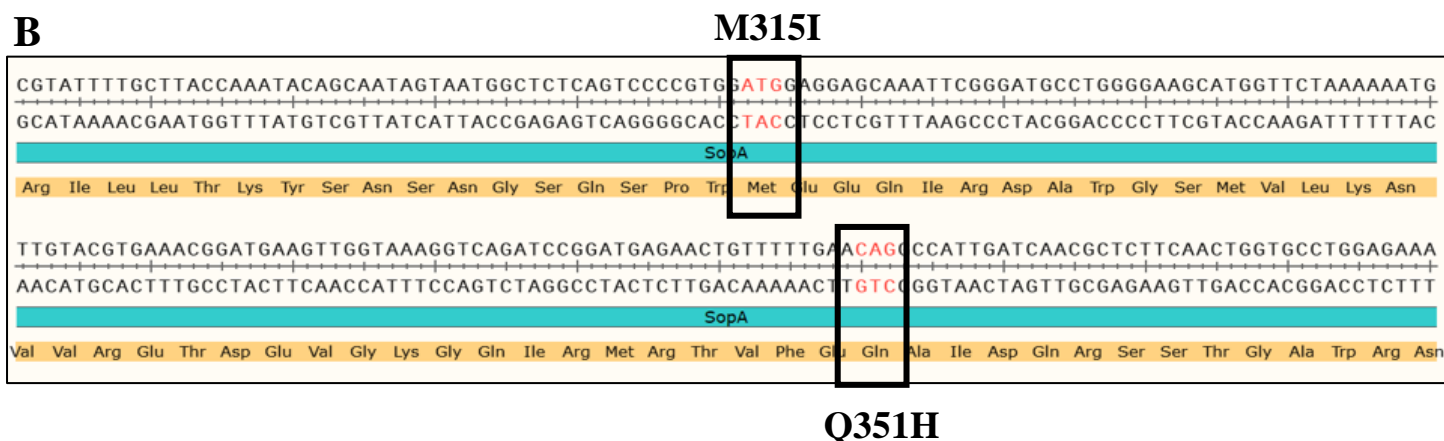
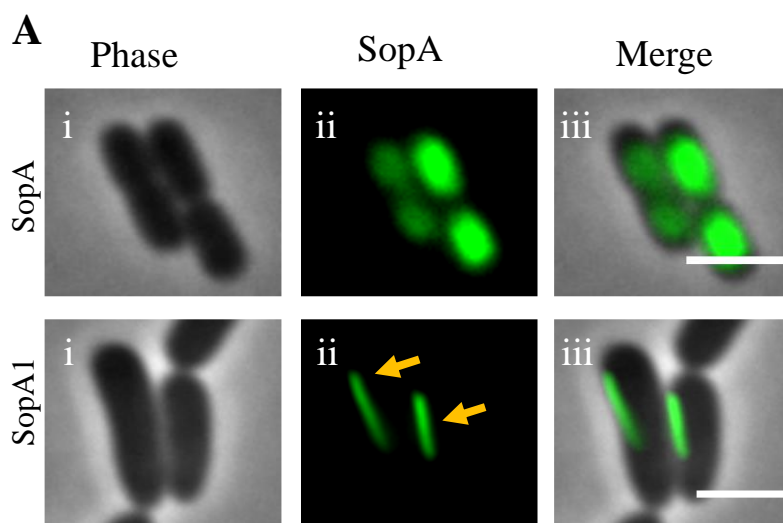
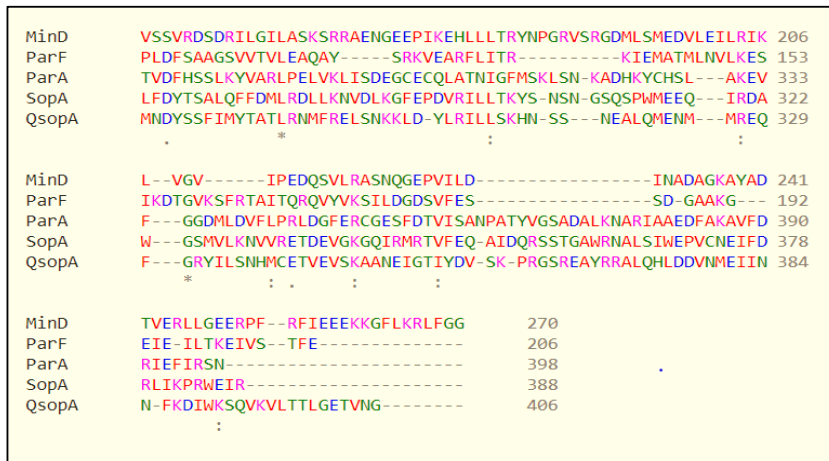


**Figure 3-1. Prediction of a C-terminal amphipathic helix in SopA.**

(A) **SopA1 assembles into polymers.** Wide-field imaging of *E. coli* MC4100 cells harbouring wt-SopA and SopA mutant plasmids. MC4100 strain with the mutant SopA plasmids was grown till OD<sub>600</sub> of 0.2 induced with 400 μM IPTG (as described in Materials and Methods) and was imaged by fluorescence microscopy. The arrows point to the filaments observed in the case of SopA1. Scale bar is 2 μm. (B) **Sequence of SopA C-terminal region.** The image was created using SnapGene™, and the residues altered in SopA1 are highlighted in red.

C



D

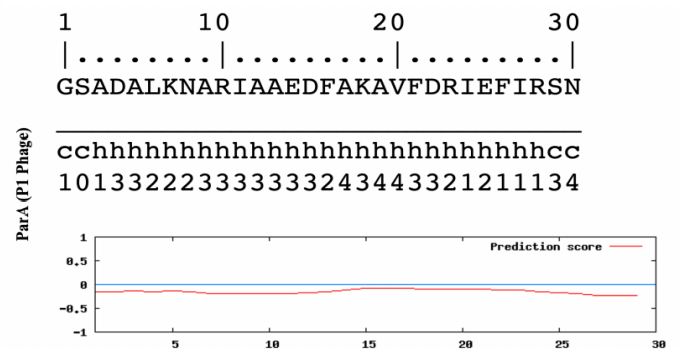
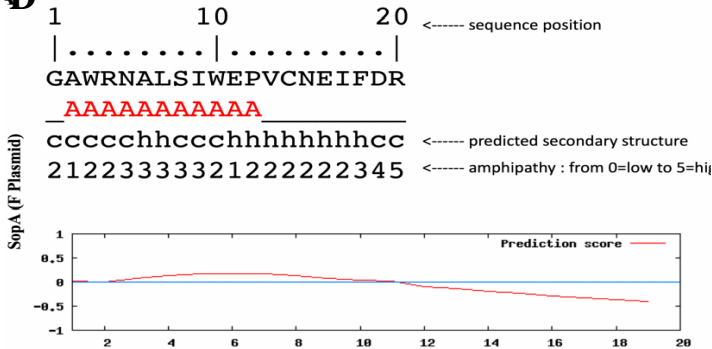


**Figure 3-1. (C) Multiple Sequence Alignment of different members of ParA superfamily.** The Multiple Sequence Alignment was created using Clustal Omega. The sequence in the C-terminal region does not show a high degree of conservation among the different members of the ParA family. **(D) Amphipathic helix prediction in SopA and P1 ParA.** AMPHIPASEEK was used to predict the presence of amphipathic helices in the C-terminal region of **(i) SopA** and **(ii) P1 ParA**. The red “A”s indicate a putative amphipathic helical region in the sequence spanning from residues A361 to V373 in SopA; however, no amphipathic helix is observed for P1 ParA.



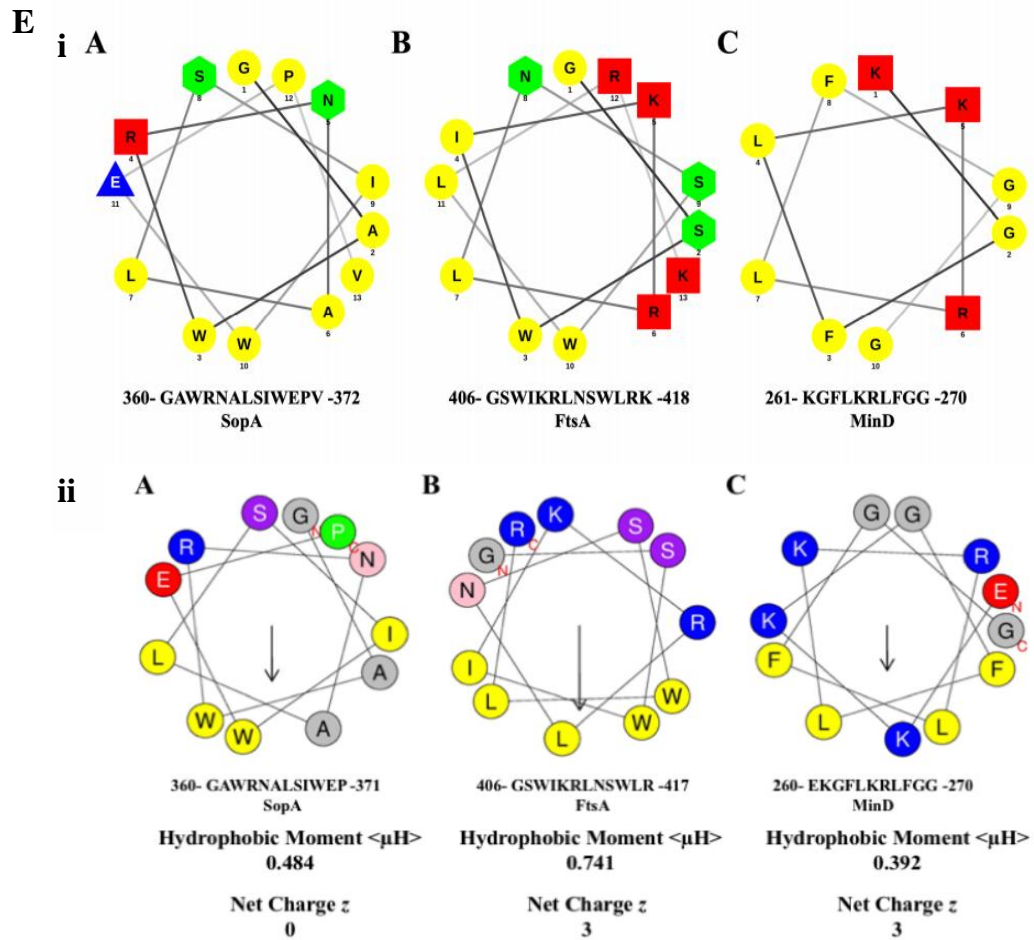


**Figure 3-1. (E) Helical wheel projection of the C-terminal amphipathic helix (G360-R379) in SopA.** Helical wheel projection diagrams were generated using (i) NetWheels and (ii) HeliQuest. (A), (B) and (C) in (i) and (ii) represent the helical wheels for SopA, FtsA and MinD respectively. They show the presence of a hydrophobic and polar face in the predicted amphipathic helix. Residues are coloured according to their properties.

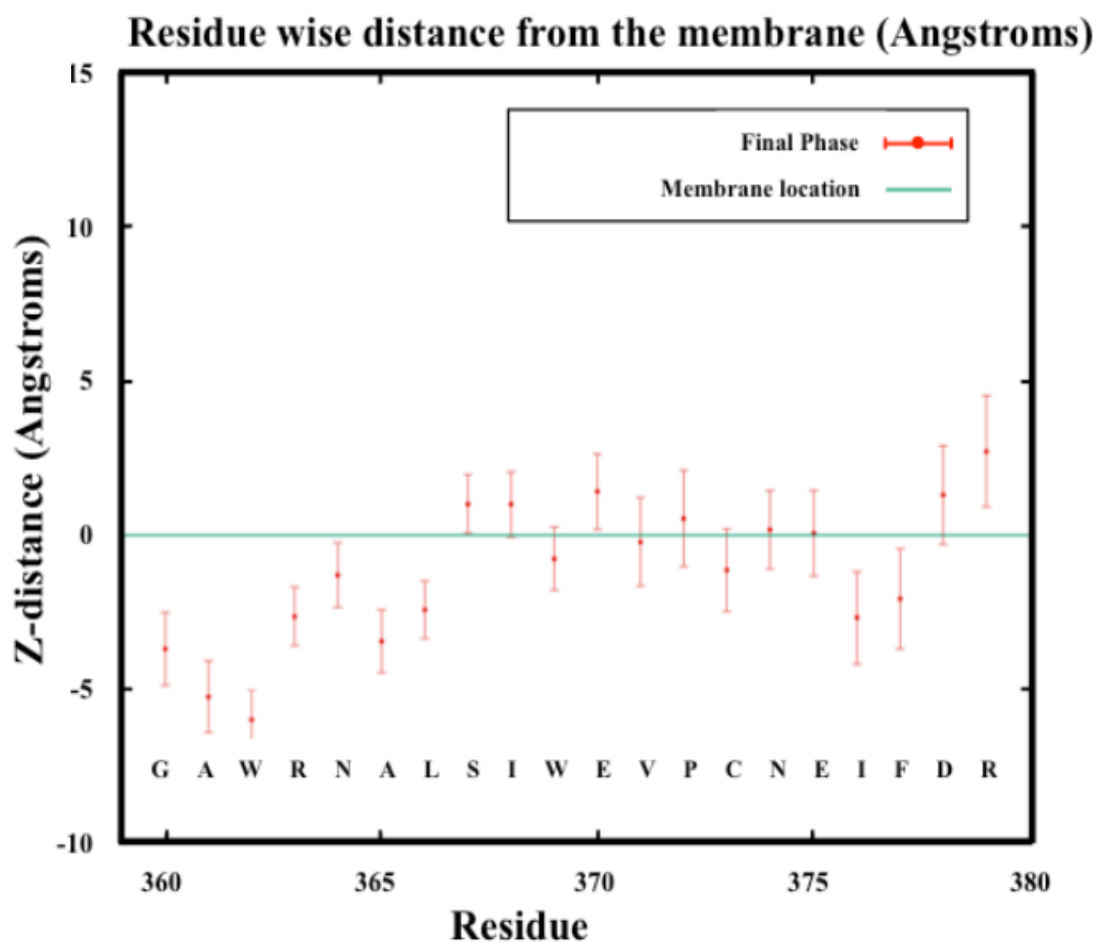


**Figure 3-1. (F) Molecular dynamics simulations of SopA C-terminus highlighting the relevance of individual residues in membrane association.** A plot of the residue wise distance from the membrane reveals that among all residues in C-terminal stretch, residues 360 (**G**), 361 (**A**), 362 (**W**), 364 (**N**), 365 (**A**), 366 (**L**), 369 (**W**), 373 (**C**), 376 (**I**) and 377 (**F**) lie closer to the phosphate plane. (Reproduced from Figure 3.D, Mishra et al., 2021)

A plot of residue wise distance from the membrane indicates that specific residues in the C-terminus lie closer to the phosphate plane, suggestive of membrane association of the SopA protein (**Fig. 3-1F**; reproduced from Mishra et al., 2021).

### **3.2.2 Association of SopA with the membrane in a $D\Psi$ -sensitive manner**

The transmembrane potential plays an important role and affects the localisation pattern of peripheral as well as integral membrane proteins. Poly-L-lysine is a chemical that dissipates the transmembrane chemical proton gradient (Katsu et al., 1984) and thus affects the localisation of bacterial peripheral proteins like FtsA, MinD, MreB and Noc (Strahl and Hamoen, 2010; Adams et al., 2015). Noc is a nucleoid-associated protein (Wu et al., 2009; Adams et al., 2015) however, the disruption of the membrane potential causes delocalisation of the Noc and results in punctate appearance near the membrane periphery (Adams et al., 2015). To test if transmembrane potential affects the localisation pattern of SopA in a similar manner, we examined cells treated with poly-L-lysine, we performed live-cell imaging of wild-type SopA protein in slides coated with 0.1 % poly-L-lysine and in agarose pads without poly-L-Lysine in HupA-mCherry strain of *E. coli* (**Fig. 3-2A and B**). Strikingly, the localisation pattern of SopA was altered after the addition of poly-L-Lysine. Consistent with our findings, SopA in the presence of poly-L- lysine formed discrete spots that were no more found on the nucleoid but rather closer to the periphery of the cell. However, in control, i.e., cells without poly-L-lysine treatment, the localisation pattern of SopA protein was on the nucleoid. This data was in similar lines to other reported membrane-binding proteins like Noc, FtsA and MreB. Further, these experiments were performed using HupA-mCherry strain (kind gift from Dr. Mohan Joshi) (Marceau et al., 2011; Fisher et al., 2013), wherein the nucleoid could be visualised.

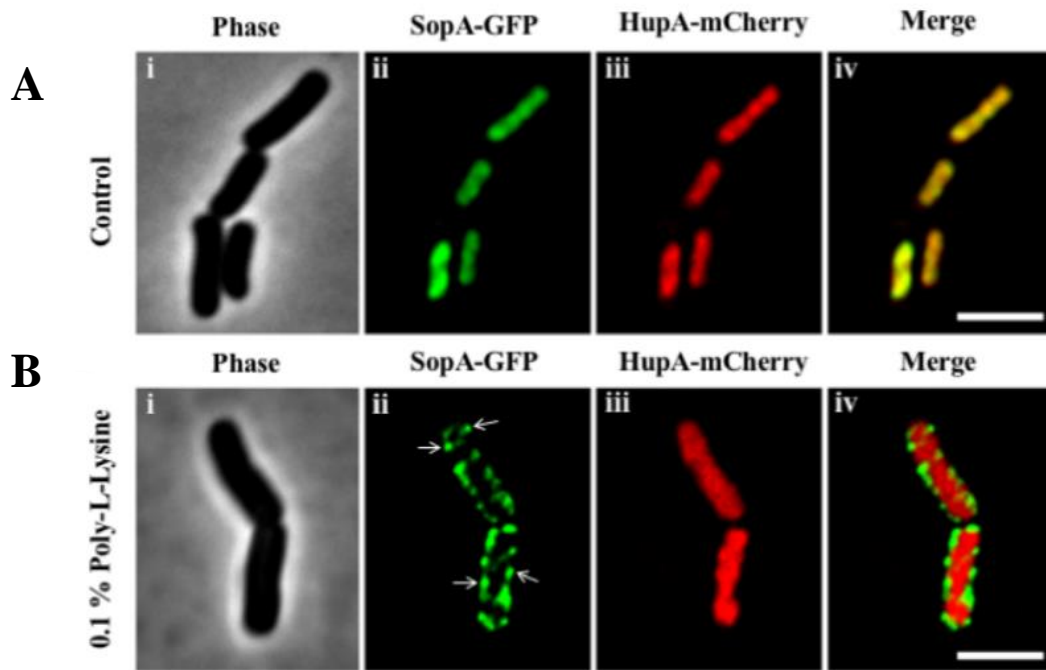


**Figure 3-2. SopA localisation to nucleoids is sensitive to the membrane potential  $\Delta\Psi$ . (A) and (B) Effect of poly-L-lysine on the localisation of SopA in HupA-mCherry strain of *E. coli*.** Cellular localisation of SopA either in the (A) absence of (NA) or (B) in the presence of 0.1 % poly-L-lysine treatment on slides. Wide-field imaging of *E. coli* HupA-mCherry cells harbouring wild-type SopA plasmids. HupA-mCherry strain carrying the wild-type SopA plasmid was grown till an OD<sub>600</sub> of 0.2 induced with 400  $\mu$ M IPTG (as described in Materials and Methods). Cells were added on slides coated with 0.1% poly-L-lysine and were examined by fluorescence microscopy.

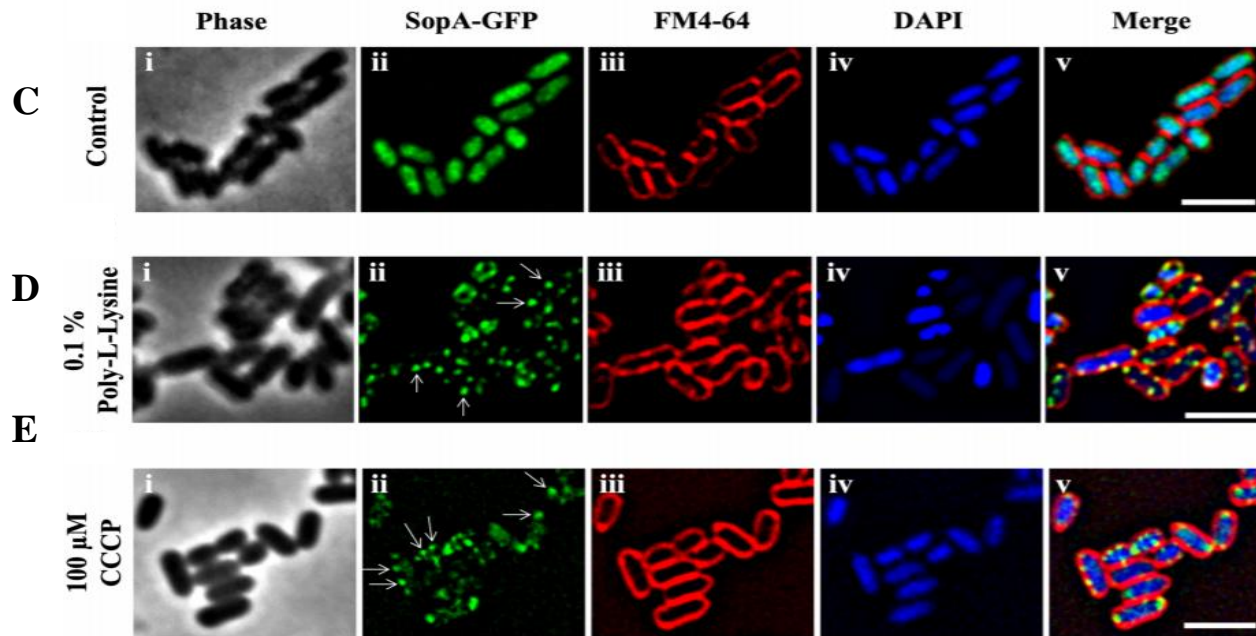


**Figure 3-2. (C – E) Effect of the ionophores, poly-L-lysine and CCCP (100  $\mu$ M for 5 min) on the localisation pattern of SopA.** *E. coli* strain MC4100 was used for these experiments. Cellular localisation of SopA either (C) without the addition (NA) of poly-L-lysine or (D) on slides treated with 0.1 % poly-L-lysine or (E) treated with CCCP on agarose pads. The nucleoids were stained with DAPI, and the cell membrane was stained with FM-4-64. Scale bar is 3  $\mu$ m.

Unlike in the case of SopA, no change in localisation of HupA-mCherry was observed in the presence of poly-L-Lysine, suggesting that the shift in localisation of SopA was not a non-specific effect of protein delocalisation from the nucleoid. The alteration of localisation pattern of SopA upon poly-L-lysine treatment was also independent of the host strain used and was similar in the case of both MC4100 and HupA-mCherry strain of *E. coli*, a derivative of MG1655.

To further test whether membrane potential plays a role in the peripheral localisation of SopA, we also examined cells treated with the ionophore carbonyl cyanide *m*-chlorophenyl hydrazone (CCCP), which dissipates both  $\Delta\Psi$  and the transmembrane chemical proton gradient ( $\Delta\text{pH}$ ). SopA localisation pattern was altered after 5 min of CCCP treatment, i.e., unlike the nucleoid localisation pattern, SopA localised as discrete spots in the cell, identical to the localisation pattern attained in the presence of poly-L-lysine. Together, these data show that the localisation of SopA, like other known membrane-binding proteins, is sensitive to the membrane potential of the cell (**Fig. 3-2C, D and E**).

### **3.2.3 Role of host factors in SopA localisation**

The above studies showed that membrane potential disruption led to relocalisation of SopA from the nucleoids to the proximity of membranes. Such localisation near the membrane periphery could possibly be mediated by membrane-bound host proteins. We suspected that UgpA could possibly be one such host factor since it has been reported that mini-F plasmids are unstable in a *ugpA* null strain (Ezaki et al., 1990). Further, UgpA is an integral membrane protein associated with sn-glycerol-3-phosphate and glycerol phosphate diester transporter proteins (Schweizer et

al., 1982). To further test if UgpA played a role in the relocalisation of SopA into discrete spots near the membrane periphery, we made use of a  $\Delta ugpA$  (KEIO collection, a kind gift from Dr. Rachna Chaba; Baba et al., 2006). We transformed our plasmid pDSW210 SopA-GFP into  $\Delta ugpA$  strain and checked for localisation of SopA-GFP in the presence of ionophore CCCP. We observed that SopA still localised as discrete spots in stark contrast to the nucleoid localisation pattern observed for the wild type SopA in the  $\Delta ugpA$  strain in the absence of CCCP (**Fig. 3-3**). Thus, *ugpA* is not directly involved in the relocalisation of SopA as discrete spots upon disruption of the membrane potential and involvement of another host factor, if any, needs to be probed further. Other than UgpA, MinD would be strong candidate as it is known in *B. subtilis* that MinD interacts with the ParA homolog Soj (Autret and Errington, 2002). The actin cytoskeleton, MreB, is another candidate as it interacts with several bacterial proteins including RnaseE (Taghbalout and Rothfield, 2006), RNAPol  $\beta$ -subunit (Kruse et al., 2006) and FtsZ (Fenton and Gerdes, 2013). Another possible candidate is the HflB/FtsH protease, whose absence has been shown to affect the F plasmid stability (Inagawa et al., 2001).

### **3.2.4 Membrane association of SopA protein**

Our *in silico* data using AMPHIPASEEK and the molecular dynamics simulation, as well as *in vivo* imaging data point at the membrane localisation of SopA protein. Moreover, biochemical assays done earlier have also revealed membrane

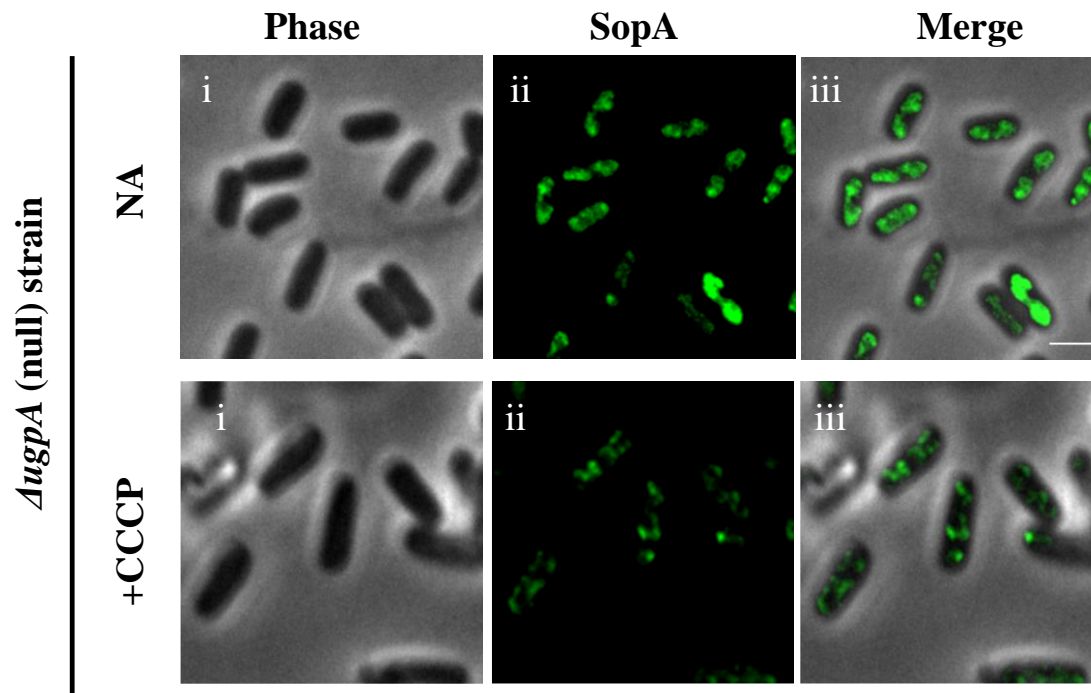


**Figure 3-3. SopA relocalisation to membrane periphery is independent of *ugpA*.**

Cellular localisation of SopA (**top panel**) or after CCCP treatment (**bottom panel**) on agarose pads in a *ΔugpA* (null) strain. Scale bar is 2  $\mu$ m.



association of SopA protein (Lin and Mallavia, 1998). To confirm the membrane association of SopA *in vitro*, we made total membrane fractions from bacteria expressing SopA and tested if SopA was detectable in these membrane fractions. We cloned SopA into a T7 promoter containing pET28a+ plasmid and over-expressed it in NiCo21 DE3 strain, prepared various fractions of the bacterial lysate and analysed them by SDS PAGE. SopA was detectable in both the cytosolic and membrane fractions, in coherence with earlier studies (**Fig. 3-4A**). The presence of SopA protein in the membrane fraction was not an over-expression artefact as a low-level expression of SopA from a tightly regulated arabinose promoter also revealed membrane association of SopA (Mishra et al., 2021). Further, the membrane to the cytosolic ratio for the protein, as determined by densitometric analysis, was  $0.9 \pm 0.12$  (SEM; n=3), suggesting clear membrane association of the protein (**Fig. 3-4B**).

We also tested whether SopA  $\Delta$ Ct29 was recovered in the membrane fraction. However, upon over-expression, unfortunately, we found that SopA  $\Delta$ Ct29 was primarily insoluble. Thus, to identify the role of C-terminal stretch in membrane association, we took advantage of a hydrophobic residue W369 in the C-terminus of the protein and exchanged it for glutamic acid. We then performed a membrane pelleting assay using this mutant SopA W369E. SopA W369E was also recovered in the membrane pellet with a membrane to cytosolic ratio comparable to wild type SopA (**Fig. 3-4B**), suggesting that mutation of the hydrophobic residue W369 to E does not affect membrane localisation of SopA. Thus, W369 is not a critical residue involved in the membrane association of SopA. Together, these data show that SopA might be a membrane-binding protein, but C-terminal hydrophobic residue W369 is not a key residue involved in the process.

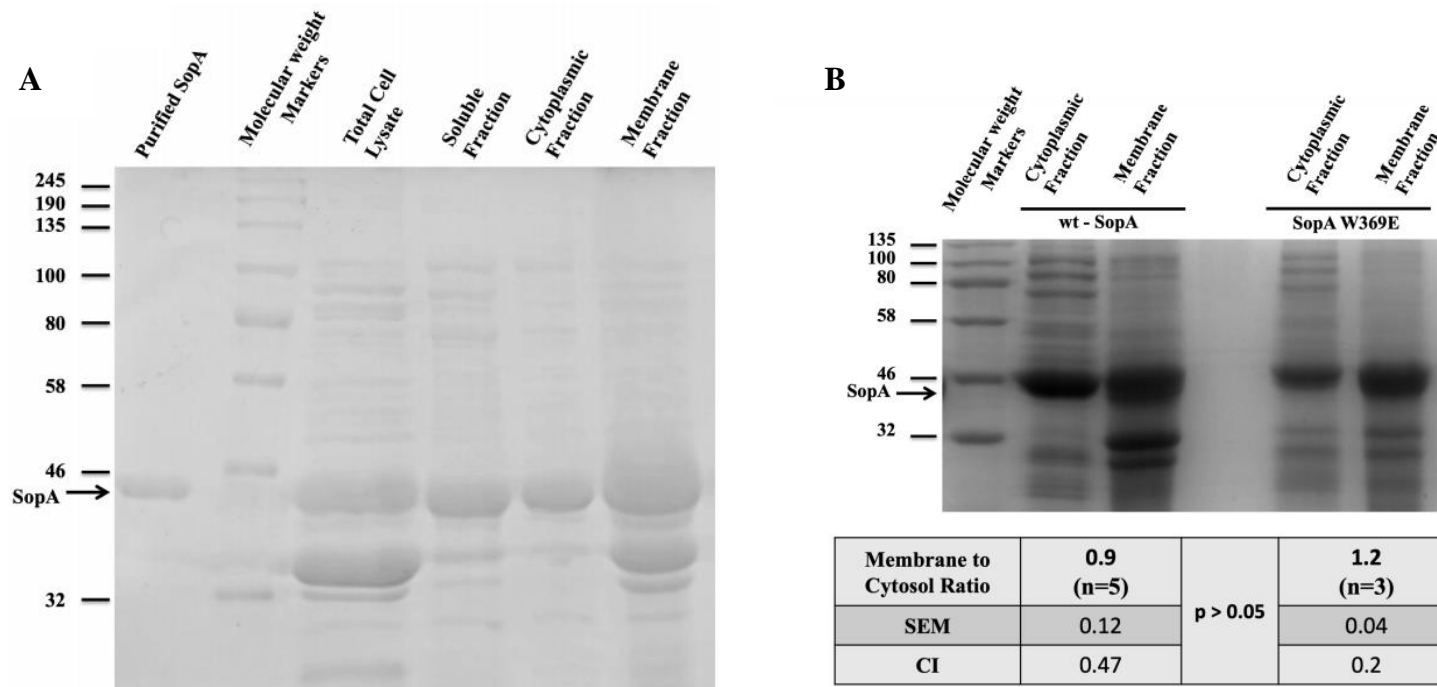


**Figure 3-4. SopA in bacterial membrane fractions.**

**(A) wtSopA is detectable in Membrane Fractions of Bacterial Lysates.** SopA was cloned and expressed from a pET28a+ vector with an N-terminal 6xHis-tag in the NiCo21 DE3 strain of *E. coli*. Over-expression of the protein was carried out by induction with 0.5 mM IPTG at OD<sub>600</sub> of 0.6 for 4 hours. The cells were pelleted, total cell lysate and membrane fractions were prepared and subjected to SDS-PAGE. **(B) Mutation of the C-terminal hydrophobic residue W369 does not affect membrane binding.** Membrane pelleting assay carried out using SopA W369E mutant showed that a significant fraction of the protein was recovered in the membrane pellet fraction. Densitometric analysis revealed that a significant proportion of SopA W369E localises to the membrane, with the membrane to cytosolic ratio being 1.2. The ratio was similar to the proportion observed in the case of wt-SopA.

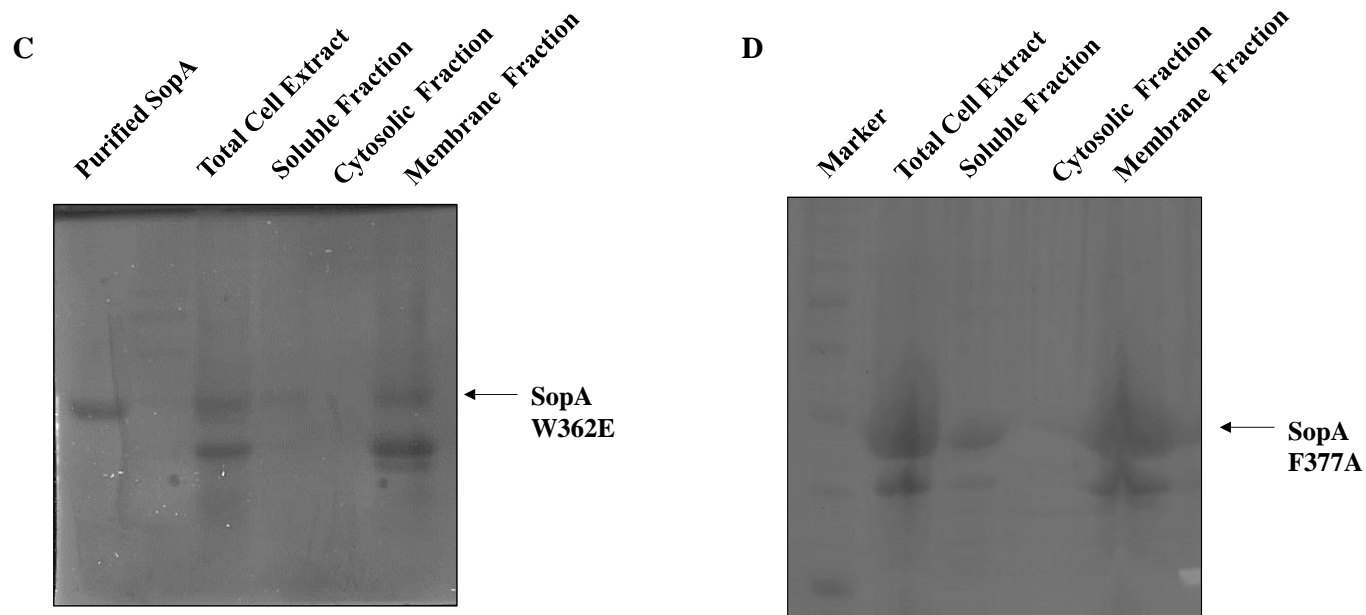


**Figure 3-4. (C) and (D) Mutation of the hydrophobic residues W362 or F377A do not affect membrane association.** Membrane pelleting assay was carried out using (C) SopA W362E and (D) SopA F377A mutant, and it showed that a significant fraction of the protein was recovered in the membrane pellet fraction, indicating that both these residues are not required for membrane association.

We also mutated the other hydrophobic residues W362 and F377 and tested for their presence in the bacterial membrane fractions. We found that both SopA W362E and F377A were recovered in membrane pellets suggesting that single mutations in neither of these hydrophobic residues abrogated the membrane association of SopA (**Fig. 3-4C and D**).

### **3.2.5 SopA association to the membrane is dimerisation independent**

Membrane association of MinD is mediated by a specific conformation. For membrane-binding protein MinD, a dimeric state of the protein is essential to bind to the bacterial membrane (Hu et al., 2002). Moreover, this dimeric conformation is achieved upon ATP binding as a MinD ATP binding mutant K16Q is impaired in binding to the membrane (Hu et al., 2002). To further explore whether SopA binding to the membrane was also dependent upon ATP or dimerisation, we generated a known ATP binding mutant of SopA. The K122 in P1 ParA and the equivalent residue K120 in F SopA have been reported to be important for ATP binding and hydrolysis, and mutating this residue to glutamic acid has been shown to affect ATP binding (Fung et al., 2001; Vecchiarelli et al., 2013). We thus generated this mutant SopA K120E, which was then tested for its ability to associate with the membrane using both *in vivo* as well as *in vitro* assays. Consistent with the essential role of ATP binding in nucleoid association, the SopA K120E mutant exhibited diffuse fluorescence. However, upon CCCP treatment, we were able to observe the localisation of SopA K120E mutant as discrete spots close to the membrane periphery similar to the wild-type SopA (**Fig. 3-5A**). Further, on similar lines, we also tested whether the mutation in another reported conserved Glycine in the Walker A motif, SopA G116V (**Fig. 3-5B**), affected localisation upon membrane potential dissipation.

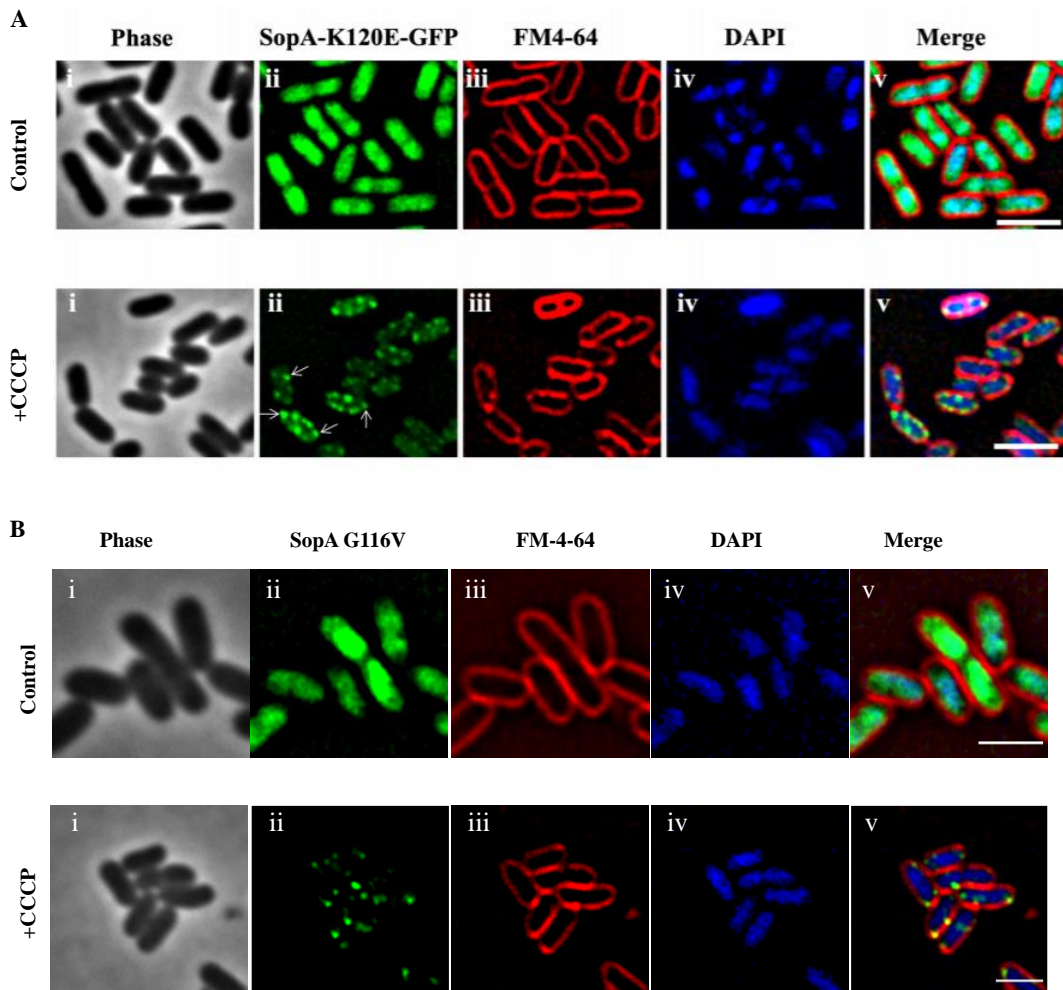
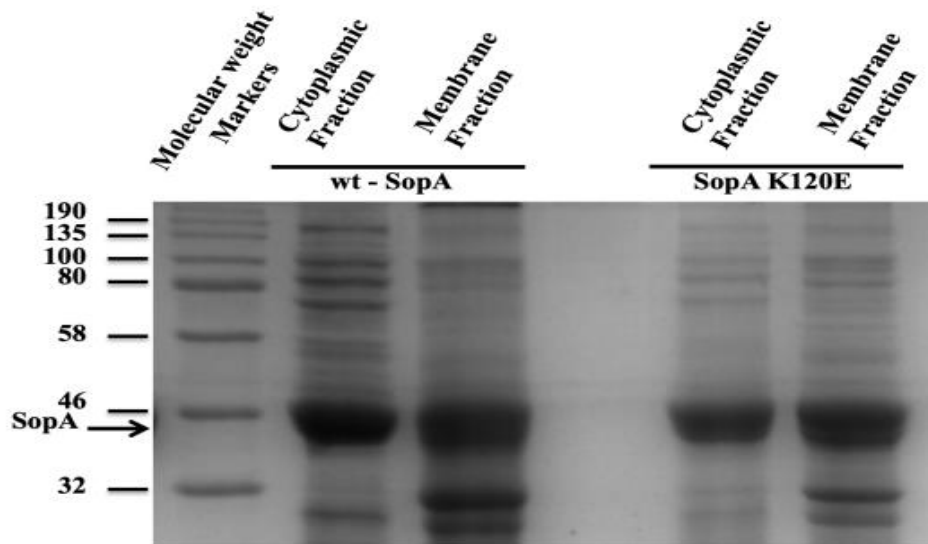


**Figure 3-5. SopA relocation to the membrane periphery is independent of its ATP binding.**

**(A) and (B) Effect of ionophore on the localisation of SopA ATP binding/dimerisation mutants.** Localisation of **(A) SopA K120E** and **(B) SopA G116V** is diffuse in the cell (top panels). However, upon treatment of CCCP, the localisation pattern changes from being diffused to spots in the cell (bottom panels in A and B). *E. coli* strain MC4100 was used for expressing SopA and imaging.



<b>Membrane to Cytosol Ratio</b>	<b>0.9 (n=5)</b>	<b>p &gt; 0.05</b>	<b>0.8 (n=3)</b>
<b>SEM (n=3)</b>	0.12		0.03
<b>CI</b>	0.47		0.1

**Figure 3-5. (C) SopA K120E is detectable in Membrane Fractions of Bacterial Lysates.** SopA K120E was cloned and expressed from a pET28a+ vector with an N-terminal 6xHis-tag in the NiCo21 DE3 strain of *E. coli*. Over-expression of the protein was carried out by induction with 0.5 mM IPTG at OD<sub>600</sub> of 0.6 for 4 hours. The cells were pelleted, total cell lysate and membrane fractions were prepared and subjected to SDS-PAGE. Densitometric analysis reveals that a significant proportion of SopA K120E localises to the membrane with the membrane to a cytosolic ratio of 0.8, close to the proportion observed in the case of wt-SopA.

This mutant G12V in the ParA homolog Soj has been reported to be ATP binding proficient but dimerisation defective mutant (Scholefield, 2011; Lutkenhaus, 2012). Even in this case, discrete spots were observed in the presence of ionophores, suggesting that dimerisation is not essential for the localisation of SopA to the membrane. We also performed a membrane fractionation assay using ATP binding defective mutant, SopA K120E. This mutant was also recovered in the membrane pellet in the presence of 20 mM NaCl in similar lines to wild type SopA (**Fig. 3-5C**). Further, a densitometric analysis also indicated that a significant proportion of the protein was present in the membrane pellet. Collectively, both the *in vitro* as well as *in vivo* data indicate that dimerisation of SopA protein is not essential for its association to the bacterial membrane.

### **3.2.6 C-terminal mutants are defective in maintaining plasmids**

Deletion of the MTS in the case of membrane-binding proteins is known to abrogate their function. Therefore, we further tested if the predicted C-terminal amphipathic helix was important for plasmid maintenance. To test this, we made use of a two-plasmid system (Ah-Seng et al., 2013) wherein one plasmid expresses the ampicillin-resistant pDSW210 SopA-GFP construct and the other plasmid was chloramphenicol resistant pCCD569 [mini-F plasmid Cam<sup>R</sup>  $\Delta$ sopA, sopBC<sup>+</sup>]. We co-transformed both the plasmids into the MC4100 strain of *E. coli*, and the colonies attained were then inoculated onto LB with both the antibiotics, grown overnight and then sub-cultured 1/100<sup>th</sup> into fresh LB with only carbenicillin (without chloramphenicol) followed by growth for 10 hours (approximately 20 generations).

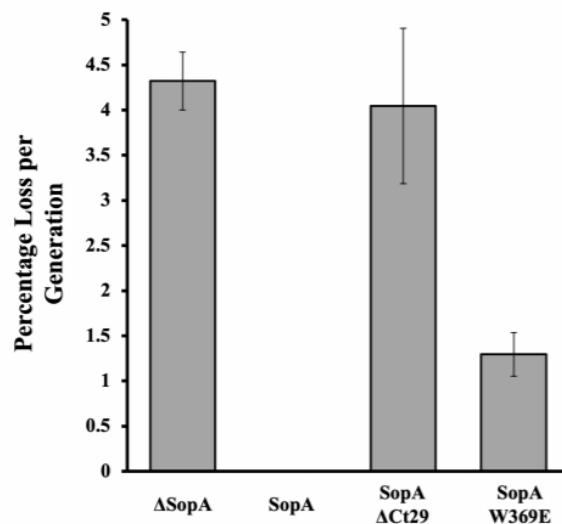
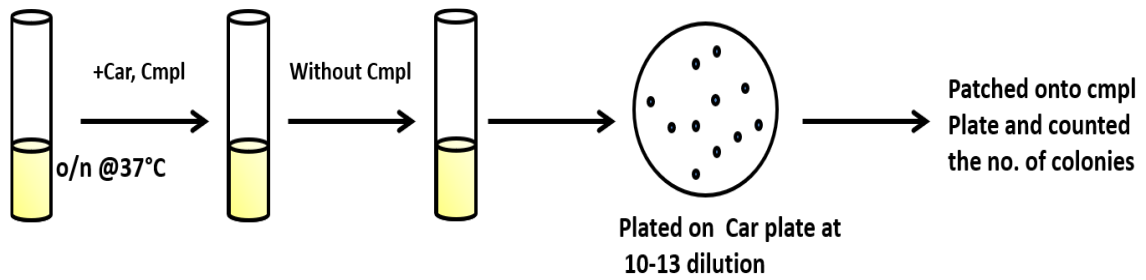


**Figure 3-6. Deletion of the predicted C-terminal amphipathic helix of SopA lead to plasmid loss.**

MC4100 cells harbouring plasmids pDSW210-SopA (and its variants) and pDAG198 (mini-F carrying  $\Delta$ sopA,  $sopBC^+$ ) were grown in LB medium with 100  $\mu$ g/ml carbenicillin and 34  $\mu$ g/ml chloramphenicol at 37°C and then transferred to LB medium with carbenicillin alone added to the media. It was allowed to grow for another 20 generations, following which serial dilutions of cultures were plated on carbenicillin containing plates and subsequently, individual colonies were replica plated into chloramphenicol containing plates to estimate the loss. The experiment was performed in triplicate. Error bars represent SEM.



After this, it was further sub-cultured 1/100<sup>th</sup> onto fresh LB with only carbenicillin, grown for 10 hours (approximately 20 generations, giving a total of 40 generations in the absence of chloramphenicol) and then plated onto carbenicillin plates. The colonies attained were further patched onto chloramphenicol plates. The percentage of loss of plasmids was calculated basing on the equation  $L = 100 * [1 - (F_t/F_i)^{(1/n)}]$  (Ravin and Lane, 1999).

In the absence of selective pressure, the plasmids would be lost from the population if the cells lacked or had a non-functional SopA. This was true for the control (lacking SopA), which was lost at a rate of 4 % per generation. Whereas wild type SopA showed 0 % loss, the mutants SopA  $\Delta$ Ct29, wherein the entire C-terminal 29 amino acids have been deleted, displayed loss rates like the control. SopA W369E, on the other hand, exhibited a 1.3 % loss (**Fig. 3-6**). Thus, deletion of the entire C-terminal stretch of SopA leads to plasmid stability defects; however, in the mutant SopA W369E, loss rates were minimal. Further, as described in Chapters 4 and 5, point mutations in other hydrophobic residues F377 and W362, respectively, also result in severe loss of mini-F plasmids from cultures. These data suggest that the C-terminal residues of SopA have a functional role and are essential for plasmid stability.

### **3.3 DISCUSSION**

**SopA might be a weak peripheral protein that reversibly associates with the membrane.**

The localisation pattern of almost all members of the ParA superfamily is on the nucleoid of the cell. Recent super-resolution microscopy data (Le Gall et al., 2016) and diffusion ratchet mechanisms also draw direct evidence of nucleoid localisation of

SopA protein (Vecchiarelli et al., 2013). Quite contrastingly, Hiraga and colleagues (Ezaki et al., 1991) provided evidence of plasmid segregation into anucleate cells and thus suggest that other players along with nucleoid might be involved in plasmid segregation. This is further supported by studies in a *mukB* deletion strain wherein plasmids are segregated efficiently into anucleate cells (Funnell and Gagnier, 1995). Biochemical assays have further added proof to the membrane association of SopA protein (Lin and Mallavia, 1998). Moreover, the formation of filaments by a spontaneous double mutant of SopA, SopA1 (Lim et al., 2005) in similar lines to other membrane-binding proteins also suggests loss of surface substrate binding.

Consistent with the above results, our AMPHIPASEEK data suggests that SopA C-terminus mediates membrane binding by forming an amphipathic helix. Like other membrane-binding proteins MinD, FtsA, MreB, and Noc (Pichoff and Lutkenhaus, 2005; Szeto et al., 2002; Salje et al., 2011; Strahl and Hamoen, 2010), dissipation of membrane potential causes the change in localisation pattern of SopA to the membrane as has been shown with poly-L-lysine as well as CCCP treatment of SopA. Also, as a direct measure of membrane binding, membrane binding assays show a major portion of SopA to be in the pellet. Taken together, these results, along with the filament-forming mutants of SopA show that SopA might be a  $D\Psi$ -sensitive weak peripheral membrane protein that associates with the cell periphery, thus facilitating the process of segregation. The deletion of the amphipathic helix in the case of membrane-binding proteins perturbs their function. In a similar way, deletion of the C-terminal 29 amino acid stretch of SopA also leads to plasmid stability defects. This suggests that the C-terminal stretch is essential for plasmid maintenance. Further, as the C-terminal domain is essential for function, we mutated the residue W369 to E and observed the membrane

association as well as plasmid loss rate. In both cases, W369E seems to be least affected, suggesting that W369 is not a critical residue mediating membrane association of SopA, and thus other residues in the C-terminus might play a critical role in the process. Further, mutation of two other hydrophobic residues W362 to E and F377 to A, also leads to recovery of the protein in the membrane pellet, indicating that neither of these residues are essential in membrane association.

Unlike other membrane-binding proteins like FtsA and MinD (Pichoff and Lutkenhaus, 2005; Szeto et al., 2002), SopA might not be a strong membrane-binding protein but rather a weak peripheral protein as the major localisation pattern of SopA is on the nucleoid of the cell. So, SopA might transiently associate with the membrane and might behave in similar lines as Noc, a weak peripheral protein that has a stretch of N terminal residues recruited to directly associate with the membrane (Adams et al., 2015). Moreover, Noc has a nucleoid localisation pattern just like SopA (Wu et al., 2009). Thus, these resemblances between SopA and Noc might hint at both the nucleoid as well as membrane association of both proteins.

Amphipathic helix prediction using AMPHIPASEEK, our *in vitro* and *in vivo* data suggests that SopA might associate with membranes via the last C-terminal helix. However, earlier reports based on PhoA fusion assays have also suggested that the N-terminal 11 residues of SopA to be sufficient for protein transport to the membrane (Lin and Mallavia, 1998). Thus, it remains to be tested if the N-terminal or C-terminal residues of SopA suffice for localisation to membranes as described in the section below under future directions. Moreover, the role of other hydrophobic residues in the process of membrane association wherein W362, W369 and F377 do not seem to be the critical residue in the process needs to be explored in the future. While this work suggests that

SopA might be membrane-associated, its role in F plasmid segregation, if any, clearly requires further work in ascertaining membrane association of SopA, elucidate the mechanism and identifying key residues involved. Further, although our data suggest that *ugpA* might not facilitate membrane association of SopA, an interesting question for future studies is whether any other host factors function as accessory modulators of F plasmid segregation.

The current models for ParA mediated DNA segregation is centred around the nucleoid binding of ParA, and thus the relevance of a partitioning protein in membrane fractions might be questionable. While the time delay is attributed to the slow conformational change upon ATP binding to the ParA-ATP\* state (Vecchiarelli et al., 2010), one could speculate that the time delay in nucleoid binding could also be affected by sequestration of SopA into membranes. Further, one could hypothesise that the binding of the protein to the bacterial membrane might lead to nucleotide exchange as in the case of DnaA (Garner and Crooke, 1996; Crooke, 2001; Makise et al., 2001) and thus facilitate the conformational change of SopA that in turn leads to the formation of SopA-ATP\* conformation leading to the rebinding onto the bacterial nucleoid. Thus, we postulate that membrane association of SopA could serve as a simple sequestration mechanism to maintain protein homeostasis or could additionally contribute and favour the generation of the chemophoretic gradients and enable equipartitioning of plasmids into daughter cells.

## **CHAPTER 4**

# **ROLE OF THE C-TERMINAL HELIX OF SOPA IN NUCLEOID BINDING AND PLASMID STABILITY**

## 4.1 INTRODUCTION

Most bacterial chromosomes and low copy number plasmids utilise the Type-I mechanism of plasmid segregation involving the ParA family of proteins. The *par* system in low copy number plasmids involves a centromere like a sequence, *parC*, an adaptor protein ParB and an NTPase ParA (Gerdes et al., 2000). SopA, a member of the ParA family of proteins, enables the segregation of low copy number F plasmid in bacteria. The basic components of the SopA mediated partitioning machinery includes a centromeric sequence *sopC*, an adaptor protein SopB and an ATPase SopA (Ogura and Hiraga, 1983). SopB binds to the centromeric sequence on the plasmid *sopC* forming fluorescent foci (Lim et al., 2005). Fluorescence microscopy has revealed that these proteins are associated with the nucleoid (Hirano et al., 1998; Marston and Errington, 1999; Ebersbach and Gerdes, 2001; Le Gall et al., 2016). Oscillation of the ParA protein majorly occurs on the nucleoid of the cell (Marston and Errington, 1999; Quisel et al., 1999; Ebersbach and Gerdes, 2001; Hatano et al., 2007; Le Gall et al., 2016). Moreover, the *in vitro* reconstitution of the plasmid partitioning system using DNA carpeted flow cell and super-resolution imaging have revealed a major role for the nucleoid in ParA mediated DNA segregation (Vecchiarelli et al., 2013; Le Gall et al., 2016). In Soj, a related member of the Walker A family of protein, the lack of the N-terminal stretch does not affect binding to nsDNA *in vitro* (Leonard et al., 2005). Also, *in vivo* and *in vitro* studies have identified two surface-exposed arginine residues in Soj that favours its interaction with non-specific DNA (Hester and Lutkenhaus, 2007). Such surface-exposed positively charged residues have also been implicated in DNA binding for pNOB8 (Schumacher et al., 2017), *HpSoj* (Chu et al., 2019), PpfA (Roberts et al., 2012) and PomZ from *Myxococcus xanthus* (Schumacher et al., 2017). Similarly, Bouet and colleagues have also identified several conserved residues in the C-terminal domain of SopA that influence its nsDNA binding

(Castaing et al., 2008). Among the residues, mutating K340 to alanine results in loss of nsDNA binding and severe plasmid loss from cells (Castaing et al., 2008). The residue K340 is highly conserved, and mutants in the equivalent residue (R351A) in P1 ParA lead to DNA binding and partitioning defects (Castaing et al., 2008; Ah-Seng et al., 2009; Dunham et al., 2009; Baxter et al., 2020).

Moreover, a spontaneous mutation designated SopA1 (M315I and Q351H) led to the assembly of SopA into filaments, a phenotype that is in stark contrast to the localisation pattern of wild-type SopA (Lim et al., 2005). Recent studies on a related protein, VcParA2, have also shown that it assembles into a polymer on DNA and have identified residues that lie close to the last C-terminal helix that is responsible for nsDNA binding (Parker et al., 2021). Further, the deletion of the last three amino acids of ParF has been reported to cause plasmid loss in the cell (Ali, 2017). Interestingly, one of the mutations in SopA1, i.e. Q351H, is close to the last C-terminal helix (H16). Notably, in MinD, deletion of the amphipathic helix comprising the last ten amino acid residues resulted in the loss of DNA binding activity (Ventura et al., 2013). Collectively, these findings suggest a role for the last C-terminal helix of the ParA superfamily for its function in DNA binding and segregation. Further, mutations in the positively charged residues within the last C-terminal helix H16 of P1 ParA (K375 and R378) have also been suggested to affect DNA binding activity (Dunham et al., 2009). Moreover, our results presented in Chapter 3 showed significant plasmid loss rates in the C-terminal deletion mutant (SopA  $\Delta$ Ct29) and the point mutant W369E (Mishra et al., 2021), suggesting a hitherto unidentified role for the last C-terminal H16 helix in SopA function and F plasmid segregation.

In this chapter, we present results from the study of several deletions and point mutants in the last C-terminal H16 helix of SopA and their ability to maintain mini-F plasmids. Further, results pertaining to non-specific DNA binding activity *in vivo* and the influence of the SopBC complex on their localisation is described. Consistent with previous studies on the role of non-

specific DNA binding in plasmid segregation, we show that certain of these C-terminal helix mutants are impaired in binding to the nucleoid and result in significant loss of plasmids from cultures.

## 4.2 RESULTS

### 4.2.1 SopA $\Delta$ Ct29 and SopA W369E mutants are defective in nsDNA binding

Plasmid maintenance was abrogated in SopA  $\Delta$ Ct29 and SopA W369E mutants. Although the W369E mutant exhibited a mild plasmid loss rate, it did not impair membrane association of the protein (described in Chapter 3; Mishra et al., 2021). Thus, it was plausible that the C-terminal 29 residues and W369 might be critical for other functions associated with SopA. One of the most critical functions of SopA is nsDNA binding that mediates plasmid segregation (Castaing et al., 2008; Vecchiarelli et al., 2013; Le Gall et al., 2016). We thus probed whether the C-terminal 29 residues and W369 played a role in the nucleoid association of SopA. To investigate this, we imaged the deletion mutant SopA  $\Delta$ Ct29 as well as the point mutant SopA W369E in a HupA-mCherry strain of *E. coli* (Marceau et al., 2011; Fisher et al., 2013) (a kind gift from Dr. Mohan Chandra Joshi). As shown previously, cells producing wild-type SopA displayed the usual characteristic nucleoid-associated fluorescence, indicating that the fusion protein was fully functional (**Fig. 4-1A**). Interestingly, both the mutants were impaired in nsDNA binding and exhibited diffuse localisation patterns throughout the cytoplasm (**Fig. 4-1A**).

Nucleoid occupies most of the space in an *E. coli* cell, making it often difficult to distinguish the nucleoid and cytoplasmic localisation of proteins. Thus, to further confirm the cytoplasmic localisation of the SopA mutants, we resorted to nucleoid condensation experiments using chloramphenicol (Zusman et al., 1973; Sun and Margolin, 2004). For this purpose, we initially induced our cells with 400  $\mu$ M IPTG for 2 hours, then treated them with



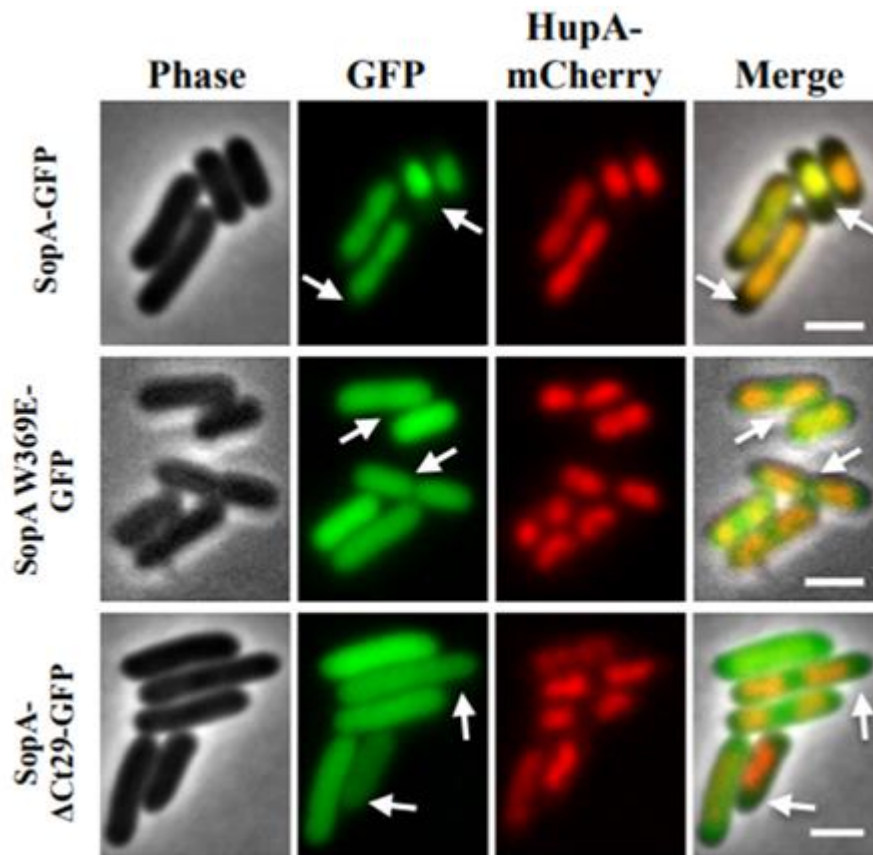


**Figure 4-1. SopA  $\Delta$ Ct29 and W369E mutants are impaired in non-specific DNA binding.**

(A) **SopA  $\Delta$ Ct29 and W369E exhibit diffuse cytoplasmic localisation.** SopA mutants ( $\Delta$ Ct29) and W369E were expressed from plasmid pDSW210 in HupA-mCherry strain by induction with 400  $\mu$ M IPTG, as described in Materials and Methods. While wild type SopA localises on the nucleoid, the deletion mutant  $\Delta$ Ct29 and point mutant W369E are cytoplasmic and do not show nucleoid localisation. The scale bar is 2  $\mu$ m.

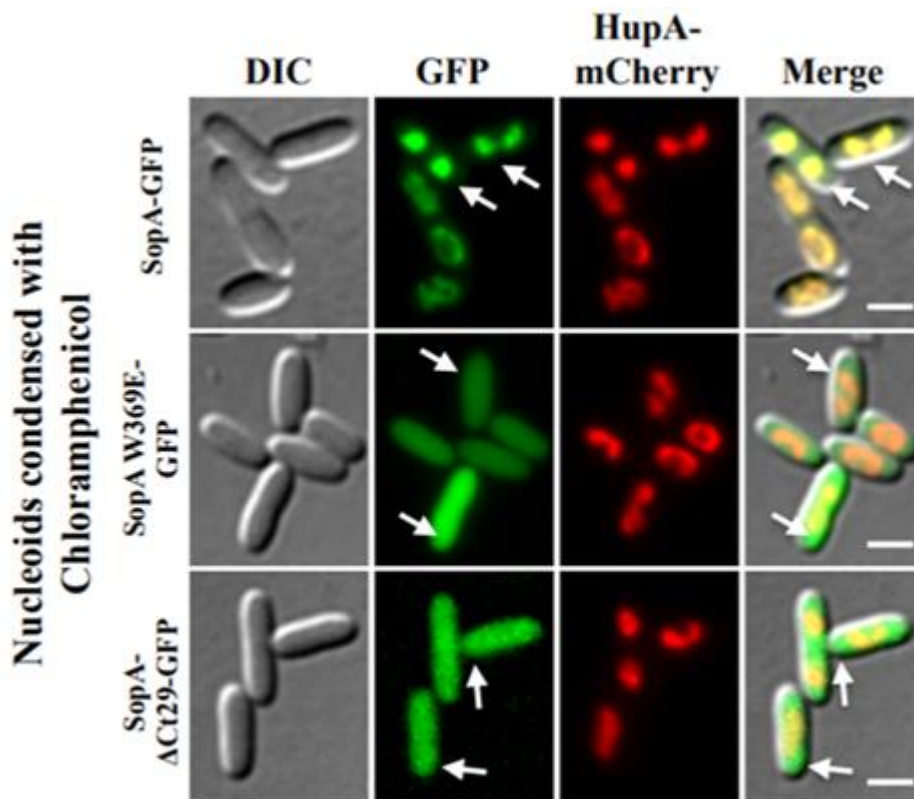


**Figure 4-1. (B) SopA  $\Delta$ Ct29 and W369E fail to localise to the nucleoid.** MC4100 cells were treated with chloramphenicol post-induction for 30 min to condense the nucleoid. The localisation pattern of wtSopA and the mutants ( $\Delta$ Ct29 and W369E) were then observed by fluorescence microscopy. Both the mutants,  $\Delta$ Ct29 and W369E, fail to colocalise with the condensed nucleoid. However, wild-type SopA exhibits complete colocalisation with the nucleoid. The scale bar is 2  $\mu$ m.

chloramphenicol (100 µg/ml) for 30 min and observed the localisation pattern in HupA-mCherry strain. After 30 min, the nucleoids were significantly condensed. While the wild-type SopA completely colocalised with the condensed nucleoid, the mutants SopA  $\Delta$ Ct29 and W369E were found to be distributed throughout the cytoplasm and did not colocalise with the nucleoid, suggesting that both these mutants were defective in association with nsDNA (**Fig. 4-1B**). Notably, W369 seemed to be critical for nsDNA binding, albeit not in membrane association. These results thus suggested that the C-terminal 29 amino acids stretch possibly played a role in nucleoid binding of SopA.

#### **4.2.2 Perturbed nucleoid binding of SopA C-terminal deletion mutants**

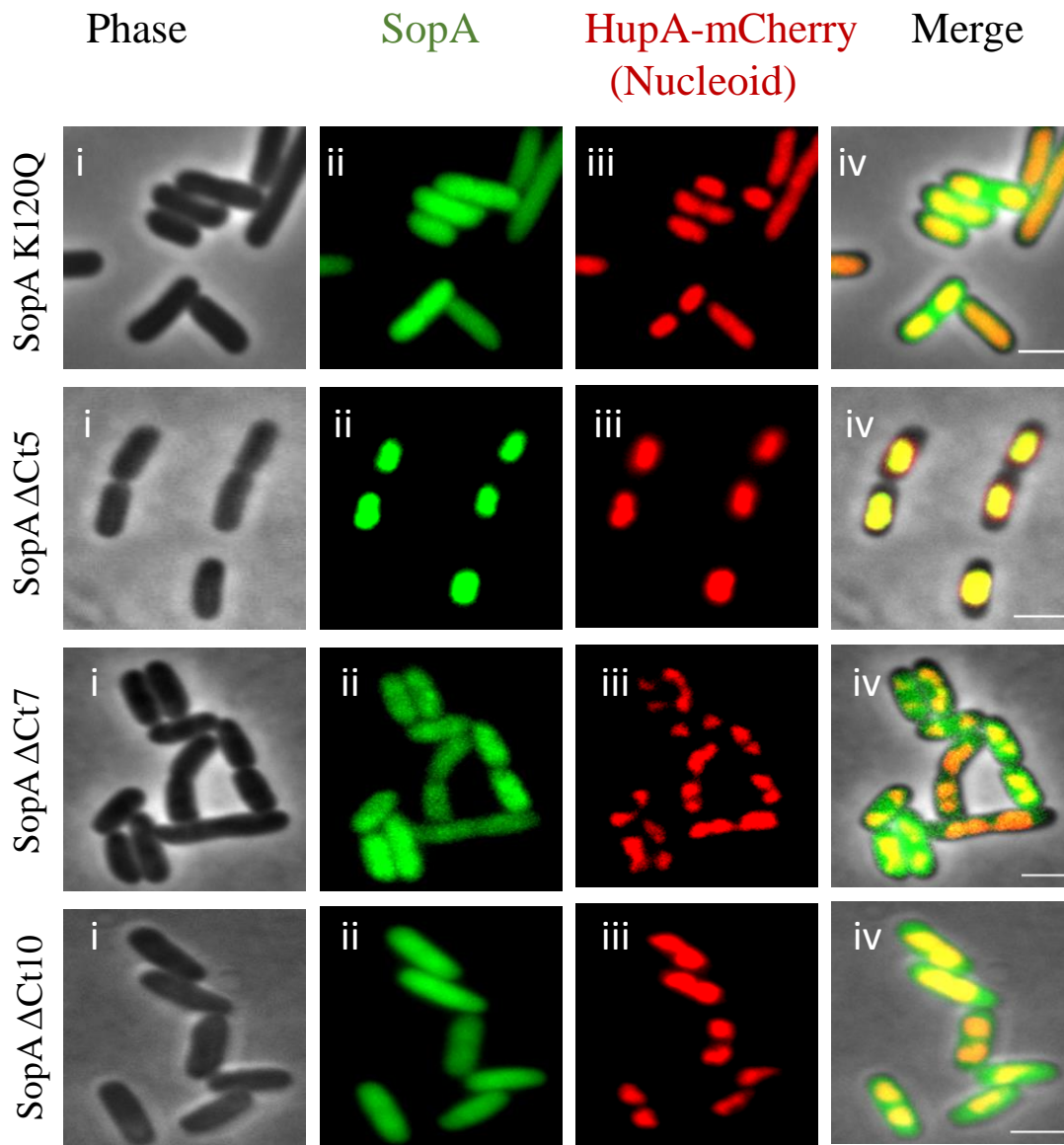
Nucleoid binding plays a key role in SopA mediated plasmid segregation, and defects in nsDNA binding activity result in failure in plasmid partitioning (Castaing et al., 2008; Roberts et al., 2012; Vecchiarelli et al., 2013; Lim et al., 2014; Le Gall et al., 2016). Further, our data presented in Chapter 3 and above suggests a role for the C-terminal 29 residues of SopA in plasmid segregation and nsDNA binding. In order to further determine the precise region and residues required for the function of SopA, we generated a series of deletion mutants and point mutations in the last C-terminal H16 helix. The deletion mutants included SopA  $\Delta$ Ct5 ( $\Delta$ 384-388), SopA  $\Delta$ Ct7 ( $\Delta$ 382-388), SopA  $\Delta$ Ct10 ( $\Delta$ 379-388) and SopA  $\Delta$ Ct20 ( $\Delta$ 369-388) (**Fig. 4-2A**). Since SopA  $\Delta$ Ct7 and SopA  $\Delta$ Ct10 resulted in significant plasmid loss rates, we did not analyse SopA  $\Delta$ Ct20 further. Hence data for only SopA  $\Delta$ Ct5, SopA  $\Delta$ Ct7 and SopA  $\Delta$ Ct10 are presented here in this chapter. As SopA  $\Delta$ Ct29, as well as W369E, were defective in nsDNA binding, we further analysed other C-terminal deletion mutants for nucleoid localisation *in vivo* using a HupA-mCherry strain of *E. coli*. Similar to the wild type, SopA  $\Delta$ Ct5 completely localised to the nucleoid, as seen in the merged image (**Fig. 4-2B**).

**A**



**Figure 4-2. The C-terminal deletion mutants exhibit abrogated nsDNA binding.**

(A) Sequence of SopA C-terminal 29 amino acid region. The image was created using SnapGene™, and it represents the sequence of the entire C-terminal stretch of SopA spanning from amino acid G360 to R388. The truncated mutants SopA ΔCt5 (Δ384-388), ΔCt7 (Δ382-388) and ΔCt10 (Δ379-388) have been represented.

**B**

**Figure 4-2. (B) C-terminal deletion mutants are defective in nsDNA binding.** SopA deletion mutants were expressed from plasmid pDSW210 by induction with 400  $\mu$ M IPTG, as described in Materials and Methods. An *E. coli* strain expressing HupA-mCherry was used to image the nucleoid. While wild-type SopA and  $\Delta$ Ct5 localise on the nucleoid, the deletion mutants  $\Delta$ Ct7 and  $\Delta$ Ct10 did not exhibit colocalisation with the nucleoid. The scale bar is 2  $\mu$ m.

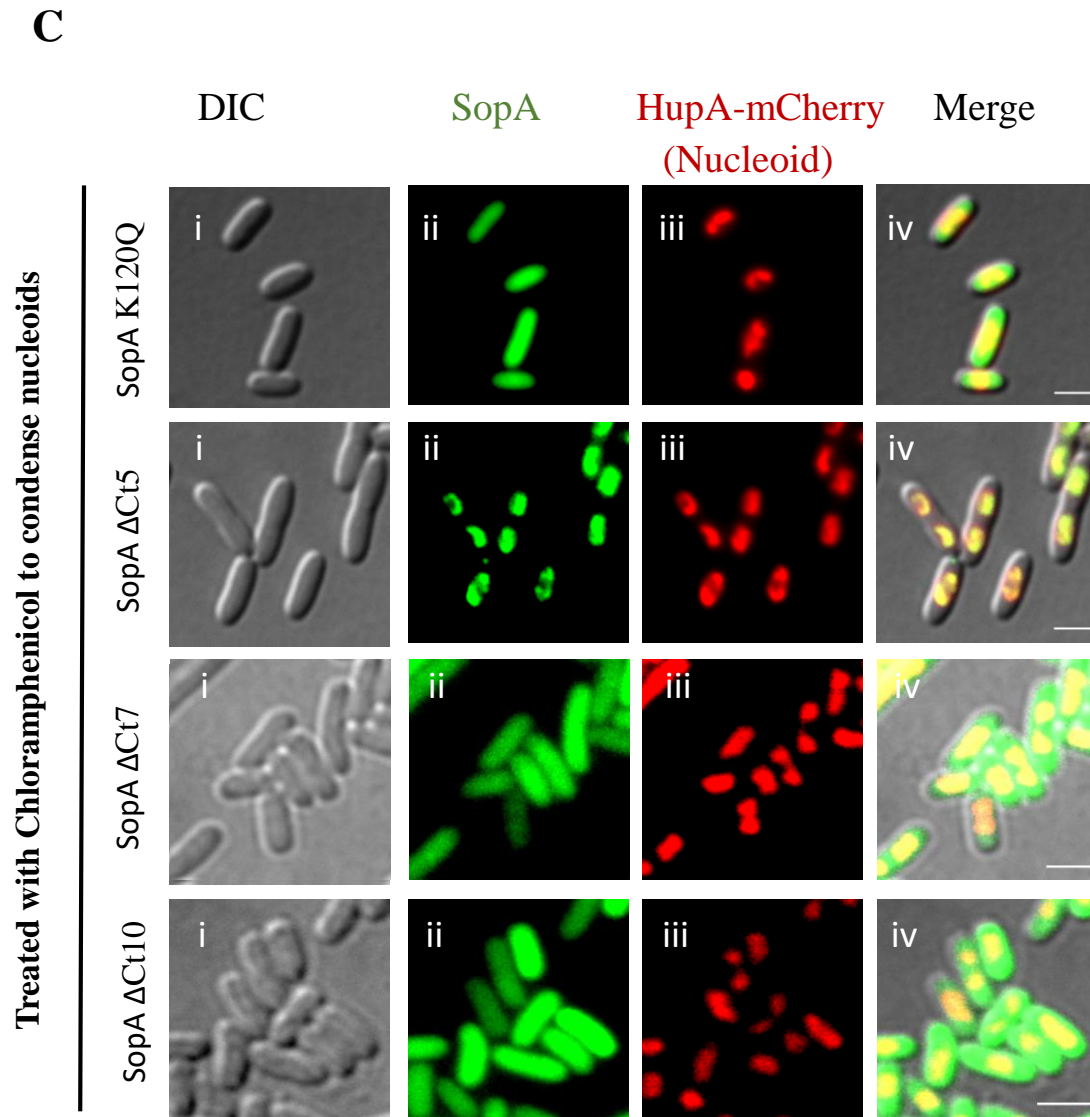


**Figure 4-2. (C) Localisation of the deletion mutants in cells with condensed nucleoids.** To further confirm nucleoid localisation, cells were treated with chloramphenicol post-induction for 30 min to condense the nucleoid and imaged. Fluorescence imaging of  $\Delta$ Ct7 and  $\Delta$ Ct10 mutants reveal that the mutants are distributed throughout the cytoplasm and do not colocalise with the condensed nucleoid. However, the  $\Delta$ Ct5 mutant exhibits complete colocalisation with the nsDNA. The scale bar is 2  $\mu$ m.

However, SopA  $\Delta$ Ct7 and SopA  $\Delta$ Ct10 mutants failed to colocalise with the nucleoid and exhibited a diffused cytoplasmic localisation. SopA K120Q, a mutant known to be defective in nsDNA binding (Hatano et al., 2007), exhibited diffused localisation as expected (**Fig. 4-2B**).

We also performed localisation studies on these deletion mutants using nucleoid condensation experiments with the help of chloramphenicol, as with the SopA  $\Delta$ Ct29 deletion mutant and SopA W369E. The mutants SopA  $\Delta$ Ct7 and SopA  $\Delta$ Ct10 did not colocalise to the condensed nucleoids. On the contrary, SopA  $\Delta$ Ct5, like wt-SopA exhibited complete colocalisation with the condensed nucleoids, suggesting that deletion of the last 5 amino acids of SopA does not impair nucleoid localisation of the protein (**Fig. 4-2C**). However, our results suggest that the deletion of the last seven amino acids in the C-terminal helix of SopA significantly affected the localisation of SopA to the nucleoid and deleting any stretch beyond the last five amino acids leads to impaired nsDNA binding.

#### **4.2.3 Influence of the SopBC partitioning complex on the nucleoid localisation of C-terminal deletion mutants of SopA**

SopA binds nucleoids and exhibits dynamic foci formation in the presence of SopBC (Lim et al., 2005; Hatano et al., 2007; Ah-Seng et al., 2013; Le Gall et al., 2016). We, therefore, tested whether these deletion mutants were capable of foci formation in the presence of SopBC. In order to do so, we co-transformed the deletion mutants and SopBC containing pDAG198 plasmid (mini-F  $\Delta$ sopA, *sopBC*<sup>+</sup>) (Castaing et al., 2008) (a kind gift from Dr. Jean-Yves Bouet) into MC4100 strain and analysed by fluorescence microscopy. As expected, wild-type SopA formed fluorescent foci in the presence of SopBC, suggesting that it interacted with the partitioning complex. However, the C-terminal deletion mutants, SopA  $\Delta$ Ct7, SopA  $\Delta$ Ct10 and SopA  $\Delta$ Ct29, resulted in diffuse fluorescence (**Fig. 4-3**).

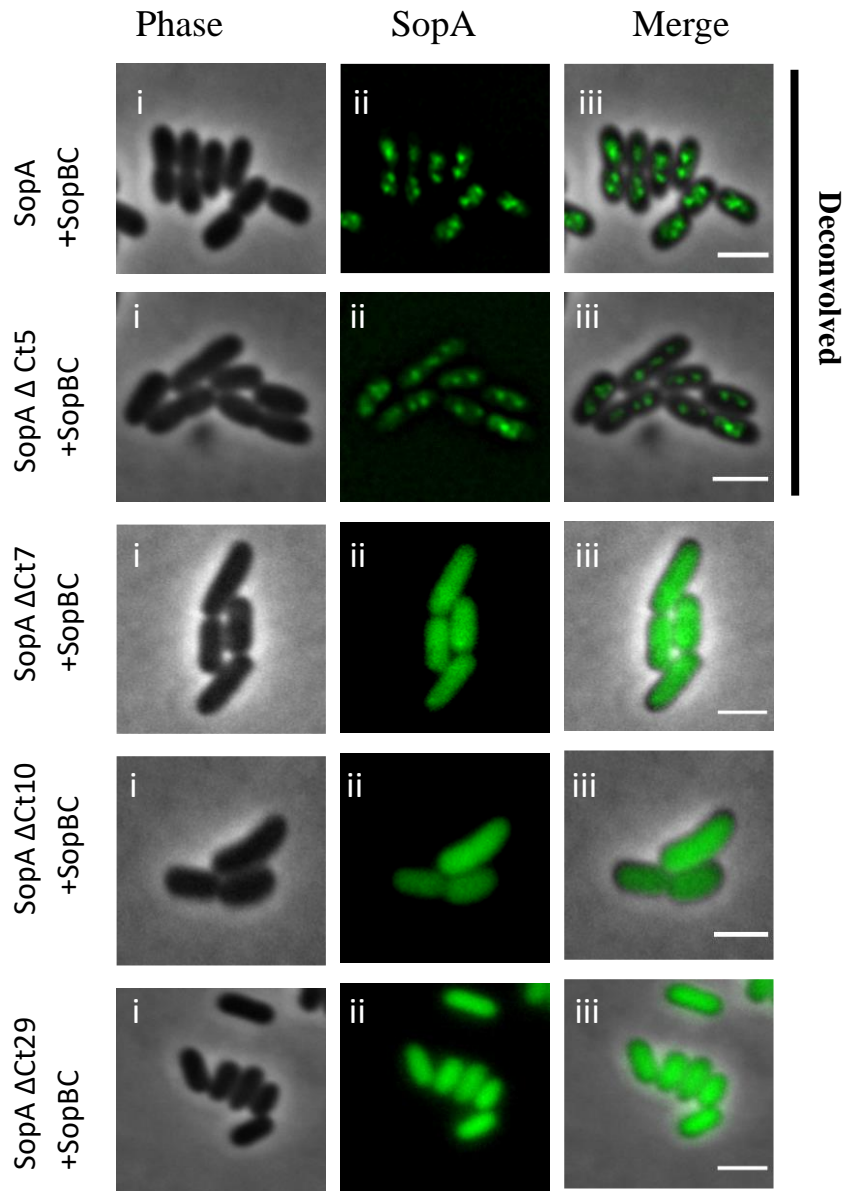


**Figure 4-3. Influence of the partitioning complex on the localisation of SopA C-terminal deletion mutants.**

Fluorescence imaging of SopA  $\Delta$ Ct7 ( $\Delta$ 382-388),  $\Delta$ Ct10 ( $\Delta$ 379-388) and  $\Delta$ Ct29 ( $\Delta$ 360-388) that the presence of SopBC does not result in foci formation in the deletion mutants. Unlike the wtSopA, the deletion mutants, SopA  $\Delta$ Ct7,  $\Delta$ Ct10 and  $\Delta$ Ct29, continue to exhibit diffuse cytoplasmic localisation patterns even in the presence of the SopBC complex. On the contrary, SopA  $\Delta$ Ct5 forms foci similar to the wtSopA in the presence of the SopBC complex. The scale bar is 2  $\mu$ m.



SopA  $\Delta$ Ct5, however, formed foci, showing that  $\Delta$ Ct5 retained its ability to interact with the SopBC complex and suggests that the last five amino acids in SopA are neither essential for nsDNA binding nor its interaction with the SopBC complex.

#### 4.2.4 SopA $\Delta$ Ct5 is defective for plasmid maintenance

As the C-terminal truncated mutants,  $\Delta$ Ct7 and  $\Delta$ Ct10 but not  $\Delta$ Ct5, exhibited abrogated nucleoid binding and impaired interaction with the partitioning machinery, we also tested another functional aspect of these mutants. We performed a plasmid stability assay to monitor the loss of plasmid from the cells. We used a two-plasmid system (Libante et al., 2001; Ah-Seng et al., 2013). One plasmid expresses SopA-GFP from the ampicillin-resistant pDSW210 construct, and another plasmid was chloramphenicol resistant pDAG198 (mini-F  $\Delta$ sopA *sopBC*<sup>+</sup>). MC4100 strain of *E. coli*, co-transformed with both the plasmids, was used to estimate the plasmid loss rates as described (Ravin and Lane, 1999) and mentioned in Chapter 2 (Materials and Methods). While the wild-type SopA exhibited no loss of plasmids in the culture, we observed a significant loss of plasmid in all the deletion mutants. Interestingly, the plasmid loss rates in the case of SopA  $\Delta$ Ct7 and SopA  $\Delta$ Ct10 were 10 %  $\pm$  0.81 (SEM, n=3) and 8 %  $\pm$  1.31 (SEM, n=3) per generation respectively, much higher than in the absence of SopA. Greater plasmid loss rates in these mutants might indicate the failure to resolve inter-plasmid clusters formed and thus impairing the usual random segregation that the plasmids undergo in the absence of SopA. Surprisingly, SopA  $\Delta$ Ct5 also exhibited plasmid loss at rates of 3.87 %  $\pm$  0.66 (SEM, n=3) per generation, which is comparable to the loss rates in the absence of SopA. However, SopA  $\Delta$ Ct5 bound nucleoids and formed foci in the presence of SopBC. These results show that all the deletion mutants exhibited significant plasmid loss and suggest that the C-terminal 29 amino acid residues play an important role in somehow regulating the nsDNA binding of SopA and plasmid segregation (**Fig. 4-4**).

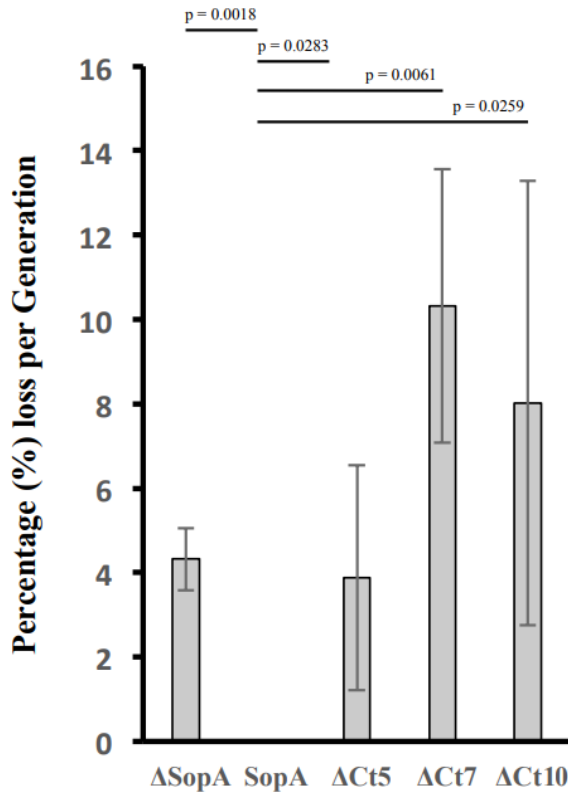


**Figure 4-4. The last five amino acids in the C-terminal helix are essential for plasmid maintenance.**

MC4100 cells harbouring plasmids pDSW210 SopA (or its variants) and pDAG198 (mini-F carrying  $\Delta sopA$ ,  $sopBC^+$ ) were grown in LB medium with 100  $\mu\text{g/ml}$  carbenicillin (Carb) and 34  $\mu\text{g/ml}$  chloramphenicol at 37°C and then transferred to LB medium with carbenicillin alone added to the media. It was allowed to grow for 40 generations, following which it was plated on Carb plates, and subsequently, individual colonies were patched onto chloramphenicol plates. The rate of plasmid loss per generation was estimated as described in the Materials and Methods as per the method of Ravin and Lane, 1999. Wild-type SopA exhibited no plasmid loss (0 %), whereas, in the case of the mutants  $\Delta\text{Ct5}$  ( $\Delta 384\text{-}388$ ), loss rates of 3.8 % was observed. The plasmid loss rate in the case of  $\Delta\text{Ct7}$  ( $\Delta 382\text{-}388$ ) and  $\Delta\text{Ct10}$  ( $\Delta 379\text{-}388$ ) were 10 % and 8 % per generation, respectively, suggesting that the entire C-terminal stretch is critical for plasmid maintenance. The experiment was performed three times ( $n=3$ ), and the error bars represent SEM.

#### 4.2.5 Residues important for DNA binding within the C-terminal helix of SopA

Earlier studies on P1 ParA have shown that mutations in two positively charged residues (K375A R378A) in the C-terminal helix abrogate DNA binding (Dunham et al., 2009). The K375 residue of P1 ParA is conserved in the case of SopA, and the equivalent residue is R363. Furthermore, studies in related ParA superfamily members have identified specific positively charged residues in the C-terminus that are essential for plasmid maintenance (Chu et al., 2018; Baxter et al., 2020; Parker et al., 2021). Also, as described above, a mutation in hydrophobic residue W369 also resulted in nsDNA binding defect. Therefore, it was of interest to probe the C-terminal stretch and, in turn, identify critical residues, if any, involved in the process of nsDNA binding and plasmid maintenance. A multiple-sequence alignment, using Clustal Omega (Madeira et al., 2019), of the C-terminal stretch of SopA with related members of ParA superfamily like Soj, ParA, ParF, P1 ParA showed four highly conserved residues (R363, E370, E375 and R379) in the C-terminal helix of SopA (**Fig. 4-5A**). We resorted to mutating the positively charged residues in the C-terminus of SopA to assess their contributions to the nucleoid binding activity of SopA. Further, since W369E showed nucleoid binding defects, we mutated the hydrophobic residue F377 as well. Thus, the mutations Q351H, W362E /A, R363A, W369E, E375A, F377A, R379A, K382A and R384A were introduced into SopA (**Table 4-1**).

Here in this section, we describe the results pertaining to R363A, W369E, E375A, F377A, R379A, K382A and R384A. While W369E has been already described above and in the previous chapter (Chapter 3), Q351H, W362E and W362A are described in the next chapter (Chapter 5). Mutation of the positively charged residues R363, R379, K382 and R384 to alanine did not seem to disrupt nucleoid localisation of the protein, as is evident in the fluorescence microscopy images. Although the exchange of hydrophobic residue W369 with glutamic acid resulted in diffuse cytoplasmic fluorescence, mutation of F377 to alanine

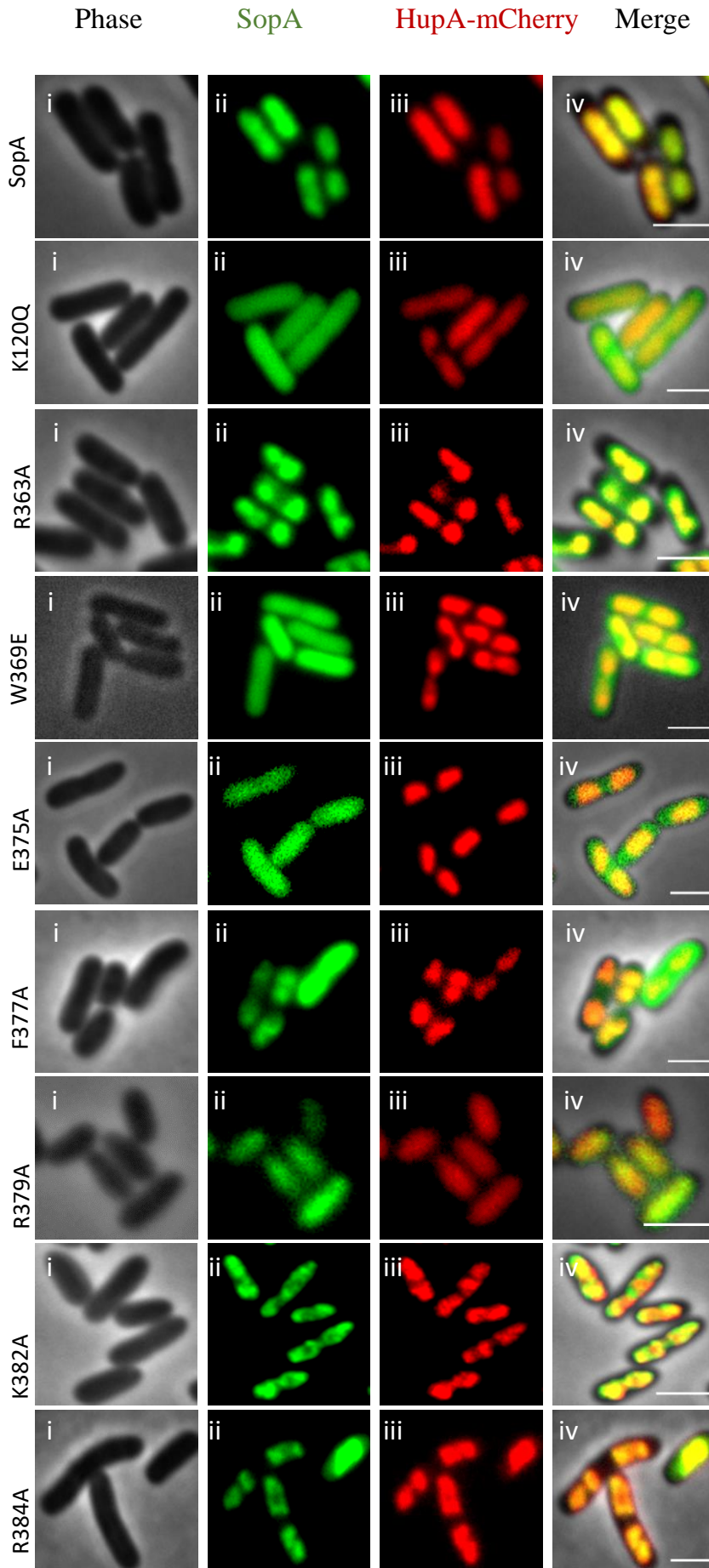
**A**



**Figure 4-5. C-terminal helix residues in SopA critical for nsDNA.**

**(A) Multiple Sequence Alignment of C-terminal 29 amino acid residues of SopA with different members of the ParA superfamily.**

The Multiple Sequence Alignment was generated using Clustal Omega. The conserved residues in the C-terminus are indicated by a ★ and residues used in this study are highlighted by a red bar on top.

**B**

**Figure 4-5. (B) W369E, E375A, and F377A residues are essential for nsDNA binding.**

Wide-field imaging of *E. coli* HupA-mCherry strain harboring wild-type SopA or mutant plasmids. The cultures carrying the plasmid pDSW210-SopA or the mutants were grown till OD<sub>600</sub> of 0.2 induced with 400 μM IPTG (as described in Materials and Methods) and was examined by fluorescence microscopy. While the mutants R363A and K382A bind to nsDNA, W369E and E375A exhibit diffuse fluorescence throughout the cytoplasm suggesting failure to bind the nucleoid. However, F377A seemed to exhibit mild localisation to the nucleoid suggesting partial binding to nsDNA. SopA K120Q, a known nsDNA binding mutant, as expected, exhibits a diffuse localisation pattern. The scale bar is 2 μm.

Residue number	Residue (amino acid)	Residue Changed (amino acid)
351	Q	H
362	W	E/A
363	R	A
369	W	E
370	E	<b>N.D</b>
375	E	A
377	F	A
378	D	<b>N.D</b>
379	R	A
382	K	A
384	R	A

N.D – Not Determined

**Table 4-1.** Residues mutated in the C-terminal stretch of SopA

seemed to affect nucleoid binding only mildly *in vivo* (**Fig. 4-5B**). Interestingly, mutating the conserved negatively charged E375 to alanine also resulted in nsDNA binding defect and failed to localise to the nucleoids. These results suggest that although F377A affects nsDNA binding mildly, mutations in the residues W369 and E375 have more severe effects on the nsDNA binding activity of SopA (**Fig. 4-5B**).

#### **4.2.6 Influence of the SopBC partitioning complex on the nucleoid localisation of C-terminal point mutants of SopA**

To further investigate whether the localisation patterns of the C-terminal mutants (R363A, W369E, E375A, F377A, R379A, and K382A) were influenced by the partitioning complex, we used the same two-plasmid system as described above. One plasmid (driven by the IPTG inducible weakened P<sub>trc</sub> promoter) was used to express SopA or its mutants, and the other mini-F plasmid derivative, pDAG198 carrying SopBC (but lacking SopA) under the P<sub>LtetO</sub> promoter (constitutive). Upon induction with 400  $\mu$ M IPTG for 2 hours, SopA formed foci in the cells, as has already been reported earlier. However, the DNA binding impaired mutants, W369E and E375A, did not form foci instead exhibited diffuse phenotype. On the contrary, R363A, R379A and K382A formed foci consistent with its nucleoid localisation, suggestive of interaction with the SopBC complex. Interestingly, F377A, which exhibited mild nucleoid localisation, also showed foci formation in the cell, indicating interaction with the SopBC complex (**Fig. 4-6**). These results reveal that while F377A might have residual nsDNA binding activity, W369E and E375A are both impaired in nucleoid binding. In similar lines, SopA K120Q, which is known to be defective in nsDNA binding, exhibited diffuse cytoplasmic localisation in the presence of SopBC as well.

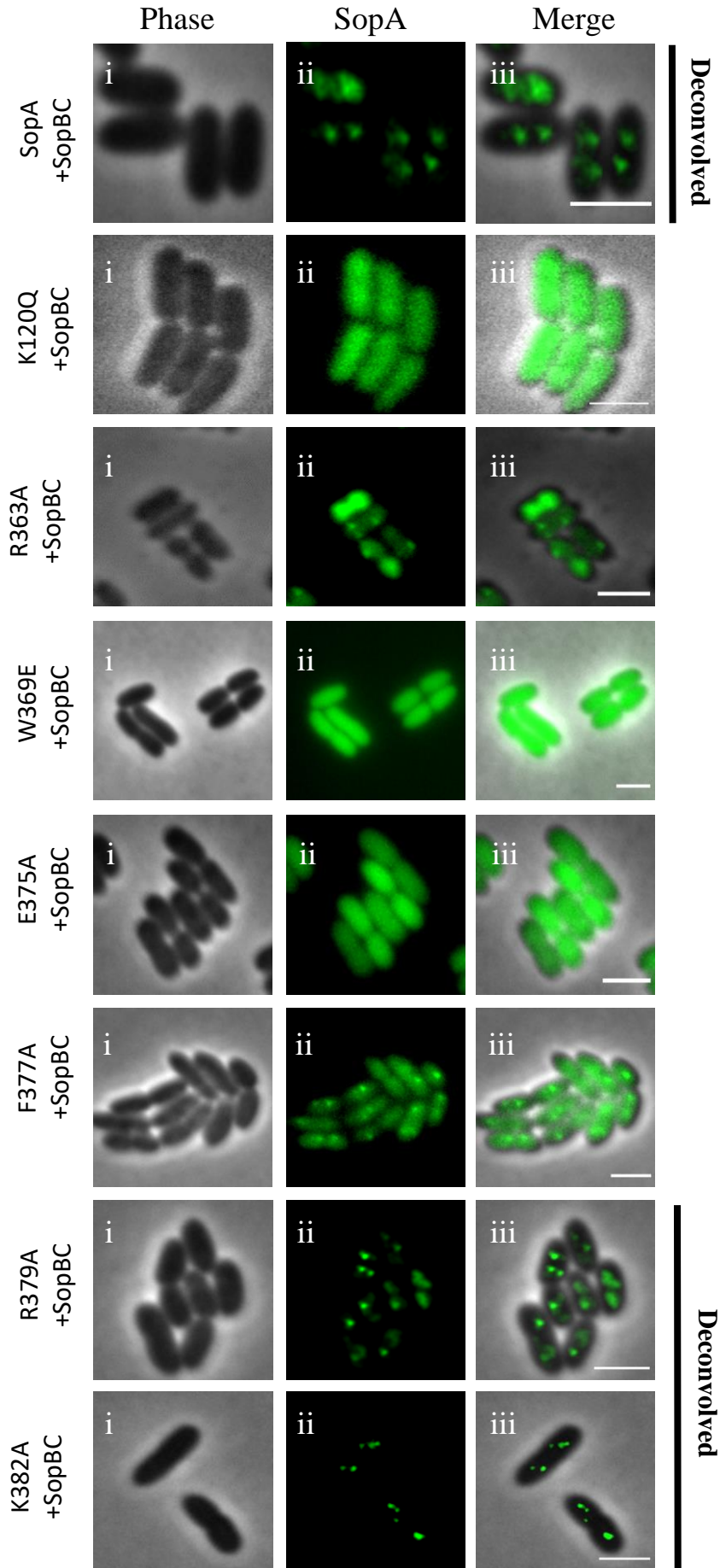




**Figure 4-6. Influence of the partitioning complex on the localisation of C-terminal point mutants.**

Fluorescence images of W369E, E375A and K120Q reveal that these mutants are impaired in SopBC interaction and thus exhibit diffuse localisation patterns in the presence of the SopBC complex. The wild-type SopA and mutants F377A and R363A, on the other hand, interact with SopBC and localise as SopA foci in the presence of the SopBC complex. The scale bar is 2  $\mu\text{m}$ .

<b>SopA mutant</b>	<b>Nucleoid Binding (nsDNA Binding)</b>	<b>SopA foci in cells</b>	<b>Plasmid Segregation</b>
$\Delta\text{Ct29}$	-	-	--
$\Delta\text{Ct5}$	+	+	-
$\Delta\text{Ct7}$	-	-	---
$\Delta\text{Ct10}$	-	-	---
<b>R363A</b>	+	+	-
<b>W369E</b>	-	-	-
<b>E375A</b>	-	-	--
<b>F377A</b>	+	+	---
<b>R379A</b>	+	+	-
<b>K382A</b>	+	+	+
<b>R384A</b>	+	<b>N.D</b>	<b>N.D</b>

N.D – Not Determined

**Table 4-2.** Table summarising the effects of deletion mutants and the site-directed mutants on SopA activity

#### 4.2.7 Plasmid maintenance is affected in C-terminal mutants

As we have identified several residues abrogated in nsDNA binding and SopBC interactions, we resorted to determine the loss of plasmid rates in these mutants by performing plasmid stability assays. The assay was done using the same two plasmid system as reported earlier (Libante et al., 2001) and described above. Surprisingly, we observed that the C-terminal residue mutants, including those that were nucleoid-associated and formed SopA foci in the presence of SopBC complex, exhibited plasmid loss (except for K382A) to varying extents. Surprisingly, R363A, which binds to both the partitioning machinery as well as non-specific DNA, exhibited mild loss rates of  $2.3 \% \pm 0.13$  (SEM, n=3) per generation as compared to the  $\sim 4 \%$  in the absence of SopA control. As expected, E375A, which failed to bind nucleoids, also exhibited similar loss rates. However, the plasmid loss rate for F377A was significantly higher, i.e.,  $7 \% \pm 0.21$  (SEM, n=3) per generation, and was the highest among all C-terminal residues tested. Although SopA F377A forms foci in the presence of the SopBC complex, the increased plasmid loss rates might suggest that upon interaction with the SopBC complex, SopA F377A is stably bound to the nucleoid forming stable plasmid clusters. No plasmid loss was detected in the case of the K382A mutant, indicating that this residue was not essential for plasmid maintenance. The other positively charged residue mutant, R379A, had a plasmid loss rate of  $1.42 \% \pm 0.085$  (SEM, n=3). Thus, we conclude that although mutations in residues R363, F377 and R379 in SopA exhibit foci in the presence of the SopBC complex, these residues are critical for plasmid maintenance. However, mutations in residues W369 and E375 result in defective plasmid partitioning due to their effects on nucleoid localisation of SopA (**Fig. 4-7**).

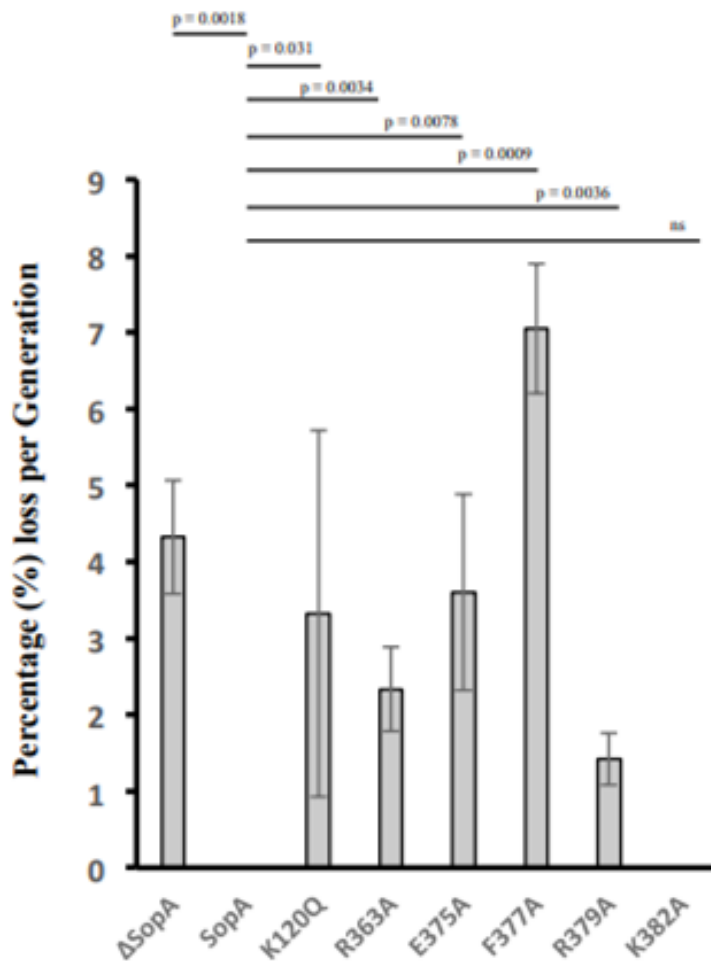


**Figure 4-7. Plasmid Stability Assay using C- terminal point mutants depicts plasmid loss in the case of most C-terminal mutants.**

Two plasmid system was used to calculate plasmid loss per generation in the cultures, details of which are described in materials and methods. Wild-type SopA exhibited no plasmid loss (0 %), whereas in the case of the mutants E375A and R363A mutants, loss rates of 3.6 % and 2.3 %, respectively, were observed. The plasmid loss rate in the case of F377A was 7 % per generation, suggesting that the entire C-terminal stretch is crucial for plasmid maintenance. The experiment was performed three times (n=3), and the error bars represent SEM.

### 4-3. DISCUSSION

A spontaneous double mutant of SopA carrying mutations in C-terminal residues, M315 and Q351, exhibits plasmid maintenance defects and forms polymeric structures (Lim et al., 2005). The C-terminal stretch of the ParA superfamily of proteins are majorly involved in nsDNA interaction, and these include VcParA2 (Parker et al., 2021), P1 ParA (Dunham et al., 2009; Baxter et al., 2020), *HpSoj* (Chu et al., 2019) etc. Moreover, similar to our results presented here, SopA  $\Delta$ Ct5, deletion of the C-terminal 3 amino acids in ParF is known to affect plasmid stability despite retaining its ability to interact with ParG (Ali, 2017). Further, in MinD, although the amphipathic helix comprising the last ten amino acid residues does not play a direct role in DNA binding, deletion of the ten amino acids resulted in the loss of DNA binding activity. Such loss of DNA binding activity could be further restored by mutation of two arginine residues to glutamate in the C-terminal region, suggesting a regulatory role for the C-terminal amphipathic helix in the conformational structure in MinD (Ventura et al., 2013). Similar to these studies, our findings here are suggestive of a critical role for the C-terminal H16 helix of SopA for its function. Although SopA  $\Delta$ Ct5 ( $\Delta$ 384-388) exhibited nucleoid localisation, other deletions like SopA  $\Delta$ Ct7 ( $\Delta$ 382-388), SopA  $\Delta$ Ct10 ( $\Delta$ 379-388), and SopA  $\Delta$ Ct29 ( $\Delta$ 360-388) were impaired in binding with nsDNA. Lack of nsDNA binding for SopA  $\Delta$ Ct7, SopA  $\Delta$ Ct10 and SopA  $\Delta$ Ct29 deletion mutants were also confirmed by localisation defects upon nucleoid condensation. Notably, these deletions (SopA  $\Delta$ Ct7, SopA  $\Delta$ Ct10, and SopA  $\Delta$ Ct29) were also incapable of forming a SopA foci in the cell even in the presence of the SopBC complex. On the contrary, the SopA  $\Delta$ Ct5 mutant retained its ability to interact with both the nucleoid and SopBC.

Further, neither of these mutants could maintain the plasmids in the cell, suggesting a more significant functional role of the C-terminal stretch in plasmid maintenance. Surprisingly, although fluorescence microscopy using SopA  $\Delta$ Ct5 revealed that the mutant could bind to the

nucleoid and form foci in the presence of the SopBC complex, this mutant exhibited plasmid partitioning defects. Despite binding to the nucleoid and interacting with the partitioning machinery, plasmid loss rates in SopA  $\Delta$ Ct5 might suggest that this mutant upon interaction with SopBC is not released from the nucleoid and thus leads to the plasmid partitioning failure. Further experiments are necessary to test this possibility.

The C-terminal point mutants like W369E, E375A, F377A fail to interact with nsDNA. However, other positively charged C-terminal mutants R363A, R379A, K382A, and R384A retained nsDNA binding activity suggesting that the positively charged residues in the C-terminal stretch are not essential for nucleoid association. While R363A, R379A, F377A and K382A formed foci in the presence of SopBC, suggesting interaction with the partitioning complex, other mutants W369E and E375A exhibited diffuse cytoplasmic localisation. Further, plasmid stability data also revealed that the mutants W369E, F377A and E375A exhibited plasmid segregation defects. Unexpectedly, we observed plasmid loss in the case of the R363A mutant as well. The loss rates in the case of R363A might be explained in similar lines to what has been suggested for SopA  $\Delta$ Ct5. No plasmid loss was observed in the case of the K382A mutant, indicating that this mutant retained all wild-type SopA properties, and the residue K382 is not critical for nucleoid association and plasmid maintenance. As with SopA  $\Delta$ Ct7 and SopA  $\Delta$ Ct10, the plasmid loss rate was very high in the case of the F377A mutant. Despite binding to the partitioning machinery, loss rates of F377A are suggestive of a critical role of this residue in plasmid maintenance.

In this work, we have characterised the role of the C-terminal stretch of SopA in nsDNA binding and thus plasmid partitioning. Deletions of SopA from  $\Delta$ Ct7 (SopA  $\Delta$ 382-388) onwards results in non-specific DNA binding defects and severe loss of plasmid from the cell, suggesting that this stretch is relevant for nsDNA binding. Further, our analysis also reveals that unlike *HpSoj* (Chu et al., 2019) and *MipZ* (Corrales-Guerrero et al., 2020), wherein

positively charged residue in the C-terminus mediates nsDNA binding, positively charged residues at the C-terminal stretch of SopA at least K382 and R363 are not relevant in nucleoid binding. However, the bulky hydrophobic residues W369, F377, and negatively charged E375 are critical for the nucleoid association of SopA. The residue E375 is a highly conserved residue among members of the ParA superfamily. Thus further studies involving E375 will help us identify the role of the C-terminus of the ParA family in nsDNA binding and plasmid partitioning.

## **CHAPTER 5**

### **C-TERMINAL RESIDUES Q351 AND W362** **REGULATE POLYMERISATION AND** **NUCLEOID BINDING OF SOPA**

## 5.1 INTRODUCTION

SopA is a member of the ParA superfamily and localises to the nucleoid within the bacterial cell (Hatano et al., 2007; Castaing et al., 2008; Roberts et al., 2012; Vecchiarelli et al., 2013; Le Gall et al., 2016). Recent super-resolution imaging data also provides direct evidence of nucleoid localisation of SopA (Le Gall et al., 2016) and additional *in vitro* reconstitution and *in vivo* experiments have led to the diffusion ratchet models (Vecchiarelli et al., 2013; Vecchiarelli et al., 2014). However, *in vitro*, SopA has also been observed to undergo polymerisation and form filaments (Lim et al., 2005). Further, these filaments have been reported to grow at a rate of  $0.18 \pm 0.05$   $\mu\text{m}$  per minute, which is similar to the rates at which plasmids and chromosomes segregate in bacteria (Lim et al., 2005). Such polymeric structures of SopA have also been reported using TEM for wild-type SopA in the presence of ATP (Bouet et al., 2007). Interestingly, the polymerisation of such filaments in SopA is mediated only by ATP, wherein non-specific DNA plays a significant role in inhibiting the formation of such polymers (Bouet et al., 2007). On the contrary, the ParA homolog Soj from *B. subtilis* and *T. thermophilus* assembles into a higher-order nucleoprotein complex in the presence of DNA (Leonard et al., 2005), and recent cryo-EM studies on VcParA2 also suggest the presence of ParA polymer-DNA complex (Parker et al., 2021).

Moreover, *in vitro* results show that SopA upon interaction with ATP and SopBC complex forms radial asters. Thus, the SopA polymeric structures are also retained in the presence of SopBC. Further, it was shown that these asters emanate radially from a centrally located SopBC complex suggesting that SopBC organises the SopA filaments into a radial aster that further promotes segregation of the plasmids (Lim et al., 2005). Such filaments in the presence of SopBC were also observed *in vivo* in 15 % of the cells (Lim et al., 2005). SopA in the presence of the SopBC complex has been reported to produce filaments whose length



remains constant during, indicating that these filaments are dynamic. These structures are also observed in anucleate cells indicating that nucleoid is not essential for the dynamic organisation of the SopA filaments (Hatano et al., 2007). These early observations had supported the cytoskeletal polymerisation-based models for plasmid segregation by SopA. However, more recent studies from several ParA members have revealed mechanisms independent of polymerisation in DNA partitioning. Models like the diffusion ratchet mechanism (Vecchiarelli et al., 2013), DNA relay mechanism (Lim et al., 2014) and the Hitch-Hiking models (Le Gall et al., 2016) have indeed questioned the physiological relevance of SopA polymerisation (Castaing et al., 2008; Vecchiarelli et al., 2013; Lim et al., 2014; Le Gall et al., 2016). However, such filaments and ATP-dependent polymers have also been observed in the case of other related ParA family members like ParF (Barilla et al., 2005; Barilla et al., 2007) and Soj (Leonard et al., 2005). More recently, work by Parker et al., 2021 has revealed that VcParA2 protein (a member of the Type-Ia superfamily) assembles into polymers in the presence of DNA. They also crystallized VcParA2 in an apo-state and an ADP nucleotide bound state, thus capturing different conformational states of ParA. The use of negative stain and Cryo-EM suggests that the VcParA2 assembles as a polymer in the presence of non-specific DNA and non-hydrolyzable analogue of ATP. The higher ordered assembly thus formed by VcParA2 has been suggested to involve the C-terminal helix of the protein (Parker et al., 2021). Thus, these recent cryo-EM studies revitalise the role of polymerisation in ParA function.

During the course of studies on SopA as described in chapters 3 and 4, we found that SopA W362E (a C-terminal helix mutant) assembled into polymeric structures. This mutant was particularly interesting as it resembled one of the spontaneous mutants, SopA1 (M314I Q351H), which was reported to assemble into filaments (Lim et al., 2005). SopA1 has been reported to be a static polymer that can co-polymerise with wt-SopA but exhibits plasmid segregation defects. In this chapter, we first show that a single mutation (Q351H) is sufficient

to recapitulate the polymers assembled by SopA1 and have further characterised the SopA Q351H and W362E mutants. We show that while SopA Q351H and SopA W362E are impaired in non-specific DNA binding, they retain their ability to interact with wt-SopA and with each other. Consistent with the previous studies on the role of non-specific DNA binding in plasmid segregation, we confirm that these mutants are impaired in the stable maintenance of the mini-F plasmid. Moreover, both Q351H and W362E act as super-repressors, strongly repress gene expression from the Psop promoter and do not respond to the presence of the SopBC complex. Finally, we show that both SopA Q351H and W362E fail to interact with SopB highlighting the relevance of the last C-terminal helix in regulating the nsDNA binding and polymerisation of SopA.

## 5.2 RESULTS

### 5.2.1 Mutations in SopA Q351 or W362 result in stabilisation of SopA polymers

All members of the ParA family of P loop ATPases involved in DNA partitioning function have non-specific DNA binding activity and is also true for F plasmid partitioning protein SopA. The localisation pattern of wild-type SopA is on the nucleoid of the bacterial cell (Hatano et al., 2007; Le Gall et al., 2016). However, a spontaneous mutation isolated in wild-type SopA, i.e., SopA1 (M315I Q351H), changed the localisation pattern from being on the nucleoid to forming static filament structures (Lim et. al., 2005). During the course of our mutagenesis studies of C-terminal helix described in the previous chapters, we also found that SopA Q351H and SopA W362E assembled into polymers similar to that of SopA1 (M315I Q351H).

**Figure 5-1A** shows the filaments formed by SopA Q351H, SopA W362E and SopA1. Further, exchanging W362 with alanine (W362A) also resulted in the assembly of similar filaments (**Fig. 5-1A**).

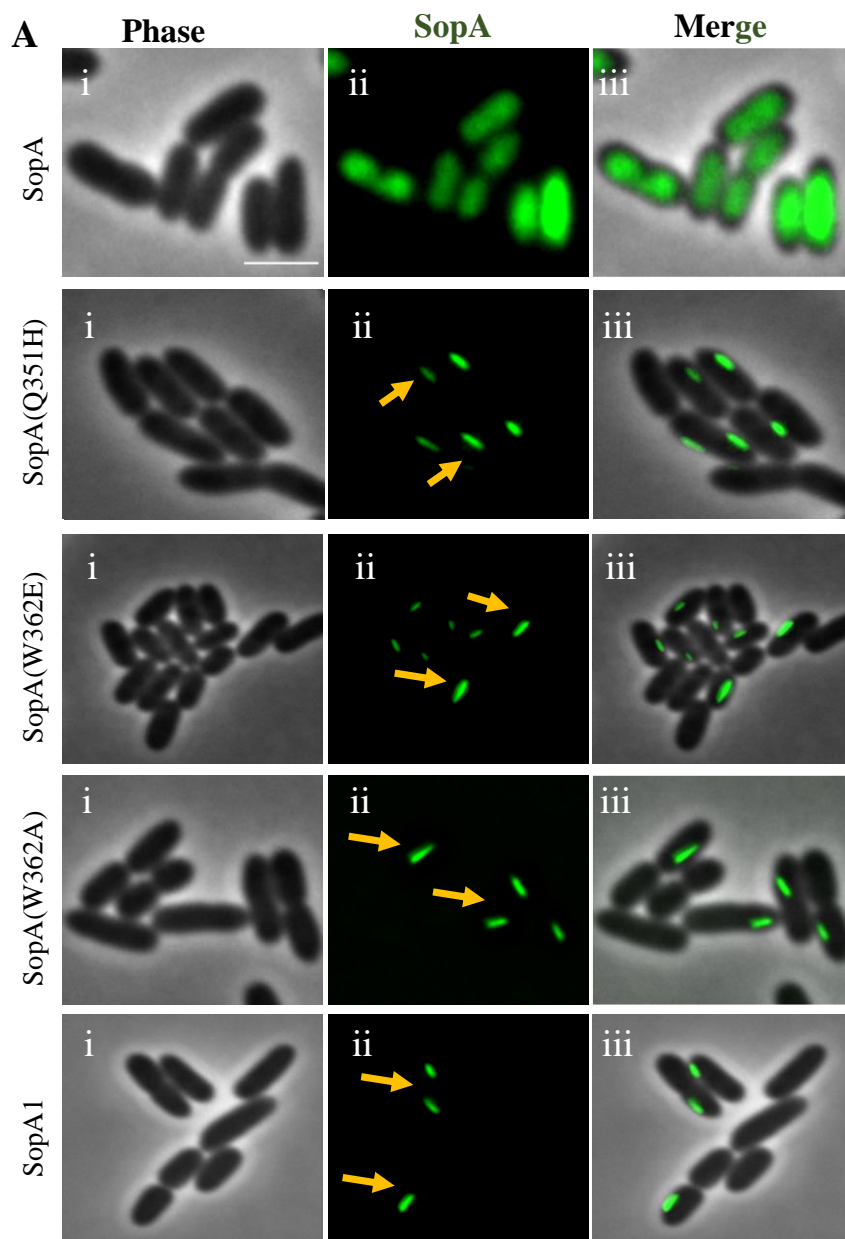


**Figure 5-1. Assembly of SopA, SopA1, Q351H and W362A/E into polymers.**

**(A) Polymers assembled by SopA mutants.** Wide-field imaging of *E. coli* MC4100 cells harboring wild-type SopA, SopA1 (M315I Q351H), SopA Q351H, SopA W362E and SopA W362A. MC4100 strain with the mutant SopA plasmids was grown till OD<sub>600</sub> of 0.2 induced with 400  $\mu$ M IPTG (as described in Materials and Methods) and was examined by fluorescence microscopy. The arrows point to the filaments observed in the case of SopA Q351H, SopAW362A/E and SopA1. The scale bar is 2  $\mu$ m.

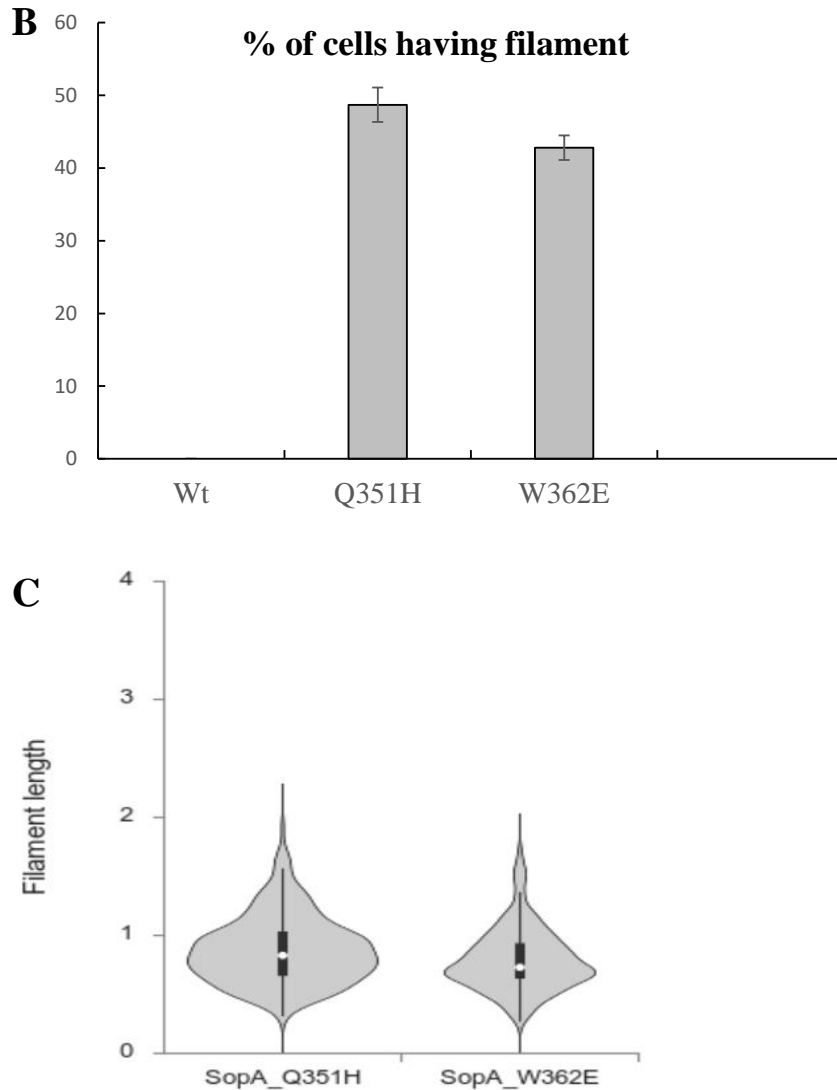


**Figure 5-1. (B) Quantification of the number of cells containing SopA polymers.** The percentage of cells having SopA polymers in cultures expressing SopA Q351H or SopA W362E is plotted. The total number of cells and the number of cells with filaments were counted manually using ImageJ and plotted in excel. Experiments were repeated at least thrice, and the error bar represents SEM. **(C) Quantitative representation of the length of the polymers formed by SopA Q351H and SopA W362E mutants in *E. coli*.** Distribution of SopA Q351H and SopA W362E filament length in *E. coli* MC4100 cells. The length of filaments was measured using ImageJ, and the representative violin plot was generated using [tastitika.mfub.bg.ac.rs/interactive-dot-plot/graph](http://tastitika.mfub.bg.ac.rs/interactive-dot-plot/graph) (Weissgerber et al., 2017). Experiments were performed in triplicate. Error bar represents S.D.

In contrast, cells expressing wild-type SopA displayed the characteristic nucleoid-associated fluorescence (**Fig. 5-1A**). Quantification of the number of cells with filaments showed that  $48.69\% \pm 2.3$  (SEM, n=3) and  $42.80\% \pm 1.8$  (SEM, n=3) of cells expressing SopA Q351H and SopA W362E, respectively contained polymers (**Fig. 5-1B**). Further, Q351H and W362E filaments showed a mean length of  $0.88\ \mu\text{m} \pm 0.28$  (SD, n=3) and  $0.75\ \mu\text{m} \pm 0.27$  (SD, n=3) respectively (**Fig. 5-1C**).

Since both SopA Q351H and SopA W362E exhibited polymerisation, we wanted to test the proximity of these residues and identify the position of these residues in the 3-dimensional structure of the protein. However, the only structures available for a Type-1a ParA are P1 and P7 ParA (Dunham et al., 2009). Therefore, we utilised iTasser (Zhang, 2008; Roy et al., 2010; Yang et al., 2015) to build a homology model of SopA protein and mapped the residues Q351H and W362E on this structure. Using Chimera (Pettersen et al., 2004) to visualise the modelled SopA structures, we observed that the residue Q351 was in close proximity to the hydrophobic residue W362 in the SopA structure and made several contacts (**Fig. 5-1D and E**). Interestingly, the model also suggests that W362 makes contact with K340, a residue known to be crucial for nsDNA binding activity (**Fig. 5-1E**).

To further confirm that these filaments formed were independent of any host factor or specific to assembly in bacteria, we tested their ability to assemble into polymers upon expression in fission yeast (*Schizosaccharomyces pombe*). We thus generated these mutants in a fission yeast expression vector pREP42. The expression of SopA-GFP or its variants were achieved from a medium strength thiamine repressible promoter *nmt41/42* and growth in a minimal medium lacking thiamine. We observed that, while wt-SopA was localised to the nucleus, probably owing to the nsDNA binding activity, both SopA Q351H and W362E mutants assembled into polymeric structures in the cytoplasm of *S. pombe* (**Fig. 5-1F**).

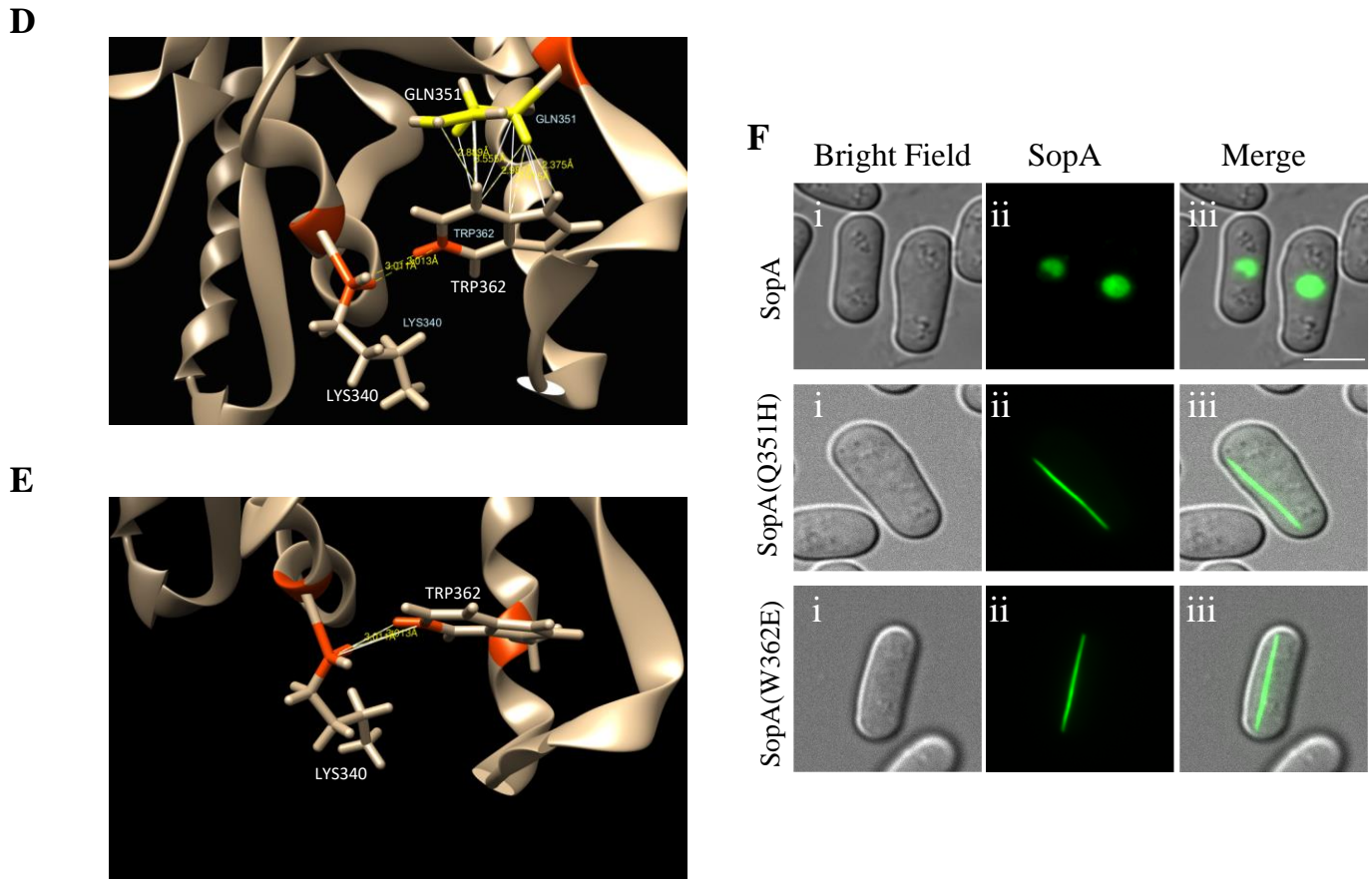


**Figure 5-1. (D) and (E) Structural model of SopA showing the residues K340, Q351 and W362.** The structure of SopA was predicted with I-TASSER (<https://zhanglab.ccmb.med.umich.edu/I-TASSER>). (D) The residues Q351 and W362 lie closer to one another, likely making several contacts in the SopA structure, and (E) that the known nsDNA binding residue K340 is in close vicinity of the hydrophobic residue W362. Molecular graphics and analyses were performed with the UCSF Chimera package (<http://www.cgl.ucsf.edu/chimera>). (F) **SopA Q351H and SopA W362E assemble into polymers in fission yeast.** Images of fission yeast cells expressing SopA-GFP and the mutants SopA Q351H-GFP or SopA W362E-GFP are shown. The polymeric mutants were cloned into pREP42 plasmids driven by thiamine repressible nmt41 promoter and were expressed in heterologous system *S. pombe*. The formation of filaments in a heterologous expression system suggests that the assembly of SopA into filaments is independent of other host factors in bacteria. similar filaments (**Fig. 5-1A**). Scale bar is 5  $\mu$ m.

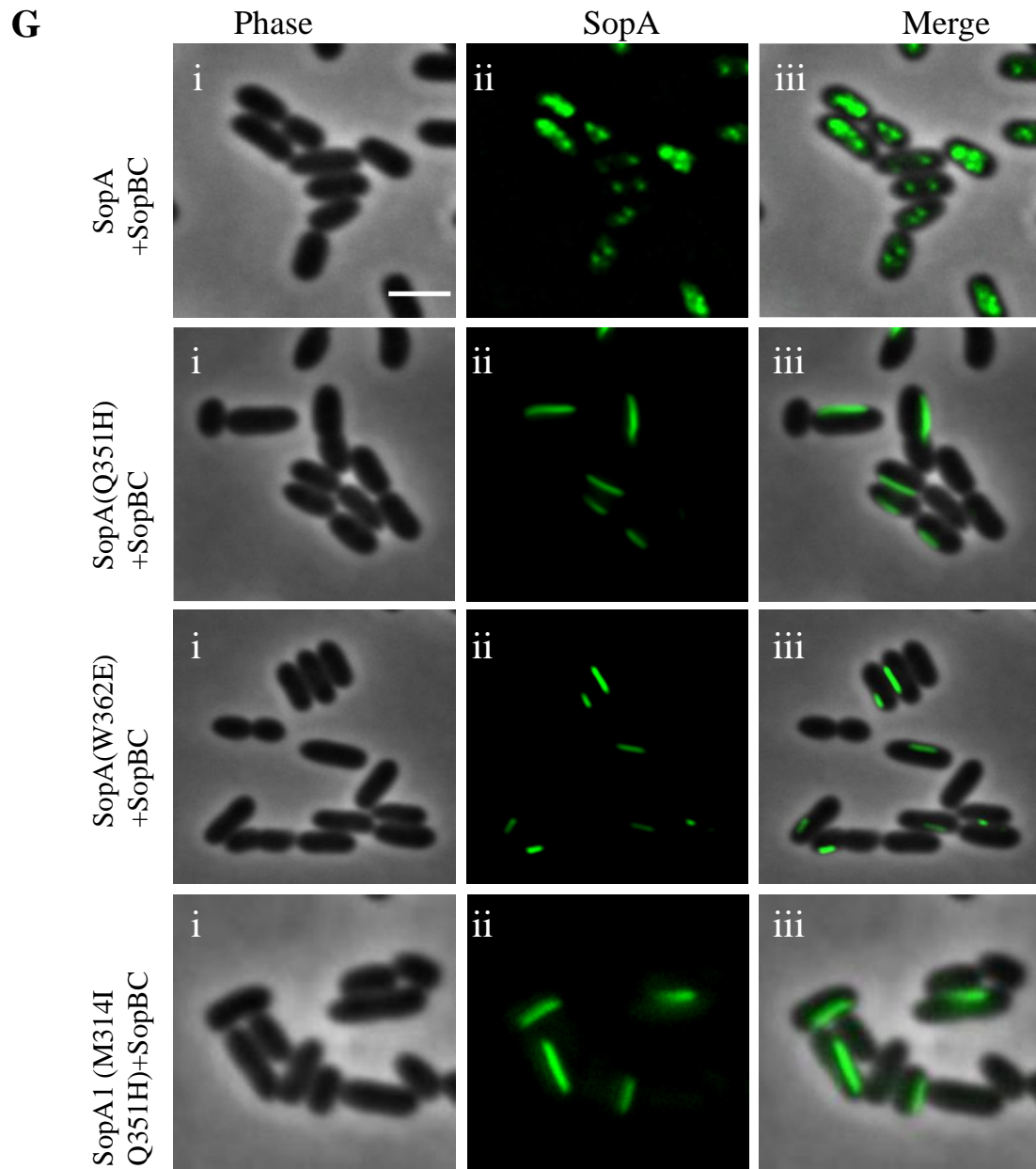


**Figure 5-1. (G) SopA1 (M315I Q351H), SopA Q351H and SopA W362E form polymers in the presence of the SopBC partitioning complex.** Fluorescence images of wild-type SopA, SopA mutants Q351H, W362E and SopA1 in the presence of SopBC complex. The wild-type SopA protein is localised as foci in the presence of the SopBC complex (top panel). Phase-contrast and fluorescence images of representative cells were overlaid and showed that SopA

mutants Q351H, W362E and SopA1 formed filaments in the presence of the SopBC complex as well. Scale bar is 2  $\mu$ m.

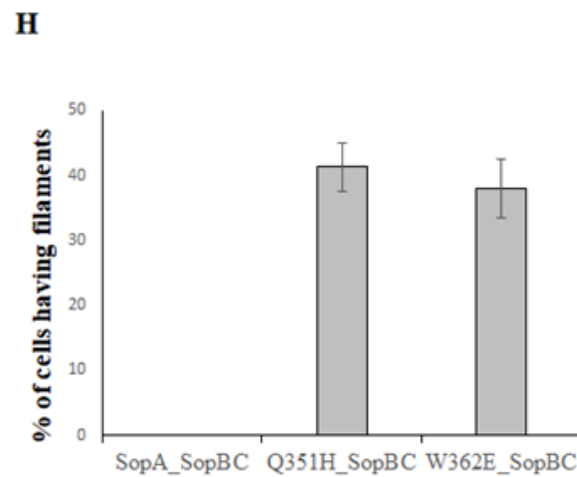


**Figure 5-1. (H) Quantification of the number of cells exhibiting SopA polymers in the presence of the partitioning complex.** Percentage of cells showing SopA Q351H and SopA W362E filaments in the presence of SopBC complex in *E. coli* MC4100 cultures. The number of cells with filaments were counted using ImageJ and plotted in excel. The data is representative of experiments performed in triplicate. Error bar represents SEM.



Interestingly, the filament length spanned the length of *S. pombe* cells and was not restricted to 1  $\mu\text{m}$  (as seen in bacterial cells), suggesting that the filament length observed in *E. coli* was a result of both the physical limit of cell length and the amount of protein available for polymerisation (also see below for cephalixin treated *E. coli* cells expressing SopA Q351H and SopA W362E).

The SopBC complex is known to interact with wild-type SopA, affecting the dynamics of SopA localisation within the cell and resulting in the assembly of SopA into foci (Lim et al., 2005; Bouet et al., 2007; Hatano et al., 2007; Ah-Seng et al., 2013; Le Gall et al., 2016). We thus tested if the presence of SopBC affected the polymers assembled by SopA1, SopA Q351H and SopA W362E. We utilised a mini-F plasmid lacking SopA but carrying SopBC ( $\Delta\text{sopA}$ ,  $\text{sopBC}^+$ ) under the constitutive  $P_{\text{LtetO-1}}$  promoter (pDAG198; a kind gift from Dr. Jean-Yves Bouet) (Castaing et al., 2008). As expected, wild-type SopA formed fluorescent spots/foci in the presence of SopBC, suggesting that it interacted with the partitioning complex. However, the presence of SopBC did not affect the polymerisation and assembly of SopA1 (M315I Q351H), SopA Q351H and SopA W362E into filaments (**Fig. 5-1G**). Quantification of percentage cells having polymers showed that  $41 \% \pm 3.69$  (SEM, n=3) of SopA Q351H and  $37 \% \pm 4.47$  (SEM, n=3) of SopA W362E expressing cells contained filaments (**Fig. 5-1H**). Thus, the number of cells having polymers were similar to the number of cells exhibiting filaments in the absence of SopBC, indicating that polymerisation of these mutants was independent of the SopBC complex.

### **5.2.2 Interaction of SopA Q351H and SopA W362E with wild-type SopA and with themselves**

Polymerisation requires interaction along a specific face among the subunits. Further, ATP binding also triggers dimerisation of ParA/ SopA, resulting in an ATP-sandwich dimer

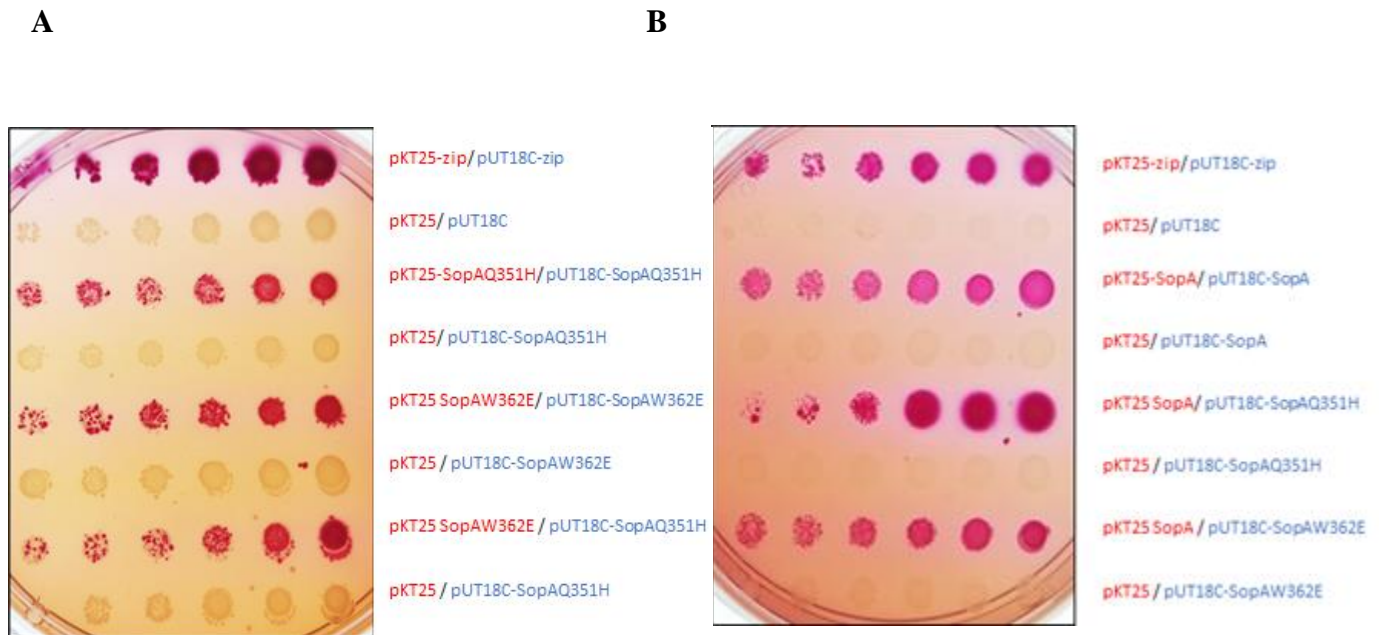


**Figure 5-2. SopA Q351H and SopA W362E retain the ability to interact with the wild-type SopA.** Bacterial two-hybrid assay showing the interaction between (A) wtSopA and SopA mutants Q351H and W362E and (B) Self-interaction of SopA Q351H and SopA W362E, cloned as N-terminal fusion in both pUT18C as well as pKT25 vectors. Experiments were performed in triplicate and plated on MacConkey agar plate with 0.5 mM IPTG as described in materials and methods. In both cases (A) and (B), the polymeric mutants exhibit interaction with wtSopA as well as with themselves, suggesting that the mutations in residues Q351 and W362 do not affect SopA interaction.

(Castaing et al., 2008; Dunham et al., 2009; Vecchiarelli et al., 2013). Thus, it was interesting to test if SopA Q351H and W362E polymers retained their ability to interact with wild-type SopA. We first probed the interaction of these filament-forming mutants with wild-type SopA using the Bacterial Two-Hybrid (BACTH) assay (Karimova et al., 1998). We observed that

both the mutants retained their ability to interact with the wild-type SopA. This result is consistent with the findings of Lim et al., 2005 wherein SopA1 was also able to interact with wt-SopA. Thus, mutations in these residues of SopA, W362 and Q351, do not affect its ability to interact with wild-type SopA (**Fig. 5-2A**).

We also investigated whether these mutants Q351H and W362E interacted with one another and among themselves using the BACTH assay. We observed that Q351H interacted with itself. Similarly, we also observed self-interaction for SopA W362E with itself. Thus, in both these cases, self-interaction was detected as would be expected for polymerizing proteins. Further, we also tested whether SopA Q351H and SopA W362E interacted with one another using the BACTH vectors, pUT18C SopA Q351H and pKT25 SopA W362E. While the control strains carrying only one of the mutant constructs failed to show a colour change on McConkey agar plates, the strains carrying both SopA Q351H and W362E turned pink (**Fig. 5-2B**). These results suggest that SopA Q351H and SopA W362E are capable of interacting with each other as well. Thus, we conclude that both SopA Q351H and SopA W362E interact with themselves and with wild-type SopA and each other.

### **5.2.3 Polymerisation of SopA Q351H and SopA W362E is ATP dependent**

*In vitro* studies of SopA and several ParA, homologs have shown that polymerisation was strictly an ATP dependent process (Lim et al., 2005; Leonard et al., 2005; Bouet et al., 2007; Parker et al., 2021). Thus, we wanted to test if the observed *in vivo* polymerisation of SopA Q351H and SopA W362E was dependent upon ATP-binding. The residue K120 in SopA has

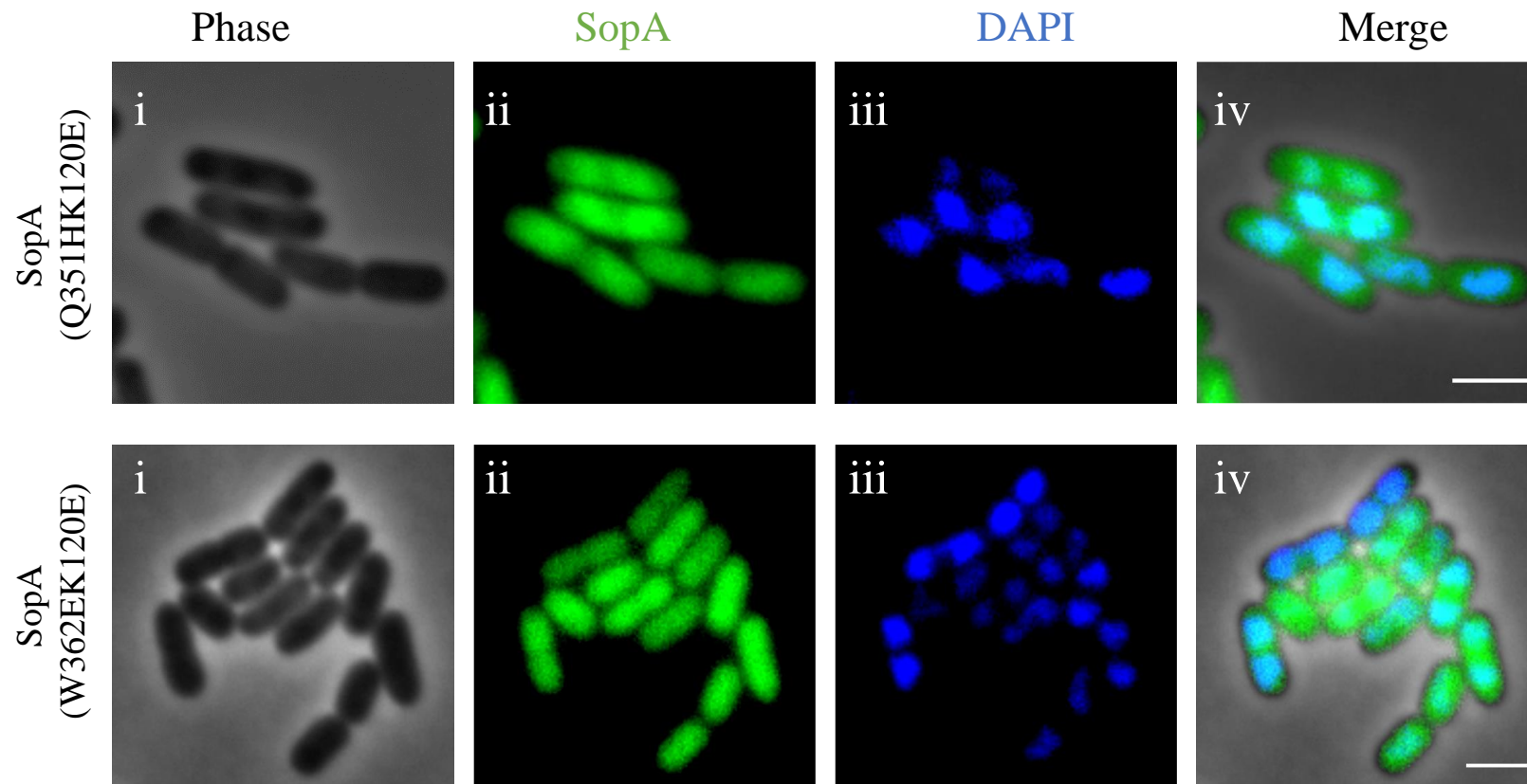


**Figure 5-3. The polymerisation of SopA Q351H and SopA W362E is dependent upon ATP binding.** Representative images of SopA double mutants, SopA Q351H K120E (top panel) and SopA W362E K120E (bottom panel) induced with 400  $\mu$ M IPTG for 2 hours and observed by fluorescence microscopy. Both the mutants fail to form filaments underlining the role of ATP binding in the polymerisation of SopA. Scale bar is 2  $\mu$ m.

been reported to be essential for ATP binding and hydrolysis, and changing this residue to glutamic acid in P1 ParA has been shown to affect ATP binding (Fung et al., 2001; Libante et al., 2001; Vecchiarelli et al., 2013). Thus, we generated SopA double mutants (SopA K120E Q351H, SopA K120E W362E in pDSW210) and assessed their ability to form polymers in *E. coli*. These double mutations abolished polymerisation entirely and resulted in diffuse fluorescence of SopA-GFP over the entire cytoplasm of the cell, underlining the role of ATP binding in the polymerisation of these SopA mutants (**Fig. 5-3**).

#### **5.2.4 Polymerisation requires continuous protein synthesis**

Polymerisation is defined by the concentration of proteins in the cell. To determine if SopA filament formation was dependent upon continual protein synthesis, we first grew cultures carrying pDSW210-SopA Q351H or pDSW210-SopA W362E with IPTG to induce polymerisation. We then placed these cells on agarose pads with or without IPTG and imaged them after 20 minutes. While in the presence of IPTG, cells continued to express SopA and retained the SopA polymers, cells predominantly exhibited diffuse fluorescence in the absence of IPTG (i.e., no further induction of protein synthesis) (**Fig. 5-4A**). The absence of polymers when IPTG was not provided suggested that the filaments had undergone depolymerisation in the absence of continued expression of SopA. Time-lapse imaging in the presence or absence of IPTG confirmed that the filaments of SopA Q351H and W362E indeed underwent depolymerisation in the absence of continued protein synthesis (**Fig. 5-4B ii**).

Further, we added chloramphenicol, a protein synthesis inhibitor and glucose (to repress SopA expression from the P<sub>Trc</sub> promoter completely) on agarose pads and carried out time-lapse imaging of SopA Q351H and SopA W362E to monitor the depolymerisation of the

**A**

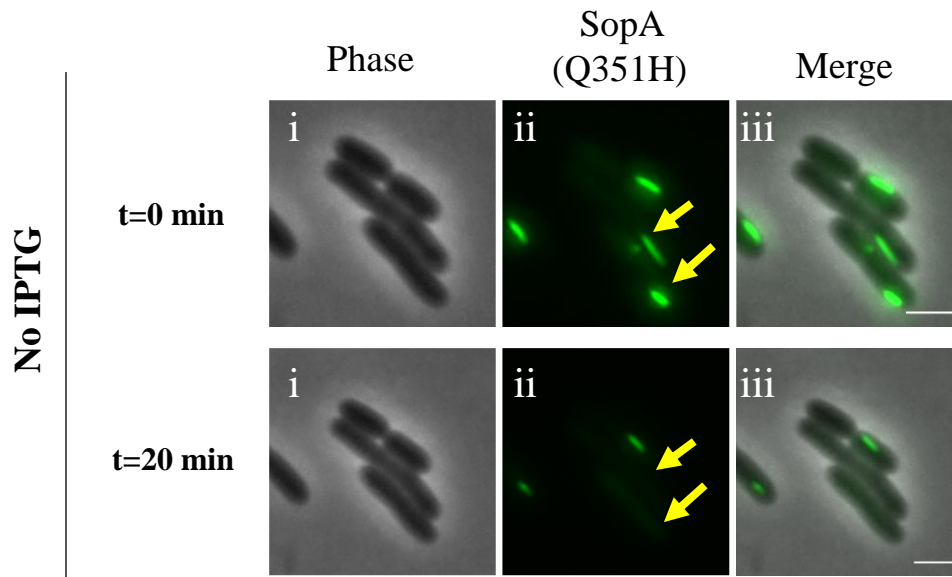
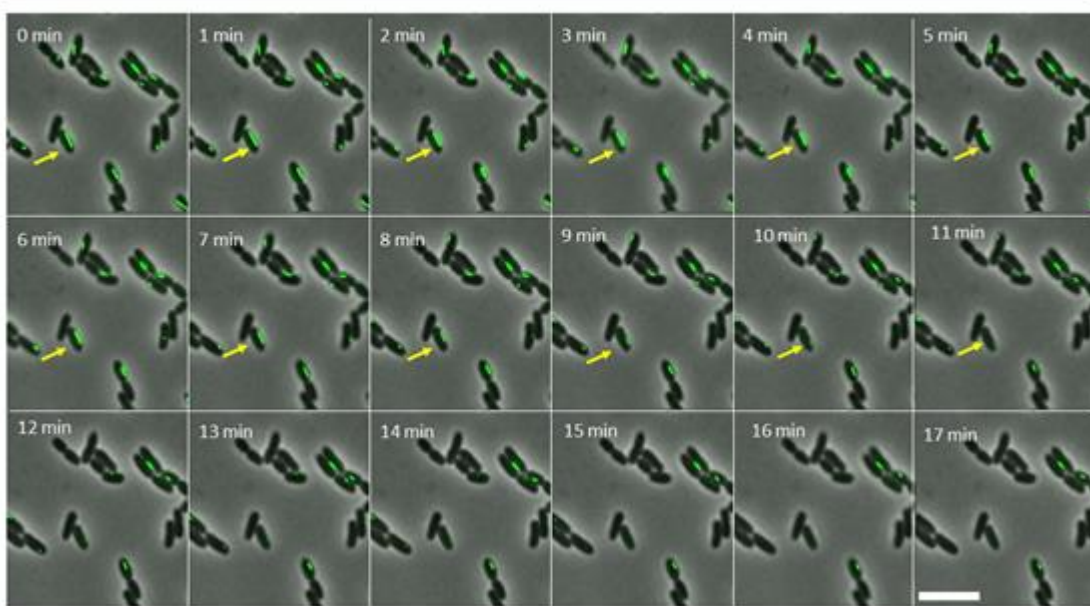


**Figure 5-4. Polymers are dynamic and exhibit the property of growth as well as shrinkage.**

**(A). Polymer formation requires continuous production of protein.** Filaments observed in cells disassemble rapidly in the absence of IPTG in 20 min. The top panel represents cells imaged at the initial (0 min) time point, and the bottom panel represents cells imaged after 20 min.

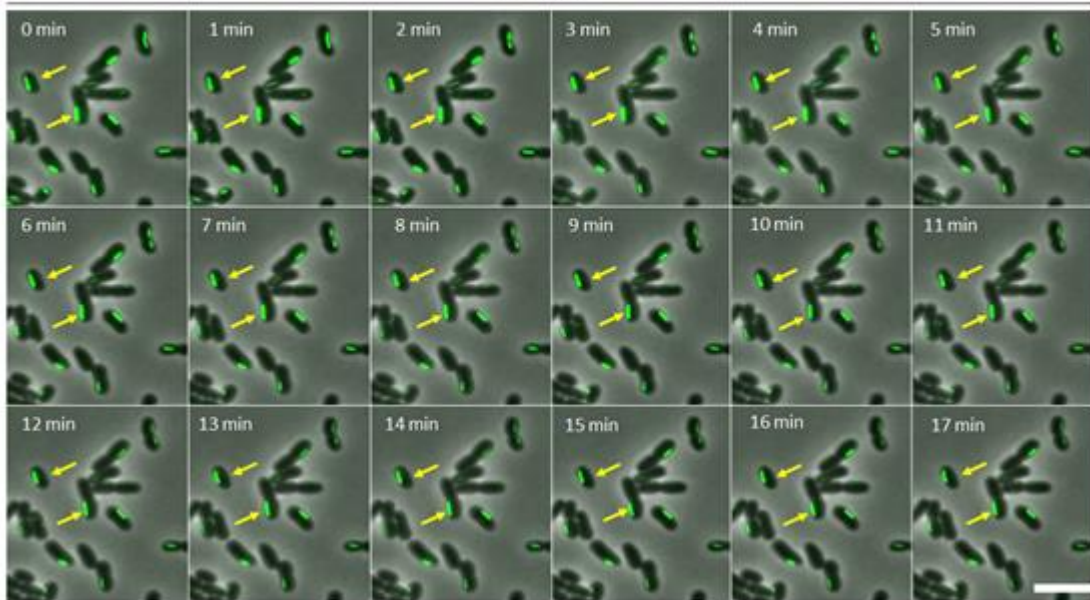
**B i**

**SopA Q351H  
(No IPTG)**



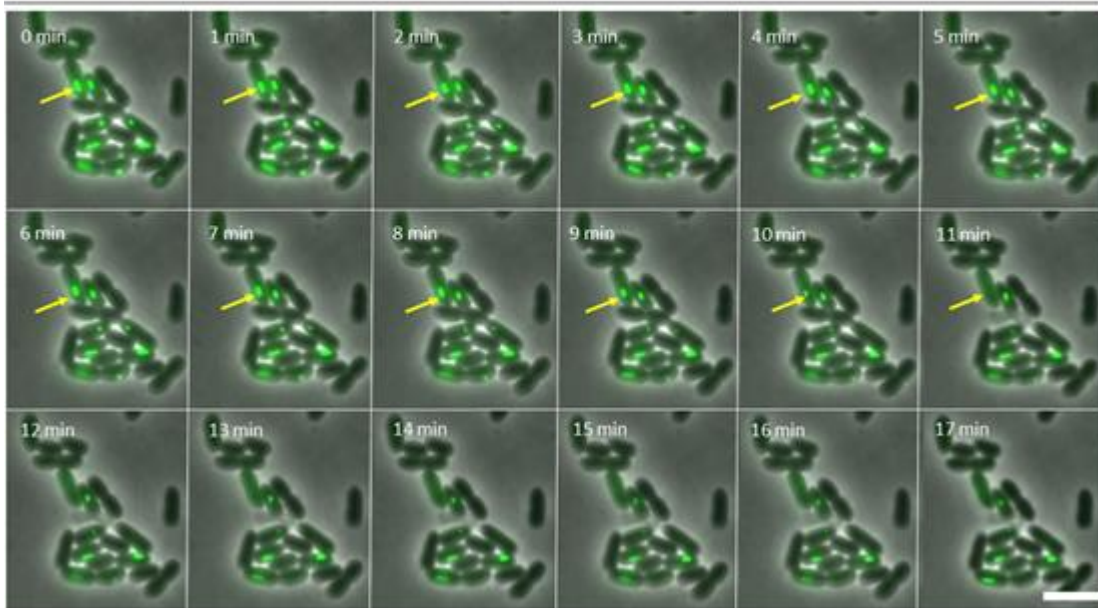
**B ii**

**SopA Q351H  
(+ IPTG)**



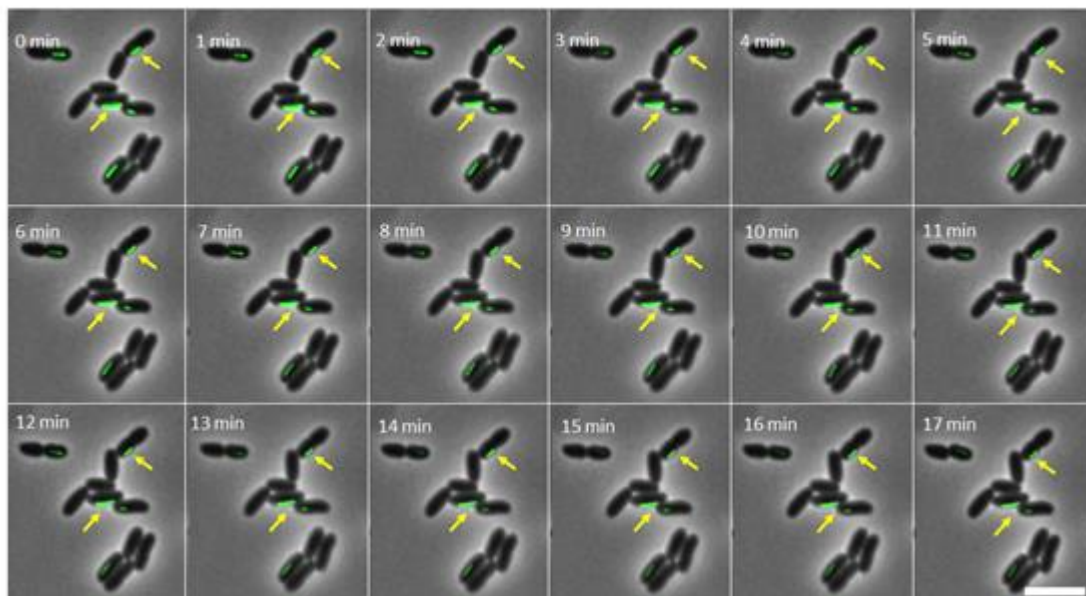
**B iii**

**SopA Q351H**  
(+ Cam ; + Glu)



**C i**

**SopA W362E**  
(+ IPTG)





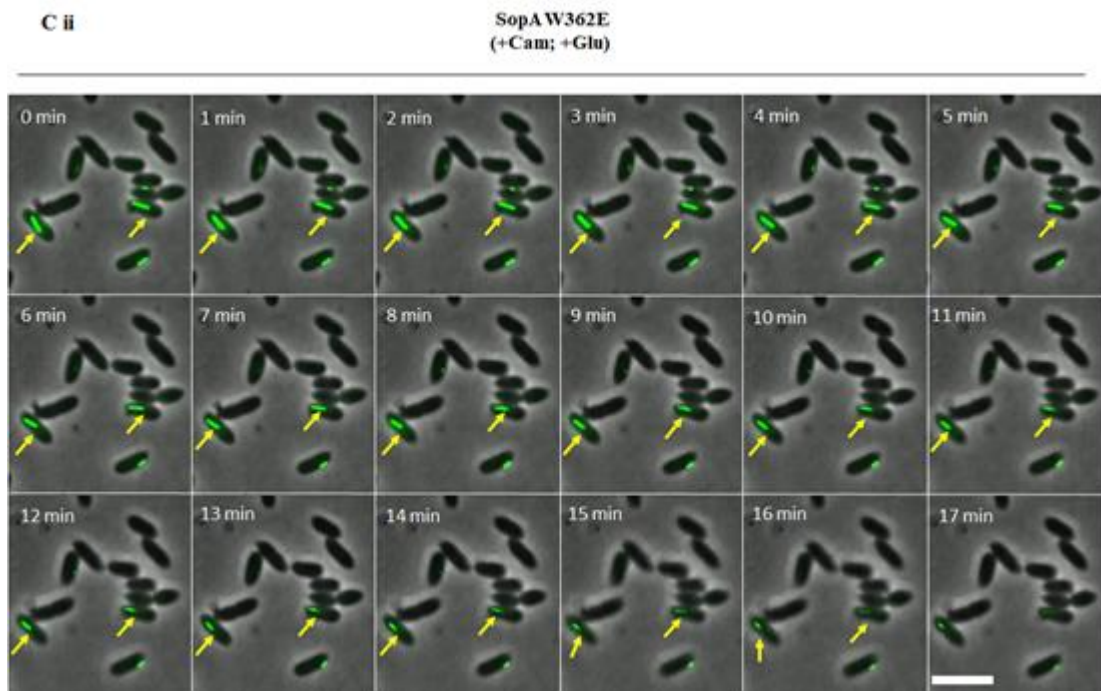
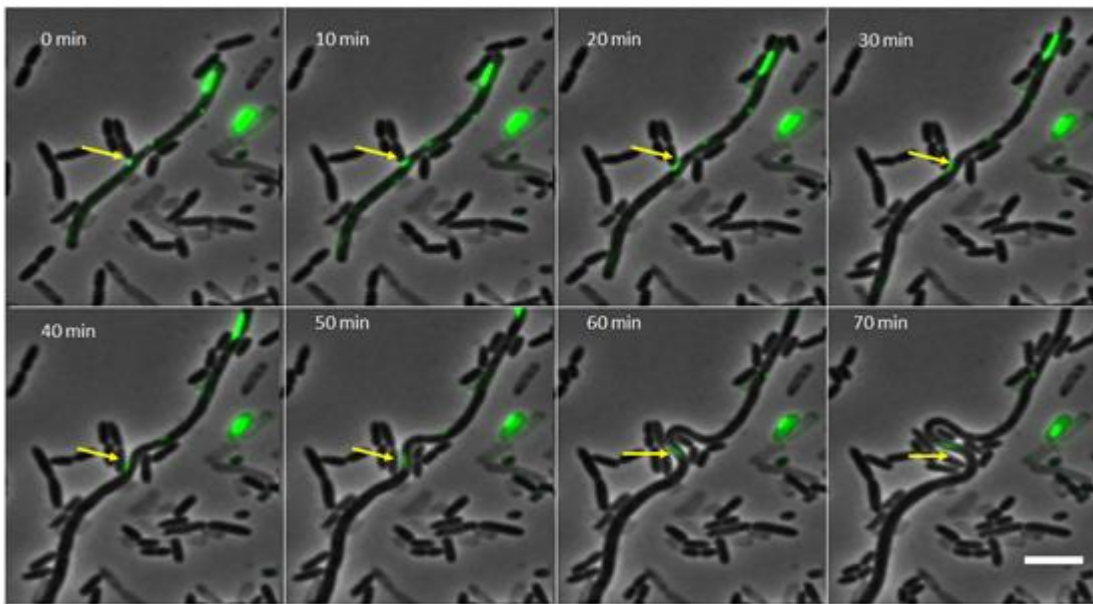


**Figure 5-4. Polymers are dynamic and exhibit the property of growth as well as shrinkage.**

**(B) and (C) Time-series of the cells showing depolymerisation of the filaments in the absence of continuous protein synthesis.** Cells were imaged every 1 min for a period of 20 min on a Delta Vision Elite<sup>TM</sup> microscope. Filaments were retained in cells supplied with IPTG in the agarose pads (**B ii and C i**). Filaments disassemble in the absence of IPTG (**B i**) or in the presence of chloramphenicol and glucose (**B iii and C ii**), suggesting that polymerisation of both Q351H and W362E requires continuous protein synthesis.

D i

SopA Q351H  
(+Cephalexin)



D ii

SopA W362E  
(+Cephalexin)

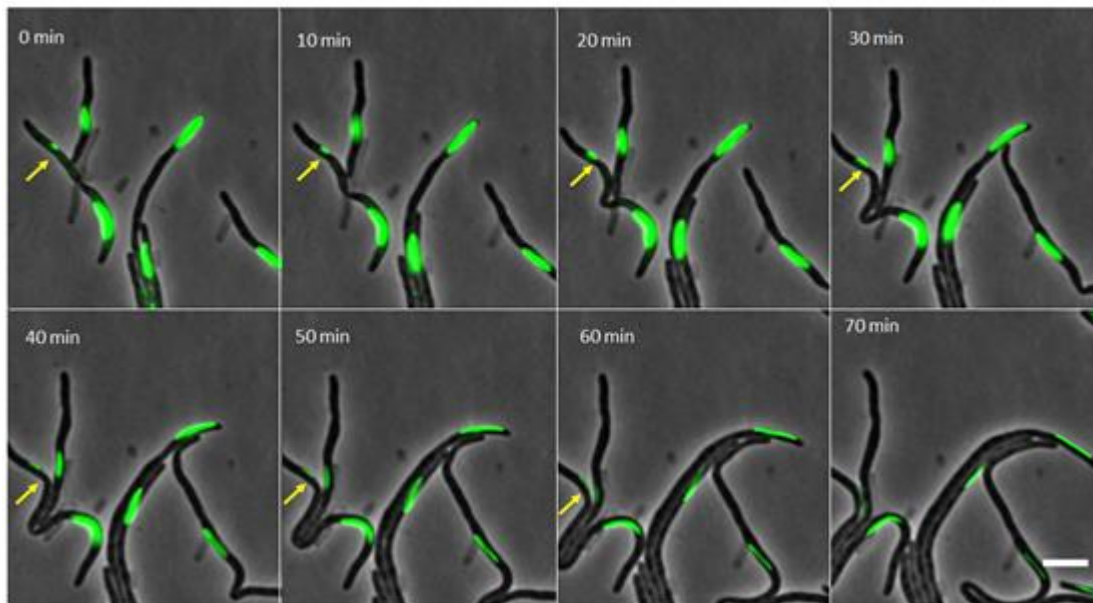


**Figure 5-4. Polymers are dynamic and exhibit the property of growth as well as shrinkage. (D) Representative montages indicating the growth of the polymers are shown.** The polymerisation of (D i) SopA Q351H and (D ii) SopA W362E was followed over time by time-lapse fluorescence microscopy. Cells were imaged every 10 min for 70 min on a Delta Vision Elite™ microscope. Arrows depict the growing filaments.

filaments. The filaments of both SopA Q351H (**Fig. 5-4B iii**) and SopA W362E (**Fig. 5-4C ii**) appeared to depolymerise over a period of approximately 20 min suggesting that continuous protein synthesis was essential for the maintenance of SopA polymers. In order to rule out that the disappearance of filaments was not due to bleaching effects, we also imaged the filaments in the presence of IPTG in agar pads and found that the polymers did not undergo any shrinkage in this period and were retained over a period of 1 hour (**Fig. 5-4B ii and C i**). These results suggest that the polymerisation of SopA was dependent upon continual protein synthesis and, in the absence of which, cellular concentrations fall below a critical threshold that the SopA filaments begin to depolymerise.

We next sought to visualise the polymerisation dynamics of SopA Q351H and SopA W362E. Although depolymerisation could be easily observed, polymerisation, i.e., the growth of a dot to a filament, could rarely be captured in our time-lapse images. Even in the case of 4-hour time-series as each cell division split the already growing filament into two halves, the increment in length could not be discerned, probably owing to limiting protein levels due to the weak promoter used (pDSW210; Weiss et al., 1999) and cell division induced dilution effects. Thus, we resorted to cephalixin treatment of cells (to inhibit cell division) and to monitor filament growth in the presence of IPTG. We were able to observe filament elongation in these non-dividing cells, albeit at a very slow rate, indicating that polymerisation of SopA was a slow process and the protein levels were possibly still limiting (**Fig. 5-4D i and ii**). Thus, we conclude that the polymers assembled by SopA Q351H and W362E are dynamic and exhibit the property of growth as well as shrinkage.

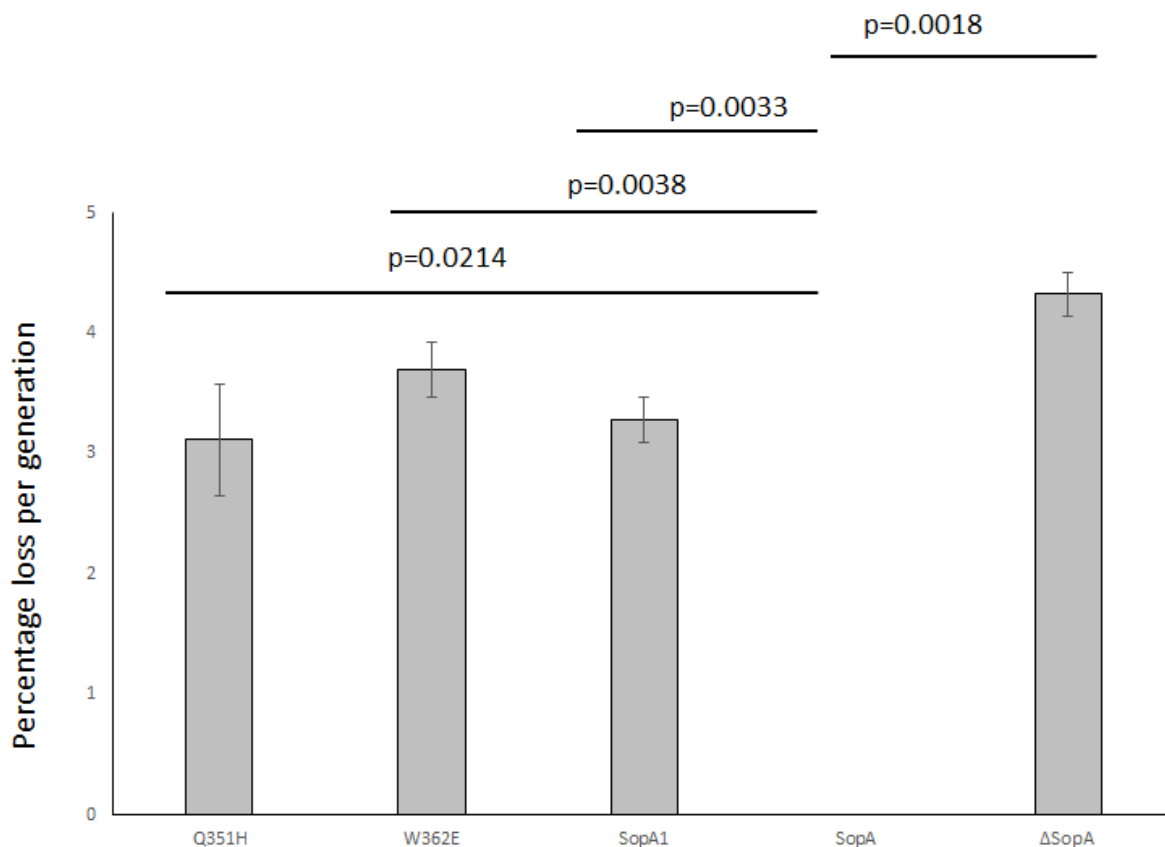


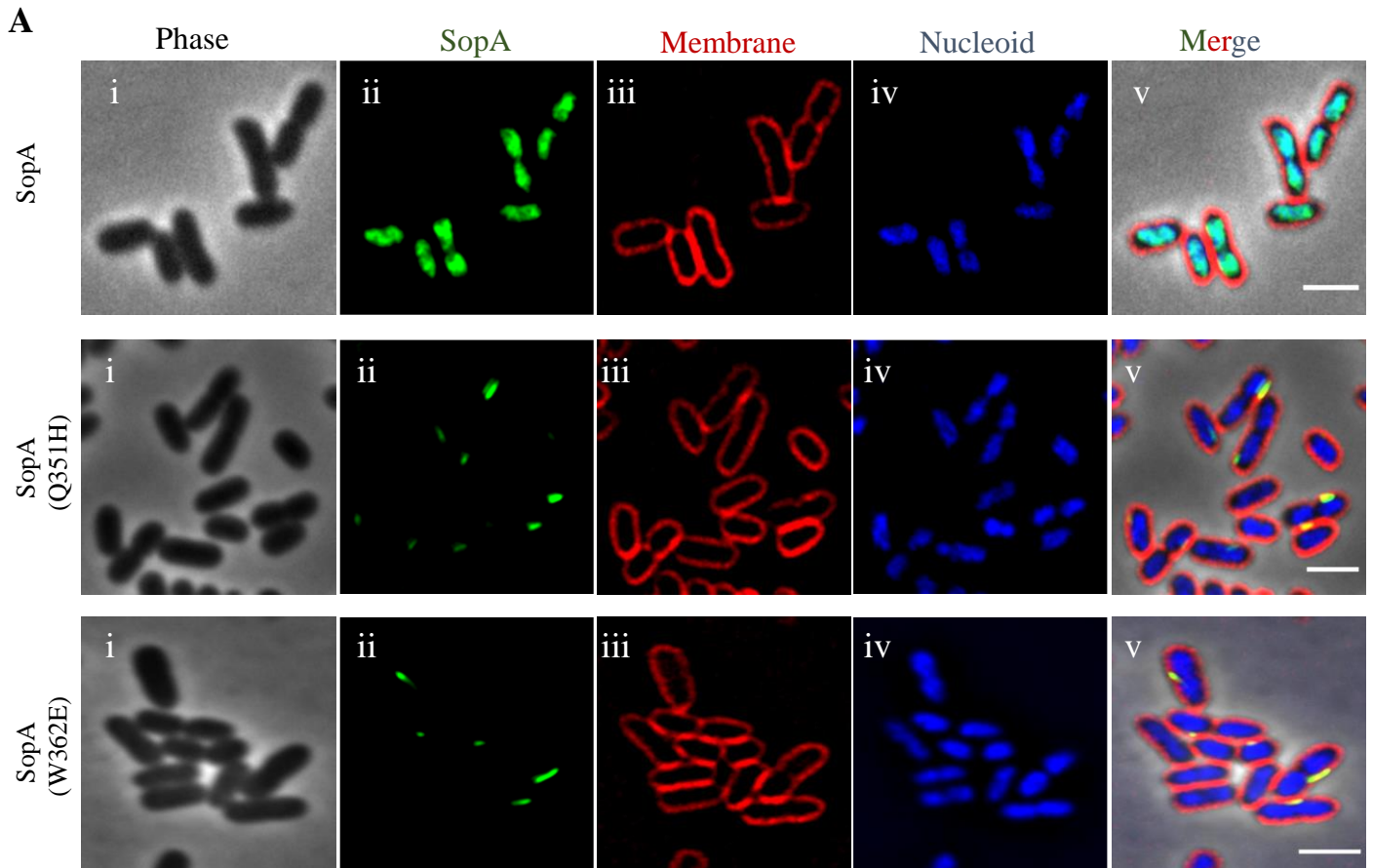
**Figure 5-5. SopA Q351H and SopA W362E are defective in plasmid partitioning.** MC4100 cells harbouring plasmids pDSW210 SopA (and its variants) and pDAG198 (mini-F carrying  $\Delta$ sopA, sopBC<sup>+</sup>) were grown in LB medium with 100  $\mu$ g/ml carbenicillin and 34  $\mu$ g/ml chloramphenicol at 37°C and then transferred to LB medium with carbenicillin alone added to the media. It was allowed to grow for 20 generations, following which it was plated on carbenicillin plates, and subsequently, individual colonies were patched onto chloramphenicol plates to estimate the loss rates. The experiment was performed three times, and representative results are shown. The error bars represent SEM. Wild-type SopA exhibited no plasmid loss, whereas, in the case of SopA Q351H and SopA W362E, a loss rate of 3.11 % and 3.69 % per generation, respectively, was observed. The loss rate in the case of SopA1 was 3.28 % and was almost similar to the loss rates observed in the case of Q351H.

### 5.2.5 SopA Q351H and SopA W362E are defective in partitioning DNA

SopA Q351H and SopA W362E formed polymers similar to SopA1 as already described above. SopA1 was isolated as a mutant that failed to maintain plasmids in cultures (Lim et al., 2005). Therefore, we next tested whether or not the polymers assembled by the mutants (Q351H and W362E) could maintain mini-F plasmids in cells. We tested the effect of SopA variants on plasmid maintenance using the two-plasmid system (Ah-Seng et al., 2013) as described in the Materials and Methods section (Chapter 2). SopA-GFP and its variants were expressed utilizing the leaky expression from the weakened  $P_{trc}$  promoter without any induction with IPTG. A mini-F plasmid lacking SopA but containing SopBC under the constitutive  $P_{LtetO-1}$  promoter (mini-F CamR  $P_{LtetO-1}::\Delta sopA, sopBC^+$ ) constituted the second plasmid whose maintenance was tested. As would be expected, in the presence of wild-type SopA, mini-F plasmids were stably maintained, whereas a loss rate of  $4.3 \% \pm 0.185$  (SEM, n=3) per generation was observed in the absence of SopA. The mini-F plasmid loss rates in cultures expressing SopA mutants Q351H and W362E were  $3.1 \% \pm 0.463$  (SEM, n=3) and  $3.6 \% \pm 0.228$  (SEM, n=3) respectively, which was comparable to those lacking SopA (**Fig. 5-5**). SopA1 (M315I Q351H) also exhibited plasmid loss from the cultures at the rate of  $3.2 \% \pm 0.189$  (SEM, n=3) as reported earlier (Lim et al., 2005), showing that these SopA mutants that assemble into polymers are impaired in partitioning plasmids.

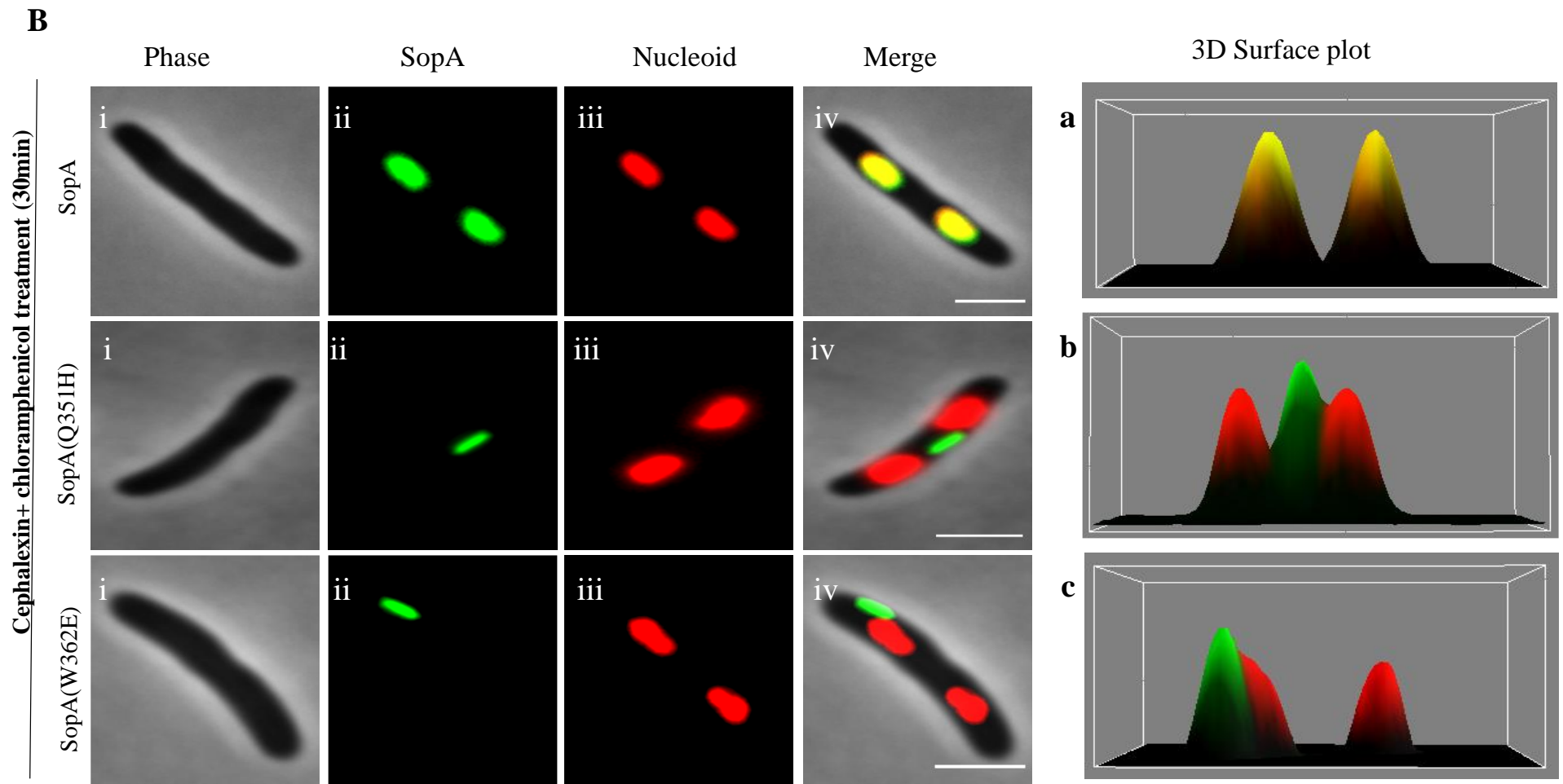
### 5.2.6 SopA Q351H and SopA W362E filaments are not nucleoid-associated

SopA mediated plasmid partitioning is majorly dependent on the nucleoid association of SopA-ATP dimers and the formation of the chemophoretic gradient through which SopB-sopC plasmid complex migrates. A positively charged lysine residue at position 340 (K340) is known to mediate non-specific DNA binding in SopA. Mutating this lysine residue to alanine (K340A) results in severe partition defects of the mini-F plasmid (Castaing et al., 2008).



**Figure 5-6. SopA Q351H and W362E are not nucleoid bound and show no DNA binding defects.**

**(A) The polymers of SopA Q351H and SopA W362E do not bind the bacterial nucleoid.** SopA mutants were expressed from plasmid pDSW210 by induction with 400  $\mu$ M IPTG, as described in Materials and Methods. Cell membranes were stained with FM 4-64 (red), and nucleoid was stained with DAPI (blue). Phase-contrast and fluorescence images of representative cells were overlaid. While SopA localises on the nucleoid, the mutants did not exhibit nucleoid colocalisation, as is evident in the merge images. Scale bar is 2  $\mu$ m.



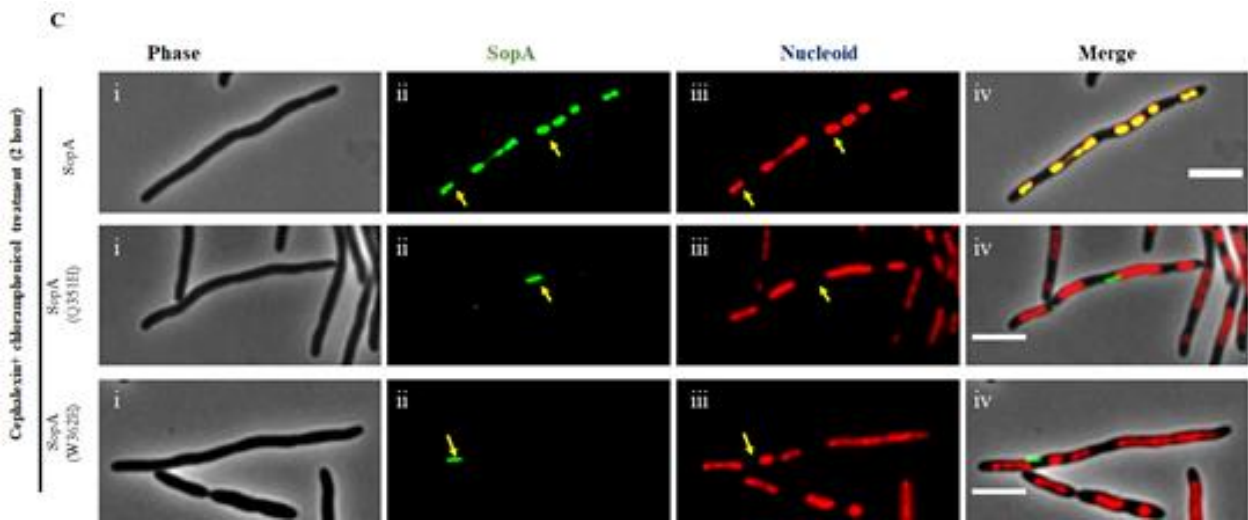


**Figure 5-6. (B) and (C) Localisation of the filaments in elongated cells with condensed nucleoids.** Cells were treated for (B) 30 minutes or (C) 2 hours post-induction with cephalexin and chloramphenicol to exacerbate the nucleoid free regions and observe the localisation of the SopA. Nucleoids were stained with DAPI but are pseudo-coloured as red. Fluorescence images of SopA Q351H and SopA W362E polymers show that the mutants do not colocalise with the condensed nucleoid. Representative 3D surface plot analysis of the selected cells for (a) SopA (b) SopA Q351H, and (c) SopA W362E show that the polymers were impaired in nucleoid binding.



D

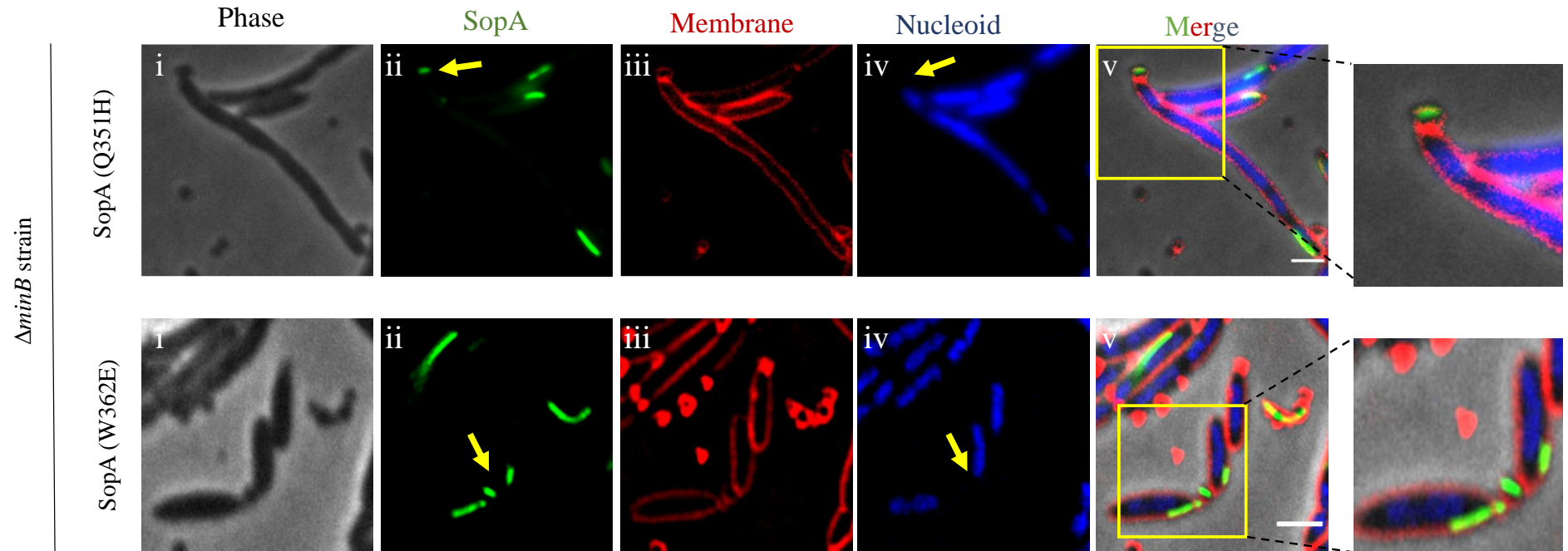


**Figure 5-6. (D) Localisation of the filaments in  $\Delta minB$  strain.** Fluorescence images of SopA Q351H and SopA W362E in a  $\Delta minB$  strain shows that both proteins localised in minicells indicating that both the mutants were not associated with the nucleoid. A magnified image of panel 3C has been shown as an inset. Scale bar is 2 $\mu$ m.

Although both the SopA mutants, Q351H and W362E, formed polymers, mutations also seemed to map to the C-terminal region with proximity to K340 (**Fig. 5-1D and E**). It was thus imperative for us to test if these mutants were also impaired in interaction with non-specific DNA. The localisation of the filaments formed by these mutant proteins was thus determined by live-cell imaging in conjunction with the nucleoid stain DAPI and the membrane marker FM 4-64. SopA Q351H and SopA W362E filaments often seemed to localise between the nucleoid and the membrane and appeared not to be co-localised with DAPI, suggesting that these mutants did not bind to the nucleoid (**Fig. 5-6A**).

In order to determine if the polymers were indeed not bound to the nucleoid, we treated cells with cephalixin (to inhibit cell division) and chloramphenicol (to condense nucleoids) and thus clearly visualise DNA free regions, stained them with DAPI as described in Materials & Methods and carried out live-cell imaging. The filaments were invariably localised to the nucleoid free regions of the cell, and we did not find any co-localisation of filaments with the nucleoid. However, wild-type SopA was seen to be entirely co-localised with the nucleoid (**Fig. 5-6B and C**). We further tested the lack of nucleoid binding of SopA Q351H or W362E filaments by analyzing their presence in anucleate cells of a  $\Delta minB$  strain of *E. coli*. Proper positioning of the FtsZ ring depends upon the presence of *minCDE* operon. A deletion of *min* genes results in aberrant polar positioning of the FtsZ rings, resulting in the production of minicells lacking chromosomal DNA (Jaffé et al., 1988; de Boer et al., 1989). When expressed in the  $\Delta minB$  strain of *E. coli*, we found polymers of SopA Q351H and SopA W362E localised to the anucleate minicells, suggesting that these SopA mutants exhibited nucleoid (non-specific DNA) binding defects (**Fig. 5-6D**).

Finally, we confirmed the lack of non-specific DNA of SopA variants using purified proteins and analyzing their DNA binding capabilities *in vitro*. SopA and the mutants (Q351H,

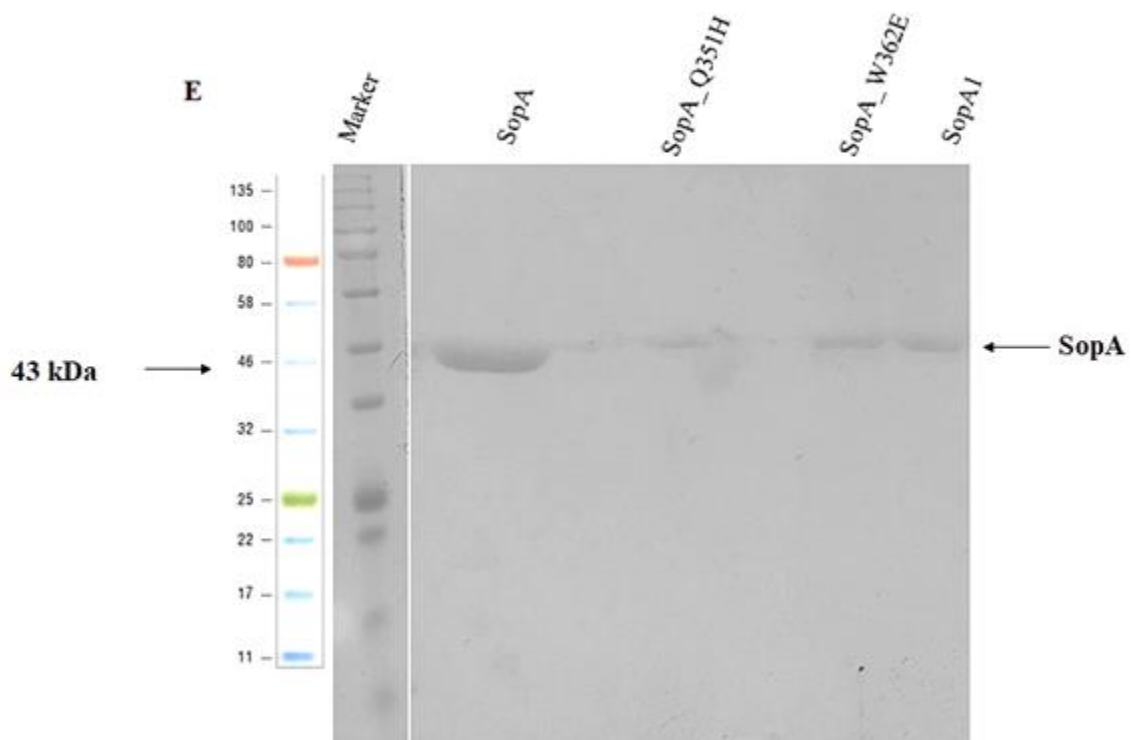


**Figure 5-6. (E) Purification of 6xHis-tagged SopA, SopA1 (M315I Q351H), SopA Q351H and SopA W362E proteins.** An N-terminal 6X His-tagged wild-type SopA, as well as the mutant proteins, were purified using affinity chromatography with the help of Ni-NTA beads. The proteins were then subjected to 12 % SDS-PAGE, followed by Coomassie staining.

**F**

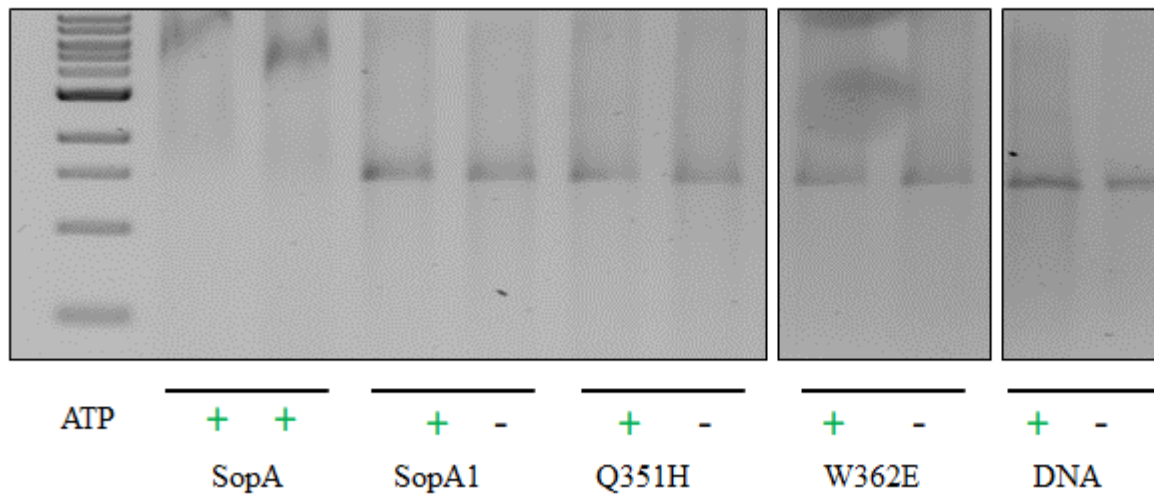


**Figure 5-6. (F) DNA binding activity of SopA mutants using a linearised PCR product by EMSA.** The proteins, SopA wild-type or mutants, were initially incubated with or without ATP, followed by the addition of linearised DNA. This was incubated for 30 min at RT, and then run on 1 % agarose gel (as described in Materials & Methods). While wild-type SopA binds to DNA in an ATP dependent manner, SopA1, SopA Q351H, and SopA W362E fail to bind nsDNA in the presence of ATP. DNA alone is shown as a control.

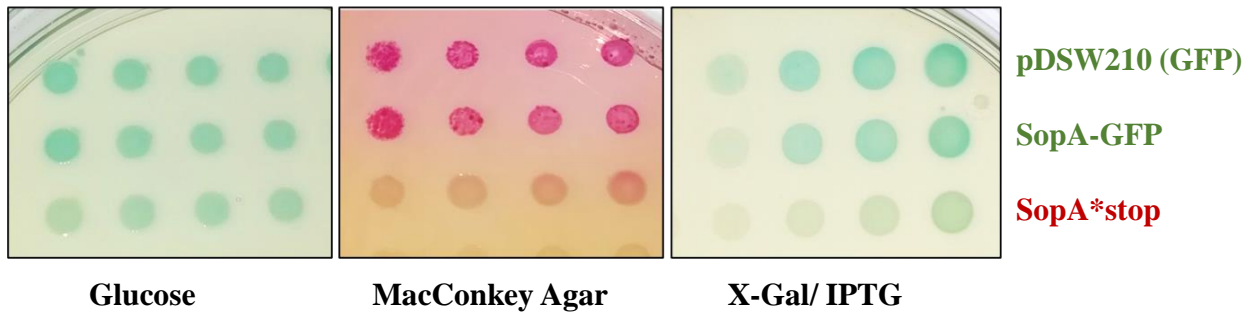
W362E and M315I Q351H) were expressed as N-terminal 6xHis tagged protein and purified using Ni-NTA chromatography as described previously (Lim et al., 2005). The purity of the protein was ascertained by SDS-PAGE and staining Coomassie staining (**Fig. 5-6E**). We tested the DNA-binding capacity of SopA Q351H, SopA W362E and SopA1 using an agarose gel EMSA (Electrophoretic Mobility Shift Assay) as described by Leonard et. al., (Leonard et. al., 2004; 2005). The purified proteins at a concentration of 12  $\mu$ M were incubated with a 1.2 kbp linear DNA in the presence of 1 mM of ATP. Whereas the wild-type protein, in the presence of ATP, strongly reduced the mobility of the DNA fragment during electrophoresis, the mutant proteins (Q351H, W362E and M315I Q351H) failed to show any binding activity either in the presence or absence of ATP (**Fig. 5-6F**). Taken together, these results show that the polymers of SopA Q351H and SopA W362E do not localise to nucleoids in *E. coli* and are impaired in nsDNA binding.

### **5.2.7 SopA Q351H and SopA W362E act as super-repressors of the *sop* promoter, P<sub>sop</sub>**

SopA is known to weakly repress transcription from its own promoter by binding to the four operator sequences (Lemonnier et al., 2000; Libante et al., 2001; Komai et al., 2011). This auto-regulatory activity of SopA is very weak, and this property is enhanced in the presence of the SopBC complex (Libante et al., 2001; Bouet et al., 2007; Komai et al., 2011). Since SopA Q351H and SopA W362E were found to be impaired in nsDNA interaction, we tested whether these mutants were also compromised for binding the specific DNA sequences in the promoter. In order to do so, we resorted to an *in vivo* reporter assay based on *lacZ* fusion to the P<sub>sop</sub> promoter and utilised the DLT1127 strain; P<sub>sop</sub>::*lacZ* (Ravin and Lane, 1999) (a kind gift from Dr. David Lane) of *E. coli*. We co-transformed our wild-type SopA and mutant plasmids into the DLT1127 strain of *E. coli* with or without SopBC plasmid ( $\Delta$ *sopA sopBC*<sup>+</sup>) and assayed for promoter repression by spotting serial dilutions of the cultures on MacConkey agar or

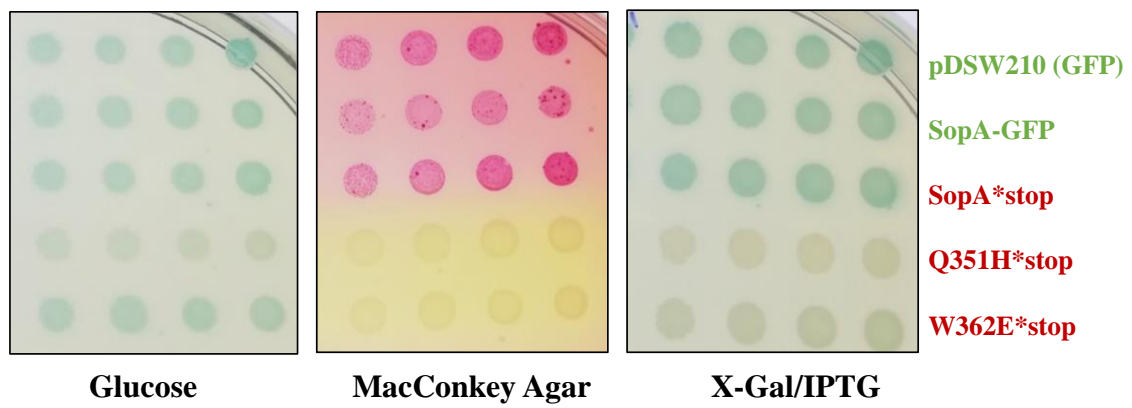
**A**

**DLT1127/SopBC/Stop Clones**



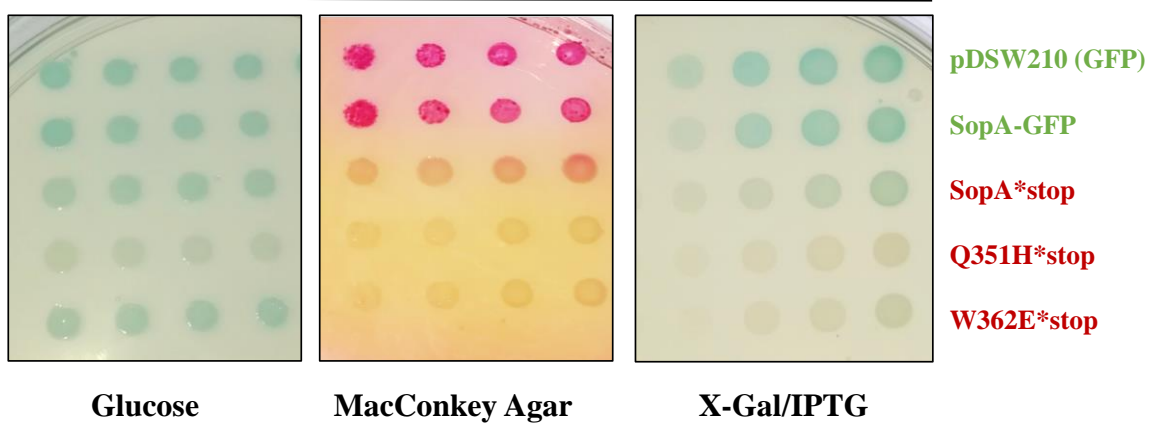
**B**

**DLT1127/SopA-Stop Clones**

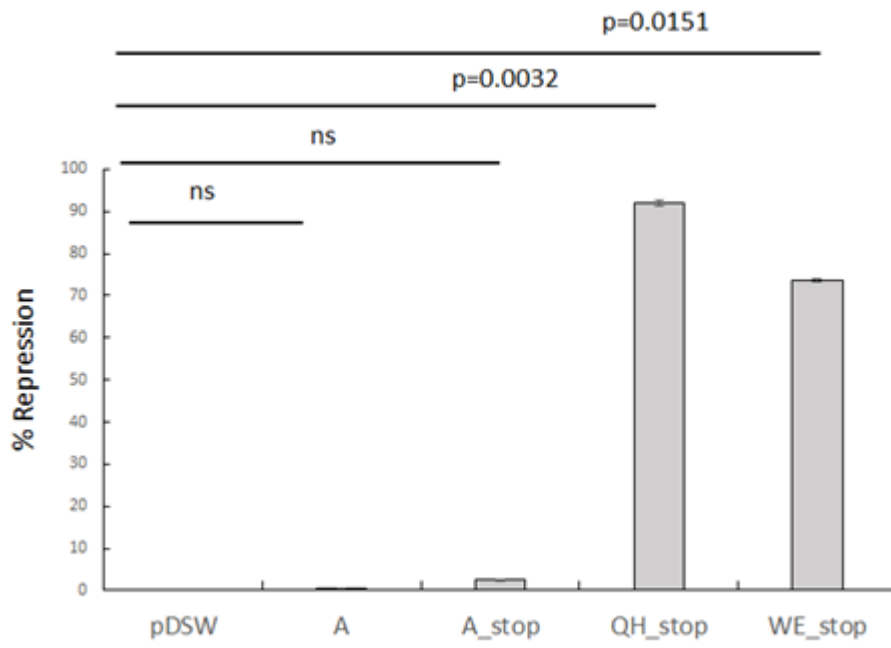


**C**

**DLT1127/SopBC/SopA-Stop clones**



**D**



**E**

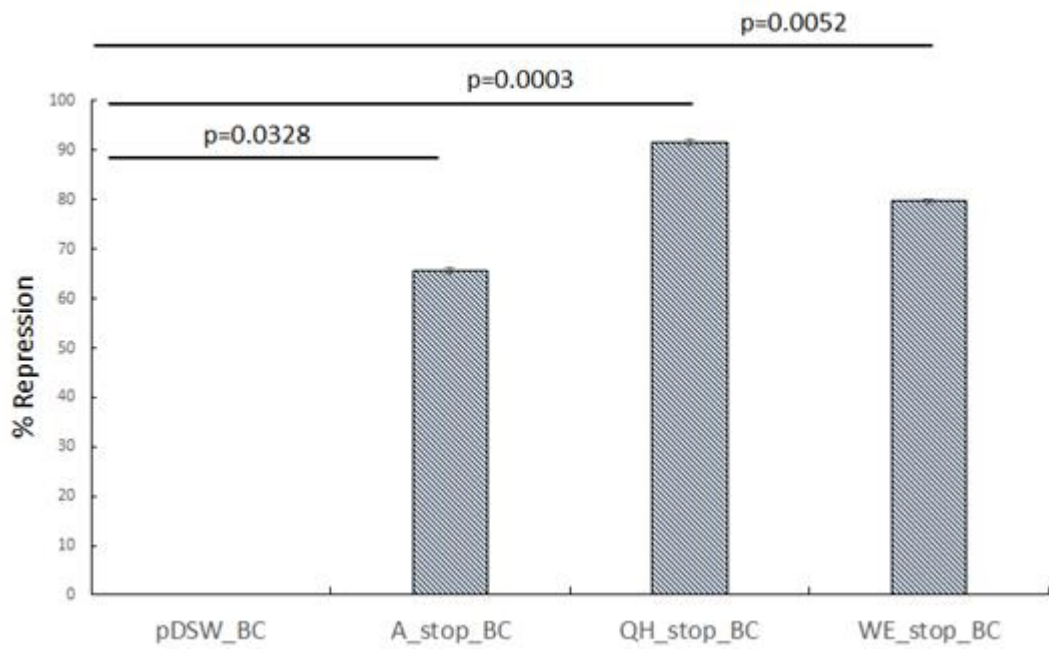


**Figure 5-7. SopA Q351H and SopA W362E can bind the SopA promoter to repress transcription. (A) SopA-GFP shows very weak repression of the SopA promoter.** Wild-type SopA-GFP and the SopA-Stop-GFP constructs were co-transformed with mini-F carrying SopBC ( $\Delta$ sopA) into DLT1127, induced for 2 hours with 400  $\mu$ M IPTG and spotted on X-Gal/IPTG plates to observe the autoregulatory effect of the wild-type SopA. Repression can be observed on the indicator plate in the case of SopA-Stop-GFP clone. However, in the case of SopA-GFP, repression was very weak. **(B and C) SopA Q351H and SopA W362E act as super-repressors.** The SopA Q351H-Stop-GFP and SopA W362E-Stop-GFP clones were transformed into **(B)** DLT1127 strain or **(C)** into DLT1127 strain carrying SopBC, induced for 2 hours with 400  $\mu$ M IPTG and spotted onto X-Gal/IPTG plates to observe the autoregulatory effect of the mutants. SopA Q351H and SopA W362E exhibit repression in both cases suggesting that promoter repression by these mutants is independent of the SopBC complex. **(D and E)** The representative results of the  $\beta$ -galactosidase/ ONPG assay (as described in materials and methods) of B and C are represented in D and E, respectively, showing the percentage reduction in the amount of  $\beta$ -galactosidase produced in cells expressing wild-type SopA or the SopA mutants in absence or presence of SopBC. The  $\beta$ -galactosidase produced in the case of vector alone (pDSW210) control has been adjusted to 0 % repressed activity, and the values were normalised accordingly for other mutants. The error bars represent SEM. SopA Q351H exhibits almost 92 % repression in all the cases. SopA W362E, on the other hand, showed repression of 74 %. However, the repression in both cases was independent of the SopBC complex suggesting that both the mutants act as super-repressors.



X- Gal + IPTG plates. However, we observed that the SopA-GFP, although fully functional for nsDNA binding and plasmid stability in our pDSW210 constructs, weakened the repression ability of wild-type SopA, even in the presence of SopBC complex (**Fig. 5-7A**). We thus resorted to using untagged versions of SopA and its mutants for carrying out the repression assays. We created an untagged version by introducing a stop codon before the first codon of GFP in all our constructs (as described in **Table 2-4**) (**Fig. 5-7A**). In the presence of SopBC, both wild-type SopA and the mutants (Q351H and W362E) strongly repressed the expression of LacZ from the  $P_{sop}$  promoter. However, in the absence of the SopBC complex, only SopA Q351H and SopA W362E showed the ability to repress the expression of *lacZ*, which was much stronger than the wild-type SopA (**Fig. 5-7B**). Moreover, in the case of mutants, repression in the absence of SopBC complex was as strong as that seen in the presence of SopBC (**Fig. 5-7B and C**). These results suggested that the repression of the SopA promoter activity by SopA Q351H and SopA W362E was independent of the SopBC complex and resulted in a super-repressor of SopA.

In order to further quantify the repression activities, we performed quantitative  $\beta$ -galactosidase (ONPG) assays using ONPG as a substrate with DLT1127 strains expressing the untagged versions of SopA, SopA Q351H or SopA W362E in the absence (**Fig. 5-7D**) or presence of SopBC (**Fig. 5-7E**). As would be expected for wtSopA, we observed a 25-fold decrease in the expression of *lacZ* in the presence of the SopBC complex. However, SopA Q351H and SopA W362E showed a  $91.9 \% \pm 5.2$  (n=3, SEM) and  $73.5 \% \pm 9.1$  (n=3, SEM) repression of transcription activity, respectively in the absence of the SopBC complex (**Fig. 5-7D**). Unlike in the case wtSopA, transcriptional repression was not further enhanced in the presence of SopBC complex for SopA Q351H and SopA W362E. The percentage of repression of *lacZ* in the presence of SopBC complex was  $91.7 \% \pm 4.9$  (n=3, SEM) and  $79.7 \% \pm 10.8$  (n=3, SEM), respectively for SopA Q351H and SopA W362E (**Fig. 5-7E**). These results show

that SopA Q351H and SopA W362E act as super-repressors, and unlike the wt-SopA, the repressor function was not responsive to the presence of the SopBC complex. These findings are consistent with the recent reports on ParA DNA binding mutant R351A. The absence of nsDNA binding results in an excess free pool of ParA that becomes available to bind the promoter and function as super-repressors (Baxter et al., 2020). Thus, the inability of SopA Q351H and SopA W362E to bind nsDNA might create an excess of free cytoplasmic pool of the protein, which can then exhibit heightened auto-repression activity.

### **5.2.8 SopA Q351H and SopA W362E fail to interact with SopB**

SopB plays an important role in facilitating segregation of the F plasmids through its interaction with SopA and spatial control of its localisation (Ogura and Hiraga, 1983; Lane et al., 1987; Mori et al., 1989; Lim et al., 2005; Hatano et al., 2007; Castaing et al., 2008; Vecchiarelli et al., 2013; Le Gall et al., 2016). However, the polymerisation and repressor activities of SopA Q351H and SopA W362E were not influenced by the presence of the SopBC complex. Therefore, we sought to determine if these mutants of SopA were impaired in their interaction with SopB. Interaction between ParA and ParB proteins have been studied using a variety of methods, including the bacterial two-hybrid assays (Dmowski and Jagura-Burdzy, 2011). We utilised the bacterial two-hybrid assay (Karimova et al., 1998) for studying the interaction between SopA and SopB. While we fused the T18 fragment to the N-terminus of SopA, we created an N-terminal and C-terminal fusion of the T25 fragment to SopB. Interaction of wild-type SopA with SopB was detected with both N-terminally and C-terminally tagged SopB (**Fig. 5-8A**). Therefore, we only used the N-terminal T25 fusion to SopB in subsequent assays. We failed to detect an interaction of SopA Q351H or SopA W362E with SopB, showing that the mutations Q351H and W362E disrupt their ability to bind the

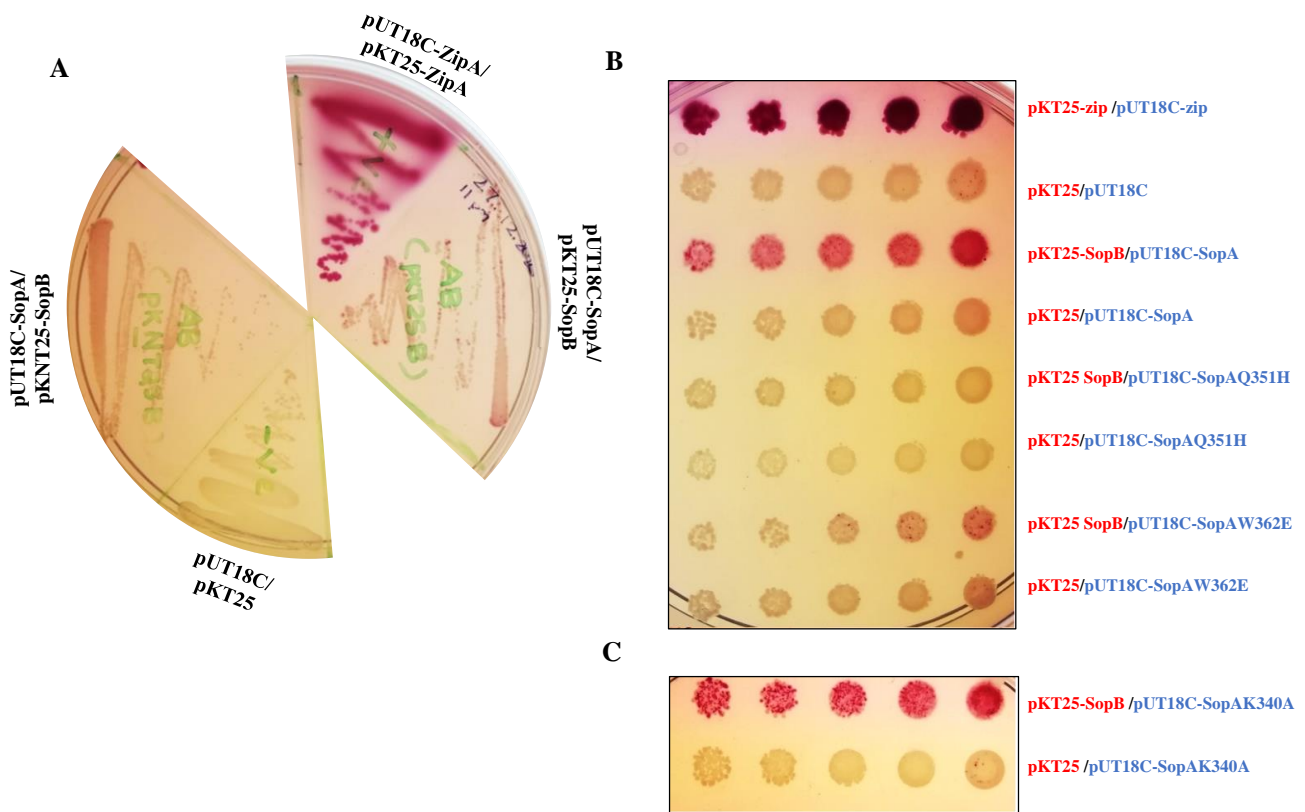


**Figure 5-8. SopA Q351H and W362E mutants are impaired in interaction with SopB.**

**(A) Interaction of the N-terminal and C-terminal fusion of SopB with SopA.** Bacterial two-hybrid assay showing the interaction between N-terminal (pKT25) and C-terminal fusion (pKNT25) of SopB with SopA cloned as N-terminal fusion. **(B) Interaction of the N-terminal fusion of SopB with SopA mutants.** Bacterial two-hybrid assay showing the interaction between SopB and SopA mutants Q351H and W362E cloned as N-terminal fusion in both pUT18C as well as pKT25 vectors. Experiments were performed in triplicate and plated on MacConkey agar plate with 0.5 mM IPTG at 30° C as described in materials and methods. SopA Q351H and W362E fail to interact with SopB, as has been shown in the indicator plate. **(C) SopA K340A, a nsDNA binding defective mutant, interacts efficiently with SopB.** SopA K340A, a known DNA binding defective mutant, is used as a control. SopA K340A exhibits strong interaction with SopB. However, in the case of negative control pKT25/pUT18C SopA K340A, no interaction was observed.

adaptor protein SopB (**Fig. 5-8B**). The inability of SopA Q351H and SopA W362E to interact with SopB was not due to their nsDNA binding defect since SopA K340A, a known nsDNA binding mutant (Castaing et al., 2008), showed efficient interaction with SopB (**Fig. 5-8C**). The ability of SopA K340 to interact with SopB is consistent with the earlier finding that SopB stimulates the ATPase activity of SopA K340A to the same extent as that of wild-type SopA (Castaing et al., 2008; Ah-Seng et al., 2009).

### 5.3 DISCUSSION

Plasmid partitioning protein SopA is predominantly seen localised to the nucleoid of the cell. It is the nucleoid bound SopA that facilitates the process of plasmid segregation by interacting with the SopB-*sopC* complex, which is essentially the plasmid cargo. SopA also undergoes polymerisation *in vitro* (Bouet et al., 2007), and a mutant of SopA (M315I Q351H) has been shown to produce static polymeric structures in *E. coli* (Lim et al., 2005). Such filaments have also been observed in certain cells expressing wild-type SopA (Lim et al., 2005). Moreover, these structures of wild-type SopA also form in the presence of the SopBC complex and exist in the form of radial asters (Lim et al., 2005). Nevertheless, DNA has been reported to inhibit the polymerisation of SopA *in vitro* (Bouet et al., 2007). Furthermore, these polymeric structures of SopA were also found in anucleate cells suggesting that non-specific DNA was not required for filament formation (Hatano et al., 2007).

SopA mutants, Q351H and W362E/A, assembled into polymers in the cell similar to those formed by SopA1 (M315I Q351H) reported earlier (Lim et al., 2005). While the mutations (Q351H and W362E) impaired the plasmid maintenance, these polymers retained their ability to interact with wild-type SopA. Further, SopA Q351H and W362E induced the polymerisation of wt-SopA, suggesting the polymerisation was not due to a drastically altered structure. Introducing an ATP-binding site mutation (K120E) into SopA Q351H and SopA

W362E completely abolished polymerisation, suggesting that polymerisation is an ATP dependent process. *In vitro* studies earlier had similarly concluded that ATP binding was essential for polymerisation of SopA (Fung et al., 2001; Vecchiarelli et al., 2013).

The polymers assembled by SopA Q351H and SopA W362E were also seen to undergo depolymerisation in approximately 20 min when protein synthesis was inhibited. However, the growth of polymers seemed to be extremely slow and could be detected only occasionally in elongated cephalixin treated cells. These results suggest that the maintenance of the polymers required continual protein synthesis and suggested a need for a critical concentration protein to be maintained in the cells for polymerisation. However, both the mutants (Q351H and W362E), like SopA1 (M315I Q351H), were defective in plasmid partitioning, suggesting that the stable polymers did not drive DNA segregation. On the contrary, localisation studies in mini-cells and upon nucleoid condensation revealed nucleoid binding defects of SopA Q351H and SopA W362E. The inability of these mutants to bind nsDNA was further confirmed *in vitro* by EMSA, suggesting that the polymers of SopA1 (M315I Q351H), SopA Q351H and SopA W362E had lost the ability to bind non-specific DNA. Although polymerisation of these mutants is ATP dependent, they are perturbed in nucleoid association. ATPase activity of SopA is stimulated by direct binding of SopB facilitating the directional movement of plasmid cargo to the two poles of the cell (Castaing et al., 2008; Vecchiarelli et al., 2013). Imaging of the polymers in the presence or absence of SopBC indicated that SopB did not affect the polymers formed by SopA Q351H or W362E and suggested that either SopB did not activate the ATPase activity of the SopA mutants or failed to interact with SopA and form an active complex. Our interaction studies of SopA and SopB using BACTH assays show that these SopA mutants (Q351H and W362E) were impaired in binding to SopB. These results might suggest that SopA and SopB interaction mainly occurs within the nucleoid, and in the absence of nucleoid association of SopA Q351H and SopA W362E, SopB interaction might be perturbed. However,

SopA K340A, a mutant defective in nsDNA binding, still retains its ability to directly bind SopA, suggesting that nsDNA binding might not regulate SopB binding. It is also feasible that polymerisation prevents SopB interaction, and future studies using other mutants should reveal the structural changes in SopA that allows interaction with SopB.

Wild-type SopA has the property of autoregulating its promoter  $P_{sop}$ ; however, such repression is weak unless stimulated by SopB (Libante et al., 2001). A reported SopA super-repressor mutant SopA K120Q had been known to bypass the stimulation by SopB to auto-repress its promoter (Lemonnier et al., 2000; Libante et al., 2001). Further, SopA K120Q also fails to bind nsDNA and localise to nucleoids (Le Gall et al., 2016). Our promoter repression assays using  $P_{sop}::lacZ$  strains suggest that SopA Q351H and SopA W362E might represent a new class of super-repressors that map to the C-terminal helix of SopA. Also, these mutants are defective in non-specific DNA binding and possibly behave as super-repressors like SopA K340A (Castaing et al., 2008) and ParA R351A (Baxter et al., 2020). SopA associates with the nucleoid in a dimeric conformation,  $(SopA-ATP^*)_2$  and thus, in the absence of nucleoid association, the free pool of  $(SopA-ATP)_2$  or SopA-ATP in the cytosol is very high. This increase in the available cytoplasmic pool of SopA-ATP offsets the balance between the active nsDNA bound form and the inactive non-DNA bound state, resulting in an increased rate of specific interaction at the promoter DNA binding sites (Baxter et al., 2020). Thus, both the mutants Q351H and W362E being defective in nsDNA binding, act as super-repressors of the  $P_{sop}$ .

Mutations in either Q351 and W362 led to plasmid segregation defects suggesting a critical role for these residues in function. Unlike wild-type SopA, these mutants are non-functional, indicating that polymerisation does not facilitate plasmid maintenance. There is ample evidence supporting non-specific DNA binding and dynamic localisation of SopA to the nucleoid driving the process of plasmid segregation. *In vitro* polymerisation studies in the

presence of nsDNA using light-scattering have implicated DNA as an inhibitor of polymerisation (Bouet et al., 2007). Thus, the lack of non-specific DNA binding by SopA1, SopA Q351H and SopA W362E possibly induce polymerisation, which is in contrast to Soj and VcParA2 that form nucleoproteins filaments in the presence of non-specific DNA (Leonard et al., 2005; Parker et al., 2021). Thus, long polymers are not a usual trait of wild-type SopA and could result from impaired non-specific DNA binding. However, SopA K340A, known to abrogate the nsDNA binding in SopA, does not assemble into such micron long filaments suggesting the C-terminal region containing Q351 and W362 play a crucial role in regulating SopA assembly and polymerisation. These results thus suggest that the last C-terminal helix of SopA might be a key player in facilitating segregation of the plasmids by regulating SopA polymerisation and nsDNA binding.

## **CHAPTER 6**

## **CONCLUSION**



## 6. CONCLUSION

Recent evidence has shown that non-specific DNA binding plays a critical role in F plasmid segregation (Castaing et al., 2008; Vecchiarelli et al., 2013; Lim et al., 2014; Le Gall et. al., 2016). Non-specific DNA binding has been the most well studied, and certain residues have been mapped and identified between 300-340 residues in the C-terminal domain of SopA that are directly involved in the process of nsDNA binding (Castaing et al., 2008). Among the several residues identified, K340 within the SopA C-terminal domain has been specifically implicated in non-specific DNA binding and mutations in the residue disrupt non-specific DNA binding and thus impairs plasmid segregation (Castaing et al., 2008). However, a spontaneous double mutant of SopA (M315 and Q351) that maps further away from the nsDNA binding domain but close to the terminal helix (H16) has been observed to assemble into static polymers and disrupt plasmid segregation (Lim et al., 2005). Further, earlier studies had also shown that SopA was membrane-associated and capable of ATP-dependent polymerisation (Lin and Mallavia, 1998; Lim et. al., 2005; Bouet, et. al., 2007; Hatano et. al., 2007).

However, the molecular details of SopA polymerisation, membrane association and interaction with non-specific DNA remain yet unclear. The broader objective of this thesis work was to characterise the role of the last C-terminal helix (H16) in SopA function and plasmid segregation. Using a combination of *in silico*, cell biological and genetic approaches, we identify that the C-terminal helix contains a hitherto unidentified amphipathic helix and also plays an important role in polymerisation, non-specific DNA binding and interaction with SopB. Further, molecular dynamics simulation analysis of the C-terminal stretch of SopA was carried out by Sakshi Pahujani (an undergraduate student in the group) in collaboration with Dr. Anand

Srivastava lab (IISc, Bengaluru) suggested weak membrane affinity for the amphipathic helix (Mishra et. al., 2021). This work thus elucidates the role of the C-terminal helix of SopA from F plasmid in membrane binding, nucleoid binding and polymerisation. The results from this work are described in Chapters 3 – 5. Chapter 3 describes the identification of a plausible membrane targeting sequence within the last C-terminal helix in SopA. Chapter 4 describes a series of C-terminal deletion mutants and several point mutants in the C-terminal helix, which affect plasmid stability and nsDNA binding activity of SopA. Finally, Chapter 5 identifies a central hub in SopA that regulates polymerisation, non-specific DNA binding, promoter binding and plasmid stability and elucidates the role of two key residues, Q351 and W362, within this hub. In conclusion, our studies here have identified a crucial role for the last C-terminal helix in the structure of F\_ParA/ SopA in non-specific DNA binding, polymerisation and potentially in membrane targeting. However, clearly further studies are required to fully elucidate the precise role of this C-terminal H16 helix in SopA structure and function. For e.g. it is important to establish the case of necessity and sufficiency of the predicted C-terminal amphipathic helix in membrane association. Moreover, preliminary sequence analysis and prediction using AMPHIPASEEK suggest that SopB also carries an amphipathic helix at its C-terminus. Experiments such as those carried out for MinD-MTS (Szeto et al., 2002) and probing direct membrane association of proteins with liposome binding assays will prove useful in testing the role of C-terminal helix in membrane binding of SopA and SopB. Further, a thorough biochemical characterisation of the C-terminal mutants for and quantitative analysis should yield insights into the SopA structure and function relationship. Finally, structural studies including cryo-electron microscopy

will be invaluable in filling our knowledge gap in the understanding of our mechanism by which the ParA family of proteins function in diverse biological aspects.

## **REFERENCES**

## REFERENCES

- Abeles, A. L., Friedman, S. A., & Austin, S. J. (1985). Partition of Unit-copy Miniplasmids to Daughter Cells III. The DNA Sequence and Functional Organization of the P1 Partition Region. *Journal of Molecular Biology*, *189*, 261–72.
- Adams, D. W., Wu, L. J., Errington, J., & William, D. (2015). Nucleoid occlusion protein Noc recruits DNA to the bacterial cell membrane. *The EMBO Journal*, *34*(4), 491–501.
- Ah-Seng, Y., Lopez, F., Pasta, F., Lane, D., & Bouet, J. Y. (2009). Dual role of DNA in regulating ATP hydrolysis by the SopA partition protein. *Journal of Biological Chemistry*, *284*(44), 30067–75.
- Ah-Seng, Y., Rech, J., Lane, D., & Bouet, J. Y. (2013). Defining the role of ATP hydrolysis in mitotic segregation of bacterial plasmids. *PLoS Genetics*, *9*(12), e1003956.
- Akil, C., Tran, L. T., Orhant-prioux, M., Baskaran, Y., Blanchoin, L., & Robinson, R. C. (2019). Complex eukaryotic-like actin regulation systems from Asgard archaea. *BioRxiv*. <https://doi.org/10.1101/768580>.
- Ali, B. (2017). The Role of the ParF Protein in Governing TP228 Plasmid Segregation: Mutational Analysis (Doctoral dissertation, The University of Manchester (United Kingdom)).
- Ana, B., & Ayora, S., Sitkiewicz, I., Fernández, S., Pankiewicz, R., Alonso, J. C., & Ceglowski, P. (1999). Plasmid copy-number control and better-than-random segregation genes of pSM19035 share a common regulator. *Proceedings of the National Academy of Sciences*, *97*(2), 728-33.
- Austin, S., Ziese, M., & Sternberg, N. (1981). A Novel Role for Site-Specific Recombination Maintenance of Bacterial Replicons. *Cell*, *25*(3), 729–36.
- Autret, S., & Errington, J. (2003). A role for division-site-selection protein MinD in regulation of inter nucleoid jumping of Soj (ParA) protein in *Bacillus subtilis*. *Molecular microbiology*, *47*(1), 159-169.
- Autret, S., Nair, R., & Errington, J. (2001). Genetic analysis of the chromosome segregation protein Spo0J of *Bacillus subtilis*: evidence for separate domains involved in DNA binding and interactions with Soj protein. *Molecular Microbiology*, *41*, 743–55.
- Aylett, C. H. S., Wang, Q., Michie, K. A., Amos, L. A., & Löwe, J. (2010). Filament structure of bacterial tubulin homologue TubZ. *Proceedings of the National Academy of Sciences*, *107*(46), 19766–771.
- Azam, T. A. L. I., Iwata, A., Nishimura, A., & Ueda, S. (1999). Growth Phase-Dependent Variation in Protein Composition of the *Escherichia coli* Nucleoid. *Journal of Bacteriology*, *181*(20), 6361–70.

- Baarle, S. Van, Celik, N., Kaval, G., Bramkamp, M., & Hamoen, L. W. (2013). Protein-Protein Interaction Domains of *Bacillus subtilis* DivIVA. *Journal of Bacteriology*, 195(5), 1012–21.
- Baba, T., Ara, T., Hasegawa, M., Takai, Y., Okumura, Y., Baba, M., Datsenko, K.A., Tomita, M., Wanner, B.L. and Mori, H., 2006. Construction of *Escherichia coli* K-12 in-frame, single-gene knockout mutants: the Keio collection. *Molecular Systems Biology*, 2(1), 2006-0008.
- Barilla, D., Rosenberg, M. F., Nobbmann, U., & Hayes, F. (2005). Bacterial DNA segregation dynamics mediated by the polymerizing protein ParF. *The EMBO Journal*, 24(7), 1453–64.
- Barillà, D., Carmelo, E., & Hayes, F. (2007). The tail of the ParG DNA segregation protein remodels ParF polymers and enhances ATP hydrolysis via an arginine finger-like motif. *Proceedings of the National Academy of Sciences*, 104(6), 1811-16.
- Barillà, D. (2016). Driving Apart and Segregating Genomes in Archaea. *Trends in Microbiology*, 24(12), 957–67.
- Baronian, G., Ginda, K., Berry, L., & Cohen-gonsaud, M. (2015). Phosphorylation of *Mycobacterium tuberculosis* ParB Participates in Regulating the ParABS Chromosome Segregation System. *PLoS ONE*, 10, 1–17.
- Bartosik, A. A., Lasocki, K., Mierzejewska, J., & Thomas, C. M. (2004). ParB of *Pseudomonas aeruginosa* : Interactions with Its Partner ParA and Its Target parS and Specific Effects on Bacterial Growth. *Journal of Bacteriology*, 186(20), 6983–98.
- Baxter, J. C., Waples, W. G., & Funnell, B. E. (2020). Nonspecific DNA binding by P1 ParA determines the distribution of plasmid partition and repressor activities. *Journal of Biological Chemistry*, 295(50), 17298–309.
- Bernard, P., Kézdy, K. E., Van Melderen, L., Steyaert, J., Wyns, L., Pato, M. L., Higgins, P.N. & Couturier, M. (1993). The F plasmid CcdB protein induces efficient ATP-dependent DNA cleavage by gyrase. *Journal of Molecular Biology*, 234(3), 534–41.
- Birge, E. A. (2006). Genetics of temperate bacteriophages. *Bacterial and Bacteriophage Genetics*, 261-303.
- Blakely, G., Colloms, S., May, G., Burke, M., & Sherratt, D. (1991). *Escherichia coli* XerC recombinase is required for chromosomal segregation at cell division. *The New Biologist*, 3(8), 789-98.
- Blakely, G., May, G., Mcculloch, R., Arciszewska, L. K., Burke, M., Lovett, S. T., & Sherratt, D. J. (1993). Two Related Recombinases Are Required for Site-Specific Recombination at dif and cer in *E. coli* K12. *Cell*, 75, 351–61.
- Boer, P. A. J. De, Crossley, R. E., & Rothfield, L. I. (1989). A Division Inhibitor and a Topological Specificity Factor Coded for by the Minicell Locus Determine Proper Placement of the Division Septum in *E. coli*. *Cell*, 56(1974), 641–49.

- Bouet, J. Y., Ah-Seng, Y., Benmeradi, N., & Lane, D. (2007). Polymerization of SopA partition ATPase: Regulation by DNA binding and SopB. *Molecular Microbiology*, *63*(2), 468–81.
- Bouet, J., & Funnell, B. E. (1999). P1 ParA interacts with the P1 partition complex at parS and an ATP – ADP switch controls ParA activities. *The EMBO Journal*, *18*(5), 1415–24.
- Bork, P., Sander, C., & Valencia, A. (1992). An ATPase domain common to prokaryotic cell cycle proteins, sugar kinases, actin, and hsp70 heat shock proteins. *Proceedings of the National Academy of Sciences*, *89*(16), 7290-94.
- Breier, A. M., & Grossman, A. D. (2007). Whole-genome analysis of the chromosome partitioning and sporulation protein Spo0J ( ParB ) reveals spreading and origin-distal sites on the *Bacillus subtilis* chromosome. *Molecular Microbiology*, *64*, 703–18.
- Broedersz, C. P., Wang, X., Meir, Y., Loparo, J. J., Rudner, D. Z., & Wingreen, N. S. (2014). Condensation and localization of the partitioning protein ParB on the bacterial chromosome. *Proceedings of the National Academy of Sciences*, *111*(24), 8809-14.
- Bukowski, M., Rojowska, A., & Wladyka, B. (2011). Prokaryotic toxin-antitoxin systems-the role in bacterial physiology and application in molecular biology. *Acta Biochimica Polonica*, *1*(58), 1-9.
- Cabeen, M. T., & Jacobs-Wagner, C. (2010). The Bacterial Cytoskeleton. *Annual Review of Genetics*, *44*, 365–92.
- Campbell, C. S., & Mullins, R. D. (2007). In vivo visualization of type II plasmid segregation: bacterial actin filaments pushing plasmids. *The Journal of Cell Biology*, *179*(5), 1059–66.
- Capiaux, H., Lesterlin, C., Péral, K., Louarn, J. M., & Cornet, F. (2002). A dual role for the FtsK protein in *Escherichia coli* chromosome segregation. *EMBO Reports*, *3*(6), 532–36.
- Casadaban, M. J. (1976). Transposition and fusion of the lac genes to selected promoters in *Escherichia coli* using bacteriophage lambda and Mu. *Journal of Molecular Biology*, *104*(3), 541-55.
- Castaing, J., Bouet, J., & Lane, D. (2008). F plasmid partition depends on interaction of SopA with non-specific DNA. *Molecular Microbiology*, *70*(4), 1000–11.
- Chen, B., Lin, M., Chu, C., Hsu, C., & Sun, Y. (2015). Insights into ParB spreading from the complex structure of Spo0J and parS. *Proceedings of the National Academy of Sciences*, *112*(21), 6613–18.
- Chodha, S. S., Brooks, A. C., Davis, P., Ramachandran, R., Chatteraj, D. K., & Hwang, L. C. (2021). Kinetic pathway of ATP-induced DNA interactions of ParA2, a protein essential for segregation of *Vibrio cholerae* chromosome 2. *BioRxiv*. <https://doi.org/10.1101/2021.02.27.433207>
- Chu, C.H., Yen, C.Y., Chen, B.W., Lin, M.G., Wang, L.H., Tang, K.Z., Hsiao, C.D. and Sun, Y.J., 2019. Crystal structures of Hp Soj–DNA complexes and the nucleoid-adaptor complex formation in chromosome segregation. *Nucleic Acids Research*, *47*(4), 2113-29.

- Christie, P. J. (2004). The *Agrobacterium* Ti plasmids. *Plasmid Biology*, 455-72.
- Colloms, S. D., Sykora, P., Szatmari, G., & Sherratt, D. J. (1990). Recombination at ColEI cer Requires the *Escherichia coli xerC* Gene Product, a Member of the Lambda Integrase Family of Site-Specific Recombinases. *Journal of Bacteriology*, 172(12), 6973–80.
- Cornet, F., Louarn, J., Patte, J., & Louarn, J. M. (1996). Restriction of the activity of the recombination site dif to a small zone of the *Escherichia coli* chromosome. *Genes & development*, 10(9), 1152-61.
- Cooper GM. The Cell: A Molecular Approach. 2nd edition. Sunderland (MA): Sinauer Associates; 2000.
- Corrales-Guerrero, L., He, B., Refes, Y., Panis, G., Bange, G., Viollier, P. H., Steinchen, W., Thanbichler, M. (2020). Molecular architecture of the DNA-binding sites of the P-loop ATPases MipZ and ParA from *Caulobacter crescentus*. *Nucleic Acids Research*, 48(9), 4769–79.
- Crooke, E. (2001). *Escherichia coli* DnaA protein – phospholipid interactions : In vitro and in vivo. *Biochimie*, 83(1), 19–23.
- Dam, M., & Gerdes, K. (1994). Partitioning of Plasmid R1 Ten Direct Repeats Flanking the ParA Promoter Constitute a Centromere-like Partition Site *parC*, that Expresses Incompatibility. *Journal of Molecular Biology*, 236(5), 1289–98.
- Davey, M. J., & Funnell, B. E. (1997). Modulation of the P1 Plasmid Partition Protein ParA by ATP, ADP, and P1 ParB. *Journal of Biological Chemistry*, 272(24), 15286–92.
- Davis, M. A., Martin, K. A., & Austin, S. J. (1992). Biochemical activities of the ParA partition protein of the P1 plasmid. *Molecular Microbiology*, 6(9), 1141–7.
- Davis, M. A., Radnedge, L., Martin, K. A., Hayes, F., Youngren, B., & Austin, S. J. (1996). The P1 ParA protein and its ATPase activity play a direct role in the segregation of plasmid copies to daughter cells. *Molecular Microbiology*, 21(5), 1029-36.
- Derman, A.I., Becker, E.C., Truong, B.D., Fujioka, A., Tucey, T.M., Erb, M.L., Patterson, P.C. and Pogliano, J. (2009). Phylogenetic analysis identifies many uncharacterized actin-like proteins (Alps) in bacteria: regulated polymerization, dynamic instability and treadmilling in Alp7A. *Molecular Microbiology*, 73(4), 534-52.
- de la Hoz, A.B., Pratto, F., Misselwitz, R., Speck, C., Weihofen, W., Welfle, K., Saenger, W., Welfle, H. and Alonso, J.C. (2004). Recognition of DNA by  $\omega$  protein from the broad-host range *Streptococcus pyogenes* plasmid pSM19035: analysis of binding to operator DNA with one to four heptad repeats. *Nucleic Acids Research*, 32(10), 3136-47.
- Dmowski, M., & Jagura-Burdzy, G. (2011). Mapping of the interactions between partition proteins Delta and Omega of plasmid pSM19035 from *Streptococcus pyogenes*. *Microbiology*, 157(4), 1009-20.



- Dmowski, M., & Jagura-Burdzy, G. (2013). Active stable maintenance functions in low copy-number plasmids of Gram-positive bacteria I. Partition systems. *Polish Journal of Microbiology*, 62(1), 3-16.
- Du, S., & Lutkenhaus, J. (2012). MipZ : One for the Pole, Two for the DNA. *Molecular Cell*, 46(3), 239–40.
- Dunham, T. D., Xu, W., Funnell, E., & Schumacher, M. A. (2009). Structural basis for ADP-mediated transcriptional regulation by P1 and P7 ParA. *The EMBO Journal*, 28(12), 1792–802.
- Easter, J., & Gober, J. W. (2002). ParB-Stimulated Nucleotide Exchange Regulates a Switch in Functionally Distinct ParA Activities. *Molecular Cell*, 10(2), 427–434.
- Ebersbach, G., & Gerdes, K. (2001). The double par locus of virulence factor pB171: DNA segregation is correlated with oscillation of ParA. *Proceedings of the National Academy of Sciences*, 98(26), 15078–83.
- Ebersbach, G., Sherratt, D. J., & Gerdes, K. (2005). Partition-associated incompatibility caused by random assortment of pure plasmid clusters. *Molecular Microbiology*, 56(6), 1430–40.
- Erb, M. L., Kraemer, J. A., Coker, J. K. C., Chaikerasitak, V., Nonejuie, P., Agard, D. A., & Pogliano, J. (2014). A bacteriophage tubulin harnesses dynamic instability to center DNA in infected cells. *Elife*, 3(e03197), 1–18.
- Erickson, H. P. (2007). Evolution of the cytoskeleton. *Bioessays*, 29(7), 668-77.
- Ettema, T. J. G., & Lindås, A. (2011). An actin-based cytoskeleton in archaea. *Molecular Microbiology*, 80(4), 1052–61.
- Ezaki, B., Mori, H., Ogura, T., & Hiraga, S. (1990). Possible involvement of the *ugpA* gene product in the stable maintenance of mini-F plasmid in *Escherichia coli*. *Molecular and General Genetics*, 223(3), 361–68.
- Ezaki, B., Ogura, T., Niki, H., & Hiraga, S. (1991). Partitioning of a mini-F plasmid into anucleate cells of the *mukB* null mutant. *Journal of Bacteriology*, 173(20), 6643–46.
- Fenton, A. K., & Gerdes, K. (2013). Direct interaction of FtsZ and MreB is required for septum synthesis and cell division in *Escherichia coli*. *The EMBO journal*, 32(13), 1953-1965.
- Firth, N., Apisiridej, S., Berg, T., O'Rourke, B. A., Curnock, S., Dyke, K. G., & Skurray, R. A. (2000). Replication of Staphylococcal Multiresistance Plasmids. *Journal of Bacteriology*, 182(8), 2170-78.
- Fisher, J. K., Bourniquel, A., Witz, G., Weiner, B., Prentiss, M., & Kleckner, N. (2013). Four-Dimensional Imaging of *E.coli* Nucleoid Organization and Dynamics in Living Cells. *Cell*, 153(4), 882–95.
- Flemming, W. (1882). Zellsubstanz, Kern und Zelltheilung. Vogel.

- Fogel, M. A., & Waldor, M. K. (2005). Distinct segregation dynamics of the two *Vibrio cholerae* chromosomes. *Molecular Microbiology*, 55(1), 125–36.
- Fogel, M. A., & Waldor, M. K. (2006). A dynamic, mitotic-like mechanism for bacterial chromosome segregation. *Genes and Development*, 20(23), 3269–82.
- Fothergill, T. J. G., Barilla, D., & Hayes, F. (2005). Protein Diversity Confers Specificity in Plasmid Segregation. *Journal of Bacteriology*, 187(8), 2651–61.
- Friedman Stanley A., & Austin, S. J. (1988). The P1 plasmid-partition system synthesizes two essential proteins from an autoregulated operon. *Plasmid*, 19(2), 103–12.
- Fung, E., Bouet, J. Y., & Funnell, B. E. (2001). Probing the ATP-binding site of P1 ParA: Partition and repression have different requirements for ATP binding and hydrolysis. *EMBO Journal*, 20(17), 4901–11.
- Funnell, B. E. (1991). The P1 Plasmid Partition Complex at *parS*. *Journal of Biological Chemistry*, 266(22), 14328–37.
- Funnell, B. E., & Gagnier, L. (1995). Partition of P1 Plasmids in *Escherichia coli mukB* Chromosomal Partition Mutants. *Journal of Bacteriology*, 177(9), 2381–86.
- Funnell, B. E. (2016). ParB Partition Proteins : Complex Formation and Spreading at Bacterial and Plasmid Centromeres. *Frontiers in Molecular Biosciences*, 3, 1–6.
- Galkin, V. E., Orlova, A., Rivera, C., Mullins, R. D., & Egelman, E. H. (2009). Structural polymorphism of the ParM filament and dynamic instability. *Structure*, 17(9), 1253–64.
- Garner, J., & Crooke, E. (1996). Membrane regulation of the chromosomal replication activity of *E. coli* DnaA requires a discrete site on the protein. *The EMBO Journal*, 15(13), 3477–85.
- Garner, E. C., Campbell, C. S., & Mullins, R. D. (2004). Dynamic Instability in a DNA-Segregating Prokaryotic Actin Homolog. *Science*, 306(5698), 1021–26.
- Garner, E. C., Campbell, C. S., Weibel, D. B., & Mullins, R. D. (2007). Reconstitution of DNA segregation driven by assembly of a prokaryotic actin homolog. *Science*, 315(5816), 1270–74.
- Gautier, R., Douguet, D., Antony, B., & Drin, G. (2008). HELIQUEST: A web server to screen sequences with specific  $\alpha$ -helical properties. *Bioinformatics*, 24(18), 2101–02.
- Gayathri, P., Fujii, T., Møller-Jensen, J., Van Den Ent, F., Namba, K., & Löwe, J. (2012). A bipolar spindle of antiparallel ParM filaments drives bacterial plasmid segregation. *Science*, 338(6112), 1334–37.
- Gayathri, P., Fujii, T., Namba, K., & Löwe, J. (2013). Structure of the ParM filament at 8.5 Å resolution. *Journal of Structural Biology*, 184(1), 33–42.

- Gerdes, K., Bech, F. W., Jorgensen, S. T., Lobner-olesen, A., Rasmussen, P. B., Atlung, T., Boe, L., Karlstrom, O., Molin, S & Von Mayenburg, K. (1986). Mechanism of postsegregational killing by the *hok* gene product of the *parB* system of plasmid R1 and its homology with the *relF* gene product of the *E. coli* *relB* operon. *The EMBO Journal*, 5(8), 2023–29.
- Gerdes, K., & Molin, S. M. (1986). Partitioning of plasmid R1: structural and functional analysis of the *parA* locus. *Journal of Molecular Biology*, 190(3), 269–79.
- Gerdes, K., Thisted, T., & Martinussen, J. (1990). Mechanism of post-segregational killing by the *hok/ sok* system of plasmid R1: *sok* antisense RNA regulates formation of a *hok* mRNA species correlated with killing of plasmid-free cells. *Molecular Microbiology*, 4(11), 1807–18.
- Gerdes, K., & Müller-jensen, J. (2000). Plasmid and chromosome partitioning : surprises from phylogeny. *Molecular Microbiology*, 37(3), 455–56.
- Gerdes, K., Howard, M., & Szardenings, F. (2010). Pushing and pulling in prokaryotic DNA segregation. *Cell*, 141(6), 927-42.
- Giraldo, R., & Andreu, M. (1998). Protein domains and conformational changes in the activation of RepA, a DNA replication initiator. *The EMBO Journal*, 17(15), 4511–26.
- Gordon, J. E., & Christie, P. J. (2014). The *Agrobacterium* Ti plasmids. *Microbiology Spectrum*, 2(6), 2-6.
- Graham, T. G. W., Wang, X., Song, D., Etson, C. M., Oijen, A. M. Van, Rudner, D. Z., & Loparo, J. J. (2014). ParB spreading requires DNA bridging. *Genes and Development*, 28(11), 1228–38.
- Griffith, K. L., & Wolf Jr, R. E. (2002). Measuring  $\beta$ -galactosidase activity in bacteria: cell growth, permeabilization, and enzyme assays in 96-well arrays. *Biochemical and biophysical research communications*, 290(1), 397-402.
- Hallet, B., & Sherratt, D. J. (1997). Xer Recombination in *Escherichia coli*. *Journal of Biological Chemistry*, 272(35), 21927–31.
- Hanahan, D. (1985). Techniques for transformation of *E. coli* DNA cloning: a practical approach, 1, 109-35.
- Hanai, R., Liu, R., Benedetti, P., Caron, P. R., Lynch, A. S., & Wang, J. C. (1996). Molecular dissection of a protein SopB essential for *Escherichia coli* F plasmid partition. *Journal of Biological Chemistry*, 271(29), 17469-75.
- Hao, J., & Yarmolinsky, M. (2002). Effects of the P1 Plasmid Centromere on Expression of P1 Partition Genes. *Journal of Bacteriology*, 184(17), 4857–67.
- Harry, E. J., Rodwell, J., & Wake, R. G. (1999). Co-ordinating DNA replication with cell division in bacteria : a link between the early stages of a round of replication and mid-cell Z ring assembly. *Molecular Microbiology*, 33(1), 33–40.

- Harry, E. J. (2001). Bacterial cell division: regulating Z-ring formation. *Molecular Microbiology*, 40(4), 795-803.
- Hatano, T., Yamaichi, Y., & Niki, H. (2007). Oscillating focus of SopA associated with filamentous structure guides partitioning of F plasmid. *Molecular Microbiology*, 64(5), 1198–1213.
- Hatano, T., & Niki, H. (2010). Partitioning of P1 plasmids by gradual distribution of the ATPase ParA. *Molecular Microbiology*, 78(5), 1182-98.
- Havey, J. C., Vecchiarelli, A. G., & Funnell, B. E. (2012). ATP-regulated interactions between P1 ParA, ParB and non-specific DNA that are stabilized by the plasmid partition site, *parS*. *Nucleic Acids Research*, 40(2), 801–12.
- Hayakawa, Y., Murotsu, T., & Matsubara, K. (1985). Mini-F Protein that Binds to a Unique Region for Partition of Mini-F Plasmid DNA. *Journal of Bacteriology*, 163(1), 349–54.
- Hayes, F., Radnedge, L., Davis, M. A., & Austin, S. J. (1994). The homologous operons for P1 and P7 plasmid partition are autoregulated from dissimilar operator sites. *Molecular Microbiology*, 11(2), 249–60.
- Hayes, F. (2000). The partition system of multidrug resistance plasmid TP228 includes a novel protein that epitomizes an evolutionarily distinct subgroup of the ParA superfamily. *Molecular Microbiology*, 37(3), 528–41.
- Hayes, F. (2003). Toxins-antitoxins: plasmid maintenance, programmed cell death, and cell cycle arrest., 301(5639), 1496–99.
- Hayes, F., & Barilla, D. (2006). The bacterial segrosome: a dynamic nucleoprotein machine for DNA trafficking and segregation. *Nature Reviews Microbiology*, 4(2), 133–43.
- Hayes, F., & Melderer, L. Van. (2011). Toxins-antitoxins: diversity, evolution and function. *Critical Reviews in Biochemistry and Molecular Biology*, 46(5), 386–408.
- Heidelberg, J.F., Eisen, J.A., Nelson, W.C., Clayton, R.A., Gwinn, M.L., Dodson, R.J., Haft, D.H., Hickey, E.K., Peterson, J.D., Umayam, L. and Gill, S.R., 2000. DNA sequence of both chromosomes of the cholera pathogen *Vibrio cholerae*. *Nature*, 406(6795), 477-83.
- Hester, C. M., & Lutkenhaus, J. (2007). Soj (ParA) DNA binding is mediated by conserved arginines and is essential for plasmid segregation. *Proceedings of the National Academy of Sciences*, 104(51), 20326-331.
- Hiraga, S., Jaffe, A., Teru, O., Mori, H., & Takahashi, H. (1986). F Plasmid ccd Mechanism in *Escherichia coli*. *Journal of Bacteriology*, 166(1), 100–104.
- Hirano, M., Mori, H., Onogi, T., Yamazoe, M., Niki, H., Ogura, T., & Hiraga, S. (1998). Autoregulation of the partition genes of the mini-F plasmid and the intracellular localization of their products in *Escherichia coli*. *Molecular and General Genetics*, 257(4), 392–403.

- Hu, Z., Gogol, E. P., & Lutkenhaus, J. (2002). Dynamic assembly of MinD on phospholipid vesicles regulated by ATP and MinE. *Proceedings of the National Academy of Sciences*, 99(10), 6761–6.
- Hu, Z., & Lutkenhaus, J. (2003). A conserved sequence at the C-terminus of MinD is required for binding to the membrane and targeting MinC to the septum. *Molecular Microbiology*, 47(2), 345–55.
- Hu, L., Vecchiarelli, A. G., Mizuuchi, K., Neuman, K. C., & Liu, J. (2015). Directed and persistent movement arises from mechanochemistry of the ParA/ParB system. *Proceedings of the National Academy of Sciences*, 112(51), E7055-64.
- Hu, L., Vecchiarelli, A. G., Mizuuchi, K., Neuman, K. C., & Liu, J. (2017). Brownian ratchet mechanism for faithful segregation of low-copy-number plasmids. *Biophysical Journal*, 112(7), 1489-1502.
- Hwang, L. C., Vecchiarelli, A. G., Han, Y. W., Mizuuchi, M., Harada, Y., Funnell, B. E., & Mizuuchi, K. (2013). ParA-mediated plasmid partition driven by protein pattern self-organization. *The EMBO Journal*, 32(9), 1238-49.
- Inagawa, T., Kato, J., Niki, H., & Karata, K. (2001). Defective plasmid partition in *ftsH* mutants of *Escherichia coli*. *Molecular Genetics and Genomics*, 265(5), 755–62.
- Ingerson-Mahar, M., & Gitai, Z. (2012). A growing family: the expanding universe of the bacterial cytoskeleton. *FEMS Microbiology Reviews*, 36(1), 256-66.
- Ireton, K., Iv, N. W. G., & Grossman, A. D. (1994). *spoOJ* Is Required for Normal Chromosome Segregation as well as the Initiation of Sporulation in *Bacillus subtilis*. *Journal of Bacteriology*, 176(17), 5320–5329.
- Jacob, F., Brenner, S., & Cuzin, F. (1963). On the regulation of DNA replication in bacteria. In *Cold Spring Harbor symposia on quantitative biology*. Cold Spring Harbor Laboratory Press, 28, 329-348
- Jaffe, A., Ogura, T., & Hiraga, S. (1985). Effects of the *ccd* function of the F plasmid on bacterial growth. *Journal of Bacteriology*, 163(3), 841-9.
- Jaffe, A., Ari, R. D., & Hiraga, S. (1988). Minicell-Forming Mutants of *Escherichia coli*: Production of Minicells and Anucleate Rods. *Journal of Bacteriology*, 170(7), 3094–101.
- Jalal, A. S. B., Tran, N. T., & Le, T. B. K. (2020). ParB spreading on DNA requires cytidine triphosphate in vitro. *ELife*, 9, 1–24.
- Jecz, P., Bartosik, A. A., Glabski, K., & Jagura-Burdzy, G. (2015). A Single *parS* Sequence from the Cluster of Four Sites Closest to *oriC* Is Necessary and Sufficient for Proper Chromosome Segregation in *Pseudomonas aeruginosa*. *PLoS ONE*, 10(3), e0120867.
- Jensen, R. B., & Gerdes, K. (1997). Partitioning of plasmid R1. The ParM protein exhibits ATPase activity and interacts with the centromere-like ParR-parC complex. *Journal of Molecular Biology*, 269(4), 505-13.

- Jensen, R. B., & Gerdes, K. (2014). Mechanism of DNA segregation in prokaryotes : ParM partitioning protein of plasmid R1 co-localizes with its replicon during the cell cycle  
Mechanism of DNA segregation in prokaryotes : ParM partitioning protein of plasmid R1 co-localizes with its replicon. *The EMBO Journal*, *18*(14), 4076–84.
- Johnson, R. C., Johnson, L. M., Schmidt, J. W., & Gardner, J. F. (2004). Major Nucleoid Proteins in the Structure and Function of the *Escherichia coli* Chromosome. *The Bacterial Chromosome*, 65–132.
- Kallioma-Sanford, A. K., Rodriguez-castañeda, F. A., Mcleod, B. N., & Latorre-roselló, V. (2012). Chromosome segregation in Archaea mediated by a hybrid DNA partition machine. *Proceedings of the National Academy of Sciences*, *109*(10), 3754–59.
- Kar, S., Edgar, R., & Adhya, S. (2005). Nucleoid remodeling by an altered HU protein : Reorganization of the transcription program. *Proceedings of the National Academy of Sciences*, *102*(45), 16397–402.
- Karimova, G., Josette, P., Ullmann, A., & Ledant, D. (1998). A bacterial two-hybrid system based on a reconstituted signal transduction pathway. *Proceedings of the National Academy of Sciences*, *95*(10), 5752–6.
- Katsu, T., Tsuchiya, T., & Yuzaburo, F. (1984). Dissipation of membrane potential of *Escherichia coli* cells induced by macromolecular polylysine. *Biochemical and Biophysical Research Communications*, *122*(1), 401–6.
- Khare, D., Ziegelin, G., Lanka, E., & Heinemann, U. (2004). Sequence-specific DNA binding determined by contacts outside the helix-turn-helix motif of the ParB homolog KorB. *Nature Structural & Molecular Biology*, *11*(7), 656–63.
- Kiekebusch, D., Michie, K. A., Essen, L.-O., Lowe, J., & Thanbichler, M. (2012). Article Localized Dimerization and Nucleoid Binding Drive Gradient Formation by the Bacterial Cell Division Inhibitor MipZ. *Molecular Cell*, 245–59.
- Kline-Smith, S. L., & Walczak, C. E. (2004). Mitotic spindle assembly and chromosome segregation: refocusing on microtubule dynamics. *Molecular Cell*, *15*(3), 317–27.
- Koch, A. L. (1985). How bacteria grow and divide in spite of internal hydrostatic pressure. *Canadian Journal of Microbiology*, *31*(12), 1071-84.
- Koehler, T. M., & Thorne, C. B. (1987). *Bacillus subtilis* (natto) plasmid pLS20 mediates interspecies plasmid transfer. *Journal of Bacteriology*, *169*(11), 5271-8.
- Komai, M., Umino, M., & Hanai, R. (2011). Mode of DNA binding by SopA protein of *Escherichia coli* F plasmid. *Journal of Biological Chemistry*, *149*(4), 455–61.
- Koonin, E. V. (1993). A superfamily of ATPases with Diverse Functions Containing Either Classical or Deviant ATP-binding motif. *Journal of Molecular Biology*, *229*(4), 1165–74.
- Kraemer, J.A., Erb, M.L., Waddling, C.A., Montabana, E.A., Zehr, E.A., Wang, H., Nguyen, K., Pham, D.S.L., Agard, D.A. and Pogliano, J. (2012). A phage tubulin assembles

- dynamic filaments by an atypical mechanism to center viral DNA within the host cell. *Cell*, 149(7), 1488-99.
- Kruse, T., Blagoev, B., Løbner-Olesen, A., Wachi, M., Sasaki, K., Iwai, N., Mann, M. and Gerdes, K. (2006). Actin homolog MreB and RNA polymerase interact and are both required for chromosome segregation in *Escherichia coli*. *Genes & development*, 20(1), 113-124.
- Kuempel, P., Høgaard, A., Nielsen, M., Nagappan, O., & Tecklenburg, M. (1996). Use of a transposon (*Tndif*) to obtain suppressing and nonsuppressing insertions of the *dif* resolvase site of *Escherichia coli*. *Genes and Development*, 10(9), 1162–71.
- Kusiak, M., Gapczyn, A., Płochocka, D., & Thomas, C. M. (2011). Binding and spreading of ParB on DNA determine its biological function in *Pseudomonas aeruginosa*. *Journal of Bacteriology*, 193(13), 3342–55.
- Lagage, V., Boccard, F., & Vallet-Gely, I. (2016). Regional Control of Chromosome Segregation in *Pseudomonas aeruginosa*. *PLoS Genetics*, 12(11), e1006428.
- Lane, D., & Ravin, N. V. (2003). Mapping of Functional Domains in F Plasmid Partition Proteins Reveals a Bipartite SopB-recognition Domain in SopA. *Journal of Molecular Biology*, 283(3), 875–89.
- Lane, D., Rothenbuehler, R., Merrillat, A., & Aiken, C. (1987). Analysis of the F plasmid centromere. *Molecular and General Genetics*, 207(2), 406–12.
- Larsen, R. A., Cusumano, C., Fujioka, A., Lim-Fong, G., Patterson, P., & Pogliano, J. (2007). Treadmilling of a prokaryotic tubulin-like protein, TubZ, required for plasmid stability in *Bacillus thuringiensis*. *Genes and Development*, 21(11), 1340–52.
- Lasocki, K., Bartosik, A. A., Mierzejewska, J., Thomas, C. M., & Jagura-Burdzy, G. (2007). Causes ParB Instability and Affects Growth Rate, Chromosome Segregation, and Motility. *Journal of Bacteriology*, 189(15), 5762–72.
- Le Gall, A., Cattoni, D.I., Guilhas, B., Mathieu-Demazière, C., Oudjedi, L., Fiche, J.B., Rech, J., Abrahamsson, S., Murray, H., Bouet, J.Y. and Nollmann, M. (2016). Bacterial partition complexes segregate within the volume of the nucleoid. *Nature Communications*, 7(1), 1–10.
- Lee, P. S., & Grossman, A. D. (2006). The chromosome partitioning proteins Soj (ParA) and Spo0J (ParB) contribute to accurate chromosome partitioning, separation of replicated sister origins, and regulation of replication initiation in *Bacillus subtilis*. *Molecular Microbiology*, 60(4), 853–69.
- Lee, M. J., Liu, C. H., Wang, S. Y., Huang, C. T., & Huang, H. (2006). Characterization of the Soj/Spo0J chromosome segregation proteins and identification of putative *parS* sequences in *Helicobacter pylori*. *Biochemical and Biophysical Research communications*, 342(3), 744-50.

- Lemonnier, M., Bouet, J., Libante, V., & Lane, D. (2000). Disruption of the F plasmid partition complex in vivo by partition protein SopA. *Molecular Microbiology*, 38(3), 493–503.
- Leonard, T. A., Butler, P. J. G., & Löwe, J. (2004). Structural analysis of the chromosome segregation protein Spo0J from *Thermus thermophilus*. *Molecular Microbiology*, 53(2), 419–32.
- Leonard, T. A., Butler, P. J., & Lo, J. (2005). Bacterial chromosome segregation: structure and DNA binding of the Soj dimer—a conserved biological switch. *The EMBO Journal*, 24(2), 270–82.
- Libante, V., Thion, L., & Lane, D. (2001). Role of the ATP-binding site of SopA protein in partition of the F plasmid. *Journal of Molecular Biology*, 314(3), 387–99.
- Lim, G. E., Derman, A. I., & Pogliano, J. (2005). Bacterial DNA segregation by dynamic SopA polymers. *Proceedings of the National Academy of Sciences*, 102(49), 17658–663.
- Lim, H. C., Surovtsev, I. V., Beltran, B. G., Huang, F., Bewersdorf, J., & Jacobs-Wagner, C. (2014). Evidence for a DNA-relay mechanism in ParABS-mediated chromosome segregation. *ELife*, 2014(3), 1–4.
- Lin, Z., & Mallavia, L. P. (1998). Membrane association of active plasmid partitioning protein A in *Escherichia coli*. *Journal of Biological Chemistry*, 273(18), 11302–12.
- Losada, A., & Hirano, T. (2005). Dynamic molecular linkers of the genome : the first decade of SMC proteins. *Genes and Development*, 19(11), 1269–87.
- Löwe, J., & Amos, L. A. (1998). Crystal structure of the bacterial cell-division protein FtsZ. *Nature*, 391(6663), 203–6.
- Lutkenhaus, J., & Sundaramoorthy, M. (2003). MicroReview MinD and role of the deviant Walker A motif, dimerization and membrane binding in oscillation. *Molecular Microbiology*, 48(2), 295–303.
- Lutkenhaus, J. (2012). The ParA/MinD family puts things in their place. *Trends in Microbiology*, 20(9), 411–8.
- MacCready, J.S., Hakim, P., Young, E.J., Hu, L., Liu, J., Osteryoung, K.W., Vecchiarelli, A.G. and Ducat, D.C. (2018). Protein gradients on the nucleoid position the carbon-fixing organelles of Cyanobacteria. *ELife*, 7, e39723.
- McLeod, B. N., & Spiegelman, G. B. (2005). Soj antagonizes Spo0A activation of transcription in *Bacillus subtilis*. *Journal of Bacteriology*, 187(7), 2532–2536.
- Madeira, F., P., Y. M., Lee, J., & Buso, N., Gur, T., Madhusoodanan, N., Basutkar, P., Tivey, A.R., Potter, S.C., Finn, R.D. & Lopez, R. (2019). The EMBL-EBI search and sequence analysis tools APIs in 2019. *Nucleic Acids Research*, 47(1), 636–41.



- Makise, M., Mima, S., Tsuchiya, T., & Mizushima, T. (2001). Molecular Mechanism for Functional Interaction between DnaA Protein and Acidic Phospholipids. *Journal of Biological Chemistry*, 276(10), 7450–6.
- Maloney, E., Madiraju, M., & Rajagopalan, M. (2011). Overproduction and localization of *Mycobacterium tuberculosis* ParA and ParB proteins. *Tuberculosis*, 89, S65–S69.
- Marceau, A. H., Bahng, S., Massoni, S. C., George, N. P., Sandler, S. J., Marians, K. J., & Keck, J. L. (2011). Structure of the SSB–DNA polymerase III interface and its role in DNA replication. *The EMBO journal*, 30(20), 4236–47.
- Marston, A. L., & Errington, J. (1999). Dynamic movement of the ParA-like Soj protein of *B. subtilis* and its dual role in nucleoid organization and developmental regulation. *Molecular Cell*, 4(5), 673–82.
- McLeod, B. N., Allison-Gamble, G. E., Barge, M. T., Tonthat, N. K., Schumacher, M. A., Hayes, F., & Barillà, D. (2017). A three-dimensional ParF meshwork assembles through the nucleoid to mediate plasmid segregation. *Nucleic Acids Research*, 45(6), 3158–71.
- Meselson, M., & Yuan, R. (1968). DNA restriction enzyme from *E. coli*. *Nature*, 217(5134), 1110–4.
- Michie, K. A., & Löwe, J. (2006). Dynamic filaments of the bacterial cytoskeleton. *Annual Review of Biochemistry*, 75, 467–92.
- Million-Weaver, S., & Camps, M. (2014). Mechanisms of plasmid segregation: have multicopy plasmids been overlooked. *Plasmid*, 36(1), 256–66.
- Mishra, D., Pahujani, S., Mitra, N., Srivastava, A., & Srinivasan, R. (2021). Identification of a potential membrane-targeting sequence in the C-terminus of the F plasmid segregation protein SopA. *The Journal of Membrane Biology*, 254, 243–57.
- Miyakoshi, M., Shintani, M., Inoue, K., Terabayashi, T., Sai, F., Ohkuma, M., Nojiri, H., Nagata, Y. and Tsuda, M. (2012). ParI, an orphan ParA family protein from *Pseudomonas putida* KT2440-specific genomic island, interferes with the partition system of IncP-7 plasmids. *Environmental Microbiology*, 14(11), 2946–59.
- Mohl, D. A., & Gober, J. W. (1997). Cell Cycle – Dependent Polar Localization of Chromosome Partitioning Proteins in *Caulobacter crescentus*. *Cell*, 88(5), 675–84.
- Mol, A. R., Castro, M. S., & Fontes, W. (2018). NetWheels: A web application to create high quality peptide helical wheel and net projections. *BioRxiv*, 416347. <https://doi.org/10.1101/416347>
- Møller-Jensen, J., Borch, J., Dam, M., Jensen, R. B., Roepstorff, P., & Gerdes, K. (2003). Bacterial Mitosis : ParM of Plasmid R1 Moves Plasmid DNA by an Actin-like Insertional Polymerization Mechanism. *Molecular Cell*, 12(6), 1477–87.

- Montabana, E. A., & Agard, D. A. (2014). Bacterial tubulin TubZ-Bt transitions between a two-stranded intermediate and a four-stranded filament upon GTP hydrolysis. *Proceedings of the National Academy of Sciences*, *111*(9), 3407–12.
- Mori, H., Kondo, A., Ohshima, A., Ogura, T., & Hiraga, S. (1986). Structure and function of the F plasmid genes essential for partitioning. *Journal of Molecular Biology*, *192*(1), 1–15.
- Moris, Y., Ichinose, C., Niki, H., Ogura, T., Katoq, A., & Hiraga, S. (1989). Purification ; and Characterization of SopA and SopB Proteins Essential for F Plasmid Partitioning. *Journal of Biological Chemistry*, *264*(26), 15535–41.
- Motallebi-Veshareh, M., Rouch, D. A., & Thomas, C. M. (1990). A family of ATPases involved in active partitioning of diverse bacterial plasmids. *Molecular Microbiology*, *4*(9), 1455–63.
- Müller-jensen, J., & Gerdes, K. (2002). Prokaryotic DNA segregation by an actin-like filament. *The EMBO Journal*, *21*(12), 3119–27.
- Nanninga, N. (1998). Morphogenesis of *Escherichia coli*. *Microbiology and Molecular Biology Reviews*, *62*(1), 110–29.
- Nasmyth, K., & Haering, C. H. (2005). The structure and function of SMC and kleisin complexes. *Annual Reviews of Biochemistry*, *74*, 595–648.
- Ni, L., Xu, W., Kumaraswami, M., & Schumacher, M. A. (2010). Plasmid protein TubR uses a distinct mode of HTH-DNA binding and recruits the prokaryotic tubulin homolog TubZ to effect DNA partition. *Proceedings of the National Academy of Sciences*, *107*(26), 11763–8.
- Niki, H., & Jaffe, A. (1991). The new gene mukB codes for a 177 kDa protein with coiled-coil domains involved in chromosome partitioning of *E.coli*. *The EMBO Journal*, *1*(1), 183–93.
- Nogales, E., Downing, K. H., Amos, L. A., & Löwe, J. (1998). Tubulin and FtsZ form a distinct family of GTPases. *Nature Structural Biology*, *5*(6), 451–58.
- Nogales, E. (2010). When cytoskeletal worlds collide. *Proceedings of the National Academy of Sciences*, *107*(46), 19609–10.
- Ogura, T., & Hiraga, S. (1983). Partition mechanism of F plasmid: two plasmid gene-encoded products and a cis-acting region are involved in partition. *Cell*, *32*(2), 351–60.
- Ogura, T., & Hiraga, S. (1986). Structure and Function of the F Plasmid Genes Essential for Partitioning. *Journal of Molecular Biology*, *192*(1), 1–15.
- Orlova, A., Garner, E. C., Galkin, V. E., Heuser, J., Mullins, R. D., & Egelman, E. H. (2007). The structure of bacterial ParM filaments. *Nature Structural & Molecular Biology*, *14*(10), 921–6.

- Osorio-Valeriano, M., Altegoer, F., Steinchen, W., Urban, S., Liu, Y., Bange, G., & Thanbichler, M. (2019). ParB-type DNA segregation proteins are CTP-dependent molecular switches. *Cell*, *179*(7), 1512-24.
- Parker, A. V., Mann, D., Tzokov, S. B., Hwang, L. C., & Bergeron, J. R. (2021). The cryo-EM structure of the bacterial type I DNA segregation ATPase filament reveals its conformational plasticity upon DNA binding. *BioRxiv*. <https://doi.org/10.1101/2021.03.22.436490>
- Pahujani, S. (2020). Role of the ParA-ATP\* state in interaction with the nucleoid and plasmid partitioning via ParABC system (Master's dissertation, National Institute of Science Education and Research (India)).
- Pettersen, E. F., Goddard, T. D., Huang, C. C., Couch, G. S., Greenblatt, D. M., Meng, E. C., & Ferrin, T. E. (2004). UCSF Chimera—a visualization system for exploratory research and analysis. *Journal of Computational Chemistry*, *25*(13), 1605-12.
- Pichoff, S., & Lutkenhaus, J. (2005). Tethering the Z ring to the membrane through a conserved membrane targeting sequence in FtsA. *Molecular Microbiology*, *55*(6), 1722–34.
- Piekarski, G. (1937). 428-439. (1937). Cytologische Untersuchungen an Paratyphus-und Colibakterien. *Archiv Für Mikrobiologie*, *8*(1), 428–39.
- Pinto, U. M., Pappas, K. M., & Winans, S. C. (2012). The ABCs of plasmid replication and segregation. *Nature Reviews Microbiology*, *10*(11), 755–65.
- Pichoff, S., Vollrath, B., Touriol, C., & Bouché, J. P. (1995). Deletion analysis of gene *minE* which encodes the topological specificity factor of cell division in *Escherichia coli*. *Molecular Microbiology*, *18*(2), 321-9.
- Popp, D., Narita, A., Oda, T., Fujisawa, T., Matsuo, H., Nitani, Y., Iwasa, M., Maeda, K., Onishi, H. and Maeda, Y. (2008). Molecular structure of the ParM polymer and the mechanism leading to its nucleotide-driven dynamic instability. *The EMBO Journal*, *27*(3), 570–9.
- Ptacin, J.L., Lee, S.F., Garner, E.C., Toro, E., Eckart, M., Comolli, L.R., Moerner, W.E. and Shapiro, L. (2010). A spindle-like apparatus guides bacterial chromosome segregation. *Nature Cell Biology*, *12*(8), 791-8.
- Pratto, F., Cicek, A., Weihofen, W. A., Lurz, R., Saenger, W., & Alonso, J. C. (2008). *Streptococcus pyogenes* pSM19035 requires dynamic assembly of ATP-bound ParA and ParB on *parS* DNA during plasmid segregation. *Nucleic Acids Research*, *36*(11), 3676–89.
- Quéré, B. Le, Ghigo, J., & Paris, R. (2009). BcsQ is an essential component of the *Escherichia coli* cellulose biosynthesis apparatus that localizes at the bacterial cell pole. *Molecular Microbiology*, *72*(3), 724–40.
- Quisel, J. D., Lin, D. C., & Grossman, A. D. (1999). Control of Development by Altered Localization of a Transcription Factor in *B.subtilis*. *Molecular Cell*, *4*(5), 665–72.

- Rajagopalan, S., & Balasubramanian, M. K. (1999). *S. pombe* Pbh1p: an inhibitor of apoptosis domain containing protein is essential for chromosome segregation. *FEBS Letters*, 460(1), 187-90.
- Ravin, N., & Lane, D. (1999). Partition of the Linear Plasmid N15 : Interactions of N15 Partition Functions with the sop Locus of the F Plasmid. *Journal of Bacteriology*, 181(22), 6898–906.
- Ravin, N. V., & Lane, D. (2003). Mapping of Functional Domains in F Plasmid Partition Proteins 1174 Reveals a Bipartite SopB-recognition Domain in SopA. *Journal of Molecular Biology*, 333(2), 875–889.
- Reece, R. J., & Maxwell, A. (1991). DNA Gyrase : Structure and Function. *Critical Reviews in Biochemistry and Molecular Biology*, 26(3–4), 335–75.
- Roberts, M. A. J., Wadhams, G. H., Had, K. A., Tickner, S., & Armitage, J. P. (2012). ParA-like protein uses nonspecific chromosomal DNA binding to partition protein complexes. *Proceedings of the National Academy of Sciences*, 109(17), 6698–703.
- Robichon, C., Luo, J., Causey, T. B., Benner, J. S., & Samuelson, J. C. (2011). Engineering *Escherichia coli* BL21 (DE3) derivative strains to minimize *E. coli* protein contamination after purification by immobilized metal affinity chromatography. *Applied and Environmental Microbiology*, 77(13), 4634-46.
- Rodionov, O., Łobocka, M., & Yarmolinsky, M. (1999). Silencing of Genes Flanking the P1 Plasmid Centromere. *Science*, 283(5401), 546–50.
- Roy, A., Kucukural, A., & Zhang, Y. (2010). I-TASSER: a unified platform for automated protein structure and function prediction. *Nature Protocols*, 5(4), 725-38.
- Salje, J., Zuber, B., & Löwe, J. (2009). Electron cryomicroscopy of *E. coli* reveals filament bundles involved in plasmid DNA segregation. *Science*, 323(5913), 509–12.
- Salje, J., Gayathri, P., & Löwe, J. (2010). The ParMRC system: molecular mechanisms of plasmid segregation by actin-like filaments. *Nature Reviews Microbiology*, 8(10), 683-92.
- Salje, J., van den Ent, F., de Boer, P., & Löwe, J. (2011). Direct membrane binding by bacterial actin MreB. *Molecular Cell*, 43(3), 478-87.
- Sapay, N., Guermeur, Y., & Deléage, G. (2006). Prediction of amphipathic in-plane membrane anchors in monotopic proteins using a SVM classifier. *BMC Bioinformatics*, 7(1), 1–11.
- Sassetti, C. M., & Rubin, E. J. (2003). Genetic requirements for mycobacterial survival during infection. *Proceedings of the National Academy of Sciences*, 100(22), 12989–94.
- Savage, D. F., Afonso, B., Chen, A. H., & Silver, P. A. (2010). Spatially ordered dynamics of the bacterial carbon fixation machinery. *Science*, 327(5970), 1258–61.

- Schindelin, J., Arganda-Carreras, I., Frise, E., Kaynig, V., Longair, M., Pietzsch, T., Preibisch, S., Rueden, C., Saalfeld, S., Schmid, B., Tinevez, J.Y. and Cardona, A. (2012). Fiji: an open-source platform for biological-image analysis. *Nature Methods*, 9(7), 676-82.
- Scholefield, G., Whiting, R., Errington, J., & Murray, H. (2011). Spo0J regulates the oligomeric state of Soj to trigger its switch from an activator to an inhibitor of DNA replication initiation. *Molecular Microbiology*, 79(4), 1089–1100.
- Scholey, J. M., Brust-Mascher, I., & Mogilner, A. (2003). Cell division. *Nature*, 422(6933), 746–752.
- Schumacher, M. A., & Funnell, B. E. (2005). Structures of ParB bound to DNA reveal mechanism of partition complex formation. *Nature*, 438(7067), 516–519.
- Schumacher, M. A., Mansoor, A., & Funnell, B. E. (2007). Structure of a four-way bridged ParB-DNA complex provides insight into P1 segrosome assembly. *Journal of Biological Chemistry*, 282(14), 10456–64.
- Schumacher, M. A. (2008). Structural biology of plasmid partition: uncovering the molecular mechanisms of DNA segregation. *Biochemical Journal*, 412(1), 1–18.
- Schumacher, M. A. (2012). Bacterial plasmid partition machinery: a minimalist approach to survival. *Current Opinion in Structural Biology*, 22(1), 72-79.
- Schumacher, M.A., Tonthat, N.K., Lee, J., Rodriguez-Castañeda, F.A., Chinnam, N.B., Kalliomaa-Sanford, A.K., Ng, I.W., Barge, M.T., Shaw, P.L. and Barillà, D. (2015). Structures of archaeal DNA segregation machinery reveal bacterial and eukaryotic linkages. *Science*, 349(6252), 1120-4.
- Schumacher, M. A., Lee, J., Zeng, W., & Duke, N. H. (2016). Molecular insights into DNA binding and anchoring by the *Bacillus subtilis* sporulation kinetochore-like RacA protein. *Nucleic Acids Research*, 44(11), 5438–49.
- Schumacher, M.A., Tonthat, N.K., Lee, J., Rodriguez-Castañeda, F.A., Chinnam, N.B., Kalliomaa-Sanford, A.K., Ng, I.W., Barge, M.T., Shaw, P.L. and Barillà, D. (2016). Structures of archaeal DNA segregation machinery reveal bacterial and eukaryotic linkages. *Science*, 349(6252), 1120–4.
- Schumacher, M. A., Henderson, M., & Zhang, H. (2019). Structures of maintenance of carboxysome distribution Walker-box McdA and McdB adaptor homologs. *Nucleic Acids Research*, 47(11), 5950–62.
- Schweizer, H., Grussenmeyer, T., & Boos, W. (1982). Mapping of Two *ugp* Genes Coding for the *pho* Regulon- Dependent sn-Glycerol-3-Phosphate Transport System of *Escherichia coli*. *Journal of Bacteriology*, 150(3), 1164–71.
- Sherratt, D. J. (1974). Plasmids Review. *Cell*, 3(3), 189–195.
- Shih, Y.-L., & Rothfield, L. (2006). The Bacterial Cytoskeleton. *Microbiology and Molecular Biology Reviews*, 70(3), 729–754.

- Soh, Y. M., Davidson, I. F., Zamuner, S., Basquin, J., Bock, F. P., Taschner, M., Veening, J.W., De Los Rios, P., Peters J.M. & Gruber, S. (2019). Self-organization of *parS* centromeres by the ParB CTP hydrolase. *Science*, 366(6469), 1129–33.
- Srinivasan, R., Mishra, M., Wu, L., Yin, Z., & Balasubramanian, M. K. (2008). The bacterial cell division protein FtsZ assembles into cytoplasmic rings in fission yeast. *Genes & Development*, 22(13), 1741-6.
- Stairs, C. W., & Ettema, T. J. G. (2020). The Archaeal Roots of the Eukaryotic Dynamic Actin Cytoskeleton. *Current Biology*, 30(10), R521–R526.
- Studier, F. W. (1990). Use of T7 RNA polymerase to direct expression of cloned genes. *Methods Enzymol.*, 185, 60-89.
- Strahl, H., & Hamoen, L. W. (2010). Membrane potential is important for bacterial cell division. *Proceedings of the National Academy of Sciences*, 107(27), 12281–6.
- Sun, Q., & Margolin, W. (2001). Influence of the nucleoid on placement of FtsZ and MinE rings in *Escherichia coli*. *Journal of Bacteriology*, 183(4), 1413-22.
- Sun, Q., & Margolin, W. (2004). Effects of Perturbing Nucleoid Structure on Nucleoid Occlusion-Mediated Toporegulation of FtsZ Ring Assembly. *Journal of Bacteriology*, 186(12), 3951–9.
- Szeto, T. H., Rowland, S. L., Rothfield, L. I., & King, G. F. (2002). Membrane localization of MinD is mediated by a C-terminal motif that is conserved across eubacteria, archaea, and chloroplasts. *Proceedings of the National Academy of Sciences*, 99(24), 15693–8.
- Szeto, T. H., Rowland, S. L., Habrukowich, C. L., & King, G. F. (2003). The MinD Membrane Targeting Sequence Is a Transplantable Lipid-binding Helix. *Journal of Biological Chemistry*, 278(41), 40050–6.
- Tadesse, S., & Graumann, P. L. (2006). Differential and Dynamic Localization of Topoisomerases in *Bacillus subtilis*. *Journal of Bacteriology*, 188(8), 3002–3011.
- Taghbalout, A., & Rothfield, L. (2007). RNaseE and the other constituents of the RNA degradosome are components of the bacterial cytoskeleton. *Proceedings of the National Academy of Sciences*, 104(5), 1667-1672.
- Tang, M., Bideshi, D. K., Park, H., & Federici, B. A. (2006). Minireplicon from pBtoxis of *Bacillus thuringiensis subsp . israelensis*. *Applied and Environmental Microbiology*, 72(11), 6948–54.
- Thanbichler, M., & Shapiro, L. (2006). MipZ, a spatial regulator coordinating chromosome segregation with cell division in *Caulobacter*. *Cell*, 126(1), 147–62.
- Thisted, T., & Kenn, G. (1992). Mechanism of Post-segregational Killing of Plasmid R1 by the *hok / sok* System Sok Antisense RNA Regulates *hok* Gene Expression Indirectly Through the Overlapping *mok* Gene. *Journal of Molecular Biology*, 223(1), 41–54.

- Thomas, C. M. (2000). Paradigms of plasmid organization. *Molecular Microbiology*, 37(3), 485–91.
- Tinsley, E., & Khan, S. A. (2006). A Novel FtsZ-Like Protein Is Involved in Replication of the Anthrax Toxin-Encoding pXO1 Plasmid in *Bacillus anthracis*. *Journal of Bacteriology*, 188(8), 2829–2835.
- Toro, E., Hong, S., Mcadams, H. H., & Shapiro, L. (2008). Caulobacter requires a dedicated mechanism to initiate chromosome segregation. *Proceedings of the National Academy of Sciences*, 105(40), 15435–15440.
- Van den Ent, F., Amos, L. A., & Lowe, J. (2001). Prokaryotic origin of the actin cytoskeleton. *Nature*, 413(6851), 39-44.
- Van den Ent, F., Møller-Jensen, J., Amos, L. A., Gerdes, K., & Löwe, J. (2002). F-actin-like filaments formed by plasmid segregation protein ParM. *The EMBO Journal*, 21(24), 6935-43.
- Van Den Ent, F., & Löwe, J. (2006). RF cloning: a restriction-free method for inserting target genes into plasmids. *Journal of Biochemical and Biophysical Methods*, 67(1), 67-74.
- Van den Ent, F., Izoré, T., Bharat, T. A., Johnson, C. M., & Löwe, J. (2014). Bacterial actin MreB forms antiparallel double filaments. *Elife*, 3, e02634.
- Vecchiarelli, A. G., Han, Y., Tan, X., Mizuuchi, M., Ghirlando, R., Biertümpfel, C., ... Mizuuchi, K. (2010). ATP control of dynamic P1 ParA – DNA interactions : a key role for the nucleoid in plasmid partition. *Molecular Microbiology*, 78(1), 78–91.
- Vecchiarelli, A. G., Hwang, L. C., & Mizuuchi, K. (2013). Cell-free study of F plasmid partition provides evidence for cargo transport by a diffusion-ratchet mechanism. *Proc Natl Acad Sci U S A, Proceedings of the National Academy of Sciences*, 110(15), e1390-7.
- Vecchiarelli, A. G., Havey, J. C., Ing, L. L., Wong, E. O., Waples, W. G., & Funnell, B. E. (2013). Dissection of the ATPase active site of P1 ParA reveals multiple active forms essential for plasmid partition. *Journal of Biological Chemistry*, 288(24), 17823-31.
- Vecchiarelli, A. G., Neuman, K. C., & Mizuuchi, K. (2014). A propagating ATPase gradient drives transport of surface-confined cellular cargo. *Proceedings of the National Academy of Sciences*, 111(13), 4880-5.
- Di Ventura, B., Knecht, B., Andreas, H., Godinez, W.J., Fritsche, M., Rohr, K., Nickel, W., Heermann, D.W. and Sourjik, V. (2013). Chromosome segregation by the *Escherichia coli* Min system. *Molecular Systems Biology*, 9(1), 686.
- Volante, A., & Alonso, J. C. (2015). Molecular Anatomy of ParA-ParA and ParA-ParB Interactions during Plasmid Partitioning. *Journal of Biological Chemistry*, 290(30), 18782–95.

- Walczak, C. E., Cai, S., & Khodjakov, A. (2010). Mechanisms of chromosome behaviour during mitosis. *Nature Reviews Molecular Cell Biology*, *11*(2), 91–102.
- Wagstaff, J., & Löwe, J. (2018). Prokaryotic cytoskeletons: protein filaments organizing small cells. *Nature Reviews Microbiology*, *16*(4), 187–201.
- Walker, J. E., Saraste, M., Runswick, M. J., & Gay, N. J. (1982). Distantly related sequences in the alpha- and beta-subunits of ATP synthase, myosin, kinases and other ATP-requiring enzymes and a common nucleotide binding fold. *The EMBO journal*, *1*(8), 945–951.
- Wang, W., Li, G. W., Chen, C., Xie, X. S., & Zhuang, X. (2011). Chromosome organization by a nucleoid-associated protein in live bacteria. *Science*, *333*(6048), 1445–9.
- Watanabe, E., Wachi, M., Yamasaki, M., & Nagai, K. (1992). ATPase activity of SopA, a protein essential for active partitioning of F plasmid. *Molecular and General Genetics*, *234*(3), 346–52.
- Weiss, D. S., Chen, J. C., Ghigo, J. M., Boyd, D., & Beckwith, J. (1999). Localization of FtsI (PBP3) to the septal ring requires its membrane anchor, the Z ring, FtsA, FtsQ, and FtsL. *Journal of Bacteriology*, *181*(2), 508–520.
- Weissgerber, T. L., Savic, M., Winham, S. J., Stanisavljevic, D., Garovic, V. D., & Milic, N. M. (2017). Data visualization, bar naked: A free tool for creating interactive graphics. *Journal of Biological Chemistry*, *292*(50), 20592–8.
- Wendler, P., Ciniawsky, S., Kock, M., & Kube, S. (2012). Biochimica et Biophysica Acta Structure and function of the AAA + nucleotide binding pocket. *BBA - Molecular Cell Research*, *1823*(1), 2–14.
- Wickstead, B., & Gull, K. (2011). The evolution of the cytoskeleton. *Journal of Cell Biology*, *194*(4), 513–25.
- Wu, L. J., Ishikawa, S., Kawai, Y., Oshima, T., Ogasawara, N., & Errington, J. (2009). Noc protein binds to specific DNA sequences to coordinate cell division with chromosome segregation. *EMBO Journal*, *28*(13), 1940–52.
- Yamaichi, Y., & Niki, H. (2000). Active segregation by the *Bacillus subtilis* partitioning system in *Escherichia coli*. *Proceedings of the National Academy of Sciences*, *97*(26), 14656–61.
- Yamaichi, Y., & Niki, H. (2004). *migS*, a cis-acting site that affects bipolar positioning of *oriC* on the *Escherichia coli* chromosome. *The Bacterial Chromosome*, *23*(1), 221–33.
- Yamaichi, Y., Fogel, M. A., & Waldor, M. K. (2006). *par* genes and the pathology of chromosome loss in *Vibrio cholerae*. *Proceedings of the National Academy of Sciences*, *104*(2), 630–5.
- Yang, J., Yan, R., Roy, A., Xu, D., Poisson, J., Arbor, A., & Arbor, A. (2015). The I-TASSER Suite: protein structure and function prediction. *Nature Methods*, *12*(1), 7–8.



- Yarmolinsky, M. B. (1995). Programmed cell death in bacterial populations. *Science*, 267(5199), 836-8.
- Yu, X., & Margolin, W. (1999). FtsZ ring clusters in min and partition mutants : role of both the Min system and the nucleoid in regulating FtsZ ring localization. *Molecular Microbiology*, 32(2), 315–26.
- Zehr, E. A., Kraemer, J. A., Erb, M. L., Coker, J. K., Montabana, E. A., Pogliano, J., & Agard, D. A. (2014). The structure and assembly mechanism of a novel three-stranded tubulin filament that centers phage DNA. *Structure*, 22(4), 539-48.
- Zhang, H., & Schumacher, M. A. (2017). Structures of partition protein ParA with nonspecific dna and ParB effector reveal molecular insights into principles governing walker-box dna segregation. *Genes and Development*, 31(5), 481–92.
- Zhang, Y. (2008). I-TASSER server for protein 3D structure prediction. *BMC Bioinformatics*, 9(1), 1–8.
- Zimmerman, S. B. (2003). Underlying regularity in the shapes of nucleoids of *Escherichia coli* : Implications for nucleoid organization and partition. *Journal of Structural Biology*, 142(2), 256–265.
- Zimmerman, S. B. (2006). Shape and compaction of *Escherichia coli* nucleoids. *Journal of Structural Biology*, 156(2), 255–61.
- Zusman, D. R., Carbonell, I. A., & Haga, J. Y. (1973). Nucleoid Condensation and Cell Division in *Escherichia coli* MX74T2 ts52 After Inhibition of Protein Synthesis. *Journal of Bacteriology*, 115(3), 1167–78.